UNIVERSIDAD DE BURGOS

Departamento de Biotecnología y Ciencia de los Alimentos

Valorización sostenible de subproductos agroindustriales para la extracción de proteínas mediante fluidos subcríticos

TESIS DOCTORAL

Pedro Barea Gómez

Burgos, 2025

UNIVERSITY OF BURGOS

Department of Biotechnology and Food Science

Sustainable valorization of agro-industrial by-products for protein extraction using subcritical fluids

PHD THESIS

Pedro Barea Gómez

Burgos, 2025

SUSTAINABLE VALORIZATION OF AGRO-INDUSTRIAL BY-PRODUCTS FOR PROTEIN EXTRACTION USING SUBCRITICAL FLUIDS

Memoria que, para optar al grado de Doctor por la Universidad de Burgos, en el programa Avances en Ciencia y Biotecnología Alimentarias, presenta:

PEDRO BAREA GÓMEZ

Burgos, 2025

AGRADECIMIENTOS

Este trabajo ha sido realizado en el marco de los siguientes proyectos de Investigación desarrollados en el seno del Grupo de Investigación: Biotecnología Industrial y Medioambiental, reconocido por la Universidad de Burgos (GIR-UBU BIOIND) y por la Junta de Castilla y León como Unidad de Investigación Consolidada UIC-128.

- VALORIZACIÓN DE SUBPRODUCTOS MARINOS MEDIANTE TECNOLOGÍAS DE FLUIDOS SUB- Y SUPERCRÍTICOS PARA LA OBTENCIÓN DE BIOCOMPUESTOS VALIOSOS (MARVALOR), financiado por la Agencia Estatal de Investigación (PID2019-104950RB-I00).

- TECNOLOGÍAS VERDES BASADAS EN EL EMPLEO DE FLUIDOS PRESURIZADOS PARA VALORIZAR BIOMASA LIGNOCELULÓSICA MEDIANTE LA PRODUCCIÓN DE FURFURAL (GREENFUR), financiado por la Agencia Estatal de Investigación (TED2021-129311B-I00).

- NUEVAS ESTRATEGIAS PARA LA PRODUCCIÓN DE ÁCIDO LÁCTICO DE SEGUNDA GENERACIÓN EMPLEANDO TECNOLOGÍAS EMERGENTES BASADAS EN FLUIDOS PRESURIZADOS (2BIOLAC), financiado por la Agencia Estatal de Investigación (PID2022-136385OB-I00).

El contrato predoctoral de Pedro Barea Gómez ha sido financiado por la Junta de Castilla y León y el Fondo Social Europeo (ORDEN EDU/1868/2022).

A mis directores de Tesis, Teresa y Rodrigo. A Tere, por su gran dedicación a esta investigación, por su confianza, su apoyo y el tiempo que ha dedicado a enseñarme tanto. A Rodrigo, por ayudarme a crecer como investigador, guiándome siempre hacia la mejora.

A Sagrario, por la confianza depositada en mí y su interés en mi progreso a lo largo de este camino. A Beti, por su ayuda siempre que la he necesitado y todo lo que me ha enseñado en el laboratorio. Y al resto de los profesores del área con los que he compartido conversaciones: Óscar, Cipri, José Manuel, Alberto y Olga.

A todos mis compañeros durante la realización de esta Tesis. En especial a Alba, que me ha acompañado durante todo este camino, resolviéndome infinitas dudas y ayudándome siempre sin dudarlo. A Helena, con quien he compartido este proceso y nos hemos apoyado mutuamente con un mismo objetivo. También al resto de compañeros que han formado parte de este trayecto: Alejandro, Esther, Almudena, Laura, Víctor, Patri, Emre, Daysi, Belén, Solomon, Amir, Eli…

A la profesora Solange Mussatto, de la Universidad Técnica de Dinamarca, por darme la oportunidad de colaborar con su grupo durante mi estancia de investigación predoctoral. Y a mis compañeros allí: Sarah, Lara, Turbo y Camilo, por compartir conmigo nuevas formas de trabajo, culturas y su tiempo libre.

A mi familia y mis amigos. En especial a mis padres y abuelos, por sus consejos, interés y apoyo incondicional. Y a mi hermana pequeña Raquel, que avanza con éxito en su propio camino, por su apoyo, humor y ánimo cada fin de semana.

Por último, a Beatriz, por su apoyo y alegría en el día a día, por su paciencia y comprensión en los días difíciles, y por acompañarme con orgullo en cada logro.

A todos, va dedicada esta Tesis.

GENERAL INDEX

GENERAL INDEX

SUMMARY

RESUMEN DE LA TESIS

El aumento de la población mundial plantea la necesidad de desarrollar fuentes sostenibles de proteínas, dado que la producción alimentaria convencional resultará insuficiente. Este desafío, junto con la gestión de los residuos agroindustriales, impulsa la valorización de subproductos proteicos no aptos para el consumo directo. En esta Tesis Doctoral se estudian dos de ellos: la harina de pescado, procedente de la industria atunera, como fuente animal, y la okara, procedente de la elaboración de leche de soja y tofu, como fuente vegetal. Ambas biomasas conservan un elevado contenido proteico, lo que las hace idóneas para su valorización, además de contener compuestos bioactivos, como las isoflavonas de la okara, con potencial nutracéutico.

El objetivo principal de esta Tesis es proponer tecnologías verdes basadas en fluidos presurizados para valorizar la fracción proteica de estos subproductos, sustituyendo procesos convencionales menos sostenibles. La hidrólisis con agua subcrítica (SWH) es la principal tecnología empleada. Se basa en el uso de agua en estado líquido a alta temperatura y presión, variables que son estudiadas además del tiempo de tratamiento y el gas presurizante. En este proceso se generan corrientes ricas en biocompuestos mediante la modificación de la temperatura de operación.

La SWH se compara con otras tecnologías verdes innovadoras, como el tratamiento con microondas, ultrasonidos, enzimas y extracciones alcalinas a presión reducida. Los hidrolizados proteicos obtenidos se fraccionaron por tamaño molecular mediante membranas y se evaluaron sus propiedades tecno-funcionales. Además, se implementó un proceso en cascada para la biomasa vegetal, orientado a la recuperación de compuestos bioactivos previa a la extracción proteica.

En conjunto, esta Tesis presenta estrategias para convertir subproductos ricos en proteínas en compuestos de alto valor, manteniendo un firme compromiso con la sostenibilidad ambiental y contribuyendo al desarrollo de enfoques de bioeconomía circular en el procesamiento de alimentos.

SUMMARY OF THE THESIS

The growth of the world population highlights the need to develop sustainable protein sources, as conventional food production will become insufficient. This challenge, together with the management of agro-industrial residues, drives the valorization of protein-rich by-products not suitable for direct consumption. In this PhD Thesis, two of them are studied: fish meal, from the tuna industry, as an animal protein source, and okara, derived from the production of soy milk and tofu, as a plant-based source. Both biomasses retain a high protein content, making them suitable for valorization, and also contain bioactive compounds, such as the isoflavones in okara, with nutraceutical potential.

The main objective of this Thesis is to propose green technologies based on pressurized fluids to valorize the protein fraction of these by-products, replacing less sustainable conventional processes. Subcritical water hydrolysis (SWH) is the main technology employed. It relies on the use of water in its liquid state at high temperature and pressure, variables that are studied along with the treatment time and the type of pressurizing gas. This process generates streams rich in biocompounds through the simple modification of the operating temperature.

SWH is compared with other innovative green technologies, such as microwave, ultrasound, enzymatic, and alkaline extraction under reduced pressure. The protein hydrolysates obtained were fractionated by molecular size using membranes, and their techno-functional properties were evaluated. In addition, a cascade process was implemented for the plant biomass, intended for recovering bioactive compounds prior to protein extraction.

Overall, this Thesis presents strategies to convert protein-rich by-products into valuable compounds while maintaining a strong commitment to environmental sustainability, contributing to the development of circular bioeconomy approaches in food processing.

INTRODUCTION

TABLE OF CONTENTS

1. Food by-products as protein source

In the context of a rapidly growing global population, food security and the sustainability of food systems are under threat, as intensifying pressures on natural resources and climate change could push them beyond safe limits (Avelar *et al*., 2022). By 2022, with the world population reaching 8 billion, approximately 735 million people faced hunger, representing 9.2 % of the total population and having increased by 19.9 % since the COVID-19 pandemic (FAO, 2023; United Nations, 2023). The global population is projected to approach 10 billion by 2050, intensifying the demands on agriculture, industry, and natural ecosystems. Food demand, and specifically protein demand, would require meat and dairy products to increase by 73 % and 58 %, respectively. In a potential context of extreme protein needs, it is interesting to highlight inefficiency of animal protein production, being needed about 7 kg of plant food to produce just 1 kg of milk or meat (Avelar *et al*., 2022).

1.1. Food waste and new protein sources

This urgent food security challenge underscores the necessity to innovate sustainable protein sources and processing methods that can meet global nutritional demands while minimizing environmental impact. The quality of food depends significantly on its protein content, both for its high nutritional value, and its structure. Proteins are even more essential in cases of extreme nutritional needs. However, meeting global protein demand is increasingly challenging due to environmental concerns and resource limitations (Corredig *et al*., 2020).

In recent decades, increasing environmental, economic, ethical, and religious concerns over animal protein production have driven research toward non-conventional protein sources, including those recovered from food industry by-products. These recovered proteins, with valuable nutritional and techno-functional properties, offer a strategic solution for both waste valorization and resource maximization under stricter environmental regulations (Avelar *et al*., 2022).

Corredig *et al.* (2020) highlighted that current food systems must transition towards more sustainable protein sources, such as plant-based protein and side streams or food waste, reducing in turn environmental impact. To complete these challenges is crucial for the development of innovative and climate-friendly food solutions capable of supporting a growing population without compromising protein quality or environmental sustainability (Corredig *et al.*, 2020).

Valorizing underused resources (including food industry by-products, non-edible plant and animal fractions, and non-food protein sources) is essential for establishing sustainable and cost-efficient protein supply chains. Achieving this transition requires technological advancements, scientific research, and a comprehensive reorganization of production, processing, and supply systems (Avelar *et al*., 2022; Corredig *et al*., 2020).

1.2. Protein hydrolysates

Proteins are highly diverse biological macromolecules, being the most abundant biomolecules in cells, participating in nearly all cellular processes and playing a crucial role in human health. They are polymers composed of sequences of 20 standard amino acids, each containing an amino group ($–NH_2$) and a carboxyl group (–COOH) bound to the same carbon, with side chains (–R groups) conferring distinct chemical properties. Amino acids are covalently linked by peptide bonds forming the primary structure (see Figure I.1), that determines the unique identity of the protein and ultimately dictates its three-dimensional shape and biological function. Any variation in the amino acid order, even minor ones, can significantly alter protein activity (Lehninger, 1984).

The secondary structure (see Figure I.1) refers to the folding patterns within specific segments of a polypeptide base structure. It includes common patterns, such as the alpha (α) helix, a right-handed spiral stabilized by internal hydrogen bonds, and the beta (β) sheet, formed by extended strands linked through inter-strand hydrogen bonds. These structural elements contribute to the protein stability and

provide a scaffold for its higher-order folding. The folding of these into unique three-dimensional tertiary and quaternary structures (Figure I.1) determines protein biological functions, ranging from enzymatic catalysis to structural support, signaling, and transport (Lehninger, 1984).

Tertiary structures are stabilized primarily by a variety of weak interactions between distant amino acid residues in the chain, including: hydrogen bonds, which form between polar side chains, helping maintain the folded shape; hydrophobic interactions, where non-polar residues group internally to shield themselves from water; van der Waals forces, arising from close packing of atoms providing additional stabilization; and ionic bonds, representing electrostatic attractions between oppositely charged side chains. Occasionally, disulfide bridges (covalent bonds between cysteine residues) also contribute to stability by crosslinking remote parts of the polypeptide chain. There are two general classes of proteins based on their tertiary structure: fibrous and globular. Fibrous proteins predominantly consist of simple repetitive secondary structure elements and primarily provide structural roles. In contrast, globular proteins exhibit more complex tertiary structures, often containing multiple types of secondary structures within the same polypeptide chain (Lehninger, 1984).

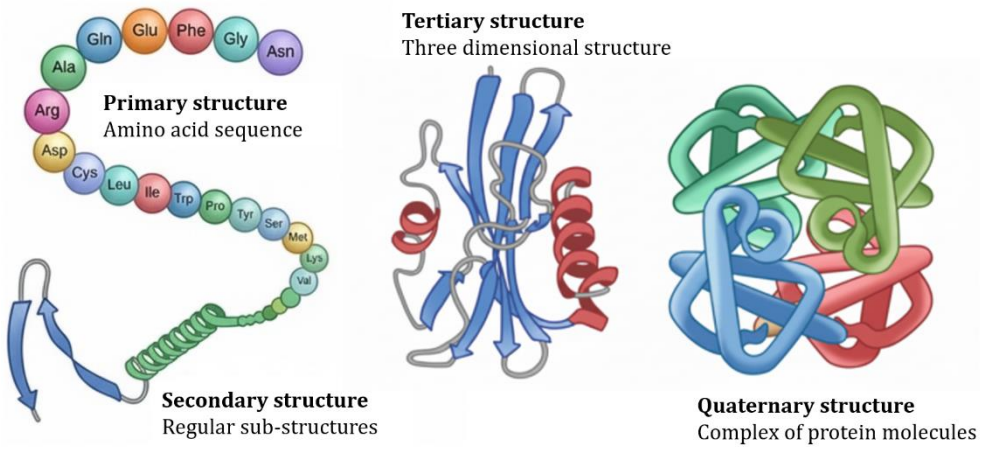

Figure I.1. Schematic representation of protein structural organization. Adapted from Labster.

The quaternary structure emerges from the association of two or more polypeptide subunits into a larger functional protein complex. Similar weak interactions, such as those in the tertiary structure, mediate these assemblies. These collectively stabilize the multi-subunit arrangement, enabling diverse biological functions that individual subunits alone could not perform (Lehninger, 1984).

Protein denaturation involves the disruption of secondary, tertiary, and quaternary structures through the breaking of weak interactions such as hydrogen bonds, hydrophobic effects, and ionic forces, while primary peptide bonds remain largely intact (Lehninger, 1984). Protein hydrolysates represent one of the most digestible and nutritionally valuable protein forms. Technically, the hydrolysis process does not diminish protein quality; rather, it enhances digestibility and bioavailability by breaking proteins down into peptides and free amino acids, which may also exhibit improved (or new) functional and bioactive properties (Aspevik *et al*., 2017). Peptide sequences that remain latent within the parent protein and only reveal their bioactive properties upon release during hydrolysis, are commonly referred to as "encrypted" peptides (Freitas *et al*., 2019).

Historically, the consumption of protein hydrolysates in human diets has been limited by undesirable residual flavors (particularly bitterness) often associated with small peptides (< 1000 Da) enriched in hydrophobic and/or aromatic amino acids. However, such sensory issues can now be mitigated through the use of flavor enhancers such as some other amino acids like glutamic acid and glycine, texturizing agents like polyphosphates and gelatin, and flavor adsorbents including activated carbon (Aspevik *et al*., 2017).

Commonly, research underscores the significance of obtaining small-sized peptides and free amino acids, primarily due to their functionalities and bioactive properties. In contrast, the acquisition of partially intact proteins and larger peptides through controlled hydrolysis processes presents several functional and technological benefits too. These larger peptides retain structural properties that facilitate the formation of gels and emulsions, which are advantageous in food

applications that require texturization, foaming, and stability (Cunha & Pintado, 2022; Wouters *et al*., 2016). Moreover, high molecular weight peptides demonstrate substantial water-holding capacity and offer a more balanced and prolonged nutritional profile, thereby enhancing their potential utility in food products (Ghalamara *et al*., 2024; Wouters *et al*., 2016).

1.3. Peptides and amino acids functionalities

The breakdown of proteins into peptides not only improves digestibility but also generates bioactive molecules with significant health and functional potential. Bioactive and functional properties are the chemical and physical qualities that affect protein behavior in food, influenced by structure, amino acid composition, charge, and interactions (Cunha & Pintado, 2022). Bioactive peptides, typically composed of 3–20 amino acids linked by peptide bonds and with molecular masses below 6000 Da, have been shown to exert antihypertensive, anticoagulant, antioxidant, and anticancer effects, as well as contribute to cardiovascular health maintenance and disease prevention (Etemadian *et al*., 2021). Their antioxidant activity is mainly attributed to free radical scavenging, metal ion chelation, and electron donation. These properties position peptides as promising nutraceutical agents, offering natural alternatives to synthetic drugs and valuable functional ingredients in food formulations (Etemadian *et al*., 2021).

Eventually, the biological activity of both proteins and peptides depends on their amino acid composition. Humans and animals require nine essential amino acids: L-valine (Val), L-leucine (Leu), L-isoleucine (Ile), L-lysine (Lys), L-threonine (Thr), L-methionine (Met), L-histidine (His), L-phenylalanine (Phe), and L-tryptophan (Trp). These amino acids cannot be synthesized endogenously and must be obtained through diet or supplementation. These amino acids, in addition to the non-essential ones analyzed in this work are represented in Table I.1. Meeting these nutritional needs has driven a rapidly growing global amino acid market, with the food sector alone absorbing approximately 50 % of total production (Sari, 2015). Free amino acids, such as glutamic acid, can also function as feeding stimulants and

palatability enhancers (Aspevik *et al*., 2017). Historically, amino acids were extracted from natural sources, but microbial fermentation is now the dominant and most efficient industrial method. Chemical synthesis remains in use for certain amino acids, such as glycine and methionine; however, it often yields racemic mixtures with limited direct food applications (Sari, 2015).

Looking forward, whether for producing protein hydrolysates, bioactive peptides, or free amino acids, sustainable methods that utilize agri-food industry by-products (rather than primary biomass or synthetic chemicals) are emerging as the most promising approaches (Sari, 2015; Tamayo-Tenorio *et al*., 2018). Large amounts of agri-food by-products are discarded annually. Some of them are utilized for bio-gas production, compost or low-value products. From livestock, between 44–49 % of the total weight from slaughterhouses is discarded; from fishery, it raises to an average of a 60 % of the raw material which is discarded: head, bones, skin, fin, trimmings and others (Etemadian *et al*., 2021; Tamayo-Tenorio *et al*., 2018).

In the vegetal food industry, the amount of waste varies depending on the type of processing applied. Regarding protein content, legumes represent the most important group, with soybean being the most cultivated and consumed legume worldwide surpassing the combined production of all other legumes by four times (Soy Nutrition Institute Global, 2025; Tamayo-Tenorio *et al*., 2018). In addition to proteins, numerous other bioactive compounds can be recovered through the valorization of various food by-products, principally from plant biomass, providing additional nutritional and functional benefits.

In summary, proteins, peptides, and amino acids are essential for nutrition and human health. Valorizing protein-rich by-products into hydrolysates allows recovery of bioactive peptides and free amino acids, enhancing nutritional and functional value. This PhD Thesis discourses these challenges by focusing on the valorization of protein from two promising agri-food industry by-products: tuna fish meal (as animal by-product) and okara (soybean residue, as vegetal by-product), aiming to develop sustainable solutions for their effective use.

Table I.1. Chemical structure of the 21 different amino acids measured and quantified in this PhD Thesis, grouped into essential (EAA) and non-essential (NEAA).

AMINO ACIDS			
EAA	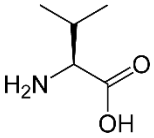 Valine (Val)	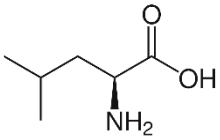 Leucine (Leu)	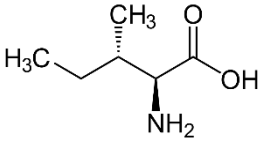 Isoleucine (Ile)
	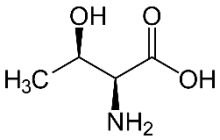 Threonine (Thr)	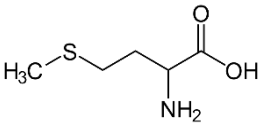 Methionine (Met)	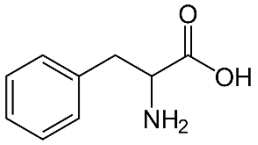 Phenylalanine (Phe)
	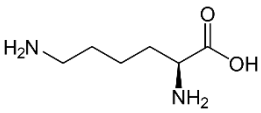 Lysine (Lys)	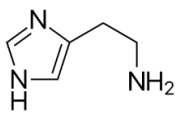 Histidine (His)	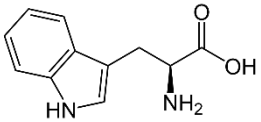 Tryptophan (Trp)
NEAA	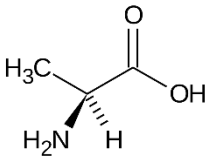 Alanine (Ala)	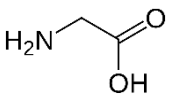 Glycine (Gly)	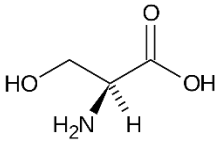 Serine (Ser)
	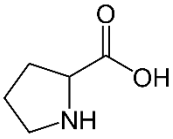 Proline (Pro)	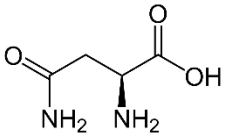 Asparagine (Asn)	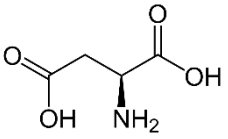 Aspartic acid (Asp)
	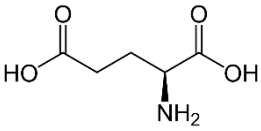 Glutamic acid (Glu)	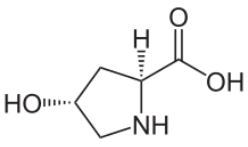 Hydroxyproline (Hyp)	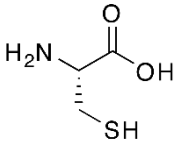 Cysteine (Cys)
	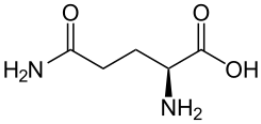 Glutamine (Gln)	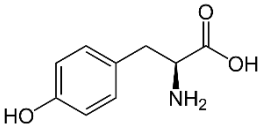 Tyrosine (Tyr)	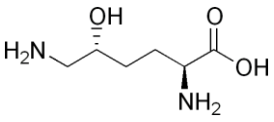 Hydroxylysine (Hyl)

2. Marine animal by-products as protein sources: Tuna fish meal

2.1. By-product generation in industry

Fish meal refers to the product obtained by drying and grinding the solid residues generated during the processing of fish for human consumption. More specifically, this procedure, described by FAO (1986) and represented in Figure I.2, involves heating raw fish residue to coagulate proteins and release oil, followed by pressing to separate liquids from solids. The liquid fraction is decanted and centrifuged obtaining crude fish oil and aqueous fraction, which is further evaporated, and its soluble solids are treated with the solid fraction. The solid fraction and evaporated solids are dried, cooled and grinded, obtaining finally the fish meal. This fish meal consists of fishery side streams, including heads, skins, bones, scales, and viscera, in addition to a large quantity of whole small fish unavoidably harvested together and non-suitable for human consumption (FAO, 2024; Windsor, 1971).

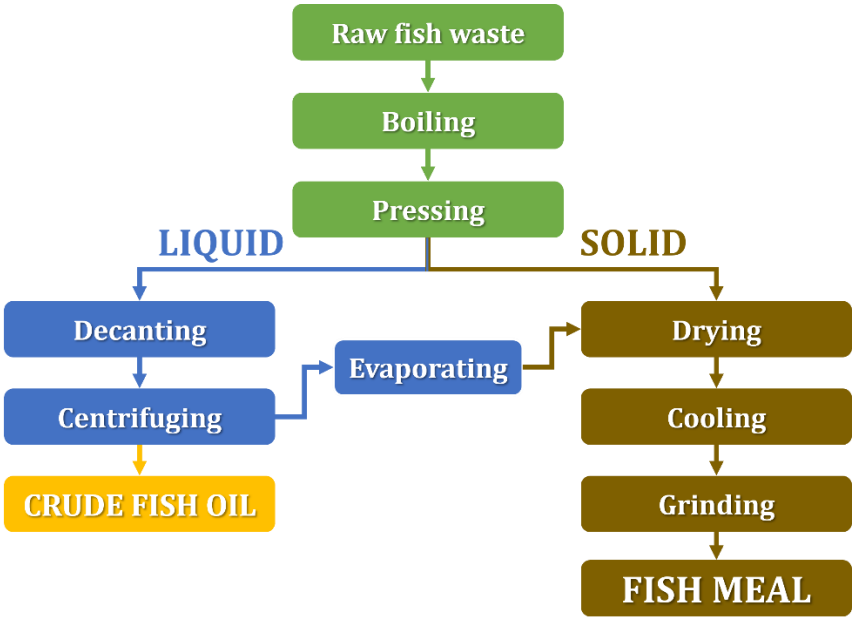

Figure I.2. Flow diagram of the conventional methodology for processing fishery waste into fish meal and fish oil at industrial scale. Adapted from FAO (1986).

In this PhD Thesis, the term fish meal will be restricted to biomass derived exclusively from fishery by-products from the tuna fish (*Thunnus sp.*) industry, which are often discarded or underutilized in animal feed production. These by-products are produced on a large scale and turned into low-value fish meal and fish oil (Shahidi *et al.*, 2019). Tuna fish meal used in this PhD Thesis (shown in Figure I.3) was supplied by *Sarval Bio-Industries Noroeste,* S.A.U. (A Coruña, Spain).

Figure I.3. Tuna fish meal biomass (*Thunnus* sp.) supplied by *Sarval Bio-Industries Noroeste,* S.A.U. (A Coruña, Spain), obtained after the industrial processing of tuna-derived products.

Tuna fish meal composition, reported in the literature (Herdina *et al.*, 2024; Montazeri Shatouri *et al.*, 2025; Zaviezo & Dale, 1994), is presented in Table I.2 to provide an overview of its main nutritional components.

Table I.2. Chemical composition of tuna fish meal based on literature.

Compound, % (w/w) (dry basis)	Zaviezo & Dale (1994)	Herdina *et al.* (2024)	Montazeri Shatouri *et al.* (2025)
Carbohydrates	0.42 – 0.53	–	0.94 ± 0.01
Proteins	55.2 – 56.9	53 – 65	60 ± 7
Lipids	10.8 – 12.7	5 – 11	13 ± 1
Ashes	26.0 – 26.5	13 – 38	23 ± 1

Protein typically accounts for more than half of the fish meal, ranging from 53 to 60 % in these studies, which makes this by-product particularly attractive for valorization. Lipid content is usually around 10 %, whereas the ash content is notably

high, averaging approximately 25 % (with a wide range of 13–38 %). In contrast, the carbohydrate fraction is negligible, generally below 1 %.

2.2. Global production

Fish processing generates between 30 and 70 % by weight of such by-products, depending on species, with an average waste of approximately 60 %. For tuna fish meal, the proportion of discarded side streams ranges from 50 to 70 %. Improving the valorization of these by-products, represents a significant challenge and opportunity for the industry, from ecological, economic, and social perspectives, while contributing to food security and consumer health (FAO, 2024).

Global fish production in 2022 accounted for 184.6 million metric tonnes (Mt), having increased by 3.65 % from 178.1 Mt in 2021. More detailed data of fisheries from the rest of the years from 2002 to 2022 are shown in Figure I.4 (Bryant, 2025), highlighting an increment of 44.4 % in those 20 years period.

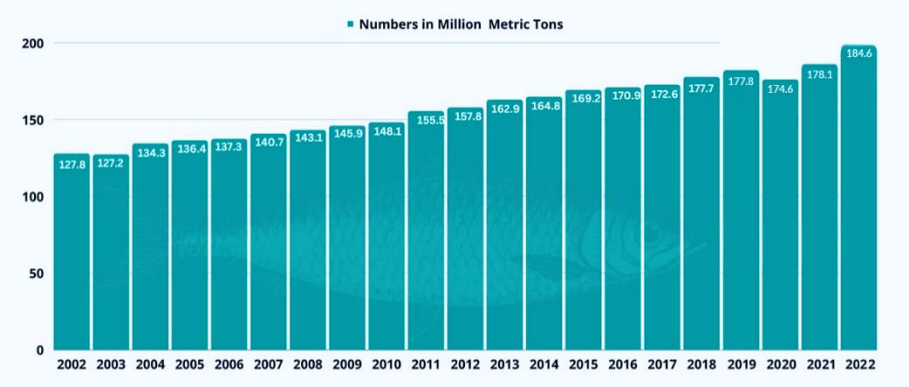

Figure I.4. Volume of global fish production from 2002–2022. Retrieved from Bryant (2025), based on FAO data from 2024.

Figure I.5a represents the global distribution of fish and seafood production in 2022 (latest available data from FAO) represented by country. China stands out as the leading producer, with 64.2 Mt, accounting for 34.8 % of global production, followed at a considerable distance by India (14.4 Mt) and Indonesia (12.7 Mt). Spain, by comparison, produced 1.2 Mt, representing 7 % of the total European

output (16.4 Mt). Figure I.5b illustrates the evolution of global fishery production from 1961 to 2022, including the trends for the three largest producers (China, India and Indonesia), Europe, and Spain (Ritchie & Roser, 2024). The graph highlights the remarkable increase in production by China, as well as by India and Indonesia, while European production only grew until the late 1980s and subsequently declined after the 1990s. Spain, although nearly imperceptible on the global scale, follows a similar trend to Europe, with its historical peak in 1976 at 1.6 Mt, and following decrement from then to now.

Regarding tuna fish species, capture reached a historical global peak in 2018, exceeding 7.9 Mt, largely driven by the Western and Central Pacific, where catches increased from approximately 2.6 Mt in the mid-2000s to more than 3.5 Mt in 2018 (FAO, 2020). Considering that tuna processing typically generates around 60 % waste, this would correspond to more than 4.7 Mt of tuna fish meal potentially produced in 2018, a value that, following tuna fishery trends, has likely continued to rise in subsequent years.

Tuna fish meal holds great potential not only as animal feed but also for human consumption, owing to its substantial protein content, which averages more than 50 % (Table I.2). This high protein level is supported by the inclusion of heads, frames, belly flaps, blood, roe, and liver and other viscera, all contributing to a high-quality amino acid profile. In addition, tuna fish meal is a valuable source of long-chain omega-3 fatty acids, serving as the principal provider of eicosapentaenoic acid (EPA) and docosahexaenoic acid (DHA) in animal diets. It also contains a wide range of vitamins (A, D and B_{12}) and essential minerals such as selenium, zinc, iodine, and iron, which are relevant to human health due to their antioxidant properties and their potential role in reducing the risk of chronic diseases (Etemadian *et al*., 2021; FAO, 2024). Therefore, valorizing tuna fish waste expands its potential applications beyond traditional uses in animal feed, particularly aquaculture, and opens new opportunities in the functional food and nutraceutical sectors.

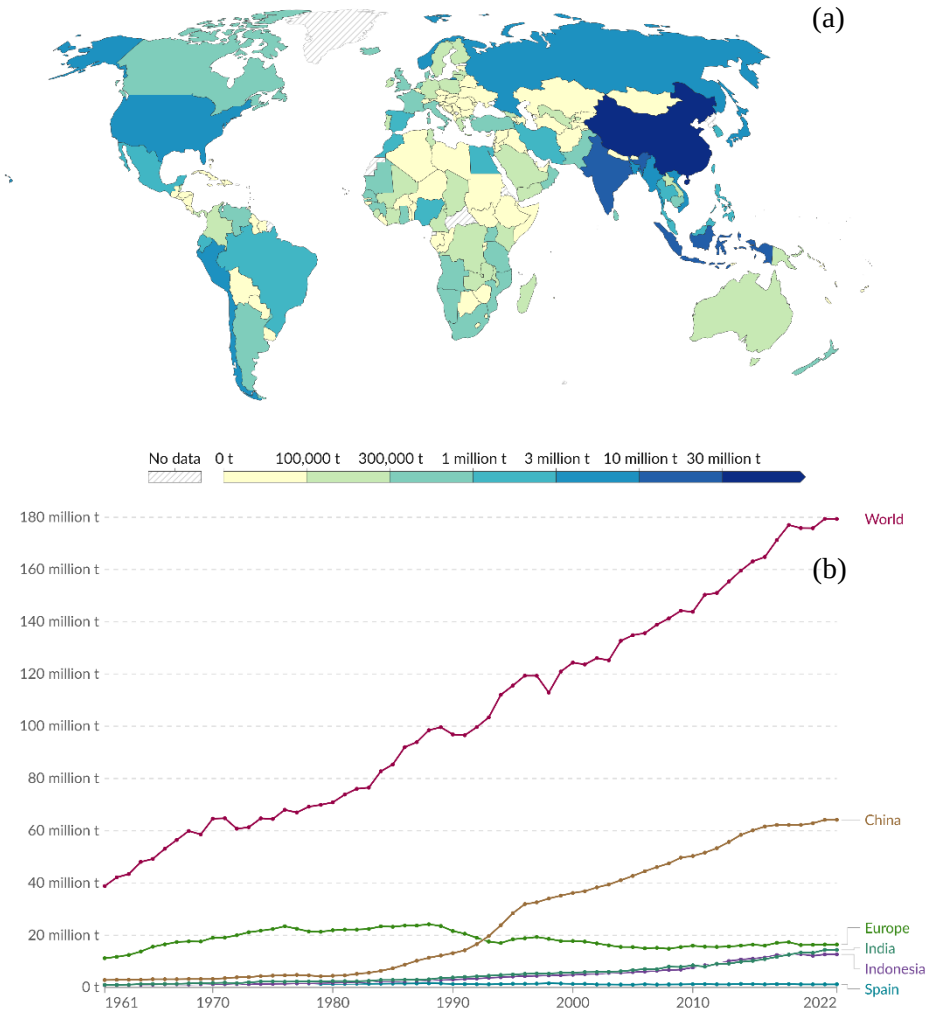

Figure I.5. (a) Fish and seafood production in 2022, distribution by countries. **(b)** Fish and seafood production globally, in the most producing countries, in Europe and in Spain, 1961–2022. Both retrieved from Ritchie & Roser (2024), based on FAO data from 2024.

According to the FAO (2024), fish meal plays a crucial role in animal nutrition, especially in aquaculture and livestock production, owing to its high protein content and well-balanced nutrient profile. Notably, 65.5 % of fish meal is produced from whole fish, not suitable for direct human consumption, while the remaining 34.5 % is originated from fish industrial processing by-products (most used in fish oil production). Fish meal is mainly utilized in aquaculture, accounting for 87 % of global fish meal use, followed by pig farming (7 %) and other applications (4 %)

(FAO, 2024). The discard of nutrient-rich by-products as these, without valorizing them, not only contributes to environmental problems but also represents the loss of valuable compounds with functional and bioactive potential (Etemadian *et al*., 2021).

2.3. Protein hydrolysates from fish meal

Tuna fish meal valorized through sustainable methodologies, particularly protein hydrolysis, can yield protein hydrolysates with diverse applications. These hydrolysates represent a valuable source of bioactive peptides with potential uses in nutraceutical, pharmaceutical, and feed industries. One of the key factors in producing protein hydrolysates with targeted bioactive and functional properties lies in their suitability for developing health-promoting materials. Fish protein hydrolysates, which remain stable across a wide pH range and at high temperatures, are known to improve water retention, texture, gelling, foaming, and emulsifying properties in food systems. Importantly, the degree of hydrolysis plays a crucial role: limited hydrolysis, generating larger peptides, tends to enhance techno-functional properties such as foaming and emulsification, whereas extensive hydrolysis may reduce these properties but can increase health-related bioactivities (Etemadian *et al*., 2021; Shahidi *et al*., 2019).

2.3.1. Bioactive properties

According to Shahidi *et al*. (2019), fish protein hydrolysates can generate peptide fractions with a wide range of biological activities. Antioxidant peptides derived from fish commonly have molecular weights between 0.5 and 4.5 kDa, with activity influenced by peptide size, sequence, and amino acid composition. When hydrolysis is more extensive, the resulting shorter peptides often display stronger antioxidant activity, primarily through their ability to donate electrons, scavenge reactive oxygen species, and chelate pro-oxidant metal ions. Specific sequences, such as those rich in glycine and proline have been shown more lipid oxidation inhibition and radical scavenging capacity (Shahidi *et al*., 2019).

Besides its high antioxidant activity, protein hydrolysates derived from tuna by-products that contain low-molecular-weight peptides, particularly those < 1 kDa, also exhibit antibacterial and antiproliferative effects against human breast carcinoma cells as described by Etemadian *et al*. (2021).

Beyond these specific effects, bioactive peptides from fish protein hydrolysates (FPH) have also exhibited: anti-inflammatory, antithrombotic, immunomodulatory, antimicrobial, anticancer, and antihypertensive activities, as well as the ability to promote calcium absorption. Some have been explored as nutritional supplements, showing potential benefits such as reducing anxiety and improving memory. Their recovery from fish processing by-products not only allows the development of protein-enriched and oxidatively stable food products but also contributes to the valorization of underutilized marine resources. (Cunha & Pintado, 2022; Hao *et al*., 2019; Shahidi *et al*., 2019).

2.3.2. Techno-functional properties

In addition to their bioactivity, fish meal protein hydrolysates are interesting due to their great physicochemical and techno-functional properties. Functional properties of fish or fish meal protein hydrolysates are largely determined by peptide size distribution, amino acid composition, hydrophilic–hydrophobic balance, pH, and processing variables such as the choice of enzyme, substrate, and degree of hydrolysis (Cunha & Pintado, 2022; Halim *et al*., 2016; Villamil *et al*., 2017).

Solubility is considered one of the most relevant parameters, as it directly influences emulsifying and foaming performance. Fish protein hydrolysates generally exhibit high solubility over a wide pH range and good heat stability as mentioned before, with higher degree of hydrolysis increasing solubility through the production of smaller, more polar peptides, although solubility tends to be lowest near the isoelectric point (Cunha & Pintado, 2022; Halim *et al*., 2016; Villamil *et al*., 2017).

Emulsifying and foaming capacities depend not only on solubility but also on peptide size, sequence, and pH. Moderate hydrolysis values, producing medium-sized peptides, often lead to improved interfacial activity and stability, whereas excessive hydrolysis yields very small peptides with reduced emulsifying and foaming performance (but commonly outperforming in bioactivity). Operating at pH values distant from the isoelectric point tends to enhance these properties (Atef & Mahdi Ojagh, 2017; Cunha & Pintado, 2022). In the case of collagen-rich hydrolysates derived from fish skin, the abundance of hydrophobic amino acids such as glycine, proline, and hydroxyproline contributes to high emulsifying capacity, while also providing bioactive potential (Atef & Mahdi Ojagh, 2017).

Water-holding capacity is an important functional attribute for maintaining texture and juiciness in processed products; however, excessive peptide breakdown during hydrolysis can reduce it. Conversely, certain low-molecular-weight fractions may enhance this property due to increased hydrophilicity. Fat-binding capacity is influenced by molecular size, density, degree of hydrolysis and hydrophobicity, making it valuable for applications in meat formulations and confectionery products (Cunha & Pintado, 2022; Halim *et al*., 2016; Villamil *et al*., 2017).

The molecular weight profile of peptides, as already mentioned above, is a central determinant of functionality: smaller peptides generally favor solubility and bioactivity, including antioxidant potential, while larger and more amphiphilic peptides contribute to the formation of stable interfacial films, improving emulsion and foam stability. Hydrolysis also increases peptide polarity by exposing amino and carboxyl groups and alters secondary structure, which further affects functional performance (Cunha & Pintado, 2022; Halim *et al*., 2016; Shahidi *et al*., 2019; Villamil *et al*., 2017).

These combined properties support the use of fish by-product protein hydrolysates as emulsifiers and stabilizers in sauces, dressings, and triturated meat products, as water-holding capacity enhancers in surimi, patties and fillets, and as fat-binding agents to modify sensory attributes in meat and confectionery. They are

also a source of bioactive peptides with potential health benefits and, in the case of collagen or gelatin hydrolysates, functional ingredients for texture improvement, edible coatings, and encapsulation systems (Atef & Mahdi Ojagh, 2017; Shahidi *et al*., 2019).

Similarly, in addition to fishery by-products, other side streams from the food industry have gained attention as potential raw materials for the production of high-value ingredients. An illustrative example is soybean pulp, or okara, which is presented in the following section.

3. Vegetal by-products as protein sources: Okara from soybean

3.1. By-product generation in industry

Okara, or soy pulp, is the soybean (*Glycine max*) by-product generated in the filtering stage during the production of soy-based beverages and soybean derivatives, principally tofu. These foods have been fundamental to East Asian diets for the last 2000 years, and have been attributed nutritional benefits, including potentially preventing malnutrition and reducing heart disease risk, in addition to be supported as a great and healthy source of quality protein (Chang & Liu, 2012).

Soymilk and tofu production (represented in Figure I.6) starts by dehulling, cleaning and blanching soybeans to rehydrate them for 8–16 hours depending on temperature and bean type. Blanching or steaming, is necessary on the slurry or soymilk for inactivation of microorganisms and trypsin inhibitors. Temperature affects flavor of soymilk by inactivating lipoxygenase enzymes that cause beany flavor, and in case of tofu, it affects its future firmness, as it denatures proteins for better coagulation, impacting protein curd formation and reducing as well off-flavors. This is followed by grinding and subsequent centrifugation and filtration (Chang & Liu, 2012).

As indicated in Figure I.6, okara is generated in the filtering stage, as the solid residue left after filtering or pressing the slurry (Chang & Liu, 2012).

Once soymilk and okara are separated, the soymilk can be further processed to produce tofu. Tofu yield and characteristics depend on factors such as the coagulation method, soymilk °Brix and pH, and processing conditions (temperature, pH, and stirring). Coagulation (that occurs between 68–95 °C) and choice of coagulant (salts, glucono-delta-lactone, or acids) determine tofu texture and flavor (Chang & Liu, 2012).

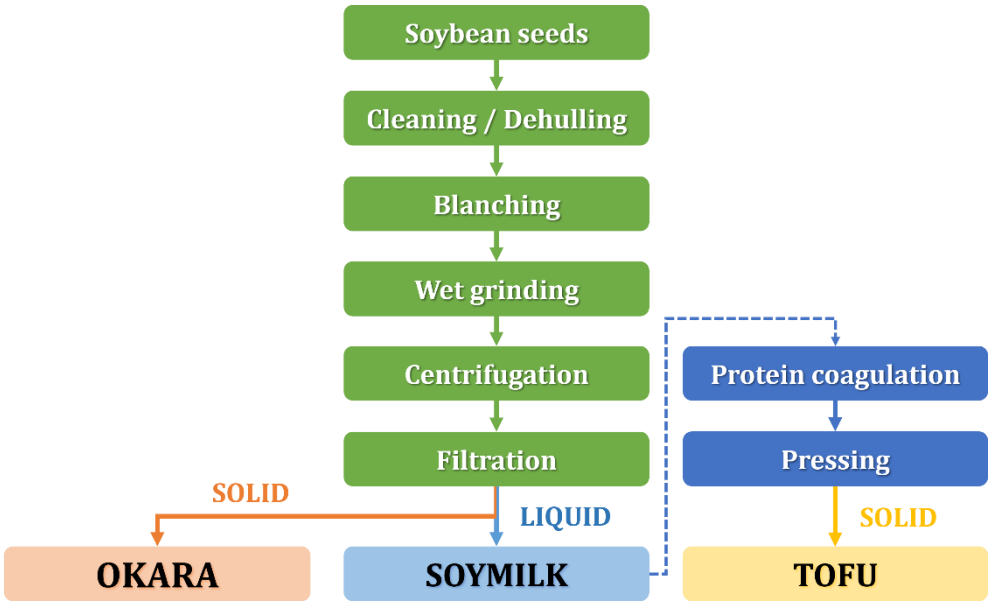

Figure I.6. Flow diagram of the generation of okara in the processing of soybean seeds into soymilk and tofu at industrial scale. Adapted from Chang & Liu (2012) and Eze (2019).

In the production of either soymilk or tofu, substantial quantities of okara are generated. Specifically, for every 1 kg of dry soybeans utilized in these processes, approximately 1.1 kg of wet okara is produced (Mok *et al*., 2019). From the same 1 kg of dry soybeans is possible to produce approximately 8 L of soymilk, as reported by Jain (2015), and with each 1 L of soymilk, it can be produced approximately 0.2 kg of tofu, as studied by Rekha & Vijayalakshmi (2013).

Consequently, 1 kg of soybeans can be employed to produce either 8 L of soymilk or 1.6 kg of tofu, with approximately 1.1 kg of okara being generated in each process. In other words, the production of 1 L of soymilk results in 0.14 kg of okara, while the production of 1 kg of tofu generates 0.69 kg of okara. These values are an estimation, as stated by Chang & Liu (2012), the quantity and characteristics of the generated okara depend on grinding and separation methods and significantly affect the yield and quality of soymilk and tofu. Okara used in this PhD Thesis (shown in Figure I.7) was provided by *Frías Nutrición* S.A.U. (Burgos, Spain).

Figure I.7. Okara from soybean (*Glycine max*) supplied by *Frías Nutrición* S.A.U. (Burgos, Spain), generated as a by-product during the industrial production of soymilk and tofu. **(a)** Frozen. **(b)** Defrosted. **(c)** Divided into small bags.

Okara composition, reported in the literature (Asghar *et al*., 2023; B. Li *et al*., 2012; O'Toole, 1999; Vong & Liu, 2016), is presented in Table I.3 to provide an overview of its main nutritional components. Okara normally presents more than 80 % of moisture when produced in industry. Its composition is characterized by its high protein content for a vegetal by-product, ranging from 25.4 to 28.4 % in dry mass according to O'Toole (1999), with a great amino acid profile; which is lower than in fish meal but still represents a high value for a plant-based by-product. Polysaccharides are the most abundant biocompounds in okara, accounting for 40–60 % when including insoluble lignin fractions. The lipid content, with beneficial fatty acids, is generally comparable to or below 10 %, while the ash content usually remains low, around 4 %, although some studies have reported abnormally high ash values. Remarkably, okara also contains B-group vitamins, essential minerals, and bioactive compounds such as the highlighted isoflavones (Mok *et al*., 2019).

Table I.3. Chemical composition of okara from soybean based on literature.

Compound, % (w/w) dry basis	O'Toole (1999)	Li *et al*. (2012) and Vong & Liu (2016)	Asghar *et al*. (2023)
Polysaccharides	40.2 – 43.6	42.4 – 58.1	46.73 ± 0.23
Lignin	*11.7 ± 1.4*	–	–
Proteins	25.4 – 28.4	15.2 – 33.4	15.86 ± 0.24
Lipids	9.3 – 10.9	8.3 – 10.9	7.54 ± 0.08
Ash	3.0 – 3.7	3.0 – 4.5	10.85 ± 0.15

3.2. Global production

Soybean is the most cultivated and consumed legume in the world. Soybean production is estimated to reach 423 million tonnes (Mt) in the present year 2025, this corresponds to a growth of approximately 6 % each year since 2023 (last available data) when 378 Mt of soybean were produced. Previous statistics also show a steady growing rate of around 5 % each year (FAO, 2025a, 2025b). However, not all soybean production is destined to human food. Between 2017 and 2019, around 7 % of total soybean produced was utilized for human direct consumption, not considering soy oils which can have different purposes. From all the soybean produced in the world, 2.6 % was processed into tofu and 2.1 % into soymilk (Ritchie, 2024).

In Figure I.8a (Ritchie *et al*., 2025), the global distribution of soybean production in 2023 is shown by country, based on data from FAO 2025. Brazil was the leading producer, with 152.1 Mt, followed by the United States with 113.3 Mt. Together, these two countries accounted for approximately 70 % of global soybean production in 2023. At a considerable distance, Argentina (25.0 Mt), China (19.5 Mt), and India (15.0 Mt) followed. In contrast, Spain produced only 7 kt, representing less than 0.05 % of the total European output (14.9 Mt) (Ritchie *et al*., 2025).

Figure I.8b (Ritchie *et al*., 2025), illustrates the evolution of global soybean production from 1961 to 2023, including the trends for the two leading producers

(Brazil and the United States), Europe, and Spain. In the case of this crop, none of the greatest producing regions show a clear decline from 1961 to 2023 at any point; Spain, as an exception, reached its historical peak in 1990 with 42.2 kt, but current production represents only 16.6 % of that value. Among all of them, Brazil demonstrates the sharpest growth, and projections, as previously noted, indicate that global soybean production will continue to increase in the coming years (Ritchie *et al*., 2025).

Based on historical percentages of tofu and soymilk production and projections of total soybean production for 2025, it is estimated that in the current year 2025, 19.9 Mt of soybean are going to be utilized for the production of tofu and soymilk, resulting in the generation of 21.9 Mt of okara. The most recent data on global okara production, reported by Mok *et al*. (2019), indicate an annual production of approximately 14 Mt. Therefore, the updated estimate of 21.9 Mt would represent a 56 % increase. Mok *et al*. (2019) were based on earlier studies assessing soy beverage consumption published in 2013 (Nguyen *et al*., 2013). Between 2013 and 2025, global soybean production has risen by more than 50 % (an increase of 52 %, from 278 Mt to 423 Mt (*Soybean Production (FAO)*, 2025)). This growth supports the higher okara production estimate (21.9 Mt) proposed for 2025 in this PhD thesis.

This great quantity of okara generated annually represents a by-product with high nutritional value and considerable potential for valorization. However, frequently is discarded due to its high moisture content, which makes it susceptible to rapid spoilage. The drying process required to stabilize okara is energy-intensive because of its large water content, and economic analyses have shown that the associated costs often exceed the market value of its useful compounds (Vong & Liu, 2016).

In the context of valorizing by-products such as okara, it is important to recognize that not only the flavonoids or the protein fraction hold value. The carbohydrate-rich residual solid obtained after protein or isoflavone recovery can be effectively repurposed in downstream processes, for instance through fermentation

to produce organic acids such as lactic acid. This integrated approach promotes a more comprehensive valorization of carbohydrate-rich plant by-products, ensuring that their composition is fully exploited rather than partially utilized and partly discarded.

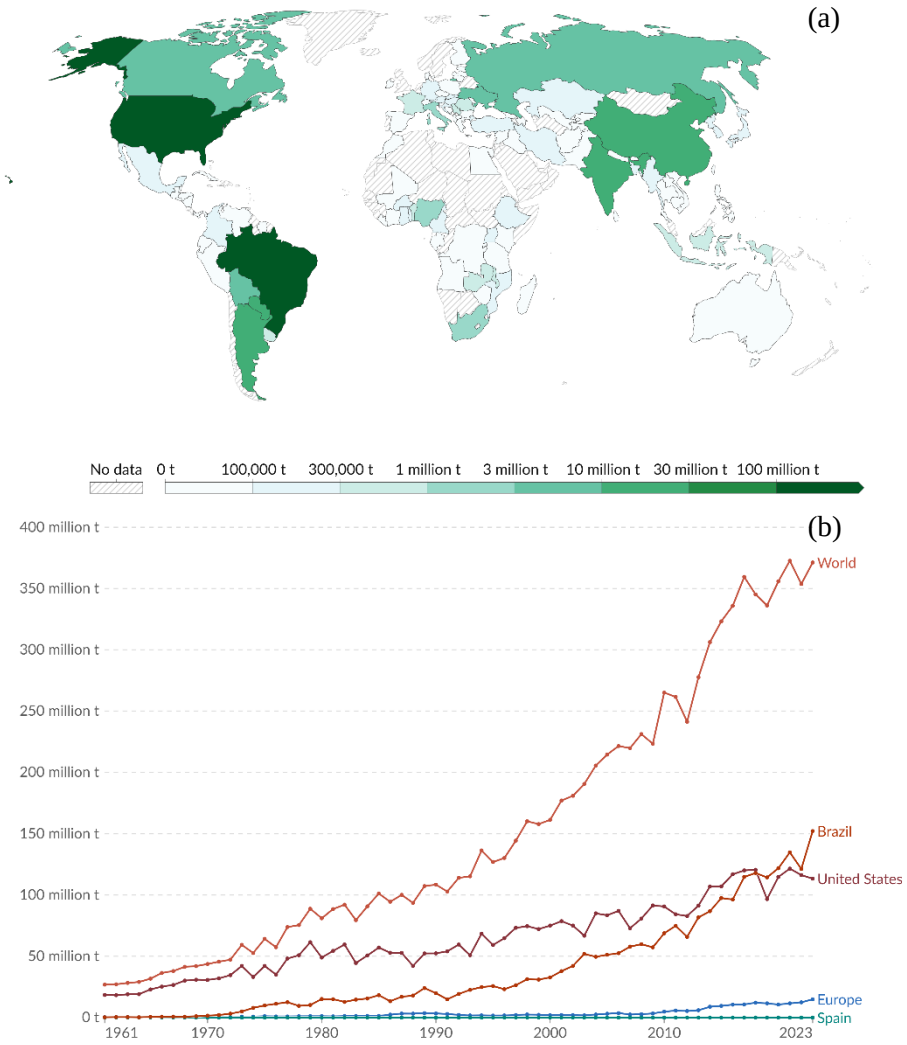

Figure I.8. (a) Soybean production in 2023, distribution by countries. **(b)** Soybean production globally, in the most producing countries, in Europe and in Spain, 1961–2023. Both retrieved from Ritchie *et al*. (2025), based on FAO data from 2025.

3.3. Protein hydrolysates from okara

3.3.1. Bioactive properties

Protein hydrolysates from soybean sources have demonstrated bioactive activities. Peptides from these extractions presented several functions as antiviral, antihypertensive, antioxidant, anticancer, mineral-binding, antidiabetic and antithrombotic activities (Marcet *et al*., 2016; Yuan *et al*., 2022). Freitas *et al*. (2019) revealed that some peptide fractions, especially those < 10 kDa (having identified some specifically), exhibit wide spectrum antimicrobial activity against Gram-positive and Gram-negative bacteria and selective cytotoxicity against glioblastoma cells, while remaining non-toxic to healthy mammalian cells (tested in mice). These encrypted peptides, originally latent within soybean proteins and released upon hydrolysis, highlight soybean by-products as promising sources of novel functional ingredients and therapeutic agents (Freitas *et al*., 2019).

The amino acid profile of okara also makes the complete hydrolysis of its peptides into monomers particularly attractive. Colletti *et al*. (2020) reported that okara proteins contain all nine essential amino acids, with especially high levels of leucine, isoleucine, and valine, which are key for muscle synthesis and overall health. In addition, the protein efficiency ratio of okara (an indicator of nutritional quality based on weight gain relative to protein intake) was found to be even higher than that of soymilk and tofu (Colletti *et al*., 2020; Ningrum *et al*., 2025). Furthermore, glutamic acid (the most abundant amino acid in okara), although non-essential, plays key roles in protein metabolism, nitrogen balance, and neurotransmitter synthesis. In industry it is also used as a flavor enhancer and precursor for biopolymers.

Although protein valorization is the main focus of this PhD Thesis, the noteworthy presence of isoflavones in okara and their recognized bioactivity make them worth to be addressed, especially given their potential contribution to the overall valorization of this by-product.

3.4. Isoflavones from okara

3.4.1. Isoflavone categories

Isoflavones are a subclass of flavonoids with an estrogen-like structure, commonly referred to as phytoestrogens, that confer both functional properties and health benefits. Soybeans are the most important natural source of isoflavones, from which twelve individual compounds have been identified. These are commonly grouped into four categories, see Table I.4: aglycones (genistein [GE], daidzein [DE], and glycitein [GYE]); β-glycosides (genistin [G], daidzin [D], and glycitin [GY]); acetyl-glycosides (acetyl-genistin [AG], acetyl-daidzin [AD], and acetyl-glycitin [AGY]); and malonyl-glycosides (malonyl-genistin [MG], malonyl-daidzin [MD], and malonyl-glycitin [MGY]) (Jankowiak *et al*., 2014).

Food processing and gastrointestinal metabolism strongly influence their chemical profile and bioavailability. Thermal treatments convert rapidly malonyl-glycosides into β-glycosides, soaking can activate endogenous β-glycosidases that release aglycones, and microbial fermentation further enhances aglycone levels. In humans, isoflavone glycosides are hydrolyzed in the gastrointestinal tract releasing aglycones that are more rapidly absorbed and further transformed in the liver resulting in several metabolites. In addition, intestinal microbiota can produce equol from daidzein, a metabolite with even higher estrogenic activity (Hsiao *et al*., 2020; Jankowiak *et al*., 2014).

In relation to their bioavailability, aglycones are absorbed more rapidly and efficiently than β-glycosides, which are less permeable to the intestinal epithelium. Malonyl and acetyl forms, despite being the most polar ones, are the least bioavailable; in any case, both are the ones that are most easily degraded, losing those groups and producing β-glycosides. Once ingested, isoflavones undergo digestion, absorption, hepatic metabolism, and enterohepatic circulation, circulating mainly as other types of conjugated metabolites. Bioavailability further depends on

gut microbiota activity, diet, age, and gender, with strategies such as encapsulation or microbiota modulation proposed to improve it (Hsiao *et al*., 2020).

Table I.4. Chemical structures of the 12 isoflavones, arranged in three columns according to their groups and in four rows according to their radicals.

	Genistin group	Daidzin group	Glycitin group
Aglycones	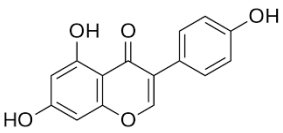 Genistein (GE)	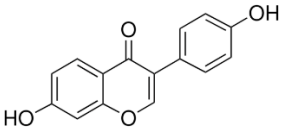 Daidzein (DE)	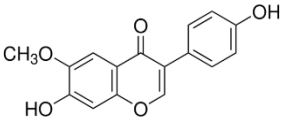 Glycitein (GYE)
β-glycosides	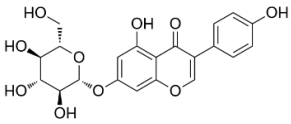 Genistin (G)	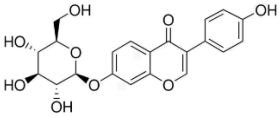 Daidzin (D)	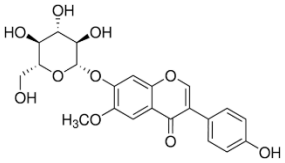 Glycitin (GY)
Acetyl-glycosides	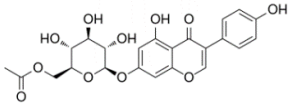 Acetyl-genistin (AG)	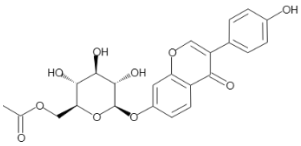 Acetyl-daidzin (AD)	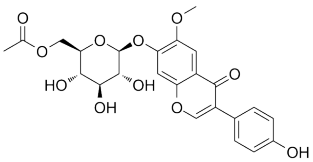 Acetyl-glycitin (AGY)
Malonyl-glycosides	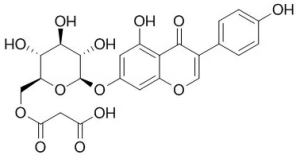 Malonyl-genistin (MG)	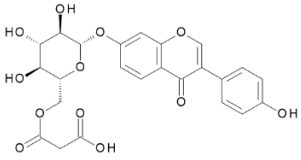 Malonyl-daidzin (MD)	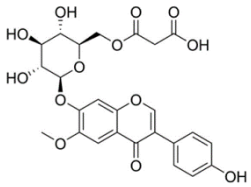 Malonyl-glycitin (MGY)

3.4.2. Bioactive properties

Their health benefits when they are present in blood plasma have been associated with anti-inflammatory effects, protection against colon cancer, anti-obesity properties, diabetes management, prevention of osteoporosis, enhancement of bone health, and support for gut microbiota. Isoflavone aglycones (non-sugar part of a glycoside, representing the bioactive form), such as genistein and daidzein (majoritarian ones), and their metabolites, including equol, are mainly responsible for these effects due to their higher bioavailability compared with glycosides. These effects are particularly relevant during periods of senescence and perimenopause, where the structural similarity of isoflavones to estrogens may provide therapeutic advantages (Hsiao *et al*., 2020).

The characteristics of okara hydrolysates strongly depend on the extraction methodology. When valorizing food residues also the sustainability of the method keeps being important, avoid generating additional environmental or health concerns during the process. In this work, we focus on subcritical water hydrolysis, a novel and green technology that uses only water as a solvent. While focusing on this methodology, several other emerging methods will also be applied to compare results and identify the most optimal strategy for each valorization process.

4. Subcritical water hydrolysis as green and sustainable technology

Subcritical water extraction and hydrolysis is a novel technology based on the use of only water as solvent, summited to high temperatures and pressures. It is a great alternative to traditional or chemical-based methodologies for biomass hydrolysis, due to its low cost and sustainability. Thanks to its unique properties, it has been recently used for extracting and break-down protein, as well as other high-value biocompounds, such as lignocellulosic materials or phenolic compounds.

Subcritical water (subW) refers to liquid water pressurized and heated in temperatures over 100 °C, maintaining it above its atmospherically boiling point but pressurized to maintain the liquid state and always below 374 °C and 22.1 MPa which is the critical point, see Figure I.9.

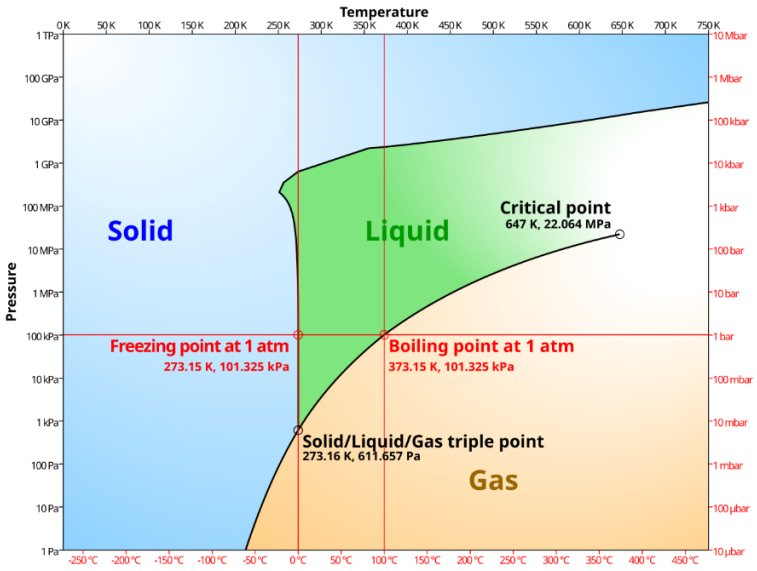

Figure I.9. Water phase diagram. Adapted from Plaza & Turner (2015).

Surpassing these critical values will be considered supercritical water, presenting very different fluid characteristics and not being a good option for extraction of biomolecules due to the harsh conditions. In the literature, subW can be also referred to as pressurized hot water (PHW), liquid hot water (LHW), hot compressed water (HCW) or similar variants; some of them can be related to specific pressure and temperature ranges (Alonso, 2018; Plaza & Turner, 2015).

4.1. Properties of subcritical water

Water is considered the most environmentally friendly solvent for biocompounds extraction; however, under standard conditions, it cannot extract a wide range of substances from biomass. In subcritical conditions, where water is maintained in a liquid state above its boiling point through pressurization, its

chemical and physical properties are altered, making subW a promising strategy for advancing sustainability in biorefinery applications, replacing traditional extraction methods, reducing chemical usage, and promoting the use of green solvents.

The dielectric constant (ε) of water, approximately ε = 80 at 20 °C, decreases significantly within the subcritical range from 100 to 374 °C. For instance, ε = 55 at 100 °C and 0.1 MPa, ε = 35 at 200 °C, ε = 24 at approximately 250 °C and 17 MPa, and ε = 14 at 350 °C and 17 MPa; acquiring values similar to some organic solvents such as methanol (ε = 32.6), ethanol (ε = 24.3), or acetone (ε = 20.7) (Park *et al*., 2019; Plaza & Turner, 2015). This temperature-adjustable polarity makes subW an excellent solvent for both polar and non-polar compounds, facilitating the selective extraction of hydrophobic organic compounds with yields and speeds comparable to conventional organic-solvent techniques, while avoiding the drawbacks of toxicity and solvent recovery. However, as noted by Carr *et al*. (2011), as the temperature increases and non-polar solubility is enhanced, the solubility of polar compounds diminishes. Figure I.10 shows an example of the most characteristic properties (dielectric constant, ionic product and density) of subcritical water at 25 MPa.

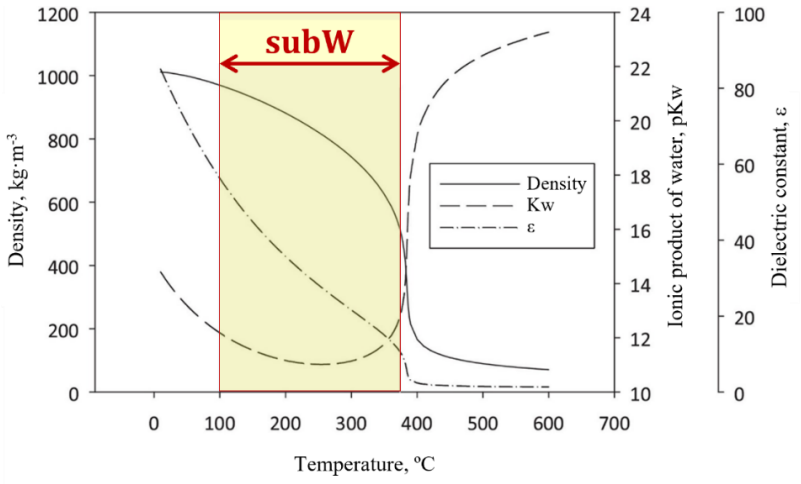

Figure I.10. Properties (density, ionic product and dielectric constant) of subcritical water at 25 MPa (yellow region) as a function of temperature. Adapted from Cocero *et al*. (2018).

The solvent properties discussed surge from alterations in the hydrogen-bonding network of water. In subW, solubility of organic compounds is determined by a balance between cavity formation, which is a positive factor for solubility, and the structuring into cages around solutes, which is a negative factor. At moderate temperatures, this balance leads to low solubility; however, above 160 °C, cavity formation becomes predominant, resulting in a marked increase in the solubility of hydrophobic compounds (the intended effect of this method). Pressure within the typical subcritical range (2–10 MPa) exerts minimal influence, although extreme pressures may modify solubility patterns (Carr *et al*., 2011).

At elevated temperatures, hydrogen bonds weaken, and both viscosity and surface tension are significantly reduced, improving matrix wetting and enhancing extraction. Additionally, diffusion rates and concentrations of H_3O^+ and OH^- increase, facilitating acid and basic hydrolysis of biomass without the need for external acid or base catalysts (Plaza & Turner, 2015; Trigueros, Sanz, *et al*., 2021). Viscosity, self-diffusivity and surface tension changes with temperature (at saturation pressure, not actually subcritical) are represented in Figure I.11.

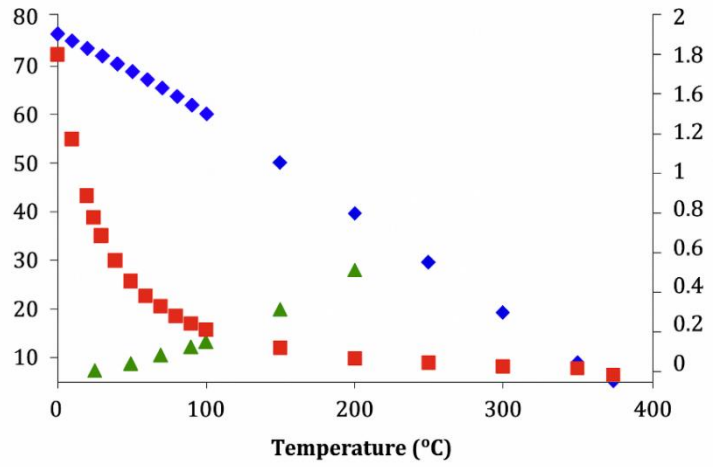

Figure I.11. Viscosity (mPa·s, ■, right axe), self-diffusivity (10^{-9} m^2/s, ▲, left axe) and surface tension (mN/m, ♦, left axe) of liquid water, as a function of temperature, at saturation pressure. Figure from Plaza & Turner (2015).

It is also pertinent to consider some energetic and operational considerations, as heating liquid water (e.g., from 25 °C to 250 °C at a constant ~5 MPa) requires approximately one-third of the energy needed for evaporating water to steam under atmospheric pressure. Furthermore, water's self-ionization constant (Kw) increases by two orders of magnitude from 25 °C to 350 °C (from 10^{-14} to 10^{-12}), reaching its maximum at 250 °C ($4.9 \cdot 10^{-12}$). This increase in acidity results in a decrease in pH from 7 to 5.5 at approximately 250 °C, further facilitating the catalytic hydrolysis of labile biomolecules (Plaza & Turner, 2015). Changes of pH with temperature (at 25 MPa of pressure) are represented in Figure I.12.

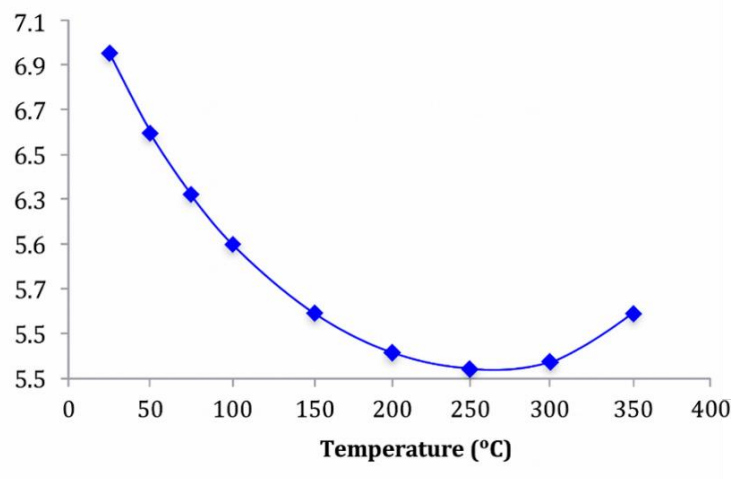

Figure I.12. pH values (♦), as a function of temperature, at 25 MPa. Figure from Plaza & Turner (2015).

In summary, subcritical water represents a powerful, environmentally friendly, and adaptable solvent. It is versatile across polarity ranges, reactive due to enhanced ion content, and efficient from both mass transfer and energy perspectives, without resorting to toxic solvents or excessive energy expenditure. It offers specific advantages for valorizing food industry residual biomass, whether animal-based like fish meal or plant-based like okara, particularly for the selective extraction or hydrolysis of components such as proteins, carbohydrates, or phenolics (e.g., isoflavones, which require minimal treatment to avoid degradation). This makes

subcritical water a compelling core methodology in sustainability-oriented residue valorization research.

The pressurizing agent can also influence the extraction process. Inert gases such as N_2 merely pressurize the system without affecting the reaction, whereas non-inert gases like CO_2 can alter the extraction behavior, as is discussed in Chapter 1. When CO_2 is used as the pressurizing gas, it dissolves in water and acidifies the medium, thereby lowering the pH. This acidification can enhance the hydrolysis of certain compounds in the biomass, acting as a catalyst that commonly strengthens the performance of subcritical water (Domenico Ziero *et al.*, 2020).

4.2 Subcritical water system configurations

Subcritical water hydrolysis (SWH) can be carried out in three different operational modes as it is represented in Figure I.13. The major difference between batch and the other two is that the treatment time for the solid biomass and the solvent (water) in batch (static) mode is the same, as they are both inside a reactor from the start to the end of the process. In case of continuous and semi-continuous configurations, the residence time (τ) for the liquid in the reactor is determined by the volume of the reactor and the flow rate. In semi-continuous (static-dynamic) configuration the biomass remains as a solid the whole process in the reactor, while the solvent is continuously pumped through it, and in continuous (dynamic) both the biomass (liquid) and the solvent are continuously pumping through the system, being in this case the τ of the biomass also variable.

In this PhD Thesis, batch configuration will be principally studied, and in Chapter 5 also semi-continuous. Both configurations are represented in more detail in the following subsections.

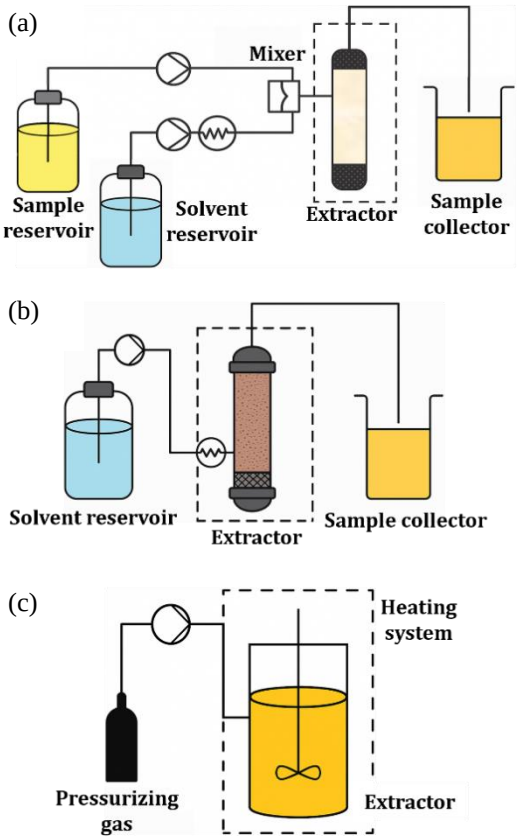

Figure I.13. Different operational modes (simplified) of subcritical water extraction systems. **(a)** continuous (dynamic), **(b)** semicontinuous (static-dynamic), **(c)** batch mode (static). Adapted from Alonso-Riaño (2022).

The performance of SWH under both operating conditions can be evaluated using the "severity factor". Severity factor is a dimensionless parameter that combines temperature and residence time to quantify hydrothermal treatment intensity, which is useful to compare the intensity of two treatments performed with the same or different equipment. The severity factor was calculated as $\log(R_0)$, where R_0 is defined by Eq. I.1. In this equation, t is the residence time (min) and T the temperature (°C). The constant 14.75 corresponds to the activation energy of glycosidic bond cleavage under first-order kinetics, and as the reference temperature (T_{ref}) is taken 100 °C (Illera *et al.*, 2025).

$$\text{Severity factor} = \log(R_0); \quad R_0 = t \cdot \exp\left(\frac{T - T_{ref}}{14.75}\right) \qquad \textbf{[I.1]}$$

Batch SWH configuration is the main system configuration used in this work. Figure I.14 represents the equipment used in these experiments, a laboratory-built reactor system with an internal volume of 0.5 L. The reactor was externally heated using a ceramic heating jacket, monitoring its internal temperature and pressure with a sensor and a manometer, respectively.

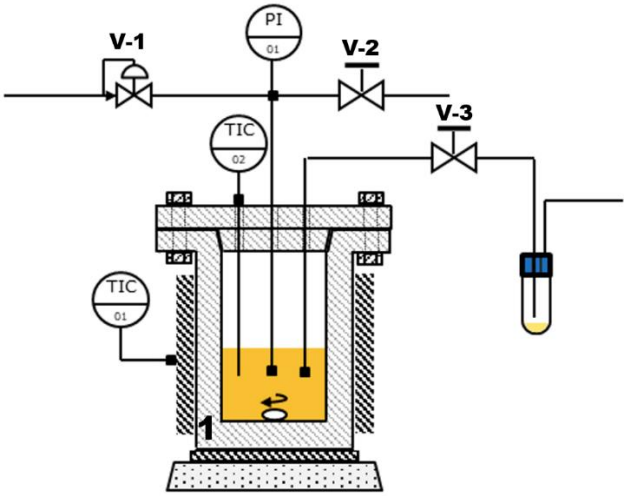

Figure I.14. Batch subcritical water extraction system configuration. 1: Steel reactor; V-1: pressurizing gas inlet; V-2: pressure purge valve; V-3: sampling valve; TIC-01: external temperature control; TIC-02: extraction temperature control; PI-01: internal pressure gauge.

This batch configuration hydrolyzes progressively the solutes, until extraction equilibrium is reached under the established conditions. The main advantage of this static configuration is that the entire process occurs in a fixed volume of water, avoiding analyte dilution, which is a disadvantage in any dynamic operational mode. However, the long residence time of the sample in contact with hot water can promote decomposition reactions, especially at high temperatures (Alonso-Riaño, 2022).

Semi-continuous SWH configuration allows constant equilibrium because fresh water is continuously supplied. This promotes mass transfer making the process faster than the discontinuous mode. Nevertheless, these modes typically

require larger volumes of water, resulting in high dilution of the target compounds. A key advantage is that the solubilized compounds are promptly removed from the reactor, reducing their exposure to high temperatures and consequently minimizing thermal degradation (Alonso-Riaño, 2022).

The semi-continuous SWH mode employed in this PhD Thesis represents a significant scale-up compared to the batch system, accommodating larger treatment volumes while operating at higher temperatures and pressures. This capability is particularly advantageous for processing okara, which contains a high concentration of complex carbohydrates and lignin that require more intense conditions than proteins for efficient breakdown. The design of this configuration, illustrated in Figure I.15, incorporates multiple sample baskets to promote uniform biomass distribution throughout the reactor, preventing agglomeration and ensuring consistent exposure to the treatment conditions. Furthermore, this versatile setup allows for sequential treatments at varying intensities within a single run, thereby maximizing the recovery of valuable components through optimized process conditions.

Residence time (τ) is the time required for a certain volume of water to pass through the reactor. It also represents the period during which the biomass is being treated, from the moment the water enters until the extract is collected as the outlet sample. For the semi-continuous configuration, the treatment time of the solid fraction coincides with the total duration of the experiment, while the treatment time of the liquid phase is calculated as shown in Eq. I.2. In this equation, V is the reactor volume in m^3, $F_{v,o}$ the flow rate measured at ambient conditions, in m^3/s, ρ_o is the water density at ambient conditions and ρ_r the water density at the reaction conditions (Alonso-Riaño, 2022).

$$\tau = \frac{V}{F_v} = \frac{V}{F_{v,o}} \cdot \frac{\rho_r}{\rho_o} \qquad \textbf{[I.2]}$$

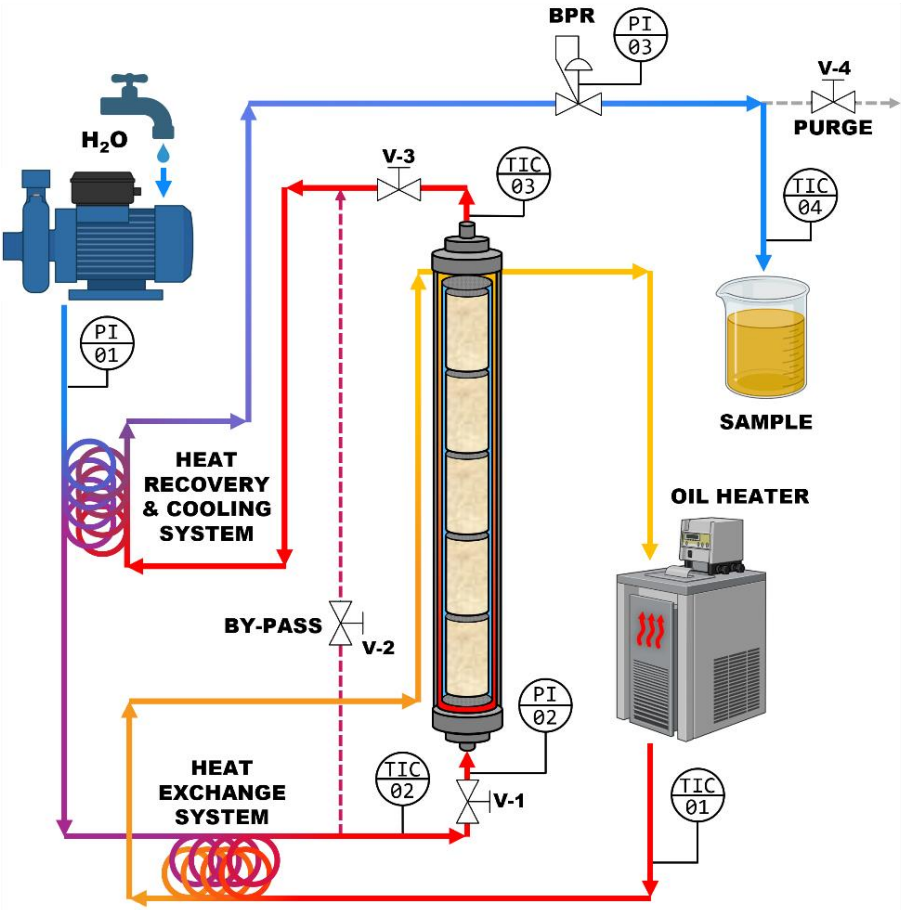

Figure I.15. Semi-continuous subcritical water extraction system configuration. BPR: system back-pressure-regulator; V-1: reactor inlet valve; V-2: by-pass valve; V-3: reactor outlet valve; V-4: purge valve; TIC-01: heating fluid temperature; TIC-02: reactor inlet temperature; TIC-03: reactor outlet temperature; TIC-04: system outlet temperature (sampling); PI-01: system inlet pressure; PI-02: reactor inlet pressure; PI-03: system (regulated by BPR) pressure.

4.3. Subcritical water influence on protein hydrolysates

In the production of protein hydrolysates, the predominant treatments reported in the literature are enzymatic methodologies, together with traditional methods that typically involve harsh conditions or solvents misaligned with sustainable processing objectives. Conversely, subcritical water has recently emerged as an innovative and environmentally friendly alternative. Although its application in

protein hydrolysis is less demonstrated than the rest of more conventional treatments, recent studies underscore its potential to merge efficiency with sustainability.

The enhanced bioactive properties of peptides post-release from biomass are extensively discussed in the initial section; however, the hydrolysis method can significantly influence the resultant bioactivities and functionalities of the hydrolysates. Marcet *et al*. (2016) emphasizes that subcritical water hydrolysis is an appealing alternative as it exclusively utilizes water and rapidly solubilizes proteins while facilitating greater peptide bond scission. Consequently, subW hydrolysates contain elevated levels of free amino acids and small peptides, which possess superior bioactive properties compared to the larger peptides typically obtained through enzymatic treatment. These authors also highlight the generation of interesting amino acid derivatives, such as pyroglutamic acid from glutamic acid, which is particularly relevant for okara due to its high glutamic acid content. These features can lead to enhanced bioactivities, such as antioxidant capacity.

Despite these advantages, Marcet *et al*. (2016) note that subW hydrolysates have certain limitations as the lack of prediction in the sequence of generated peptides. However, the recovery of amino acids and peptides is simple, as only water is used, and conventional downstream techniques such as ultrafiltration or spray-drying can be directly applied. Overall, subW still holds unexplored potential, combining efficiency and sustainability, thus representing a valuable alternative for the valorization of protein-rich by-products.

5. Other novel sustainable extraction methods

In this PhD thesis, subcritical water extraction will be the primary strategy examined for protein hydrolysis, but it will be also compared with other methodologies. Fish meal SWH protein recovery, peptide size and functional properties will be compared versus enzymatic treatment in Chapters 1–3, and okara isoflavone recovery potential of SWH will be compared versus alternative

methodologies such as microwave-assisted extraction and ultrasound-assisted extraction in Chapter 4.

In addition to SWH, several innovative and sustainable extraction techniques have been explored in this work as alternatives to conventional methods. Four of these were applied at different stages and evaluated in comparison with subcritical water hydrolysis, showing promising results in terms of yield and functionality. Enzymatic hydrolysis, the most widely used method in the literature for protein recovery not involving chemicals, was performed to assess whether the results were improved by SWH, which is supposed to be, as mentioned before, a greener, faster and more efficient technology. Furthermore, less studied sustainable technologies such as ultrasound-assisted extraction (UAE) and microwave-assisted extraction (MAE) were also employed. Finally, through a collaboration with Technical University of Denmark (DTU), reduced pressure alkaline pre-treatment (RPAP) was tested as a mild protein extraction method, though relying on an alkaline solvent.

5.1. Enzymatic hydrolysis

Enzymes are protein biocatalysts that facilitate chemical reactions without being consumed. Proteases, a subgroup of hydrolases, hydrolyze proteins by cleaving peptide bonds through the incorporation of a water (H_2O) molecule, thereby releasing peptides of lower molecular weight and restoring the amino and carboxyl groups of the resulting amino acids (Polgár, 1989). The specificity of proteases determines the peptide profile generated, which in turn influences both the nutritional and functional properties of the hydrolysates. Their activity depends strongly on parameters such as pH, temperature, enzyme-to-substrate ratio, and reaction time, which collectively shape the efficiency and outcome of hydrolysis.

Compared to chemical hydrolysis of proteins, enzymatic processes are milder and more sustainable, avoiding harsh conditions, preserving bioactive sequences, and offering greater control over the degree of hydrolysis (Marcet *et al*., 2016). However, they often require longer reaction times and stricter control of operating

conditions than physical methods such as SWH, MAE, UAE, or RPAP. Furthermore, enzymatic processes typically necessitate buffering agents to maintain optimal pH, and the enzymes themselves remain in the reaction medium unless immobilized. This requirement for additives and downstream purification can reduce their environmental advantages.

In this PhD thesis, two commercial endo-proteases from Novozymes A/S (Bagsværd, Denmark) were used: Alcalase® and Novozym® 11028. Alcalase® is characterized by broad proteolytic activity, leading to extensive protein degradation and the generation of bioactive peptides with enhanced solubility and antioxidant properties (Novozymes, 2025a). It has been widely applied to both animal and plant-derived proteins when high degrees of hydrolysis are desired. Novozym® 11028 by contrast, provides milder and more controlled proteolysis, producing primarily peptides rather than free amino acids. This results in reduced bitterness, making it particularly useful in applications where subtle sensory modifications are important (Novozymes, 2025b).

Both enzymes have been reported to improve protein solubility, though Alcalase® tends to induce a higher degree of hydrolysis, while Novozym® 11028 offers gentler modification. Vogelsang-O'Dwyer *et al*. (2023) demonstrated that both enzymes extensively degraded major protein fractions in lentil protein concentrate and significantly increased solubility under acidic conditions, with Novozym® 11028 achieving the highest values. These findings highlight the potential of broad-specificity proteases for enhancing protein solubility and broadening the application range of plant and animal protein concentrates.

5.2. Microwaves and Ultrasounds

Both microwave-assisted extraction (MAE) and ultrasound-assisted extraction (UAE) are considered sustainable, novel techniques that enhance the recovery of target compounds from biomass. Like subcritical water hydrolysis (SWH), they do not require the addition of enzymes or chemical reagents.

Microwave-assisted extraction (MAE) is based on something so common nowadays as microwaves, not only in its ability to heat water accelerating its molecules, but also in its ability to break chemical bonds. Microwaves are a form of electromagnetic radiation; their wavelength exists between radio waves and infrared waves. The microwave region extends from 1,000 to 300,000 MHz (or 30 cm to 1 mm wavelength). This radiation can penetrate biomass, as food, and any other material containing water. In microwave heating, the energy is absorbed by polar molecules, causing them to rapidly rotate and generate heat from the inside out (see Figure I.16). This internal heating effect is much faster than conventional methods, making microwaves highly efficient for cooking or for extraction processes in which heat promotes the release or break-down of target compounds (Fritzsche & Phillips, 2025).

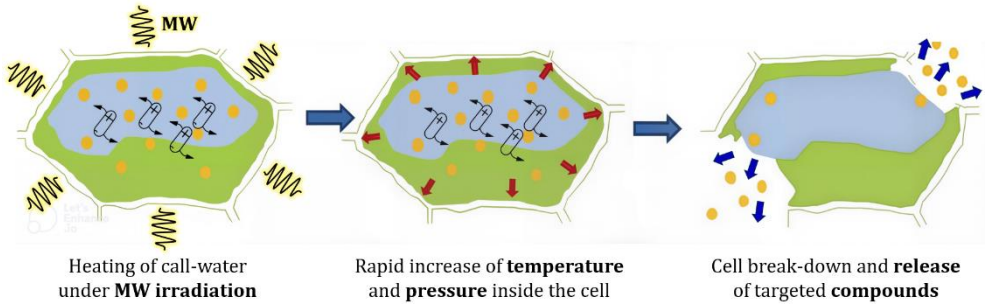

Figure I.16. Mechanism of Microwave-assisted extraction (MAE) for intracellular biocompounds extraction. Adapted from Vinatoru *et al*. (2017).

Non-biological materials that lack water, such as glass, ceramics and majority of plastics, are transparent to microwaves (not being heated), and metals block microwave penetration, reflecting microwaves and potentially causing electric arcs. Polytetrafluoroethylene (PTFE), commonly known as Teflon, is a synthetic fluoropolymer valued for its chemical inertness, hydrophobicity, and low-friction properties. These characteristics make it the ideal reactor material for microwave-assisted extractions, as it is heat-resistant, transparent to microwaves, and ensures efficient and uniform sample heating. Additionally, its non-stick surface minimizes contamination and simplifies cleaning, providing a practical and reliable material for conducting extractions.

Ultrasound-assisted extraction (UAE) is a sustainable and efficient technique used to enhance the release of compounds from biomass. It relies on the physical effects of acoustic cavitation, such as bubble collapse, microstreaming and other mechanical forces, which disrupt cell structures and facilitate mass transfer (see Figure I.17). UAE is considered environmentally friendly, simple, and effective, making it a valuable tool for extracting proteins, bioactive compounds, and other target molecules from plant or food matrices (Illera, Sanz, Varona, *et al*., 2018).

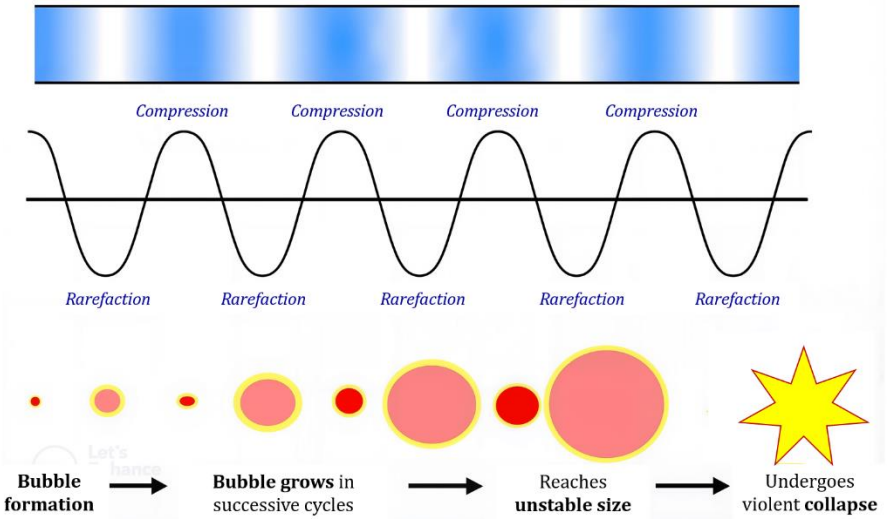

Figure I.17. Creation of cavitation bubbles and their collapse when using Ultrasound-assisted extraction (UAE). Adapted from Vinatoru *et al*. (2017).

Despite their differing mechanisms, MAE and UAE share advantages such as faster extraction, reduced solvent use, and milder conditions relative to conventional methods. Compared to enzymatic hydrolysis, they require shorter processing times and do not depend on strict pH or temperature control, while unlike SWH, they operate under lower temperatures and pressures, offering simpler and more energy-efficient alternatives for the extraction of proteins and bioactive compounds.

In Chapter 4, these two technologies are evaluated for the extraction of isoflavones, bioactive compounds which have been less studied as target than proteins, despite the promising extraction results reported by authors as Tsubaki *et al*. (2009).

5.3. Reduced pressure alkaline pre-treatment (RPAP)

Reduced-pressure alkaline pre-treatment (RPAP) represents a sustainable alternative to conventional alkaline extraction. Conventional alkaline extractions typically operate at temperatures ranging from 104 °C to 121 °C, in contrast, RPAP facilitates protein recovery at lower temperatures and with diminished oxygen exposure. By incorporating low pressure into the traditional alkaline approach, RPAP reduces energy consumption, preserves thermosensitive compounds, and enhances selectivity by limiting the co-extraction of sugars and other components, thereby improving the efficiency and environmental sustainability of downstream processing (da Fonseca *et al*., 2023). Nevertheless, the use of alkaline solvents such as NaOH continues to contribute to the chemical footprint, and achieving full sustainability necessitates the optimization of solvent use, energy efficiency, and process scalability. Optimizing RPAP variables enhances extraction yield, selectivity, processing capacity, and reduces the carbon footprint, thereby supporting technology readiness and scalability (da Fonseca *et al*., 2023).

The main advantage of RPAP technology lies in its ability to operate at very low temperatures (using remarkably less energy on heating), enabling the extraction of intact proteins and large peptides with minimal degradation. The primary advantage of this method is the purity of the protein hydrolysate, achieved through high selectivity, particularly by avoiding the co-extraction of sugars common in other techniques. Selectivity was calculated as the ratio of protein to protein plus carbohydrates released under each condition (da Fonseca *et al*., 2023). This results not only in a protein fraction of high quality but also in a solid residue that remains rich in carbohydrates and only lightly treated. This residue is highly suitable for subsequent valorization as fermentable residue, such as through enzymatic hydrolysis followed by fermentation for lactic acid production.

6. Membrane fractionation process

Membrane filtration is a sustainable separation method that operates at low temperatures with minimal energy consumption, requiring no solvents or additives and being easily scalable to higher flow rates. Compared to chromatographic methods commonly proposed for peptide fractionation, it offers higher efficiency and simpler operation. While chromatography provides high selectivity, it relies on toxic and costly solvents, suffers from low mass transfer and yield, and is therefore unsuitable for large-scale production of bioactive peptides in the food and pharmaceutical industries. Membrane processes are increasingly applied to protein and bioactive compound recovery from food by-products, offering significant advantages over conventional methods (Alavi & Ciftci, 2023).

The operation of membrane filtration relies on the selective permeability of a semi-permeable membrane that allows molecules smaller than its pore size to pass into the permeate, while larger ones remain in the retentate. The process is pressure-driven, and its efficiency depends on both permeate flux and selectivity. Higher pressure increases flux, but operating conditions must balance productivity with minimal fouling (Alavi & Ciftci, 2023).

Bioactive and functional peptides are increasingly demanded due to functional food trends, aging populations, and chronic diseases. After its production through hydrolysis of food by-products, the next step is recovery and isolation by effective and sustainable methods, which constitutes a key improvement in this area. In this way, membrane fractionation appears as a great mechanism to separate the wide range of compounds present in the hydrolysates mainly by its MW (but also influenced by charges and physicochemical properties), in addition to facilitating or approach its purification due to the separation of the other non-bioactive biomolecules initially present also in solution (Alavi & Ciftci, 2023).

As previously described in Section 1, peptides of different molecular weights (MW) derived from protein hydrolysates exhibit distinct functionalities, making

them suitable for various industrial applications depending on their size. This is further discussed in Chapter 2, where the functional properties of fish meal protein hydrolysates are analyzed in relation to their molecular size and charge, showing how these factors influence their characteristics and potential applications. Large (high-MW) peptides and barely broken-down proteins present more interest in a physical, structural or techno-functional way, and small (low-MW) peptides and amino acids, in addition to being useful for their techno-functional properties too, stand out more for their wide range of bioactive properties (Etemadian *et al*., 2021; Wouters *et al*., 2016). Therefore, Chapter 3 of this PhD thesis focuses on membrane fractionation to separate fish meal hydrolysates based on molecular weight.

Membrane filtration is commonly differenced in four types depending on its pore size, from larger to smaller pore size: microfiltration, ultrafiltration, nanofiltration and reverse osmosis. Commonly, as smaller is the pore size, higher is the pressure needed to work with the membrane, lower is the working flux, and higher is the influence of the charge in the membrane and the molecules (Alavi & Ciftci, 2023; Shon *et al*., 2013).

Microfiltration (MF) presents the higher pore size of these four (of about 0.1–10 μm), is normally used to remove cell debris of fermentation media or hydrolysates, and also solid particles in solution (Martin-Orue *et al*., 1998; Shon *et al*., 2013).

Ultrafiltration (UF) englobes the size pores of about 5–20 nm and it is the most widely used to recover peptides and proteins from hydrolysates, as well as any other macromolecules or colloids. This pore sizes are able to be used for concentrate molecules from above 1000 Da, as protein and high-MW peptides and permeate other peptides of smaller size, as oligopeptides and amino acids (Alavi & Ciftci, 2023; Ratnaningsih *et al*., 2021; Shon *et al*., 2013). In the Chapter 3 of this PhD Thesis, UF membrane will be used to separate the peptides of high-MW obtained by enzymatic treatment, where the hydrolysis is not as sharp as in subW.

Nanofiltration (NF), with pore sizes commonly between 1–5 nm, allow to separate molecules in the range of 300–1000 Da (sometimes even higher depending on their charge). These membranes are great to separate peptides of small sizes and permeate only free amino acids, dipeptides and small oligopeptides. Charge effect of the membrane gain importance in NF, being more selective to charged molecules and being also a good one to separate even ions (Alavi & Ciftci, 2023; Martin-Orue *et al*., 1998; Shon *et al*., 2013). In the Chapter 3 of this PhD Thesis, NF will be used to separate the peptides of medium and low-MW obtained by SWH, or the ones obtained by enzymatic treatment but already permeated from UF membrane. These ranges of pore sizes are optimal for separate medium-small peptides from smallest oligopeptides and free amino acids.

Reverse osmosis (RO) is based on diffusivity of solutes, membranes are nonporous and only allow to permeate very small peptides or ions depending principally on their charge, even for the smallest particles (Alavi & Ciftci, 2023; Shon *et al*., 2013).

OBJECTIVES

OBJECTIVES

The **Main Objective** of this PhD Thesis is to develop and optimize sustainable extraction technologies for the comprehensive valorization of food industry by-products, specifically targeting protein and bioactive compound recovery from tuna fish meal and soybean okara through subcritical water extraction, being compared also with other novel technologies.

Chapters 1–3 address the valorization of tuna fish meal focusing on its high protein content and assessing the quality and functionality of the peptide fractions extracted by subcritical water under different conditions as well as comparing the results with those obtained through enzymatic treatments. These are their respective specific objectives:

Chapter 1. *Production of small peptides and low molecular weight amino acids by subcritical water from fish meal: Effect of pressurization agent*: To optimize subcritical water extraction parameters (temperature, pressure, and pressurization agent) for protein hydrolysis from tuna fish meal and evaluate the efficiency compared to enzymatic treatments using Alcalase® and Novozym® proteases.

Chapter 2. *Green fractionation and hydrolysis of fish meal to improve their techno-functional properties*: To characterize the techno-functional properties of protein hydrolysates obtained by subcritical water and Alcalase®, from fish meal as itself, its water-soluble fraction and its non-water-soluble fraction, including emulsifying capacity, solubility, surface tension, and protein fluorescence.

Chapter 3. *Membrane fractionation of hydrolysates of the water-soluble protein from tuna fish meal obtained by subcritical water and enzymatic treatments. Comparison of physical and chemical properties*: To purify and fractionate tuna fish meal protein hydrolysates obtained by subcritical water and Alcalase® through

membrane separation (ultrafiltration and nanofiltration) and correlate molecular weight distribution with functional properties.

Chapters 4–6 focus on the valorization of isoflavones and proteins from soybean okara. The aim is to identify the most suitable extraction methodology for each target compound, adopting a cascade valorization strategy through subcritical water extraction and comparing it with other novel and green methodologies such as microwave-assisted, ultrasound-assisted, and reduced-pressure alkaline extractions. These are their respective specific objectives:

Chapter 4. *Green extraction of isoflavones from okara using subcritical water: Kinetics, optimization, and comparison with other water-based sustainable methods*: To extract and characterize isoflavones from soybean okara using subcritical water extraction under mild conditions, studying isoflavone profiles, extraction kinetics and interconversion pathways. Comparing the technology with conventional extractions using hydroalcoholic mixtures and other novel and green methodologies as microwave- and ultrasound-assisted extraction.

Chapter 5. *Cascade valorization of okara by subcritical water hydrolysis: assessment of protein and amino acid profile in batch and semi-continuous systems:* To implement cascade valorization of okara through sequential isoflavone extraction followed by protein hydrolysis using subcritical water in batch and semi-continuous configurations, evaluating protein recovery and bound and free amino acid profiles.

Chapter 6. *Protein recovery from okara by reduced-pressure alkaline pre-treatment: Optimization and techno-economic assessment*: To assess reduced-pressure alkaline pre-treatment as an alternative methodology for okara protein extraction, optimizing operational parameters to maximize protein recovery while minimizing carbohydrate co-extraction, and conducting techno-economic evaluation for industrial scalability aiming to select the optimal conditions at industrial scale.

RESULTS

RESULTS

The more relevant results of this PhD Thesis are presented as different chapters which correspond to the scientific publications detailed below. A brief summary in Spanish language of each publication is included at the beginning of each chapter.

Chapter 1: Production of small peptides and low molecular weight amino acids by subcritical water from fish meal: Effect of pressurization agent.

Chapter 2: Green fractionation and hydrolysis of fish meal to improve their techno-functional properties.

Chapter 3: Membrane fractionation of hydrolysates of the water-soluble protein from tuna fish meal obtained by subcritical water and enzymatic treatments. Comparison of physical and chemical properties.

Chapter 4: Green extraction of isoflavones from okara using subcritical water: Kinetics, optimization, and comparison with other water-based sustainable methods.

Chapter 5: Cascade valorization of okara by subcritical water hydrolysis: assessment of protein and amino acid profile in batch and semi-continuous systems.

Chapter 6: Protein recovery from okara by reduced-pressure alkaline pre-treatment: Optimization and techno-economic assessment.

CHAPTER 1

Production of small peptides and low molecular weight amino acids by subcritical water from fish meal: Effect of pressurization agent

Adapted from the article:

P. Barea, R. Melgosa, A.E. Illera, P. Alonso-Riaño, E. Díaz de Cerio, O. Benito-Román, S. Beltrán, M.T. Sanz (2023).

"Production of small peptides and low molecular weight amino acids by subcritical water from fish meal: effect of pressurization agent"

Food Chemistry, *418*, 135925.

DOI: https://doi.org/10.1016/j.foodchem.2023.135925

Capítulo 1

Producción de pequeños péptidos y aminoácidos de bajo peso molecular por agua subcrítica a partir de harina de pescado: Efecto del agente de presurización

Resumen

La hidrólisis de la fracción de proteína soluble en agua (WSP) de la harina de atún se evaluó mediante el uso de agua subcrítica (subW) con N_2 y CO_2 como diferentes agentes de presurización en el rango de temperatura de 140 a 180 °C. Para ambos gases, la liberación del grupo amino aumentó al aumentar la temperatura de trabajo, mientras que la respuesta de Lowry disminuyó debido a la producción de péptidos de menor tamaño y aminoácidos libres.

El contenido de aminoácidos libres fue mayor con CO_2 que con N_2. A 180 °C, se liberaron 344 ± 5 y 275 ± 3 mg de aminoácidos libres por g de WSP, respectivamente; aunque, en ambos sistemas, los aminoácidos de menor peso molecular, glicina y alanina, fueron liberados preferentemente. El contenido de aminoácidos libres obtenidos por hidrólisis enzimática con proteasas comerciales Alcalase® y Novozym® fue mucho menor, con el mayor rendimiento de hidrólisis determinado para la histidina. Estos resultados han sido respaldados por el análisis de cromatografía de exclusión por tamaño.

Palabras clave: Proteína soluble de harina de pescado, hidrólisis, agua subcrítica, dióxido de carbono.

Chapter 1

Production of small peptides and low molecular weight amino acids by subcritical water from fish meal: Effect of pressurization agent

Abstract

The hydrolysis of the water-soluble protein (WSP) fraction from tuna fish meal was evaluated by subcritical water (subW) by using N_2 and CO_2 as different pressurization agents in the temperature range from 140 to 180 °C. For both gases, the amino group release increased by increasing working temperature while the Lowry response decreased due to production of smaller-size peptides and free amino acids.

The free amino acid content was higher with CO_2 than with N_2. At 180 °C, 344 ± 5 and 275 ± 3 mg of free amino acids per g of WSP were released, respectively; although, in both systems the smallest molecular weight amino acids, glycine and alanine, were preferentially released. The free amino acids content obtained by enzymatic hydrolysis with commercial proteases Alcalase® and Novozym® was much lower with the highest hydrolysis yield determined for histidine. These results have been supported by size exclusion chromatography analysis.

Key words: Soluble fish meal protein, hydrolysis, subcritical water, carbon dioxide.

1. Introduction

Fish meal is an essential ingredient in aquaculture and pet-food industry since it presents a high protein content as well as a valuable lipid fraction composition. However, new sources of protein, such as those derived from fermentation processes, plant-based or insect protein, force fish meal producers to look for new valuable products in the fishmeal production chain.

Protein from marine origin is of high nutritional value and presents a good profile of essential amino acids (Guérard *et al*., 2001). Exploring the production of small peptides and valuable free amino acids from marine protein, and specifically from fish meal protein, is of great interest according to their well-documented functional properties and other interesting bioactivities. New functional and healthy products can be obtained creating more sustainable and environmentally friendly processes (Petrova *et al*., 2018; Slizyte *et al*., 2016).

Hydrolysis converts protein into small peptides of great interest in the food, pharmaceutical and cosmetic industries. Chemical and enzymatic hydrolysis are widely employed in the hydrolysis process of proteins. However, enzymes are expensive and time consuming, while chemical hydrolysis usually requires the use of concentrated acids or alkalis and generates a high salt content in the final product after neutralization (Ahmed & Chun, 2018).

Large scale production of peptides will require the development of new alternative cost-effective approaches to meet the quality and functionality specifications demanded by the market (Melgosa *et al*., 2020). In this regard, the use of subcritical water as hydrolytic agent offers a green and modern alternative to the traditional methods.

Subcritical water (subW) is water in its liquid state in the range from 100 to 374 °C and pressures up to 22 MPa. Under these conditions, water presents unique properties, the dielectric constant decreases facilitating the solubilization of

non-polar components. Furthermore, the viscosity and density decrease. Under subcritical water conditions there is also an increase of the ionic product. The increment in the concentration of H^+ and OH^- in the aqueous medium raises its activity as an acid- or base-like catalyst for hydrolysis reactions (Marcet *et al*., 2016). Based on these properties, the mechanism of hydrolysis of peptide bonds in the protein structure in the presence of subW is due to the acid-catalysis effect due to the increase of the ionic product (Lamp *et al*., 2020). subW has been successfully applied to hydrolyze and fractionate the protein content of different herbaceous and aquatic biomass (Rivas-Vela *et al*., 2021; Trigueros, Sanz, *et al*., 2021) as well as from crops (Alonso-Riaño *et al*., 2021; Sganzerla *et al*., 2022). subW treatment may be a promising alternative to produce different bio-compounds from different biomasses; however, there appears to be a lack of data for subcritical biomass process reactor systems, in particular for the production and recovery of proteins and amino acids at a larger scale (Domenico Ziero *et al*., 2020). Regarding scaling up process, temperature control becomes primordial, since the increasing temperature rate for different capacity reactor systems can play an effect on the hydrolysis yield of some of the biopolymers (Alonso-Riaño *et al*., 2023; Domenico Ziero *et al*., 2020). Therefore, temperature is one of the most critical parameters in subW treatment.

During processing of fish and fish canning, considerable amount of fish-derived water-soluble proteins are discarded into the wastewater (Iwata *et al*., 2000). Therefore, a two-stage process for fish meal valorization is proposed based first on the valorization of the water-soluble protein (WSP) fraction and subsequently the non-water-soluble protein, in a cascade approach, contributing to increase the value of the marine resources. The easy fractionation of the protein from the fish meal will offer an economical route for amino acid production. The WSP is no longer bound to the matrix of the raw material, and it is expected a high yield of free amino acid release compared with the total protein fraction treatment.

There are only a few works dealing with the choice of the gas to generate the working pressure in subW treatment. However, it has been proved to be a factor to consider (Domenico Ziero *et al*., 2020). According to the literature, the hydrolysis of biopolymers in subW can be significantly enhanced by adding carbon dioxide to the medium since it leads to a more acidic medium due to the formation of carbonic acid that serves as a catalyst according to Rogalinski *et al*. (2008):

$$CO_2 + H_2O \rightarrow H_2CO_3 \rightarrow H^+ + HCO_3^- \rightarrow 2\,H^+ + CO_3^{2-} \qquad \textbf{[1.1]}$$

The effect of carbon dioxide on the subW hydrolysis of different biopolymers has been reported in the literature. Rogalinski *et al*. (2008) reported that the addition of carbon dioxide led to an increase in amino acid production from bovine serum albumin (BSA) compared to pure subW. With other polymers such as xylan, Van Walsum (2001) showed that carbonic acid substantially increased hydrolysis activity in comparison to water alone. However, for aspen wood and corn stoves the addition of carbonic acid during subW treatment did not bring any further improvement in the subsequent enzymatic hydrolysis step. This was attributed to the autocatalytic effect of acetyl groups released from the raw materials during hydrolysis, which performed a similar role to that of carbonic acid and obscured its action when added to the reaction media (Yourchisin & Van Walsum, 2004).

The objective of this work was to investigate the hydrolysis of the water-soluble protein fraction of the fish meal by subW regarding the production of peptides and free amino acids. Hydrolysis kinetics were determined at different temperatures and with different pressurization agents, including an inert gas, such as nitrogen and carbon dioxide as an improvement agent for protein hydrolysis. Hydrolysis driven by subW was compared with enzymatic hydrolysis by commercial proteases considering the amount and profile of free amino acids released and antioxidant capacity. The different results obtained for subW and enzymatic hydrolysis were correlated with the molecular weight distribution of the hydrolysates. This treatment

could lead to a feasible solution for a first step for fish meal valorization via previous fraction and hydrolysis of the WSP.

2. Experimental

2.1. Raw material

The raw material used in this work was fish meal from tuna (*Thunnus* sp.) kindly supplied by *Sarval Bio-Industries Noroeste*, S.A.U. (A Coruña, Spain). The raw material was kept at 4 °C until used. Moisture content was 3.4 % ± 0.1 % (w/w) as determined gravimetrically after drying preweighted samples at 105 °C for 24 h.

Ash content was determined after subjecting the sample at 500 °C for 12 h. Lipid content of the fish meal was determined by Soxhlet extraction (Buchi B-8111) using hexane as solvent. Protein content of the raw material was determined from the nitrogen elemental content applying the corresponding N-factor obtained by the amino acid profile of the fish meal protein.

2.2. Water soluble protein extraction

Water soluble protein, WSP, was extracted by putting the fish meal in contact with water in a thermostated extractor. Extraction was carried out at different fish meal:water ratios (4:100, 8:100, 16:100 and 24:100) and different temperatures (20, 50 and 80 °C). Protein extraction kinetic was followed along time by withdrawing samples at regular time intervals. Samples were stored at -18 °C until analysis. The quantification of the protein was carried out by the Lowry method. The yield of WSP was evaluated according to:

$$\text{Yield of WSP} = m_{WSP}/m_{\text{total protein}} \quad \textbf{[1.2]}$$

where m_{WSP} is the amount of WSP in the supernatant solution after extraction with water and $m_{\text{total protein}}$ is the total amount of protein in the fish meal.

2.3. Equipment for subcritical water hydrolysis

Subcritical water hydrolysis of WSP fraction was carried out in a lab-assembled batch system with a reactor of 0.5 L capacity. The reactor was covered by a ceramic heating jacket (230 V, 4000 W, ⌀ 95 mm, 160 mm height) to reach the selected working temperature. A Pt100 sensor placed inside the reactor and the PID system to which it is connected allowed to control and register the temperature during the extraction. A needle valve (Autoclave Engineers) followed by a cooling system was connected to collect samples along the hydrolysis.

In a typical run, 200 mL of the WSP extract was charged into the reactor. Three different temperatures were essayed, 140, 160 and 180 °C and the working pressure was set at 5 MPa by using different gases. This pressure was chosen based on previous studies of the research group for biomass valorization from different sources (Alonso-Riaño *et al*., 2023; Trigueros, Alonso-Riaño, *et al*., 2021). The use of mild reaction pressure, 40 to 60 bar, has been found also as optimum for the hydrolysis of proteins of biomass waste (fish) to produce free amino acids (Cheng *et al*., 2008). Furthermore, according to literature (Rivas-Vela *et al*., 2021) the effect of pressure on performance of hydrolysis in different studies has been observed as a non-significant, compared with temperature and time, as long as water remains in the liquid state.

Pressurization of the vessel was performed with inert N_2 or CO_2, fed through a sintered stainless steel micro-filter with a pore size of 10 μm submerged in the liquid sample (Illera, Sanz, Beltran, *et al*., 2018). The same amount of CO_2 (8.3 g) was added to all the experiments by using a syringe pump with pressure and volume controllers (ISCO 260 D), yielding a ratio of 2 g CO_2/g WSP). Once the pressure was reached, there was no need of further gas addition into the high-pressure reactor.

Hydrolysis kinetics were followed by carefully withdrawing samples at regular time intervals through the sampling port. After 300 minutes, the vessel was let to cool down, and depressurized when the temperature was lower than 90 °C.

2.4. Enzymatic hydrolysis

Two different commercial proteases, kindly donated by Novo Industry, were selected in this work, specifically Alcalase® and Novozym®. Firstly, the protease activity of the two commercial enzymes was determined by the casein method according to Pokhum *et al*. (2015) with some modifications. One mL of casein solution (2 % w/v) prepared in potassium phosphate buffer (50 mM) was incubated in a water bath at 37 °C for 5 min. Then, 500 µL of the commercial protease enzyme was added and incubated at 37 °C for 10 min. The reaction was stopped by adding 3 mL of 0.4 M trichloroacetic acid. After that, the mixture was filtrated through a 0.45 µm filter. One mL of the filtrated mixture was mixed with 1 mL of the Folin Ciocalteu's reagent and 5 mL of 0.50 M Na_2CO_3. The mixture was incubated at 37 °C for 30 min. The protease digests casein and the amino acid tyrosine is liberated, along with other amino acids and peptide fragments, that react with the Folin's reagent producing a blue-colored chromophore.

Protease activity was determined by measuring the absorbance at 660 nm in a Jasco (V-750) spectrophotometer. The blank sample was prepared by adding the stopping reagent to the mixture before the sample of enzyme. A calibration curve was prepared by reacting known quantities of tyrosine with the Folin's reagent and protease activity was expressed as µmol of tyrosine released per mL of enzyme, resulting 1157 ± 74 and 826 ± 33 µmol of tyrosine/mL for Alcalase® and Novozym®, respectively.

In the enzymatic hydrolysis study, 100 mL of the WSP extract obtained was incubated at 60 °C and pH of 8 by adding 225 U of each protease. Samples were withdrawn at regular time intervals and subsequently heated in boiling water for 5–10 min to inactivate the protease. Samples were frozen at -18 °C until analysis.

2.5. Analytical methods

2.5.1. Lowry method for protein determination

The Lowry method was carried out to determine the WSP fraction during its extraction, as well as during the subW and enzymatic hydrolysis treatments (Lowry *et al*., 1951). Briefly, the samples were conveniently diluted to 1 mL with deionized water. 5 mL of Lowry reagent were added (Lowry reagent: 20 $g \cdot L^{-1}$ sodium potassium tartrate, 20 $g \cdot L^{-1}$ copper sulfate pentahydrate and 20 $g \cdot L^{-1}$ sodium carbonate in 0.1 M NaOH; in proportion 1:1:100). Samples were incubated for 15 min in the dark. Afterwards, 0.5 mL of Folin-Ciocalteu's phenol reagent, diluted 1:3 in distilled water, were added, and the mixture was let to stand for 30 min in the dark. Finally, absorbance was measured at 750 nm using a Jasco spectrophotometer and protein content was obtained based on a calibration curve using bovine serum albumin as standard.

2.5.2. Ninhydrin assay

The ninhydrin reaction method was carried out according to the Sigma Aldrich protocol. Ninhydrin assay results in the formation of soluble chromophores by all primary amines, including amines, amino acids, proteins and even ammonia (Friedman, 2004). Briefly, 2 mL of the diluted protein sample were gently mixed with 1 mL of ninhydrin reagent solution and placed into a boiling water bath for 10 min. After cooling, 5 mL of 95 % ethanol were added. Ninhydrin reagent solution was purchased from Sigma-Aldrich and leucine was used as standard (Friedman, 2004). Absorbance was measured at 570 nm.

2.5.3. Amino acid profile

The amino acid profile was analyzed by gas chromatography after derivatization by using the EZ:faast^{TM} kit (Phenomenex) and a GC-FID instrument (Hewlett Packard, HP 2890 Series). Details can be found elsewhere in Alonso-Riaño

et al. (2021) and Trigueros, Sanz, *et al*. (2021). Amino acid profile of fish meal and WSP fraction was determined after hydrolysis using 6 N HCl at 100 °C during 24 h. Tryptophan and cysteine are lost by acid hydrolysis, and methionine can be partially destroyed by acid hydrolysis, so an alkaline hydrolysis was also carried out to determine these amino acids (Alonso-Riaño *et al*., 2021). Arginine cannot be detected by this kit, whereas asparagine and glutamine were quantified as aspartic and glutamic acids, respectively.

For WSP extracts, amino acids were determined before the HCl hydrolysis and referred to as free amino acids. After hydrolysis with HCl of the WSP, total amino acids were determined and the difference between the value of amino acids obtained after HCl hydrolysis and free amino acids were referred to as constituted amino acids of the WSP. Free amino acids were also determined during enzymatic and subW hydrolysis.

2.5.4. Elemental analysis

Elemental composition (C, H, N, S) was determined by an organic elemental micro-analyzer equipment (Thermo Scientific Model Flash 2000). Nitrogen composition of the sample and its amino acid profile were used to calculate the N factor of the fish meal protein.

2.5.5. Determination of antioxidant capacity

The antioxidant activity of the WSP and its hydrolysates was assessed by the Ferric Reducing Antioxidant Power (FRAP) assay (Benzie & Strain, 1996). As standard, a solution of $FeSO_4 \cdot 7H_2O$ (0.1 M) was used. Results were expressed in μmol of Fe^{2+} per gram of dry WSP.

2.5.6. Size Exclusion Chromatography

The molecular weights (MW) of the WSP and its hydrolysates were determined employing high-pressure size exclusion chromatography coupled to a refraction index detector (HPSEC-RID, 1260 HPLC system, Agilent Technologies, CA, USA). Samples and standards were filtered through 0.45 μm syringe filters. A PL Aquagel guard column was linked in series with PL Aquagel-OH 30 (from 0.1 to 60 kDa) and PL Aquagel-OH 40 (from 10 to 200 kDa) columns from Agilent Technologies (300 mm × 7.5 mm, particle size 8 μm). Characterization of WSP and its hydrolysates was performed in isocratic mode with 0.01 M NH_4Ac, at a flow rate of 0.7 mL/min at 40 °C. A PEO/PEG standard set (117.9–0.194 kDa) was used for calibration and data were analyzed with Agilent OpenLab Data Analysis 2.5 software.

2.6. Statistical analysis

All values were expressed as mean ± standard deviation of at least two replicates. The significance differences between the mean value from the different factors was determined based on an analysis of the variance with the Fisher's Least Significant Difference (LSD) method at *p*-value ≤ 0.05. Correlation between the reducing capacity of the hydrolysates and the amino group released and Lowry assay results were determined by using the Pearson's Correlation Test. The software Statgraphics19 X64 was used.

3. Results and discussion

3.1. Characterization of the fish meal

Results were presented in a dry basis taking into account the moisture content of the fish meal. Ash content of fish meal was 21.7 ± 0.2 % (w/w). Total lipid content was 6.5 ± 0.2 % (w/w) as determined by Soxhlet extraction. The elemental analysis composition was: 40 ± 1 % (w/w) of C, 10.3 ± 0.3 % (w/w) of N, 5.8 ± 0.1 % (w/w) of H and 0.45 ± 0.07 % (w/w) of S. Crude protein was obtained from the nitrogen

content and the corresponding conversion factor to estimate the crude protein content. The Nitrogen factor was calculated from the amino acid profile of the fish meal (see Table 1.1) according to the NREL standard protocols (Hames *et al*., 2008). For the fish meal used in this work, a N-factor of 5.0 was determined. This value was in the same range as the one reported by Salo-Väänänen & Koivistoinen (1996) for fish and fish products with a N-factor of 4.94. This value indicated that a significant amount of nitrogen comes from other non-amino acids structures, such as those compounds derived from degradation of proteins or other non-protein nitrogen compounds. The N-factor values of 5.0 yielded a crude protein content of 51 ± 2 % (w/w). However, in literature many authors still consider 6.25 as the N-factor to convert nitrogen into crude protein values for fish and fish products (Ween *et al*., 2017). A N-factor of 6.25 will yield a crude protein of 64 % (w/w), which is closer to the value reported by the provider.

3.2. Extraction and characterization of the water-soluble protein fraction of fish meal

WSP was extracted at different temperatures (from 20 to 80 °C) at a fish meal to solvent ratio of 8 g fish meal:100 mL of distilled water. Total protein content in the liquid supernatant was determined according to the Lowry assay. Extraction kinetics curves are presented in Figure 1.1a. Faster initial extraction rates were obtained by increasing temperature. Additionally, final WSP yield was also slightly higher at the highest temperature essayed in this work yielding values of 14.1 ± 0.5 g of WSP per 100 g of dry fish meal, which represented 28 % of the total protein content in the fish meal.

Table 1.1. Amino acid profile of the raw fish meal product and of the water-soluble protein (WSP). Free amino acid profile of subW and enzymatic hydrolysates.

Amino acid	Fish meal, mg aa/g prot	WSP, mg aa/g WSP		Free amino acids generated during hydrolysis, mg aa/g WSP							
				subW hydrolysis in N_2		subW hydrolysis in CO_2				Alcalase	Novozym
		Free aa	Bound aa	140 °C	160 °C	Free aa	Bound aa	160 °C	180 °C	Free aa	Bound aa
Ala	89 ± 3	8.2 ± 0.1	80 ± 7	18.8 ± 0.1^{b}	52.6 ± 0.1^{d}	66.0 ± 0.4^{e}	19.8 ± 0.4^{c}	66.3 ± 0.2^{f}	72.8 ± 0.4^{g}	9.7 ± 0.1^{a}	9.8 ± 0.1^{a}
Gly	86 ± 2	3.5 ± 0.1	195 ± 9	30.3 ± 0.2^{c}	95 ± 2^{d}	110 ± 1^{e}	27 ± 0.1^{b}	118.4 ± 0.3^{f}	130.4 ± 0.3^{g}	5.4 ± 0.1^{a}	4.3 ± 0.3^{a}
Val	43 ± 3	4.0 ± 0.1	25 ± 5	4.5 ± 0.2^{a}	7.9 ± 0.9^{c}	10.4 ± 0.1^{d}	6.7 ± 0.1^{b}	8.0 ± 0.1^{c}	13.3 ± 0.1^{e}	5.03 ± 0.07^{a}	4.7 ± 02^{a}
Leu	63 ± 4	5.0 ± 0.1	31 ± 2	5.1 ± 0.3^{a}	8.5 ± 0.2^{d}	11.0 ± 0.1^{e}	6.8 ± 0.1^{c}	11.0 ± 0.1^{e}	13.4 ± 0.1^{f}	5.9 ± 0.1^{b}	5.7 ± 0.1^{b}
Ile	36 ± 2	2.7 ± 0.1	15 ± 2	2.2 ± 0.1^{a}	2.1 ± 0.2^{a}	3.4 ± 0.1^{b,c}	3.5 ± 0.1^{c}	2.2 ± 0.1^{a}	3.8 ± 0.1^{b,c}	3.4 ± 0.1^{c}	3.2 ± 0.1^{b}
Thr	43 ± 2	2.4 ± 0.1	29 ± 2	1.7 ± 0.4^{c}	0.7 ± 0.2^{a,b}	0.43 ± 0.03^{a}	2.4 ± 0.1^{d}	0.59 ± 0.05^{a,b}	5.0 ± 0.1^{b,c}	2.5 ± 0.4^{d}	2.7 ± 0.1^{d}
Ser	44 ± 3	1.6 ± 0.1	34 ± 5	6.3 ± 0.1^{g}	0.42 ± 0.05^{a}	0.43 ± 0.02^{a}	6.0 ± 0.1^{f}	1.1 ± 0.2^{c}	0.8 ± 0.1^{b}	2.44 ± 0.04^{e}	2.0 ± 0.2^{d}
Pro	58 ± 3	3.2 ± 0.1	108 ± 5	8.3 ± 0.1^{c}	25.7 ± 0.8^{d}	41.9 ± 0.6^{f}	8.4 ± 0.1^{c}	27.9 ± 0.1^{e}	52 ± 1^{g}	3.6 ± 0.1^{b}	3.2 ± 0.1^{a}
Asp	94 ± 2	2.8 ± 0.1	67 ± 7	7.8 ± 0.7^{b}	2.2 ± 0.8^{a}	2.0 ± 0.1^{a}	11.4 ± 0.1^{c}	3.0 ± 0.1^{a}	2.4 ± 0.1^{a}	3.0 ± 0.1^{a}	2.8 ± 0.1^{a}
Met	27 ± 3	1.6 ± 0.1	11 ± 2	1.8 ± 0.1^{a}	2.7 ± 0.4^{c}	2.2 ± 0.1^{b}	2.5 ± 0.1^{c}	5.7 ± 0.2^{d}	6.0 ± 0.3^{d}	2.00 ± 0.03^{a,b}	2.0 ± 0.1^{a,b}
Hyp	24 ± 3	n.d.	58 ± 9	3.0 ± 0.1^{b}	7 ± 1^{b}	6.9 ± 0.1^{b}	2.3 ± 0.1^{b}	7.8 ± 0.7^{b}	12 ± 1^{c}	0.36 ± 0.01^{a}	0.24 ± 0.03^{a}
Glu	110 ± 6	2.5 ± 0.1	100 ± 14	0.7 ± 0.1^{a,b}	0.8 ± 0.1^{b}	4.8 ± 0.03^{e}	2.0 ± 0.1^{c}	0.63 ± 0.03^{a}	9.2 ± 0.2^{f}	1.93 ± 0.02^{c}	3.7 ± 0.1^{d}
Phe	34 ± 2	2.5 ± 0.1	18 ± 2	2.6 ± 0.1^{a}	4.0 ± 0.1^{c}	5.3 ± 0.1^{d}	3.1 ± 0.1^{b}	5.2 ± 0.1^{d}	6.3 ± 0.1^{e}	3.1 ± 0.1^{b}	3.0 ± 0.1^{b}
Lys	57 ± 4	2.4 ± 0.1	35 ± 6	3.5 ± 0.1^{a}	6 ± 1^{b}	3.7 ± 0.1^{a}	3.8 ± 0.1^{a}	6.8 ± 0.2^{c}	6.2 ± 0.2^{b,c}	3.5 ± 0.1^{a}	4.0 ± 0.1^{a}
His	22 ± 2	13.3 ± 0.1	13 ± 2	7.9 ± 0.4^{c}	5 ± 2^{b}	2.8 ± 0.1^{a}	12.6 ± 0.4^{d}	6.9 ± 0.2^{b,c}	6.9 ± 0.1^{b,c}	19.0 ± 0.7^{f}	16.1 ± 0.2^{e}
Hyl	1.9 ± 0.4	0.5 ± 0.1	52 ± 18	0.5 ± 0.1^{c}	0.40 ± 0.05^{a,b}	0.43 ± 0.03^{b,c}	1.0 ± 0.1^{e}	0.8 ± 0.1^{d}	n.d.	0.25 ± 0.02^{a}	0.39 ± 0.04^{a,b}
Tyr	26 ± 2	1.9 ± 0.1	13 ± 3	2.1 ± 0.1^{a}	2.2 ± 0.3^{a,b}	2.5 ± 0.1^{b,c}	2.6 ± 0.1^{c}	2.7 ± 0.1^{c,d}	2.9 ± 0.1^{d}	2.7 ± 0.1^{c,d}	2.5 ± 0.1^{b,c}
Trp	8 ± 1	0.5 ± 0.1	53 ± 12	0.26 ± 0.02^{a}	0.27 ± 0.03^{a}	0.94 ± 0.02^{e}	0.40 ± 0.04^{b}	0.27 ± 0.03^{a}	0.81 ± 0.05^{b}	0.72 ± 0.03^{d}	0.66 ± 0.04^{c}
Cys	2.3 ± 0.6	0.3 ± 0.1	25 ± 9	0.2 ± 0.1^{a,b,c}	0.28 ± 0.06^{b,c}	0.16 ± 0.02^{a,b}	0.30 ± 0.06^{b,c}	0.27 ± 0.06^{c}	0.26 ± 0.03^{b,c}	0.11 ± 0.01^{a}	0.26 ± 0.09^{b,c}
TAA	868 ± 48	59 ± 2	962 ± 121	108 ± 4^{b}	224 ± 10^{d}	275 ± 3^{e}	123 ± 2^{c}	276 ± 3^{e}	344 ± 5^{f}	75 ± 1^{a}	71.0 ± 0.6^{a}
EAA	333 ± 23	34.3 ± 0.3	230 ± 35	30 ± 2^{a}	37 ± 5^{b}	40.1 ± 0.7^{c}	31.9 ± 0.7^{c,d}	42.4 ± 0.9^{e}	51.4 ± 0.2^{f}	45 ± 1^{e}	42.0 ± 0.2^{d}
Yield %				11 ± 1^{b}	22 ± 2^{d}	27 ± 3^{e}	12 ± 1^{c}	27 ± 3^{e}	34 ± 3^{f}	7.3 ± 0.9^{a}	7.0 ± 0.9^{a}

TAA: total amino acids, EAA: total essential amino acids, n.d.: non detected. Values with different letters in each raw are significantly different when applying the LSD method at p-value ≤ 0.05. Ala: alanine, Gly: glycine, Val: valine, Leu: leucine, Ile: isoleucine, Thr: threonine, Ser: serine, Pro: proline, Asp: aspartic acid, Met: methionine, Hyp: hydroxyproline, Glu: glutamic acid, Phe: phenylalanine, Lys: lysine, His: histidine, Hyl: hydroxylysine, Tyr: tyrosine, Trp: tryptophan, Cys: cysteine.

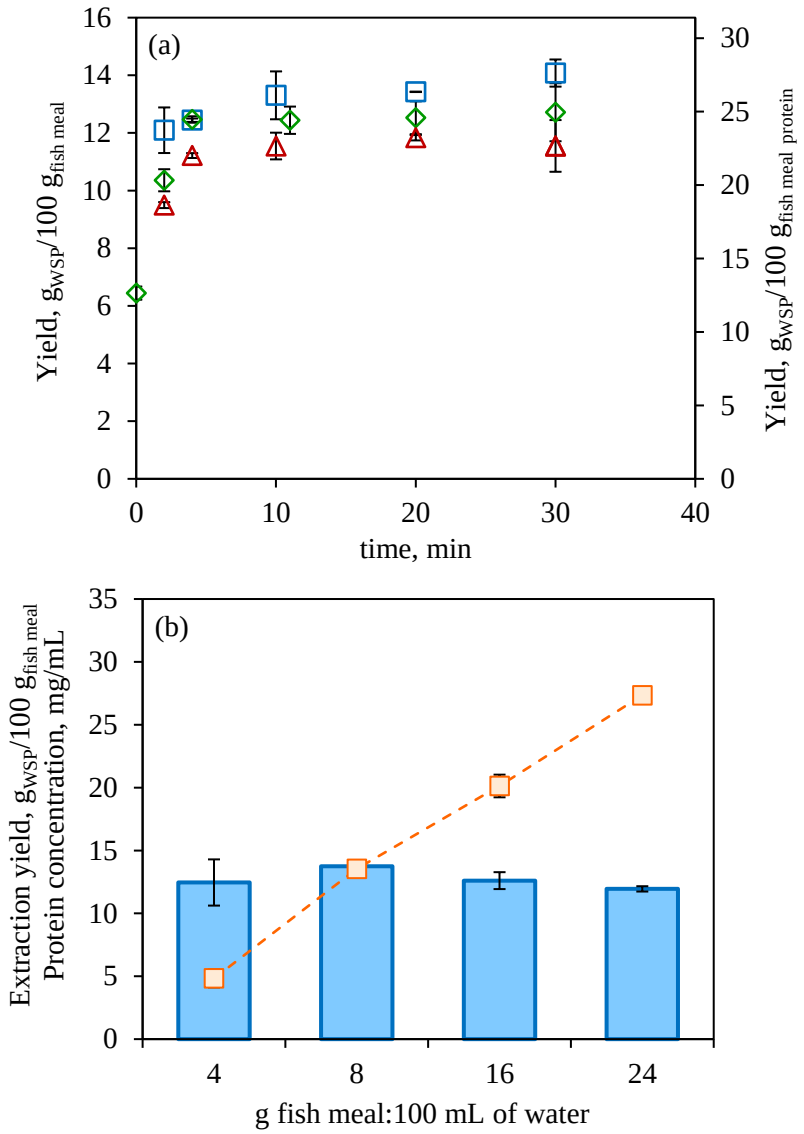

Figure 1.1. (a) WSP extraction kinetics at different temperatures (△ 20 °C, ◇ 50 °C, □ 80 °C) and a fixed ratio of 8 g of fish meal:100 g of water. **(b)** Effect of the solid solvent ratio on the WSP extraction yield (g_{WSP}/100 g fish meal, ▢) and protein concentration (mg/mL, ▢). Different letters in the extraction yield indicate means significantly different by using the LSD procedure at *p*-value ≤ 0.05.

The effect of fish meal to solvent ratio (w/v) on the WSP extraction was studied at 80 °C in the range from 4 to 24 g of fish meal per 100 mL of distilled water. Results at the final extraction time of 30 min are presented in Figure 1.1b. Figure

1.1b shows that the extraction yield, WSP/100 g fish meal, remained more or less constant in the range considered in this work, while the WSP concentration in the extract (mg WSP/mL) increased as the fish meal to solvent ratio increased. Since the extraction yield was of the same order, the WSP fraction was therefore more concentrated by decreasing the amount of solvent. However, the WSP extract obtained at the ratio 16 g fish meal:100 mL of distilled water was used for further hydrolysis studies instead of the highest fish meal:solvent ratio essayed (24:100) due to poor separation of the non-water soluble solid after extraction at this condition, since small particles and suspended solids were perceptible by the human eye after centrifugation of the extracts. The ratio of total soluble solids (SS) per g of dry fish meal was around 0.25 g SS /$g_{\text{dry fish meal}}$ for any of the fish meal to solvent ratios studied. Therefore, according to the Lowry assay, half of the soluble solids correspond to solids of protein nature.

Characterization of the WSP was done in terms of the amino acid profile. Free and bound amino acids of the WSP have been listed in Table 1.1. The percentage of free amino acids regarding the total content of amino acids in the WSP extract was 5.8 % (w/w). Similar to the original fish meal, the major amino acids in the WSP extract were alanine, glycine, proline and glutamic acid; however, the content of glycine and proline was nearly double in the WSP extract than in the original fish meal protein.

3.3. Hydrolysis of water-soluble protein by subcritical water

The WSP extract was subjected to hydrolysis by subW at different temperatures from 140 to 180 °C. Pressure was fixed at 5 MPa by using two different gases as pressurization agents, N_2 and CO_2.

3.3.1. Release of amino group

To follow the hydrolysis of the protein fraction, samples were withdrawn during the experiment and the ninhydrin assay was performed to determine the total number of primary amines released to the medium. Firstly, the initial content of primary amines in the WSP extract was determined, resulting 34 ± 1 meq leucine/L (1.7 ± 0.2 meq leucine/g WSP). However, the number of free amino acids determined in the characterization of the WSP extract (see Table 1.1) was much lower as determined by the sum of individual free amino acids determined by GC (59 ± 2 mg/g WSP or 0.475 ± 0.004 mmol/g WSP or 9.4 ± 0.1 mM). The difference could be attributed to the compounds determined by the ninhydrin test, since the test would include all type of primary amines such as peptides, proteins, amino acids, amines and even ammonia (Friedman, 2004). As it has been widely reported in the literature, during processing of fish products, degradation of proteins can take place, leading to the formation of different non-protein nitrogen compounds such as biogenic amines, total volatile basic nitrogen, trimethylamine, dimethylamine and ammonia (Folador *et al*., 2006). Some of these compounds can yield the characteristic chromophore of ninhydrin with primary amino groups.

Figures 1.2a and 1.2b show the kinetics for the release of amino groups in subW, as determined by the ninhydrin assay, at the three different temperatures studied, 140, 160 and 180 °C, by using nitrogen or CO_2 as pressurizing agents, respectively. During protein hydrolysis, peptide bonds were broken, which resulted in an increase of primary amine concentration corresponding to an increase in the degree of hydrolysis of WSP.

An increase in temperature led to a faster and higher release of amino groups due to the hydrolytic action of subW for both pressurization gases. The initial rate of amino groups released was evaluated at the three temperatures, determining statistically significant differences in the initial slopes considering the temperature as the factor at the 99 % confidence level for both pressurization agents (Table 1.2). Similar effect of temperature on protein hydrolysis degree has been previously

reported for different types of biomass and model proteins such as bovine serum albumin (Alonso-Riaño *et al*., 2021; Koh *et al*., 2019; Trigueros, Sanz, *et al*., 2021) where an increase in temperature led to an increase in the release of amino group under subW conditions. In the temperature range covered in this work, the ionic product of water, K_w, increases with temperature due to the high levels of hydronium (H_3O^+) and hydroxide (OH^-) ions that favor protein hydrolysis.

Table 1.2. Initial rate of release of amino groups, meq leucine/L min, in subW at different temperatures in different atmospheres, N_2 and CO_2.

T, °C	N_2	CO_2
140	$0.0107 \pm 0.0006^{a, A}$	$0.0136 \pm 0.0006^{a, B}$
160	$0.0345 \pm 0.0007^{b, A}$	$0.040 \pm 0.002^{b, B}$
180	$0.055 \pm 0.002^{c, A}$	$0.051 \pm 0.003^{c, A}$

Different lowercase letters in each column indicate that there are statistically significant differences among the slopes at the 99 % of higher confidence level for the different pressurization agents at the different temperatures.
Different capital letters in each row indicate that there are statistically significant differences among the slopes at the 99 % of higher confidence level at each temperature level considering the effect of the pressurization agent.

Regarding the effect of the addition of CO_2 as pressurization agent instead of N_2, slightly higher values of the initial release of amino groups were obtained by using CO_2 at the different temperatures essayed, except for 180 °C; however, the final value of amino group release was similar for both systems. Therefore, the expected enhancement of the acidic behavior of the medium due to the addition of CO_2 was hardly observed by the ninhydrin method. It could be concluded that the ninhydrin assay allowed us to qualitatively follow the protein hydrolysis, but the presence of different primary amines in the medium could interfere in the determination of free amino acid release.

3.3.2 Total protein content in the subW hydrolysates of soluble water protein

Total protein content was also monitored by the Lowry assay along subW treatment. During the experiments, a decrease in the total protein content was observed, being more pronounced at higher operating temperatures for both pressurization agents (N_2 and CO_2, Figures 1.2c and 1.2d, respectively).

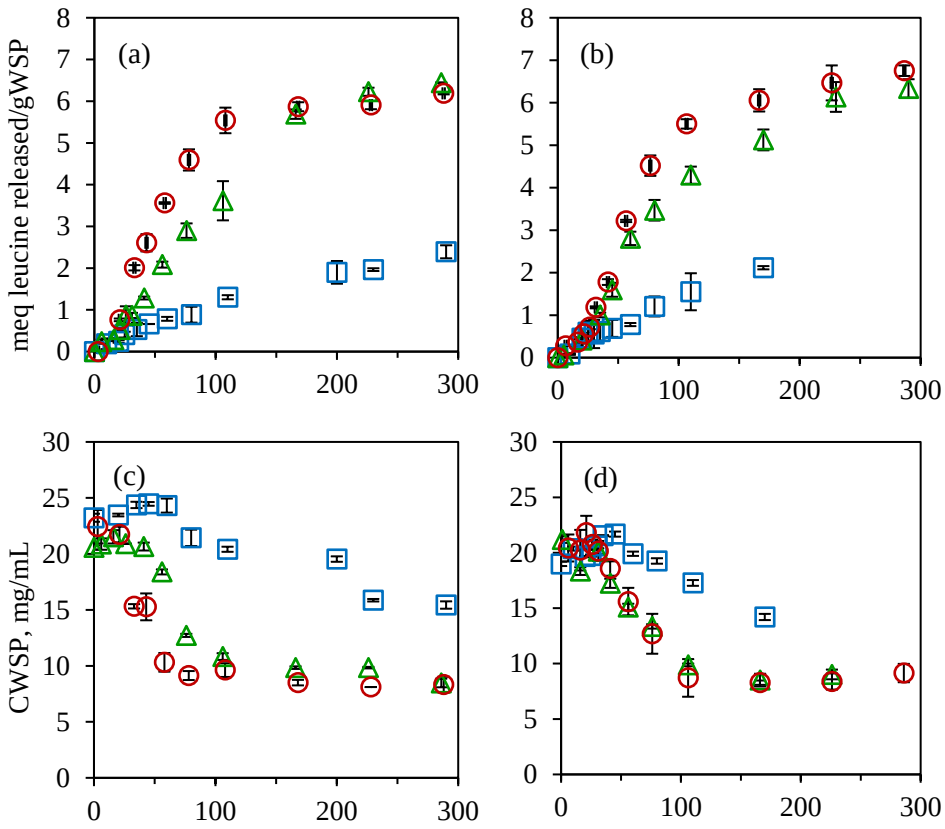

Figure 1.2. (a, b) Amino groups release kinetics by subW. **(c, d)** Evolution of the total protein content in subW hydrolysates. **(a, c)** N_2 and **(b, d)** CO_2, at different temperatures (□ 140 °C, △ 160 °C, ○ 180 °C).

The hydrolysis of the WSP into small peptides and free amino acids might be responsible for the decrease response in the Lowry assay. According to the literature, with the exception of tyrosine and tryptophan, free amino acids will not produce a

colored product with the Lowry reagent, although most dipeptides can be detected (Schaich, 2016). Furthermore, for peptides, color formation increases with peptide size as well as with the presence of tyrosine, tryptophan, cysteine, histidine and asparagine in the peptide or protein backbone. This fact has been also observed in this work, since a mixture of pure amino acids standards (in a similar concentration as the one obtained in the hydrolysis of WSP by subW at 180 °C in the presence of CO_2, see section 3.3.3) did not produce an appreciable colored product. Additionally, solutions of protein standards of different molecular weight (see Figure 1.3) were prepared at the same concentration (0.2 mg/mL) and the Lowry response, as absorbance, was determined. Figure 1.3 shows that proteins above 40–50 kDa yielded a similar response to the Lowry assay. However, for smaller proteins and peptides the response is generally lower than for molecules of higher molecular weight and it seems to be affected by the amino acid composition. Similar conclusions were reached by Rodrigues *et al*. (2021) in the protein hydrolysates from shellfish waste streams obtained by using subW extraction.

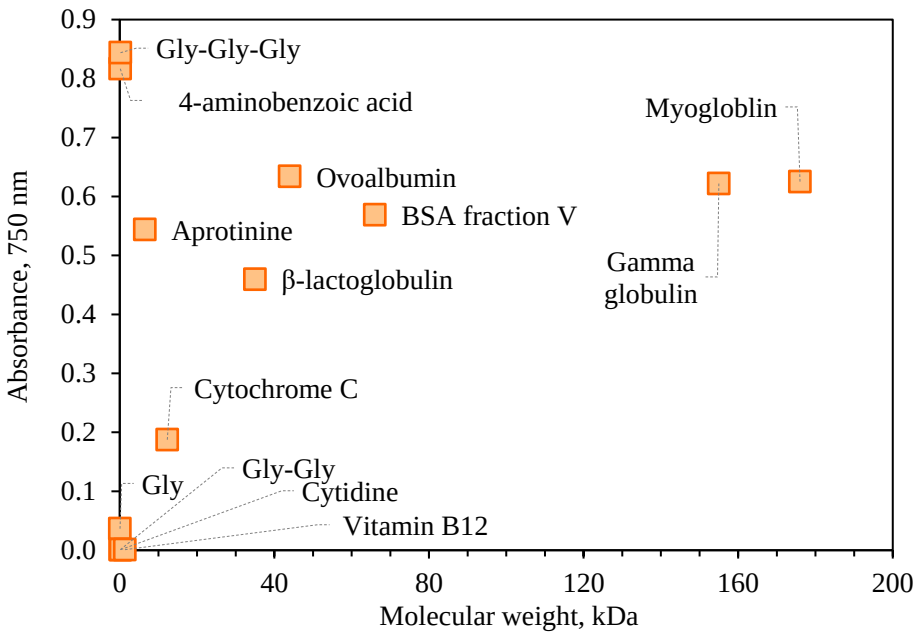

Figure 1.3. Response of different standard proteins and peptides at the same concentration (0.2 mg/mL) by the Lowry assay method.

To ensure that no protein or peptides degradation was taking place at the working conditions essayed in this work, total nitrogen was determined by TOC analysis during the subW treatment carried out at 180 °C in the presence of CO_2. Assuming the same N-factor as for total WSP, the total protein fraction in the subW extracts remained constant with values of 22 ± 2 mg/mL. Therefore, it can be concluded that when the Lowry method is used to quantify the total solubilized protein in different hydrolysis studies, small peptides obtained could lead to a lower response, as it has been demonstrated in this work.

3.3.3 Free amino acid profile in the subW hydrolysates

Determination of amino group release by the ninhydrin assay could overestimate the WSP hydrolysis yield into free amino acids and small peptides, since the test would include other primary amines (Friedman, 2004). Therefore, it is important to quantify the total undamaged free amino acids formed in the hydrolysate.

Individual free amino acids content expressed as mg aa/g WSP is listed in Table 1.1 for subW treatment. It can be clearly observed that total free amino acid content, evaluated as the sum of the individual free amino acid determined by GC, increased by increasing temperature due to an increase of the dissociation constant of water creating a more acidic medium. Other works have found a maximum in the total free amino acid content in subW hydrolysates from different protein sources at much higher temperature than the maximum temperature studied in this work. For instance, Quitain *et al*. (2001) determined a maximum at 523 K, 4 MPa and 60 min of reaction time in a batch configuration in the subW hydrolysis of the protein from shrimp shells (around 233 mg of free amino acids per g of shell protein).

Although the maximum temperature would be different for each amino acid, for the predominant amino acids determined in the WSP hydrolysate, no degradation was taking place at the working conditions of this work (maximum temperature of 180 °C and 288 min treatment time). A common factor used when working with

subW is the severity factor that combines the effect of treatment time and temperature according to the following expression(Alonso-Riaño *et al*., 2021):

$$\log R_o = \log\left(t \cdot \exp\left(\frac{(T-T_{ref})}{14.75}\right)\right) \quad \textbf{[1.3]}$$

where t is the treatment time (min), T is the operating temperature (°C) and T_{ref} is equal to 100 °C. In the literature, a maximum in the free amino acids production was obtained at severity factors around 5.9–6.2 from different protein sources (Quitain *et al*., 2001; Rogalinski *et al*., 2005); while the highest severity factor applied in this work corresponds to 4.8 (at 180 °C and 288 min treatment time). Therefore, according to the maximum observed in the literature for free amino acids at higher severity factors no degradation was observed in this work, at least for the predominant free amino acids formed in the subW hydrolysate.

The amount of free amino acids in subW hydrolysates was significantly higher in the presence of CO_2 compared with N_2, at all the working temperatures essayed in this work. For instance, by working at 180 °C, 275 ± 3 and 344 ± 5 mg free aa/g WSP were obtained in N_2 and CO_2, respectively (25 % higher in CO_2 than in N_2). According to Rogalinski *et al*. (2005) the solubility of CO_2 in water increases significantly in the subcritical region, increasing the concentration of protons in the medium enhancing the formation of free amino acids. These authors determined that the addition of CO_2 in the hydrolysis of bovine serum albumin as model protein induced the formation of 150.3 mg aa/g_{BSA}, obtaining 36.6 mg aa/g_{BSA} in the absence of CO_2. In the present work, the addition of CO_2 did not lead to such big increase, but around 14–25 % of increase was observed . These values were of the same order as the one reported by Zhu *et al*. (2010) who determined that the addition of CO_2 had also an effect on the amino acid production from bean dregs, with values around 20 % higher by using CO_2 instead of air. However, other works found different trends for each individual amino acid by using N_2, CO_2 and air as pressurization agents in the hydrolysis of fish meat by subW (Zhu *et al*., 2008).

In any case, in either of the two pressurization agents, N_2 or CO_2, free amino acids were produced with a similar qualitative profile. As it can be observed in Table 1.1, the major amino acids in the different hydrolysates were mainly alanine and glycine, followed by proline. These three amino acids accounted for 81 % and 74 % of the total free amino acids determined in the subW hydrolysates in N_2 and CO_2, respectively. Alanine and glycine were also determined as the most abundant amino acids in the subW hydrolysates of other protein sources such as hog hair (Esteban *et al*., 2010), entrails of fish meat (Kang *et al*., 2001), shrimp shells (Quitain *et al*., 2001) and pure protein such as bovine serum albumin (Rogalinski *et al*., 2005). These authors also determined arginine as one of the most abundant free amino acids in the subW hydrolysates, unfortunately, arginine cannot be determined with the EZ:Faast kit used in this work. The high content of these simple amino acids has been attributed to their stability under the working conditions, but also to the possibility of formation from decomposition of complex amino acids to simpler ones (Koh *et al*., 2019; Rogalinski *et al*., 2005). Production of these low molecular weight amino acids is important since they can be used as sweetness enhancing agents for use as food additives and taste enhancers (Quitain *et al*., 2001).

Figure 1.4 shows the recovery yield of each individual amino acid determined as:

$$Y_i = m_{i,subW}/m_{i,WSP} \qquad \textbf{[1.4]}$$

where $m_{i,subW}$ is the amount of amino acid "i" determined in the subW hydrolysates and $m_{i,WSP}$ the total amount of the amino acid "i" in the initial raw material, WSP, including the free and bound amino acids. Global yield, evaluated by considering the sum of all the individual free amino acids, has been also evaluated and listed in Table 1.1. Recovery yield of total free amino acids increased with temperature and in the presence of CO_2, observing significant differences at the different temperatures essayed and between both pressurization agents, reaching a maximum value of 34 ± 3 % at 180 °C.

According to the results presented in Figure 1.4, the highest recovery yield was achieved by alanine followed by glycine, achieving more than 80 % of alanine recovery at 180 °C in the presence of CO_2 (more than 70 % in N_2). As a general trend, the highest values of the individual recovery yield were obtained for most of the hydrophobic amino acids (leucine, phenylalanine, proline and valine) and the sulfur containing amino acid methionine. For these amino acids, there was a clear trend of increasing recovery yield by increasing temperature. This trend was also found by Hao *et al*. (2019) in the subW hydrolysates of Abalone viscera; however, for other free amino acids there was no trend with temperature or even a slightly decrease by increasing the working temperature (isoleucine, serine, threonine, serine or aspartic acid). Therefore, as concluded by Esteban *et al*. (2010), although some trends could be determined according to the type of side chain of the amino acid, not all the amino acids considering a specific side chain type were obtained in proportional amounts according to the amino acid composition of the protein source.

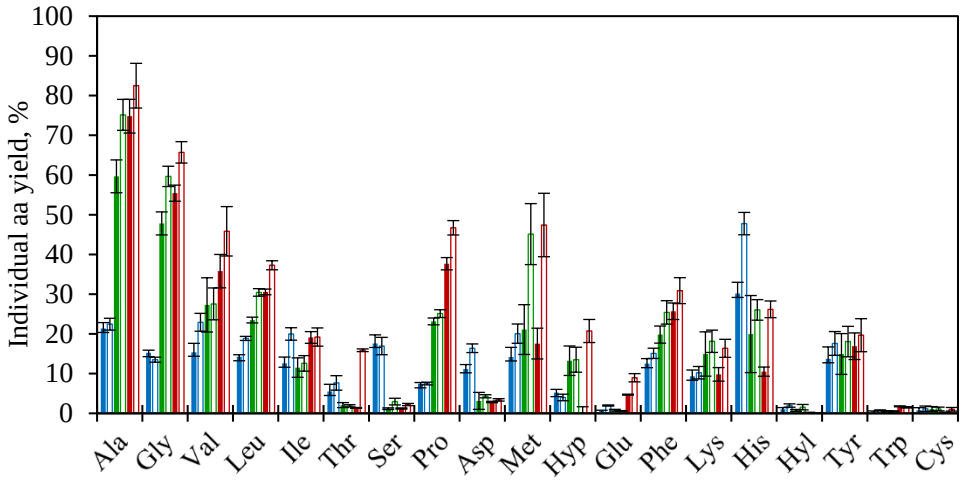

Figure 1.4. Individual amino acid yield obtained by subW with different pressurization agents and temperatures after 300 min treatment (140 °C: ■ N_2, □ CO_2) (160 °C: ■ N_2, □ CO_2) (180 °C: ■ N_2, □ CO_2).

The kinetics of the release of total and individual free amino acids from the WSP extract in subW have been determined at 180 °C in the presence of CO_2 and N_2. Some of the most representative free amino acids have been represented in

Figures 1.5a and 1.5b for N_2 and CO_2, respectively. In these figures, the amount of free amino acids at zero treatment time corresponds to the free amino acids that are initially soluble in water.

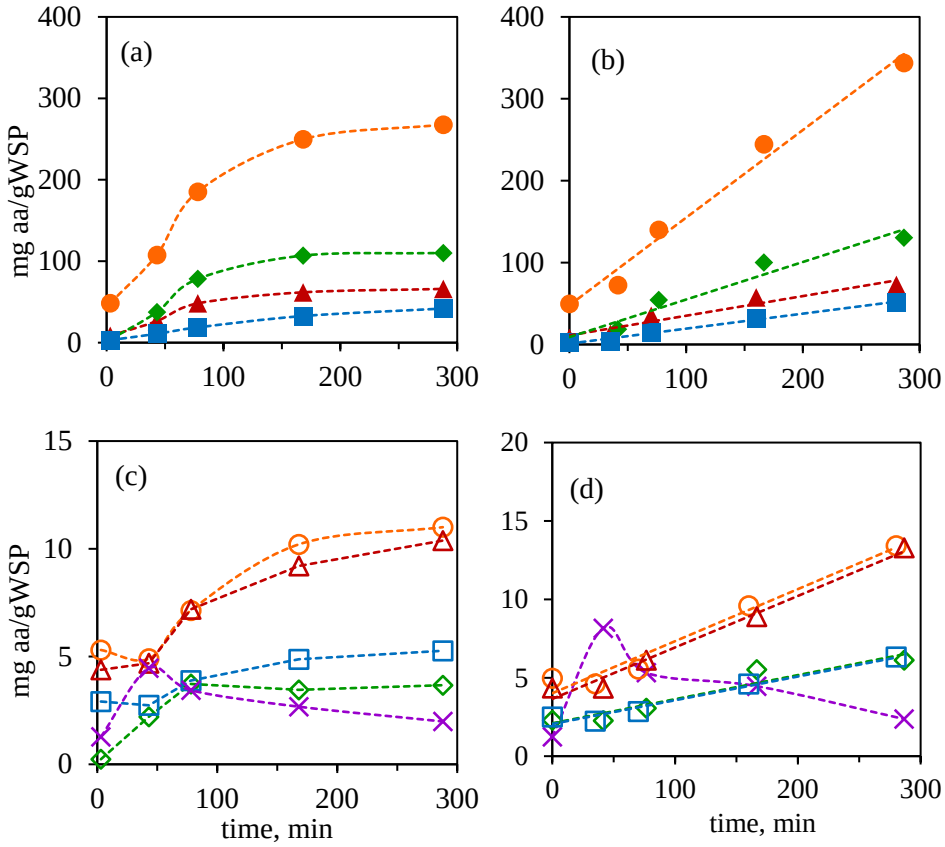

Figure 1.5. Total and individual amino acids release kinetic by subW at 180 °C. Total and major free amino acids **(a)** in N_2 **(b)** in CO_2: ■ proline, ◆ glycine, ▲ alanine, ● total amino acids. Other amino acids: **(c)** in N_2 **(d)** in CO_2: □ phenylalanine, ◇ lysine, △ valine, ○ leucine, × aspartic acid.

The qualitative profile for free amino acids was similar for CO_2 and N_2 pressurization agents; however, for total free amino acids and most of the major free amino acids it was observed a linear increase with reaction time in the presence of CO_2 suggesting that the maximum yield could not have been achieved. On the contrary, in the presence of N_2, there was a continuous increase with hydrolysis time up to 170 min and afterwards a plateau was reached and no further hydrolysis was

taking place. These results also indicated that the predominant free amino acids were stable under the employed conditions.

Figures 1.5c and 1.5d also show the evolution of aspartic acid. Although aspartic acid was not one of the major free amino acids determined in subW hydrolysate of WSP, it has been represented to show its maximum peak in the first minutes of treatment time and then a continuous decrease with reaction time. In this regard, it must be highlighted that aspartic acid belongs to the amino acid class of negatively charged group that has been found to be very liable in the hydrolysis of other protein sources such as BSA (Abdelmoez & Yoshida, 2013) or vegetable proteins (Alonso-Riaño *et al*., 2021).

3.3.4 Antioxidant capacity of subW hydrolysates

The antioxidant capacity of the subW hydrolysates of WSP was determined along treatment time and results are presented in Figures 1.6a and 1.6b in the presence of N_2 and CO_2, respectively. Reducing capacity at zero treatment time corresponds to the reducing power of the WSP extract with a value of 0.569 ± 0.002 mM Fe^{2+}.

All WSP hydrolysates showed an increasing reducing capacity due to subW treatment and it increased with operation temperature. Correlation coefficients between the reducing capacity of the hydrolysates and the amino group released have been determined according to the Pearson product moment correlation. Correlation has been also established between the reducing capacity and the results obtained by the Lowry assay since the decrease in the total protein content (Figure 1.2c and 1.2d) might indicate formation of smaller peptides with higher antioxidant capacity. Analysis indicated a statistically significant non-zero correlations at the 95.0 % confidence level coefficients between both variables with positive and negative correlation coefficients between reducing capacity and amino group release and Lowry assay, respectively. Correlation coefficients were 0.9316, -0.8624 for amino group release and Lowry assay, respectively in the presence of CO_2 (n=35, the

number of pairs of data values used to compute each coefficient) and 0.9159, -0.9238 for NH_2 release and Lowry assay, respectively in the presence of N_2 (n=30). Based on these coefficients, the strength of the correlation between reducing capacity and amino groups and the Lowry assay, as an indicator of smaller peptides size production, was of the same order.

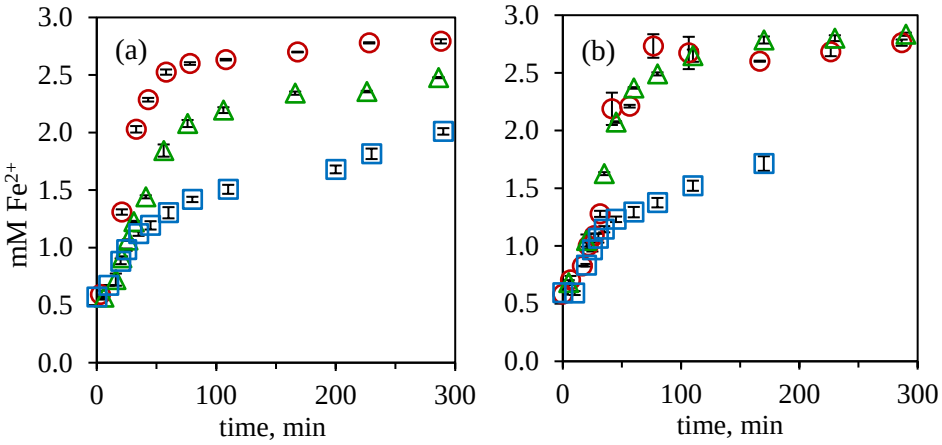

Figure 1.6. Evolution of the reduction capacity of subW hydrolysates with different pressurization agents. **(a)** N_2 and **(b)** CO_2, at different temperatures (□ 140 °C, △ 160 °C, ○ 180 °C).

3.4. Enzymatic hydrolysis of WSP

The results obtained in the hydrolysis of WSP by subW have been compared with conventional enzymatic hydrolysis by using two different commercial proteases, Alcalase® and Novozym®. Figures 1.7 a, b, c and d show the amino group release, the total protein content and the reducing activity obtained along time, respectively.

For both enzymes, the release of $–NH_2$ group is much lower than the release observed in subW, less than 1.2 meq leucine/g WSP were released after 240 min by enzymatic hydrolysis. By comparing both enzymes, final significant higher $–NH_2$ group release was observed for Alcalase® than for Novozym® (nearly a 30 % higher),

although there was not observed a significantly higher initial $–NH_2$ group release for both enzymes (Figure 1.7a).

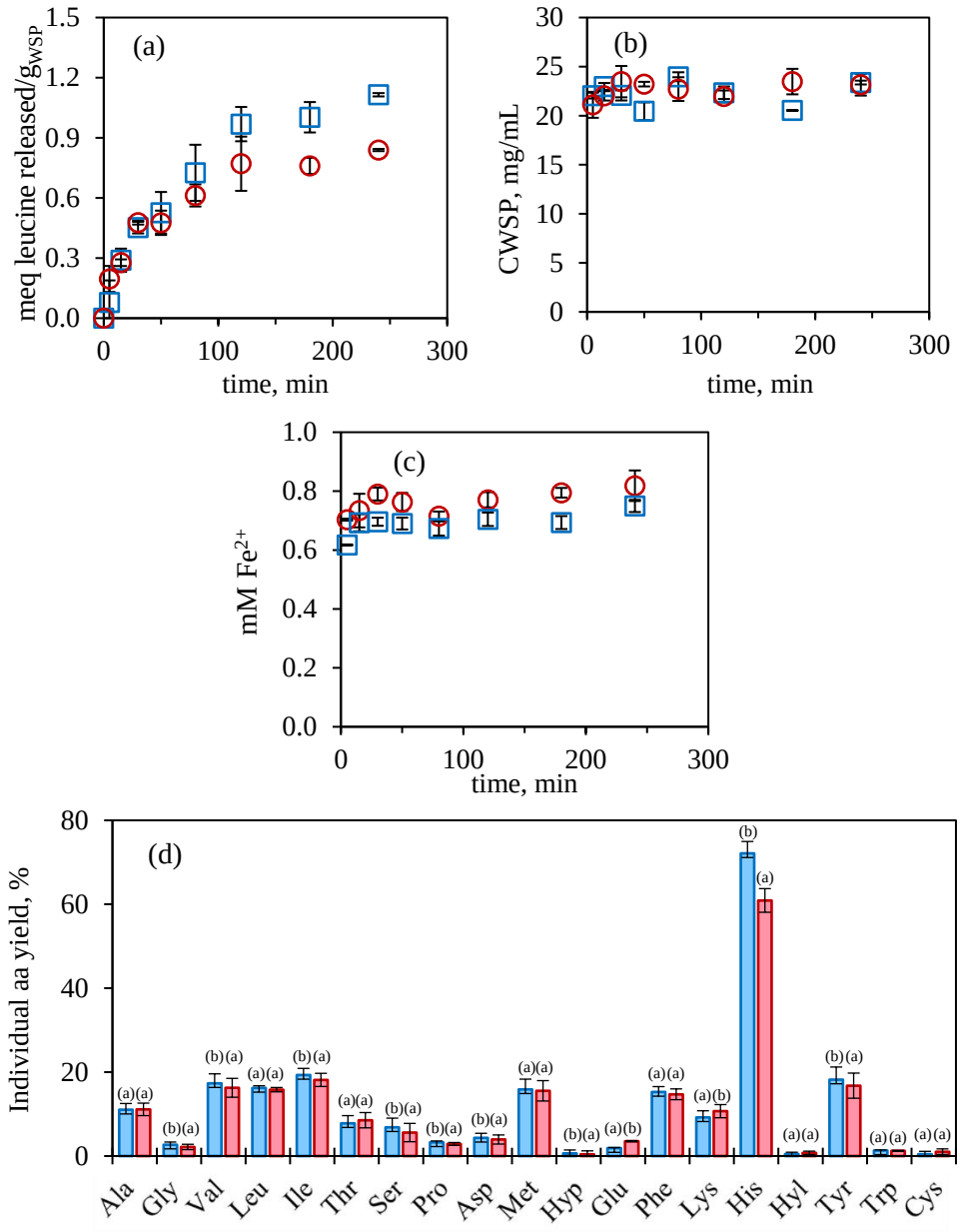

Figure 1.7. Enzymatic hydrolysis of WSP at 60 °C, pH = 8 and 225 U/100 mL of WSP extract. **(a)** amino group released **(b)** total protein content **(c)** reducing capacity: ◻ Alcalase®, ○ Novozym®. **(d)** Individual amino acid yield: ■ Alcalase®, ■ Novozym®.

Regarding total protein content, a clear decrease was observed by subW hydrolysis attributed to the production of small peptides and free amino acids; however, not a clear trend was observed in the total protein content by enzymatic hydrolysis that could be attributed to the generation of peptides of bigger size than by subW hydrolysis as it will be presented in section 3.5 (see Figure 1.7b). Furthermore, there were no statistically significant differences between the medium total protein content both enzymes along the kinetic process.

Figure 1.7c shows an initial slight increase in the reducing capacity of the enzymatic hydrolysates for both enzymes. The medium value of reducing capacity along enzymatic treatment was significantly higher for Novozym® than for Alcalase®; however, the reducing activity, for both enzymes, was much lower than the one observed by subW hydrolysis.

Total and individual free amino acids were also determined in the final enzymatic hydrolysates with similar values for both enzymes (75 ± 1 and 71.0 ± 0.6 mg/g WSP for Alcalase and Novozym, respectively) but much lower than the amount of free amino acids generated by subW hydrolysis. Table 1.1 shows the individual amino acid profile expressed as mg aa/g WSP obtained by Alcalase® and Novozym®, observing a similar free amino acid profile for both enzymes. The highest concentration corresponds to histidine (19.0 ± 0.7 and 16.1 ± 0.2 mg aa/g WSP for Alcalase® and Novozym®, respectively) followed by alanine (9.7 ± 0.1 and 9.8 ± 0.1 mg aa/g WSP for Alcalase® and Novozym®, respectively). The yield of the individual free amino acids was also evaluated according to Eq. 1.4 and results are presented in Figure 1.7d. The highest hydrolysis yield was obtained for histidine, with values of 75 ± 1 % and 71 ± 0.1 %, for Alcalase® and Novozym®, respectively. For the rest of amino acids, hydrolysis yields were lower than 20 %. The lower yield obtained for glycine, less than 3 %, must be highlighted, since this small size amino acid was one the major free amino acid obtained in subW hydrolysates. Both commercial enzymes are sold as endopeptidases, which may explain the low production of free amino acids. Comparison with literature data regarding the free

amino acid profile after enzymatic hydrolysis of marine protein is difficult since most of the studies do not present the individual free amino acid profile. Ovissipour *et al*. (2009) reported individual free amino acid yields after enzymatic hydrolysis of Persian sturgeon viscera by Alcalase® yielding the highest value for arginine (93 %), histidine (79 %) and methionine (75 %). The yield of histidine was of the same order as the one obtained in this work; unfortunately, arginine could not be determined by the analytical methods used in this work.

3.5. Molecular weight distribution of WSP hydrolysates

Molecular weight of the protein hydrolysates will play an important role in their functional properties. Therefore, to obtain information about the hydrolysate-length distribution and variations according to the different hydrolysis treatments, final subW hydrolysate obtained by subW in the presence of CO_2 at 180 °C and the enzymatic hydrolysate obtained by Alcalase® were analyzed by size-exclusion chromatography, and the results are shown in Figure 1.8, together with the molecular weight distribution of the WSP extract.

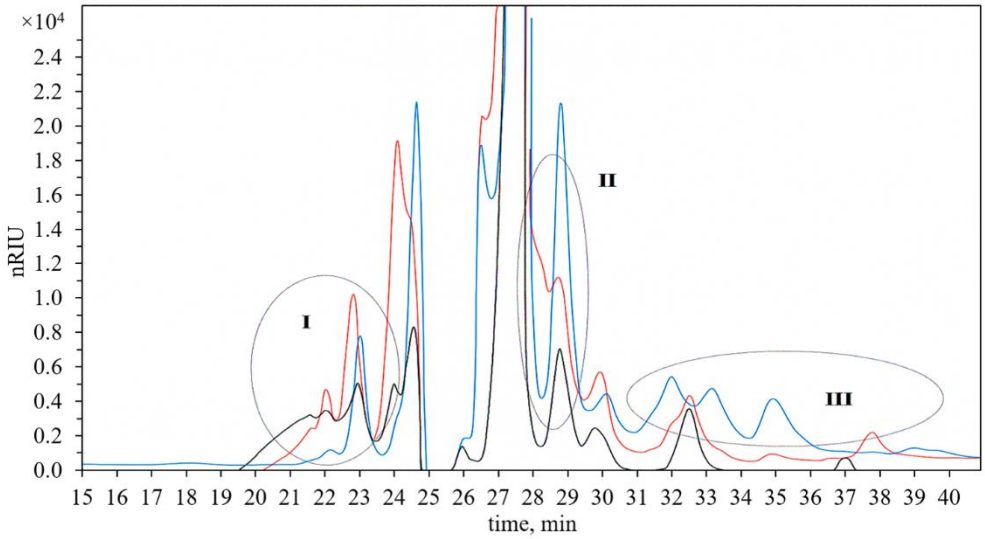

Figure 1.8. Molecular weight distribution of WSP extract (**black**), subW hydrolysate in CO_2 at 180 °C (**blue**), and enzymatic hydrolysate by Alcalase® (**red**).

Three major fractions were distinguished in the chromatogram presented in Figure 1.8: fraction I corresponds to the higher molecular size distribution proteins and peptides (> 17 kDa), fraction II corresponds to the peptides with molecular sizes around 0.4–0.5 kDa, whereas fraction III corresponds to the lower molecular ranged determined by the equipment configuration, < 0.1 kDa.

Both hydrolysis treatments, subW and enzymatic reduced the peptide size lengths compared with those of the original WSP extract. It was observed that the presence of the highest molecular weight species (fraction I) in the samples was more abundant in WSP, followed by Alcalase® hydrolysate and subW hydrolysate. These results support previous results presented in this work, in which the high molecular weight fraction present in the WSP extract was reduced after the enzymatic treatment and even more after the subW treatment. The hydrolysis was more intense in the subW hydrolysate, which showed more minor peaks in fraction III than WSP extract and the enzymatically hydrolyzed sample. The molecular weight distribution obtained in Fraction III agreed with the results presented in Table 1.1 where the total amount of free amino acids released by subW in CO_2 at 180 °C was higher than the amount of free amino acids released by enzymatic treatment or the free amino acid present in the WSP extract. Molecular weight of amino acids ranges from 75 Da for glycine ($C_2H_5NO_2$) to 204 Da for tryptophan ($C_{11}H_{12}N_2O_2$). Therefore, the higher distribution obtained for subW hydrolysate in Fraction III would correspond to the higher amount of free amino acids generated by subW (344 ± 5 mg aa /g WSP at 180 °C in CO_2) compared to enzymatic hydrolysates (71.0 ± 0.6 mg free aa/g WSP for Alcalase®). Similar area distribution of the lowest molecular weight range (Fraction III) was obtained for the WSP extract and the enzymatic hydrolysates supporting by the similar amount of free amino acids in both samples (59 ± 2 mg free aa/g WSP for WSP extract, see Table 1.1).

It is also worth highlighting that the signals of peptides of Fraction II was much higher for subW hydrolysate than for the enzymatic hydrolysate. Taking into account the molecular weight distribution of individual amino acids (from 75 Da to 204 Da),

the small peptides generated in this fraction would consist of 2–6 amino acids units. Fraction II was more prominent in the subW hydrolysate supporting the fact that smaller peptides were generated than by enzymatic hydrolysis. These results were supported by the Lowry assay that might indicate the generation of smaller size peptides by subW than by enzymatic hydrolysis due to the decreasing signals as decreasing the peptide molecular size.

4. Conclusions

Protein hydrolysates from fish meal can be an excellent source of nitrogen for different food applications. The combination of analytical techniques performed in this work, such as the amino group release, protein content by Lowry method, (free and bound) amino acid profile, antioxidant capacity and molecular weight distribution, has been carried out in order to characterize the protein hydrolysis and explore alternatives to the conventional process.

According to the amino group release profiles and the production of free amino acids, temperature in the 140–180 °C range has a positive effect in the WSP hydrolysis by subW. The use of CO_2 as pressurization agent favored the production of free amino acids, likely due to the carbonate formation and the associated pH reduction of subW, compared to the inert N_2. The Lowry analysis showed lower responses when increasing hydrolysis temperature and treatment time, which is likely related to the reduction in peptide size and the liberation of non-reactive free amino acids, rather than to protein degradation. The molecular weight distribution supported the results obtained in the amino group release and free amino acid analyses.

Compared to enzymatic hydrolysis with commercial proteases, hydrolysis of the WSP fraction of fish meal by subW achieved much higher release of amino groups and free amino acids in a similar reaction time, and with no need of additional catalysts or reagents. Small amino acids such as glycine and alanine were

preferentially released by subW treatment compared to enzymatic hydrolysis. These results show the benefits of subW technology for protein valorization.

CHAPTER 2

Green fractionation and hydrolysis of fish meal to improve their techno-functional properties

Adapted from the article:

P. Barea, R. Melgosa, Ó. Benito-Román, A.E. Illera, S. Beltrán, M.T. Sanz (2024).

"Green fractionation and hydrolysis of fish meal to improve their techno-functional properties"

Food Chemistry, *452*, 139550.

DOI: https://doi.org/10.1016/j.foodchem.2024.139550

Capítulo 2

Fraccionamiento e hidrólisis sostenibles de harina de pescado para mejorar sus propiedades tecno-funcionales

Resumen

Se ha adoptado una estrategia sostenible que emplea agua como disolvente (SWH) para obtener hidrolizados de proteínas a partir de harina de pescado (FM), de su fracción soluble en agua (WSP) y de su fracción no soluble en agua (NSP). Se han investigado las propiedades tecno-funcionales de estos hidrolizados y se han comparado con los hidrolizados obtenidos con Alcalasa®. En general, los hidrolizados de SWH presentaron mayor contenido de aminoácidos libres y mayor grado de hidrólisis, lo que se reflejó en la distribución del tamaño molecular. Sin embargo, los hidrolizados de Alcalasa® presentaron una mejor solubilidad (de 74 ± 4 % con NSP a pH = 2 hasta 99 ± 1 % con WSP a pH = 4–7). Según los experimentos de fluorescencia, los hidrolizados de FM y NSP mostraron la mayor hidrofobicidad superficial, lo que se ha relacionado con mejores propiedades emulsionantes y una mayor estabilidad de la emulsión. Las emulsiones estabilizadas con 2 % p/v de NSP tratadas con SWH mostraron los tamaños de partícula más pequeños, con D[4,3] = 155 nm en el día 0, y buena estabilidad, con D[4,3] = 220 nm en el día 7, lo que demuestra que el fraccionamiento con agua seguido de tratamiento SWH es un buen método para mejorar las propiedades tecno-funcionales de los hidrolizados.

Palabras clave: Proteína de harina de pescado, fraccionamiento con agua, hidrólisis, agua subcrítica, emulsión.

Chapter 2

Green fractionation and hydrolysis of fish meal to improve their techno-functional properties

Abstract

A green strategy employing water as solvent (SWH) has been adopted to obtain protein hydrolysates from fish meal (FM), its water-soluble fraction (WSP), and its non-water-soluble fraction (NSP). The techno-functional properties of the hydrolysates have been investigated and compared to hydrolysates obtained with Alcalase®. In general, SWH hydrolysates presented higher content of free amino acids and higher degree of hydrolysis, which reflected on the molecular size distribution. However, Alcalase® hydrolysates presented better solubility (from 74 ± 4 % for NSP at pH = 2 up to 99 ± 1 % for WSP at pH = 4–7). According to fluorescence experiments, FM and NSP hydrolysates showed the highest surface hydrophobicity, which has been related to better emulsifying properties and higher emulsion stability. The emulsions stabilized with 2 % (w/w) of SWH-treated NSP showed the smallest particle sizes, with D[4,3] = 155 nm at day 0, and good stability, with D[4,3] = 220 nm at day 7, proving that water fractionation followed by SWH treatment is a good method to improve the techno-functional properties of the hydrolysates.

Key words: Fish meal protein, water fractionation, hydrolysis, subcritical water, emulsification.

1. Introduction

Fish meal is the main co-product of the fish industry, together with fish oil. Fish meal production has increased over the last years, reaching > 16 million tonnes in 2020 (FAO, 2022), mainly linked to its utilization in aquaculture and as an ingredient in the pet-food industry. Fish meal presents a high protein content as well as a valuable lipid fraction composition. However, the rise of novel sources of protein resulting from the increasing demand of a growing and aging population, urge fish meal producers to explore new processing methods and obtain novel valuable products. Increasing processing yield and efficiency in the utilization of these resources may further reduce the environmental footprint of food produced from marine resources. Therefore, optimal utilization of fish co-products as part of the biomass, which is unavoidably harvested, and development of technologies enabling their value addition to high quality proteins is urgently needed.

Fish co-products contain valuable proteins, polyunsaturated fatty acids (PUFAs), essential amino acids, vitamins, and minerals (Wisuthiphaet & Kongruang, 2015; H. Wu *et al*., 2022). Moreover, fish-derived protein hydrolysates have been reported to have remarkable bioactive effects, such as antioxidant, anticancer, antimicrobial, antihypertensive, immunomodulatory, and anti-thrombotic activities, among others (Shahidi *et al*., 2019). Techno-functional properties of fish protein hydrolysates have also been reported, including good solubility, foaming, gelling, and emulsifying properties. These functional properties are closely related to the physicochemical characteristics of the proteins, peptides, and amino acids, such as molecular weight, amino acid composition and surface hydrophobicity (Chen *et al*., 2019), and play a very important role in the texture and sensory quality of food during processing and storage (Brishti *et al*., 2020; N. Li *et al*., 2022).

Subcritical water hydrolysis (SWH) of proteins has been proposed as an environmentally friendly alternative to exploit the valuable compounds present in

fish co-products. Subcritical water treatment uses liquid water at temperatures between 100 and 374 °C. At these conditions, decreases as temperature rises due to hydrogen bond dissociation, making water an effective solvent for moderately polar to non-polar substances. Moreover, the ionic product of water (K_W) increases significantly with temperature, enhancing the concentrations of hydronium and hydroxide ions. This enables water to function as an acid or base catalyst, facilitating the hydrolysis of biomass from different origins, such as lignocellulosic polymers and proteins, into smaller oligomers and peptides without requiring additional catalysts (Ali *et al*., 2023; Melgosa *et al*., 2021). For these reasons, SWH can be considered greener than the widely employed chemical and enzymatic methods, providing a purer final extract without need of reprocessing.

Previous works have already reported important benefits of SWH compared to enzymatic hydrolysis, such as the higher degree of hydrolysis and release of amino groups that can be achieved in a similar reaction time and with no need of additional catalysts or reagents (Barea *et al*., 2023). Moreover, increasing temperature and acidifying the reaction media with pressurized CO_2 enhanced the hydrolysis process and the free amino acid release, which have been also associated to better physicochemical and bioactive properties of the FPHs, such as higher antioxidant capacity (Barea *et al*., 2023). However, few studies have explored the influence of the preparation method on important techno-functional properties of fish meal hydrolysates, such as solubility, surface hydrophobicity, and emulsifying capacity. These properties may be influenced by environmental factors and processing conditions and make the fish protein hydrolysates much more interesting in a wide variety of fields, highlighting food, cosmetic and pharmacy industry. The different fractionation and hydrolysis processes conducted on a protein sample determine the molecular structure of the hydrolysates and their further capacity as a techno-functional ingredient (Lv *et al*., 2023).

In this work, the double role of the greenest solvent, water, is emphasized. First, water has been used as a solvent for the fractionation of fish meal proteins. On the

other hand, water in subcritical conditions has been used as hydrolytic agent, avoiding the use of chemical solvents and strong acids and alkalis in the production of fish protein hydrolysates. The products obtained from the hydrolysis of the different substrates: fish meal (FM), and the water-soluble protein (WSP) and non-water-soluble protein (NSP) fractions, will be characterized in terms of protein content and amino acid composition. Besides, the different techno-functional properties of the hydrolysates obtained by using only water as solvent and hydrolytic agent will be evaluated. The results obtained can be further used to enhance the use of fish protein hydrolysates in different applications (e.g.: feed and food, cosmetics, or pharmaceutical products), enhancing the sensory, nutritional, and physicochemical properties, while simultaneously improving the economy of its production.

2. Experimental

2.1. Raw Material

Fish meal from tuna (*Thunnus* sp.) was kindly supplied by *Sarval Bio-Industries Noroeste*, S.A.U. (A Coruña, Spain). It was provided in a powdered formulation and used as it is. Characterization has been carried out in a previous work (Barea *et al*., 2023), finding a moisture content of 3.4 ± 0.1 % (w/w); the crude protein, ash, and lipids, expressed in a dry basis, were 51 ± 2 %, 21.7 ± 0.2 %, and 6.5 ± 0.2 % (w/w), respectively. Until use, the fish meal was stored in sealed air-tight polypropylene bags under refrigeration conditions (4 °C) and protected from light.

2.2. Fractionation of fish meal

Fish meal fractionation was achieved by water extraction. Based on previous studies (Barea *et al*., 2023), fish meal was mixed with water at a ratio of 16 g fish meal/100 mL water (16:100) in a stirred reactor thermostated at 80 °C for 30 min. Subsequently, the resulting slurry was cooled down and filtered through a cheese

cloth to obtain a liquid fraction, the water-soluble protein (WSP), and a solid fraction, the non-water-soluble protein (NSP), which was gently dried in an oven at 40 °C for 48 h.

Further characterization analysis and hydrolysis experiments were performed with the original fish meal (FM) and the WSP and NSP fractions, which were stored at -18 °C prior to analysis.

2.3. Subcritical water hydrolysis (SWH)

Subcritical water hydrolysis (SWH) of FM, and WSP, and NSP fractions was performed in a lab-built discontinuous reactor with an internal volume of 0.5 L. The equipment has been described elsewhere (Barea *et al*., 2023).

For the solid samples, 20 g of FM or NSP were charged into the reactor and suspended in 200 mL of distilled water. In the case of the liquid WSP fraction, SWH process was carried out in a similar way, except that 200 mL of the filtered liquid were directly charged into the reactor and no additional water was used. In a typical experiment and based on previous studies (Barea *et al*., 2023), hydrolysis temperature was set at 180 °C and pressure at 5 MPa. Pressurization of the reactor was achieved using CO_2, which causes acidification of the reaction medium and promotes efficient protein hydrolysis (Barea *et al*., 2023). After 300 min of SWH process, the vessel was cooled down and depressurized when the temperature was lower than 90 °C. Subsequently, the hydrolysates were withdrawn, filtered through Whatman no. 5 filter paper to separate the solids in the case of the FM and NSP extracts, and frozen at -18 °C for further analysis.

2.4. Enzymatic hydrolysis

Based on previous studies (Barea *et al*., 2023), the commercial protease Alcalase®, kindly donated by Novo Nordisk A/S, was selected in this work. The protease activity was already determined in a previous work (Barea *et al*., 2023) by

the casein method, resulting in 1157 ± 74 μmol of tyrosine/mL of enzyme preparation.

In the enzymatic hydrolysis study, 10 g of solid (FM, or NSP) were charged into a jacketed glass reactor and suspended into 100 mL of phosphate buffer at pH 8. When the temperature reached 60 °C, the reaction was started by adding 225 U of pre-warmed Alcalase®. In the case of WSP, 100 mL of the liquid obtained in the fractionation step were filtered and charged into the reactor, which was preheated at 60 °C, and mixed with 225 U of preconditioned Alcalase®. Enzymatic hydrolysis was carried out for 24 h at constant temperature of 60 °C. After that, the mixture was immersed in boiling water for 5 min to inactivate the enzyme and subsequently cooled down in an ice bath, filtered through Whatman no. 5 filter paper and frozen at -18 °C for further analysis.

2.5. Freeze drying

Freeze-dried protein hydrolysates (FDH) were obtained from the liquid and filtered hydrolysates produced in the SWH process and in the enzymatic hydrolysis. First, liquid hydrolysates were placed in a Petri dish and equilibrated at -80 °C for 2 h. Then, the frozen samples were submitted to freeze-drying at $1.5 \cdot 10^{-4}$ mbar (Telstar Lyoquest) until moisture was lower than 3 % (w/w).

After lyophilization, the FDHs were weighed in order to calculate the final hydrolysis yield. FDHs were stored in dark hermetic flasks under refrigeration conditions (4 °C) for further analysis.

2.6. Characterization

Samples from the FM, WSP and NSP substrates and their corresponding FDHs were analyzed in order to evaluate the fractionation and hydrolysis process.

2.6.1. Elemental analysis

The elemental composition (C, H, N, S) of the original FM, WSP and NSP fractions and the FDHs was determined by elemental microanalysis in an EA Flash 2000 apparatus (Thermo Scientific, USA), equipped with a thermal conductivity detector (TCD). Oven temperature was set at 900 °C and gas flows were 250 mL/min for oxygen and 140 mL/min for helium, used as the carrier gas. A second flow of helium (100 mL/min) was used as a reference for the detector, whereas the calibration curve was prepared with different concentrations of 4-aminobenzenesulfonamide.

2.6.2. Amino acid profile

The amino acid profile was analyzed by gas chromatography (Hewlett-Packard, 6890 series) with an EZ:Faast^{TM} AAA GC kit, following the method described by Trigueros, Sanz, *et al*. (2021). Amino acid profile of FM, WSP and NSP substrates was determined after hydrolysis using 6 N HCl at 100 °C during 24 h and further derivatization. Since tryptophan and cysteine are lost by acid hydrolysis, and methionine can be partially destroyed, an alkaline hydrolysis was also carried out to determine these amino acids (Trigueros, Sanz, *et al*., 2021). Arginine cannot be detected by this kit and asparagine and glutamine were quantified as aspartic and glutamic acids, respectively.

Free amino acids in the FM, WSP and NSP substrates were determined by derivatization and GC-FID analysis, following the previously described method (Trigueros, Sanz, *et al*., 2021) without prior HCl or alkaline hydrolysis. The difference between total amino acids after hydrolysis and free amino acids were referred to as bound amino acids. Free amino acids were also determined for the FDHs.

2.6.3. Degree of hydrolysis

The degree of hydrolysis (DH) was estimated by the ninhydrin reaction method according to the Sigma Aldrich protocol. 1 mL of ninhydrin reagent solution was gently mixed with 2 mL of sample and heated for 10 min at 100 °C using a boiling water bath. Afterwards, the samples were cooled, and 5 mL of 95 % ethanol were added. The absorbance was measured at 570 nm. A calibration curve was constructed using a leucine solution daily prepared (Friedman, 2004). The DH was evaluated according to Eq. 2.1 (Adler-Nissen, 1979):

$$\text{DH}\ (\%) = \frac{\text{h}}{\text{h}_{\text{tot}}} \times 100 \qquad \textbf{[2.1]}$$

where h is the number of equivalent peptide bonds hydrolyzed, expressed as meq/g protein and h_{tot} is the total amount of millimoles of individual amino acids per gram in the unhydrolyzed protein that can be evaluated from the amino acid profile.

2.7. Physicochemical and techno-functional properties

2.7.1. Protein solubility (PS)

PS was determined according to the method described by N. Li *et al*. (2022) with some modifications. In brief, 10 mg of lyophilized extracts were dispersed in 20 mL of distilled water maintained at different pH values (pH 2.0, 4.0, 7.0 and 10.0) by adding HCl or NaOH. The mixture was stirred for 15 min and then centrifuged at 8000 g for 30 min. The nitrogen content of the supernatants was measured using the Lowry method as described by Barea *et al*. (2023). PS was expressed as percentage ratio of the protein content of the supernatant to the total protein content. Results are expressed as the mean of three replicates.

2.7.2. Surface tension

Surface tension was measured in an optical tensiometer (Attension Theta, Biolin Scientific), using the pendant drop method. Briefly, 2 g of FDH were dispersed in 95 mL of distilled water at ambient temperature. Droplets of ca. 4 µL were created with the help of a micro-syringe, which was fixed to the apparatus and aligned to a high-resolution camera. Images of the pendant drop were taken during 10 s to measure the drop volume and radius, and the surface tension was calculated from these measurements using the OneAttension software (Biolin Scientific). Results are reported as the average of three measurements.

2.7.3. Molecular weight distribution of the hydrolysates

The molecular size distribution of the FDHs was measured by Gel Permeation-Size Exclusion Chromatography (GPC-SEC) in an HPLC system (Agilent 1260 infinity II) coupled to a refraction index detector (RID). The column system consisted of a Proteema precolumn (4.6 x 30 mm) and a micro column (4.6 x 250 mm) with a porosity of 100 Å and a particle size of 3 µm (PSS Polymer Standards Service GmbH), which allowed for good separation in the range from 150 Da to 100 kDa. The mobile phase was 0.01 M ammonium acetate at a flow rate of 0.3 mL/min. Separation and detection were conducted at 35 °C. Data acquisition and GPC-SEC calculations were performed using OpenLab CDS 3.2 and its GPC-SEC add-on. For calibration, a standard set of pullulans (PSS Polymer Standards Service GmbH) was used. Both standards and FDH samples were dissolved in ultrapure water at a concentration of 10 g/L. After filtration through 0.45 µm syringe filters, a volume of 10 µL was injected.

2.7.4. Protein fluorescence

2.7.4.1. Intrinsic fluorescence

Intrinsic fluorescence analysis was performed as described by Arogundade *et al*. (2016) with slight modifications. FDHs were dissolved in phosphate buffer solution (pH = 6.8–7.0) at a concentration of 0.5 mg/mL. Intrinsic fluorescence emission spectra were obtained by a fluorescence spectrophotometer (Cary Eclipse, Agilent Technologies). Sample solutions were excited at 280 nm, and emission spectra were recorded from 300 nm to 800 nm. Slit width was set at 5 nm, both for excitation and emission, in order to minimize the effect of tyrosine residues.

2.7.4.2. Quenching experiments

Fluorescence quenching experiments were also performed by adding different concentrations of potassium iodide (KI) to the FDH solutions, based on methodology previously developed (Benito-Román *et al*., 2019). Maximum fluorescence data of each sample against a blank with no added KI was recorded in order to obtain the Stern-Volmer plots and calculate the quenching constant (K_{SV}) according to the following equation:

$$\frac{I_0}{I} = 1 + K_{SV}[Q] \qquad \textbf{[2.2]}$$

where $[Q]$ is the concentration of quencher (KI).

Results are reported as the means of three replicates. Blank samples with no added KI were diluted with the same volume of phosphate buffer in order to account for the dilution effect.

2.7.5. Emulsifying properties

2.7.5.1. Preparation of emulsions

Oil-in-water (O/W) emulsions were prepared using FDHs as emulsifying agents. Emulsions were prepared as follows: First, 2 g of FDH were dispersed in 95 mL of distilled water. Then, 3 g of sunflower oil were added dropwise and continuously stirring. This coarse emulsion was subsequently homogenized in a Miccra D-9 homogenizer-disperser for 3 min at 21000 rpm. The resulting pre-emulsion was immediately passed through a microfluidizer (Microfluidcs LM20) equipped with an F20Y interaction chamber. Final microemulsions were obtained at a fixed pressure of 150 MPa and 7 passes through the microfluidizer. A cooling coil immersed in ice water was used to keep the emulsion at controlled temperature throughout the homogenization process. Each emulsion was duplicated to account for experimental error.

For each FDH, droplet size distribution was measured after each pass in the microfluidizer. The stability of the final microemulsions was assessed by droplet size measurements over 14 days of storage under refrigeration conditions (4 °C).

2.7.5.2. Droplet size distribution and stability of the emulsions

The droplet size of the emulsions was measured by static light scattering (SLS) using a Mastersizer 2000 (Malvern Instruments) immediately after emulsification. Emulsion droplet size values are reported as the volume-weighted mean diameter (De Brouckere mean diameter; D[4,3]) and as droplet size distributions from 20 nm to 2000 μm. Results are reported as the mean of three measurements.

2.7.5.3. Electrokinetic potential of emulsions

The electrokinetic potential (i.e., ζ potential) of emulsion droplets stabilized with FDHs was measured by electrophoretic mobility using a Zetasizer Nano Series equipment (Malvern Instruments, UK). ζ potential measurements were conducted

after dilution of emulsions in ultrapure water (1:20). Then, with the help of a gel-loading tip, samples were added to the bottom of a disposable capillary cell specifically designed for this measurement (O'Sullivan *et al.*, 2015). Results are reported as the average and standard deviation of ten replicates, with 50 stabilization cycles per replicate.

3. Results and discussion

3.1. Fractionation of fish meal protein according to water solubility

According to previous studies (Barea *et al.*, 2023), the initial protein content of FM is 51 ± 2 % (w/w), as determined by the analysis of elemental N and the corresponding conversion factor, which was calculated from the amino acid profile (Table 2.1). Water fractionation yielded a liquid extract containing around 4 % (w/v) soluble solids and 20.5 ± 0.8 mg protein/mL, according to the Lowry assay (Barea *et al.*, 2023), which represents half of the soluble solids and one third of the total protein content in the fish meal. The other two thirds of protein in FM plus other non-soluble components4 formed the NSP fraction, with an estimated protein content of 50 % (w/w) according to the mass balance.

The amino acid profile of FM and its fractions, WSP and NSP, is reported in Table 2.1. From these data and according to the NREL standard protocols (J. B. Sluiter *et al.*, 2010), the nitrogen-to-protein conversion factors (NPCFs) were calculated. For the FM, and the WSP and NSP fractions, NPCFs of 4.98, 4.59, and 4.91 were obtained, respectively. Similar NPCF values have been reported in the literature for fish and derivatives (Boisen *et al.*, 1987; Diniz *et al.*, 2013; Salo-Väänänen & Koivistoinen, 1996), indicating a higher-than-average proportion of N in the fish meal proteins (around 20 % (w/w)). With these factors and the elemental analysis of N (results not shown), the crude protein content of the samples was estimated to be 51.3, 54.4, and 54.7 g protein/100 g for FM, WSP and NSP, respectively, finding good agreement with the mass balance calculations.

Despite the similarities in the NPCFs of the FM and its fractions, some differences in the amino acid profiles can be observed. As indicated in Table 2.1, the percentage of large non-polar amino acids (Ile, Leu, Met, Phe, Trp) is higher in the NSP fraction, followed by the original FM and lastly the WSP fraction. On the contrary, the content of small amino acids such as Ala, Gly, Pro and Cys is greater in the WSP fraction compared to the NSP, indicating some selectivity of the fractionation process with water at 80 °C. As we describe in the following sections, the different amino acid profiles of FM, WSP and NSP substrates further affect the extension of the hydrolysis process and especially the properties of the final hydrolysates.

3.2. Hydrolysis of fish meal and its fractions

FM, WSP and NSP were subjected to SWH and enzymatic hydrolysis. Liquid hydrolysates were freeze-dried to obtain the FDHs. Chemical characterization of the FDHs was carried out in terms of free amino acid release to the medium. As shown in Table 2.1, production of free amino acids during the hydrolysis process was most pronounced when the WSP fraction was used as the starting material, and almost 5 times higher with the SWH method, compared to the enzymatic hydrolysis with Alcalase®. Among the free amino acids released, the proportion of large non-polar amino acids follows the same trend as in the non-hydrolyzed samples, being higher in the NSP hydrolysate compared to FM and WSP. Moreover, the WSP hydrolysates showed a lower ratio than the original WSP, indicating low hydrolysis of the non-polar domains and the potential transformation of these large non-polar amino acids into smaller amino acids and degradation products, following different reaction pathways (Abdelmoez *et al*., 2007).

Table 2.1. Amino acid profile of the fish meal (FM) and of the water-soluble protein (WSP) and non-water-soluble protein (NSP) fractions. Free amino acid profile of the hydrolysates obtained by subcritical water hydrolysis (SWH) and enzymatic hydrolysis with Alcalase® (Alc-H) of FM, WSP, and NSP substrates.

Amino acid	Fish meal, mg aa/$g_{protein}$	WSP, mg aa/$g_{protein}$	NSP, mg aa/$g_{protein}$	Free amino acids generated during hydrolysis, mg aa/$g_{protein}$					
				FM		WSP		NSP	
				SWH	Alc-H	SWH	Alc-H	SWH	Alc-H
Ala	89 ± 3	88 ± 7	64 ± 2	15 ± 2	0.9 ± 0.1	72.8 ± 0.4	9.7 ± 0.1	11.6 ± 0.1	0.38 ± 0.01
Gly	86 ± 2	199 ± 9	63 ± 1	16 ± 3	0.5 ± 0.05	130.4 ± 0.3	5.4 ± 0.1	9.7 ± 0.1	0.12 ± 0.01
Val	43 ± 3	29 ± 5	45.8 ± 0.9	3.8 ± 0.5	0.73 ± 0.05	13.3 ± 0.1	5.03 ± 0.07	3.9 ± 0.1	0.13 ± 0.01
Leu	63 ± 4	36 ± 2	83 ± 1	4 ± 1	1.04 ± 0.05	13.4 ± 0.1	5.9 ± 0.1	3.6 ± 0.1	0.27 ± 0.02
Ile	36 ± 2	18 ± 2	36.2 ± 0.6	2.1 ± 0.4	0.54 ± 0.05	3.8 ± 0.1	3.4 ± 0.1	2.6 ± 0.1	0.05 ± 0.01
Thr	43 ± 2	31 ± 2	48 ± 1	1.1 ± 0.1	0.53 ± 0.05	5.0 ± 0.1	2.5 ± 0.4	1.10 ± 0.03	0.10 ± 0.02
Ser	44 ± 3	36 ± 5	38 ± 2	2.1 ± 0.5	0.56 ± 0.05	0.8 ± 0.1	2.44 ± 0.04	1.83 ± 0.05	0.13 ± 0.01
Pro	58 ± 3	111 ± 5	48.9 ± 0.8	5.6 ± 0.9	0.62 ± 0.05	52 ± 1	3.6 ± 0.1	4.3 ± 0.1	0.09 ± 0.02
Asp	94 ± 2	70 ± 7	130 ± 4	9.7 ± 0. 2	2.47 ± 0.05	2.4 ± 0.1	3.0 ± 0.1	8.0 ± 0.1	0.55 ± 0.07
Met	27 ± 3	13 ± 2	35 ± 0.7	2.4 ± 0.5	0.66 ± 0.03	6.0 ± 0.3	2.00 ± 0.03	2.0 ± 0.1	0.23 ± 0.03
Hyp	24 ± 3	58 ± 9	1.9 ± 0.6	3.2 ± 0.04	0.13 ± 0.01	12 ± 1	0.36 ± 0.01	4.63 ± 0.03	0.19 ± 0.05
Glu	110 ± 6	103 ± 14	127 ± 8	n.d.	n.d.	9.2 ± 0.2	1.93 ± 0.02	0.47 ± 0.03	n.d.
Phe	34 ± 2	21 ± 2	47 ± 3	5.1 ± 0.1	1.1 ± 0.1	6.3 ± 0.1	3.1 ± 0.1	4.8 ± 0.1	0.37 ± 0.07
Lys	57 ± 4	37 ± 6	53 ± 5	5.0 ± 0.1	1.8 ± 0.07	6.2 ± 0.2	3.5 ± 0.1	4.9 ± 0.1	0.7 ± 0.1
Hys	22 ± 2	26 ± 2	22.6 ± 0.8	3.4 ± 0.1	3.8 ± 0.1	6.9 ± 0.1	19.0 ± 0.7	2.9 ± 0.1	0.8 ± 0.1
Hyl	1.9 ± 0.4	53 ± 18	2.3 ± 0.2	n.d.	0.82 ± 0.01	n.d.	0.25 ± 0.02	0.78 ± 0.05	0.8 ± 0.2
Tyr	26 ± 2	15 ± 3	36 ± 1	2.3 ± 0.5	0.6 ± 0.1	2.9 ± 0.1	2.7 ± 0.1	2.3 ± 0.1	0.31 ± 0.05
Trp	8 ± 1	54 ± 12	11 ± 1	0.7 ± 0.3	0.2 ± 0.1	0.81 ± 0.05	0.72 ± 0.03	0.7 ± 0.1	0.40 ± 0.02
Cys	2.3 ± 0.6	25 ± 9	3.0 ± 0.3	0.67 ± 0.01	0.60 ± 0.01	0.26 ± 0.03	0.11 ± 0.01	0.64 ± 0.03	0.40 ± 0.1
Total	868 ± 48	1021 ± 121	896 ± 36	84 ± 4	18 ± 1	344 ± 5	75 ± 1	71 ± 2	6.5 ± 0.9
NP*, %	22.3	15.2	27.7	19.8	23.0	9.7	23.8	22.5	25.1

Ala: alanine, Gly: glycine, Val: valine, Leu: leucine, Ile: isoleucine, Thr: threonine, Ser: serine, Pro: proline, Asp: aspartic acid, Met: methionine, Hyp: hydroxyproline, Glu: glutamic acid, Phe: phenylalanine, Lys: lysine, Hys: histidine, Hyl: hydroxylysine, Tyr: tyrosine, Trp: tryptophan, Cys: cysteine. n.d.: non detected. *NP: Non-Polar, very large, amino acids: Leu, Ile, Met, Phe, Tyr and Trp, according to IMGT amino acid classes (Pommié *et al*., 2004).

In the literature, several authors have demonstrated that SWH is a suitable method to produce free amino acids from fish and shellfish by-products. For instance, semi-continuous SWH of sardine viscera produced a free amino acid yield of 161.2 mg/g dry hydrolysate at 140 °C (Melgosa *et al*., 2020), whereas Chun *et al*. (2022) reported free amino acid yields of 65.3–74.8 mg/g dry extract for the SWH of comb pen shell viscera in a batch reactor at 170–230 °C during 15 min.

In the literature, the optimal SWH temperature and time to obtain free amino acids vary greatly (Marcet *et al*., 2016). Higher temperatures generally lead to higher amino acid productions, as shown by Park *et al*. (2022) in the extraction of amino acids from eel by-products. In that work, an eel extract containing 6.7 g/L of free amino acids was obtained by using SWH in a discontinuous reactor at 220 °C for 15 min (Park *et al*., 2022). However, higher temperatures and longer exposure times lead to decreased yields due to thermal degradation into organic acids (Marcet *et al*., 2016).

Elemental (CHNS) analysis of the FDHs obtained in this work is reported in Table 2.2. These data allowed the calculation of the elemental H/C and N/C ratios, which range between 1.85–1.96 and 0.24–0.30, respectively, for all the hydrolysates. O/C values are missing due to limitations in the analytical procedure. Despite these limitations, we can see that these values fall very well within the Multidimensional Stoichiometric Compound Classification Constraints (MSCCC) proposed by Rivas-Ubach *et al*. (2018) for protein compounds. The crude protein content of the hydrolysates can be also calculated by using the NPCFs previously calculated for FM, WSP and NSP. Except for the WSP fraction hydrolyzed with Alcalase®, the hydrolysates presented similar or slightly more crude protein than their non-hydrolyzed counterparts. This is especially true for the SWH-treated FM and NSP hydrolysates, with around 70 % of these FDHs being of protein nature. It seems clear that the enhanced protein content has been achieved through selective hydrolysis of proteins and solubilization of peptides and amino acids, as shown in the results for the hydrolysis yield. For WSP, hydrolysis yield, expressed as the amount of FDH

obtained from 100 g of solid material, was close to 100 % in all cases since all the solids were already solubilized; therefore, no selectivity could be achieved, and the protein content was similar to that of the non-hydrolyzed NSP. On the other hand, FM and NSP fraction showed hydrolysis yields ranging 20–35 %. As expected, the hydrolysis of FM presented higher yield than that of NSP due to the presence of soluble solids, whereas all the solids in the NSP fraction were initially not soluble. In any case, these rather low hydrolysis yields came with the benefit of a higher protein selectivity.

Together with the hydrolysis yield, the degree of hydrolysis (DH) is an indicative of the extension of the hydrolysis process. DH values are reported in Table 2.2 as the percentage of cleaved bonds over the total peptide bonds present in the original protein, which can be calculated from the amino acid profile. These results showed that SWH achieved much higher DH compared to enzymatic hydrolysis with Alcalase® regardless of the starting material. Considering both the DH and the crude protein content of the hydrolysates, we can observe similarities with enzymatic hydrolysis as reported by other authors (Aspevik *et al*., 2016), since protein recovery remained constant and even decreased when DH increased. In this work, the different substrates and hydrolysis methods affect the composition and characteristics of the final hydrolysate. This way, Alcalase® hydrolysis provided low protein recovery and DH values. On the contrary, SWH of the same fractions achieved higher DHs, with the lowest protein content and highest DH of all the hydrolysates obtained in this work for WSP fraction. Overall, the SWH process presents higher efficiency in the hydrolysis and solubilization of fish proteins than enzymatic hydrolysis with Alcalase®, since results obtained in this work showed slightly higher selectivity, increased hydrolysis yields and higher DHs.

Table 2.2. Elemental composition, hydrolysis yield, and degree of hydrolysis of the freeze-dried hydrolysates (FDHs) obtained from fish meal (FM), its water-soluble fraction (WSP), and its non-water-soluble fraction (NSP) by subcritical water hydrolysis (SWH) and enzymatic hydrolysis with Alcalase® (Alc-H).

	C, %	H, %	N, %	Protein*, % (w/w)	Hydr. Yield, g_{FDH}/100 g	DH**, %
SWH						
FM	44.9 ± 0.3	7.4 ± 0.3	13.5 ± 0.2	67.5 ± 1	31.9 ± 0.5	72 ± 2
WSP	34.1 ± 0.4	5.4 ± 0.1	11.9 ± 0.1	54.6 ± 0.5	99.8 ± 0.2	86.5 ± 0.5
NSP	50.6 ± 0.1	7.8 ± 0.1	14.7 ± 0.1	72.2 ± 0.6	28.5 ± 0.5	52 ± 1
Alc-H						
FM	34.2 ± 0.6	5.6 ± 0.1	10.7 ± 0.1	53.5 ± 0.5	26.3 ± 0.5	23.6 ± 0.2
WSP	28.1 ± 0.7	4.6 ± 0.2	9.6 ± 0.2	44 ± 1	98.9 ± 0.7	33.8 ± 0.5
NSP	30.2 ± 0.7	4.8 ± 0.1	11.3 ± 0.1	55.7 ± 0.2	19.7 ± 0.3	9.4 ± 0.3

*NPCF = 4.98 for FM; 4.59 for WSP; 4.91 for NSP.
**Eq. 2.1.

3.3. Molecular weight distribution of the hydrolysates

Molecular weight distribution of hydrolysates showed complex elution profiles, with similarities between samples that can be attributed to their common origin. Differences in size and abundance can be also observed and might be related to the techno-functional properties of the hydrolysates, as it will be discussed in the following sections. Results obtained are represented in Figure 2.1 as a normalized distribution of slice molecular weights against the estimated MW according to column calibration.

Figure 2.1a shows large peaks in the range 200–1000 Da, indicating that SWH process promotes the formation of small peptides. While FM and NSP presented 2 groups of compounds with MW centered around 300 and 600 Da, WSP only showed one peak centered at 400 Da that may correspond to di- or tri-peptides as it has been also observed in a previous work (Barea *et al*., 2023). SWH hydrolysates presented some larger peptides and proteins, with estimated MWs centered at 4 kDa, 11–12 kDa, and 28–30 kDa, which are more abundant in FM and NSP hydrolysates than in

WSP, probably due to the abundance of these compounds in the original substrates. On the other side, free amino acids are likely represented in the small peak centered around 100 Da, since their MWs range from 75 Da for glycine ($C_2H_5NO_2$) to 204 Da for tryptophan ($C_{11}H_{12}N_2O_2$). The abundance of these compounds is notable in the SWH hydrolysates, especially in that from WSP, and is much lower in Alcalase® hydrolysates, which is in accordance with the previously described results for the amino acid profile and degree of hydrolysis.

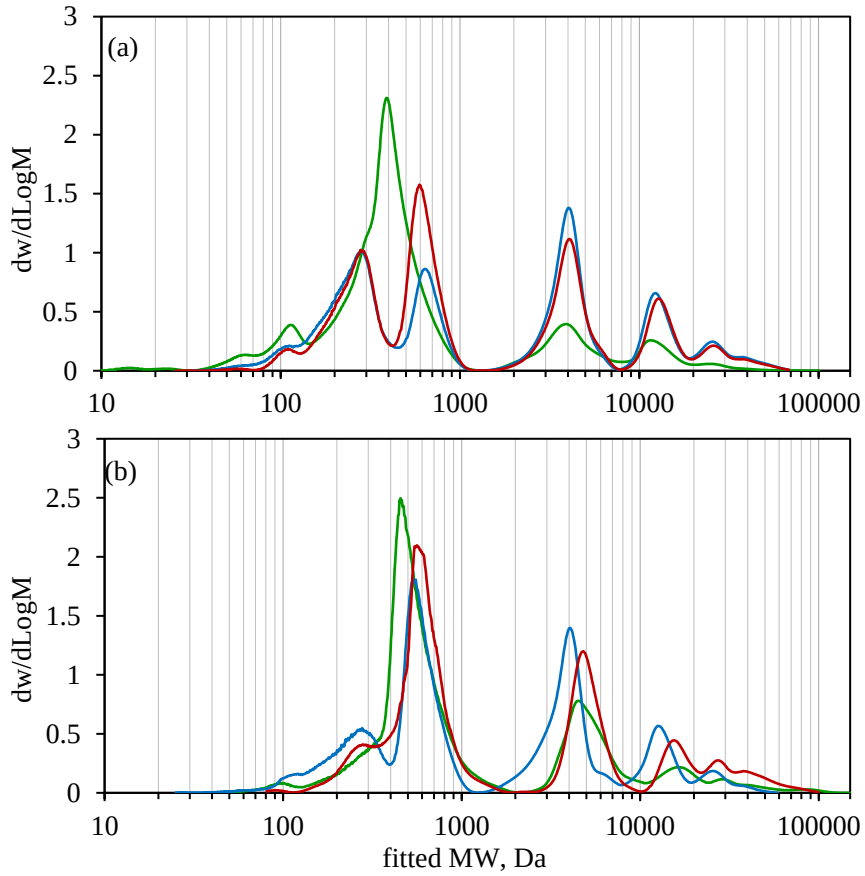

Figure 2.1. Normalized slice distributions of hydrolysates obtained from fish meal (FM, **red**), its water-soluble fraction (WSP, **green**), and its non-water-soluble fraction (NSP, **blue**). **(a)** subcritical water hydrolysis (SWH). **(b)** enzymatic hydrolysis with Alcalase® (Alc-H). Samples resuspended in ultrapure water at 10 g/L.

In the case of the hydrolysates obtained with Alcalase® (Figure 2.1b), most of the compounds were also in the range 200–1000 Da. Again, WSP only presented one peak at 400 Da whereas FM and NSP presented two groups of compounds at 300 and 600 Da. However, the peak at 300 Da was much smaller than in the SWH hydrolysates, indicating less abundance of small peptides in the Alcalase hydrolysates. In general, the normalized distributions of Alcalase® hydrolysates at MW larger than 1000 Da are rather similar and have as well some resemblances with the SWH hydrolysates. Three main families of compounds can be observed at MW = 4–6, 11–14 and 28–30 kDa. Differences in abundance and displacement of the peaks to lower MW give an idea of the susceptibility of each substrate to enzymatic hydrolysis with SWH and Alcalase®. Area calculations allowed to estimate a weighted-average molecular size for each hydrolysate, being: 4835, 2021 and 5335 Da for FM, WSP and NSP obtained by SWH, respectively; and 6792, 4057 and 4065 Da for FM, WSP and NSP obtained by enzymatic hydrolysis.

3.4. Protein solubility (PS)

Solubility of FDHs in aqueous buffer at different pH is reported in Figure 2.2. Comparing the different hydrolysates, the WSP hydrolysates presented the higher solubility, reaching values close to 100 % at mild pH conditions (pH = 4.0–7.0) for WSP hydrolyzed with Alcalase®. In the case of WSP hydrolyzed with SWH, total solubility is only achieved at pH = 4.0. Outside of this pH range, solubility of WSP hydrolysates would decrease down to ca. 95 %, which is still very high. This is not unexpected since the original protein was obtained by water solubilization at a similar pH, and its further hydrolysis would increase its solubility in a wider range of pH and temperatures due to the smaller size of the obtained protein residues. The explanation may lie in the higher content of polar groups of WSP, compared to the other substrates, which gives place to electrostatic interactions between water molecules and protein residues (Gehring *et al*., 2009).

On the contrary, the presence of hydrophobic amino acid residues would promote protein-protein interactions and aggregation into insoluble species (Gehring *et al.*, 2009), leading to lower solubility values as observed for the NSP hydrolysates. In this case, a more significant effect of pH on solubility can be observed, varying in the ranges 82–97 % and 64–82 % in the FDHs obtained by enzymatic hydrolysis and SWH, respectively. Both Alcalase® and SWH hydrolysates followed the same trend, with the lowest solubility at pH = 2.0, increasing dramatically up to the maximum solubility at pH = 4.0 and then decreasing again at higher pH values. The enzymatic FDHs, despite having a larger molecular size than SWH hydrolysates according to the GPC-SEC results, present significantly higher solubility than their SWH counterparts for all the pHs studied in this work.

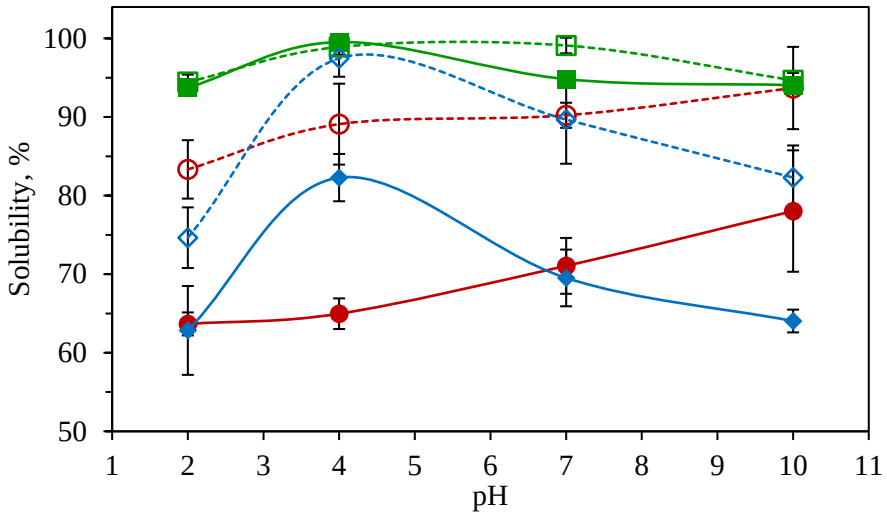

Figure 2.2. Effect of pH on the solubility of freeze-dried hydrolysates (FDHs) obtained from fish meal (FM, ● ○), its water-soluble fraction (WSP ■ □), and its non-water-soluble fraction (NSP, ◆ ◇) by subcritical water hydrolysis (SWH, full symbols) and enzymatic hydrolysis with Alcalase® (Alc-H, hollow symbols). Samples were resuspended at 500 mg/L in buffer solutions at pH = 2.0–10.0. Lines are drawn to guide the eye.

It has been proposed that Alcalase®, being an endopeptidase, acts by cleaving larger proteins into more soluble polypeptide chains (Barea *et al.*, 2023); whereas SWH mostly liberates small peptides and free amino acids, which are also soluble

but affect less the solubility parameter since the parent protein is still large and insoluble. Another possible reason for the lower solubility of SWH hydrolysates might be related to the high temperatures of SWH treatment, which may have promoted the denaturation and unfolding of the polypeptide chains, rendering some of the proteins and peptides insoluble due to the higher exposure of hydrophobic domains (López *et al*., 2019). For FM hydrolysates, higher solubility was also obtained with Alcalase® compared to SWH in all the pHs studied. We can also observe that solubility increases with pH, from 80 % and 60 % at pH = 2.0 to 95 % and 75 % at pH = 10.0, for Alcalase® and SWH, respectively. At high pH, carboxyl groups are charged but not amine groups; thus, repulsive intermolecular interactions between local negatively charged groups may promote protein-water interactions and the observed increase in solubility (Das *et al*., 2021).

3.5. Surface tension

The potential use of the protein hydrolysates obtained in this work as emulsifiers is based on the modification of interfacial and surface properties of emulsions and solutions. Figure 2.3 a and b show an example of the measurement of the surface tension of water using the optical tensiometer. Figure 2.3c shows a screenshot of the software used by this equipment, which analyzes the surface tension by photographing the drop as it emerges from the tube for each sample.

As shown in Figure 2.4 and taking ultrapure water as a reference, the surface tension at room temperature (20 °C) notably decreases when the hydrolysates are present. The more drastic decrease was observed for the SWH-treated WSP fraction, whereas the highest surface tension was found in FM subjected to enzymatic hydrolysis. Results obtained in the measurement of surface tension of the protein hydrolysates show the potential of FDHs as emulsifying and stabilizing agents. Thanks to their molecular structure and amphiphilic nature, small peptides and amino acids can adsorb into the oil-water interphase, decreasing the energy required to form the emulsion and stabilizing the emulsion droplets.

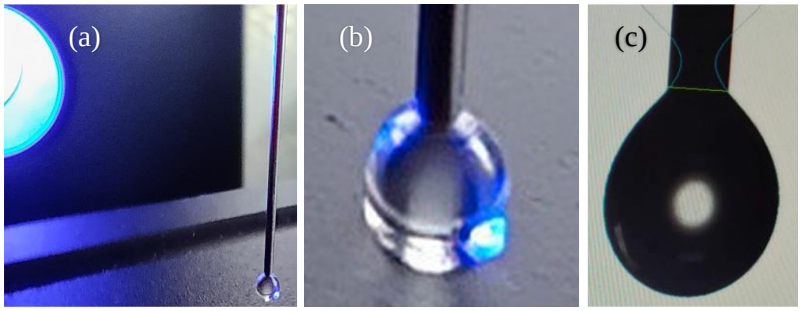

Figure 2.3. Measurement of water surface tension using an optical tensiometer. **(a)** Light beam of the optical tensiometer's camera focusing on the drop emerging from the tube. **(b)** Close-up photograph of the liquid droplet coming out from the tube tip. Effect of surface tension clearly visible. **(c)** Image monitored by the tensiometer software, which calculates the surface tension value.

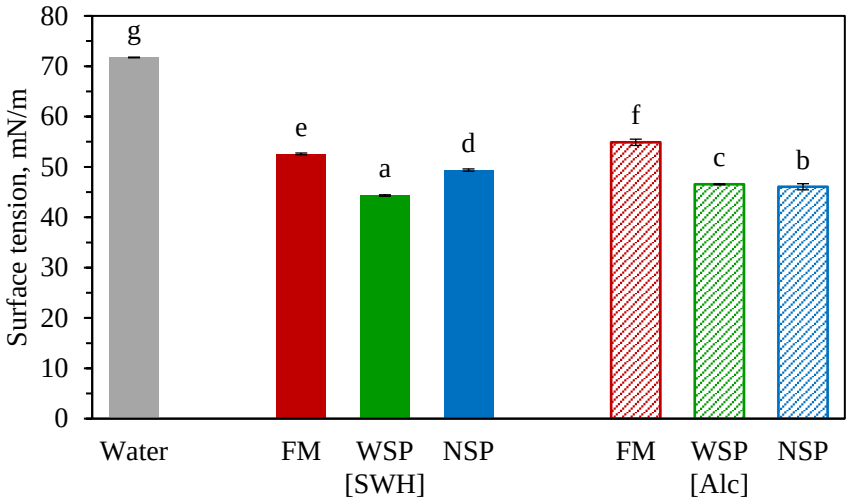

Figure 2.4. Surface tension measured at room temperature (20 °C) of freeze-dried hydrolysates obtained from fish meal (FM, **red**), its water-soluble fraction (WSP, **green**), and its non-water-soluble fraction (NSP, **blue**) by subcritical water hydrolysis (SWH, full columns) and enzymatic hydrolysis with Alcalase® (Alc-H, patterned columns). All samples consisted of 2 g of solid resuspended in 93 mL of ultrapure water. Different letters represent statistically significant differences at p-value < 0.05.

3.6. Intrinsic fluorescence

It has been reported that the intrinsic fluorescence of proteins is primarily due to the presence of tryptophan residues within its structure (Bobone *et al*., 2014), among other hydrophobic amino acids such as tyrosine. Denaturation of the protein, protein hydrolysis, and changes in its environment may cause changes in protein folding and the exposure of hydrophobic domains, where tryptophan is more abundant. These changes can be monitored through the determination of the fluorescence emission spectra of the protein (Antonov *et al*., 2015).

As shown in Figure 2.5, enzymatically hydrolyzed FDHs had lower emission maximum (λ_{max}) values than those obtained by SWH. These results indicate that the tryptophan residues were mostly embedded into the protein structure, within a hydrophobic environment (C. Li *et al*., 2014). Based on these results, the enzymatically hydrolyzed FDHs would present more hydrophilic domains on the surface of the FDH, promoting interactions with water molecules and possibly explaining their higher solubility at different pH (2–10) when compared to those obtained by SWH.

On the other hand, intrinsic fluorescence of FDHs obtained by SWH presented higher fluorescence intensity than its Alcalase® counterparts at the same concentration. Moreover, the fluorescence emission maxima of SWH hydrolysates are red shifted in relation to the enzymatic FDHs, especially for FM and the NSP fraction. This phenomenon may occur when the fluorophores are highly exposed to the solvent, and indicates deep changes in the molecular structure of the protein (C. Li *et al*., 2014), which are likely due to the extensive hydrolysis and unfolding of the proteins by SWH treatment. SWH and enzyme-mediated protein hydrolysis leads to protein unfolding and a gradual transition of the more hydrophobic domains from the core of the protein to the surface, yielding a more flexible protein conformation. Hence, these flexible proteins with higher surface hydrophobicity could have excellent emulsifying properties since they would adsorb to the oil-water interface,

decreasing the surface tension and establishing interactions with both hydrophobic and hydrophilic molecules (N. Li *et al*., 2022).

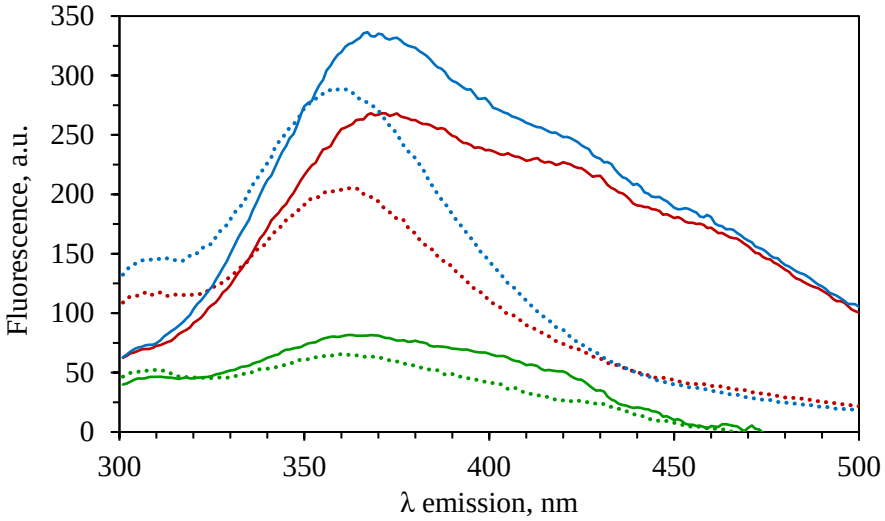

Figure 2.5. Intrinsic fluorescence emission spectra of freeze-dried hydrolysates (FDHs) obtained from fish meal (FM, **red**), its water-soluble fraction (WSP, **green**), and its non-water-soluble fraction (NSP, **blue**) by subcritical water hydrolysis (SWH, continuous lines) and Alcalase® hydrolysis (Alc-H, dotted lines). Samples resuspended at 0.5 mg/mL in phosphate buffer, pH = 6.8.

Comparing by substrates, it is highly noticeable that the hydrolysates obtained from WSP presented the lower fluorescence intensities, followed by those from FM, and NSP with the highest emissions. Since tryptophan and other fluorescent amino acids are hydrophobic, it seems likely that the WSP fraction contains lower quantities of these residues, whereas the NSP fraction presented a higher proportion of this hydrophobic amino acid. Besides, the shoulder centered around 310 nm observed in the spectra of Alcalase®-hydrolyzed samples, and not in the SWH hydrolysates, may be due to the tyrosine residues of the enzyme (Paiva dos Santos *et al*., 2020).

3.7. Surface hydrophobicity of the FDHs

Fluorescence quenching is an adequate method to determine the presence and exposure to the solvent environment of tryptophan residues within the protein

structure; hence, it is a good indicator of the surface hydrophobicity of the protein (N. Li *et al*., 2022). From the results obtained in the quenching experiments, a Stern-Volmer plot was obtained for each FDHs. The fitting parameters are shown in Table 2.3, with K_{SV} values ranging from 3.16 ± 0.08 to 12.9 ± 0.2 M^{-1} and intercepts close to 1. In general, SWH hydrolysates showed higher K_{SV} values than their Alcalase® counterparts, indicating a larger number of hydrophobic groups exposed to the solvent environment. It is likely that the higher degree of hydrolysis achieved by this method would have led to protein unfolding and higher exposure of hydrophobic groups in proteins. This is especially true for the FM and NSP hydrolysates. On the other hand, low K_{SV} values have been frequently attributed to partial denaturation and subsequent aggregation of hydrophobic residues (He *et al*., 2014; M. Ma *et al*., 2018), which may be the case for the WSP hydrolysates. However, it is more likely that the lower presence of hydrophobic residues in the original substrate had led to a lower K_{SV} value.

Table 2.3. Stern-Volmer parameters of the FDHs obtained from fish meal (FM), its water-soluble fraction (WSP), and its non-water-soluble fraction (NSP) by subcritical water hydrolysis (SWH) and enzymatic hydrolysis with Alcalase® (Alc-H). Free amino acid concentration in the synthetic solution as in Table 2.1 for WSP [SWH].

	K_{SV}*, M^{-1}	**Intercept**	**R^2**
Free aa solution	*16.7 ± 0.3*	*0.88 ± 0.07*	*0.9970*
		SWH	
FM	12.3 ± 0.2	1.31 ± 0.06	0.9963
WSP	3.9 ± 0.4	1.23 ± 0.07	0.9510
NSP	12.9 ± 0.2	1.07 ± 0.05	0.9970
		Alc-H	
FM	8.3 ± 0.3	1.04 ± 0.06	0.9902
WSP	3.16 ± 0.08	1.12 ± 0.02	0.9949
NSP	7.82 ± 0.08	1.08 ± 0.02	0.9990

*K_{SV}: Stern-Volmer constant.

The results obtained in this work are not easy to compare with the literature since different quenching methodologies are frequently used, and the effects of the quencher may be different depending on the origin of the protein hydrolysate. M. Ma *et al*. (2018) obtained K_{SV} values in the range 100–700 M^{-1} for ANS-binding of protein isolates of cottonseed meal, indicating a much higher surface hydrophobicity than the FDHs obtained in this work although deviations could be in part attributed to the different methodology. On the other hand, He *et al*. (2014) obtained K_{SV} values of the same order for peanut protein isolates quenched by ANS-binding. Since quenching rate can be also influenced by the presence of free amino acids with fluorescence emission, an additional quenching experiment was performed with a synthetic solution of free amino acids, which was obtained by mixing commercially available (Sigma Aldrich) standards in ultrapure water according to the free amino acid profile of the WSP hydrolysate obtained by SWH (Table 2.1). From this experiment, a higher but rather similar K_{SV} value was obtained compared to those of FM and NSP. This result suggests that fluorescence emission of FDHs obtained by SWH is not only due to surface hydrophobicity but also to the release of free amino acids and small peptides during SWH, which present high fluorescent intensities but at the same time high sensitivity to changes in the solvent environment.

3.8. Droplet size measurements

The droplet size distribution of fresh and stored emulsions was used to evaluate the emulsifying ability of FDHs and physical stability of the emulsions during storage for 14 days, as shown in Figure 2.6. The droplet diameter, expressed as a volume weighted mean (D[4,3]) can be also used to monitor the evolution of the emulsions along storage and is reported in Table 2.4.

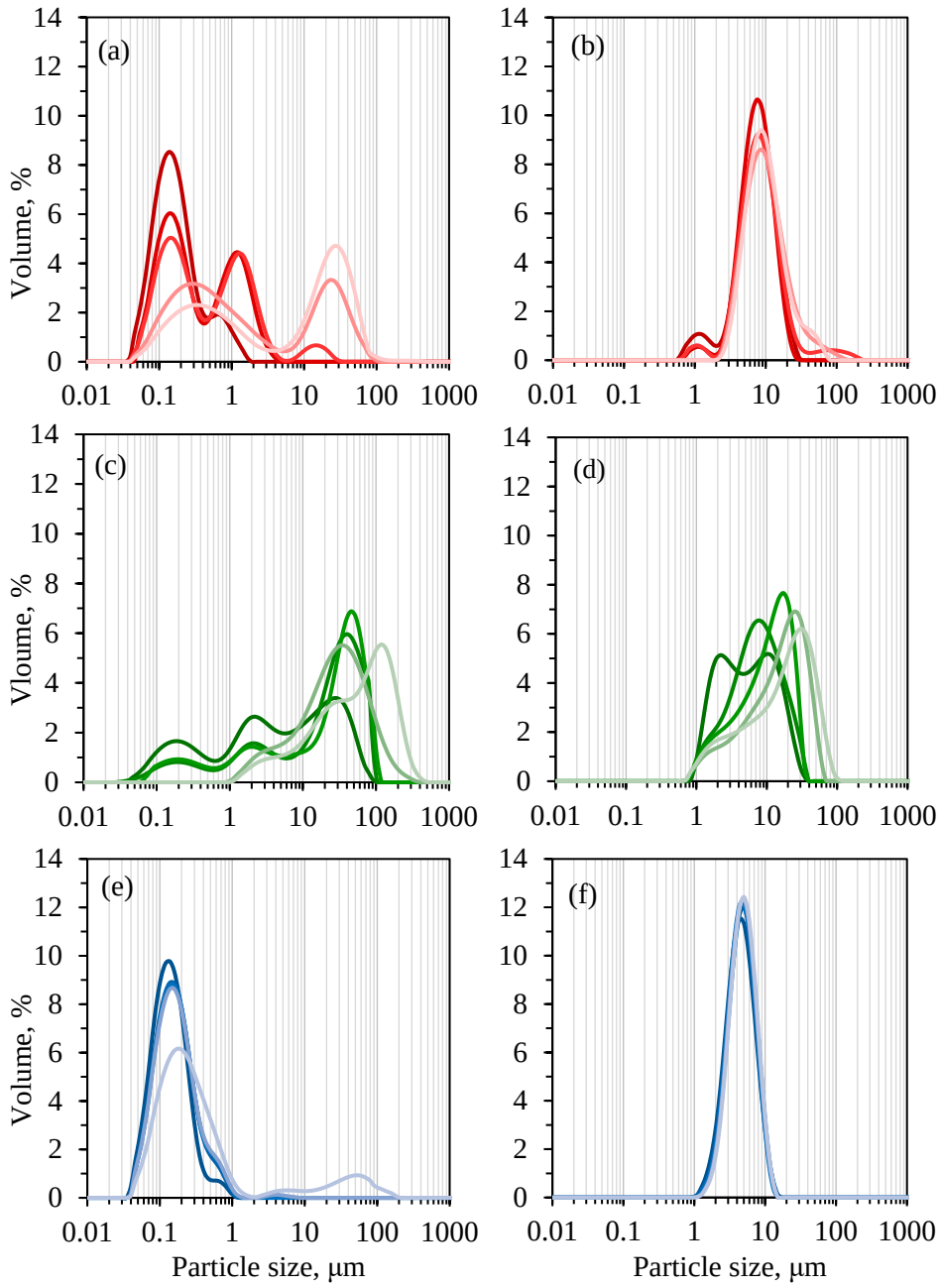

Figure 2.6. Droplet size distributions of emulsions stabilized with 2 % freeze-dried hydrolysate (FDH) from fish meal (FM, **red**), its water-soluble fraction (WSP, **green**), and its non-water-soluble fraction (NSP, **blue**). **(a, c, e)** SWH treatment. **(b, d, f)** Alcalase® treatment. Each color intensity decreases progressively, reflecting the particle size increment as elapsed time increases: fresh, ▬ ▬ ▬; 1 day, ▬ ▬ ▬; 3 days, ▬ ▬ ▬; 7 days, ▬ ▬ ▬; 14 days, ▬ ▬ ▬.

Table 2.4. Evolution of the volume weighted mean droplet size (D[4,3]) of emulsions stabilized with freeze-dried hydrolysates (FDHs) during storage. FDHs obtained from fish meal (FM), its water-soluble fraction (WSP), and its non-water-soluble fraction (NSP) by subcritical water hydrolysis (SWH) and enzymatic hydrolysis with Alcalase® (Alc-H).

	D [4, 3] - Volume weighted mean, µm					
Days	**0**	**1**	**3**	**7**	**14**	**14 + SDS**
SWH						
FM	0.224	0.582	1.289	9.206	15.468	2.045
WSP	11.733	25.555	28.035	37.399	73.092	18.144
NSP	0.155	0.184	0.190	0.220	6.041	0.323
Alc-H						
FM	7.939	7.678	11.678	12.316	11.609	2.382
WSP	9.096	11.306	14.537	27.628	58.150	10.089
NSP	4.586	4.803	4.669	4.816	4.901	4.234

Fresh emulsions were obtained after 7 passes through the microfluidizer, monitoring the D[4,3] parameter after each pass and observing the droplet size reduction. Droplet size reduction was much more significant in the FM and NSP samples obtained by SWH with reductions from 12–14 µm of the coarse emulsion to 0.15–0.2 µm of the final emulsion. Similar results were obtained for pea protein-maltodextrin mixture in the micro-emulsification of rice bran oil, with a droplet size reduction from 9 µm to 0.2 µm after 8 passes through a microfluidizer (Benito-Román *et al.*, 2020). On the other hand, WSP samples did not show a significant improvement in D[4,3] and droplet size distribution when increasing the number of passes, whereas the FM and NSP samples treated with Alcalase® suffered a reduction from 40 µm to 7.9 µm and from 12 to 4.6 µm, respectively. Moreover, as it can be seen in Figure 2.6, the emulsions obtained with FM and NSP hydrolyzed with Alcalase® (Figure 2.6b and f, respectively) presented a larger droplet size than their SWH counterparts (Figure 2.6a and e).

As shown in Figure 2.6a, emulsions stabilized with FM hydrolysates obtained by SWH exhibited a small droplet size distribution, centered around 0.14 µm just

after high-pressure homogenization. This droplet size distribution is similar to those reported by Lu *et al*. (2016) for emulsions stabilized by soy protein hydrolysates obtained by SWH, and Benito-Román *et al*. (2020) for emulsions stabilized with pea protein and maltodextrin mixtures. However, the emulsions obtained in this work showed lower physical stability, since larger populations (> 1.25 μm) started to grow after just 1 day of storage. It has been proposed that protein unfolding and the Maillard reaction products formed during SWH process could decrease the energy barrier for interfacial adsorption during high-speed homogenization (Lu *et al*., 2016). Moreover, small droplet sizes have been also related to highly hydrolyzed peptides (Lu *et al*., 2016), although we have observed that the small peptides and amino acids resulting from extensive hydrolysis by SWH process do not contribute to emulsion stability, possibly due to its small size and the inability to form stable surface interactions. On the other hand, the larger peptides obtained from FM treated with Alcalase® (Figure 2.6b), which presented a much larger droplet size distribution centered at 7.6 μm, were more stable under storage for 14 days. These larger peptides are more likely to present both hydrophobic and hydrophilic domains, which allow for a more effective and stable interfacial adsorption.

From Figure 2.6c and d, we can see that the WSP hydrolysates did not promote the formation of stable emulsions, no matter the hydrolysis method. As shown in the previous analysis, the higher solubility and the low surface hydrophobicity of these hydrolysates possibly prevented surface adsorption and the formation of the strong hydrophobic interactions that are necessary to form a stable emulsion.

The NSP hydrolysates obtained by SWH (Figure 2.6e) and Alcalase hydrolysis (Figure 2.6f) presented molecular size distributions similar to their FM counterparts, although some improvements in emulsifying properties can be observed. The SWH hydrolysates of NSP allowed the formation of an emulsion with smaller droplet size distribution, compared to FM, that still retains its characteristics after 7 days of storage (Figure 2.6e). Moreover, the emulsion obtained using the Alcalase® hydrolysate from NSP maintained the same droplet size for 14 days of storage. These

results suggest better emulsifying properties of NSP hydrolysates, possibly related to higher surface hydrophobicity, the intermediate peptide size and the higher degree of hydrolysis achieved through enzymatic treatment, which leads to a remarkable improvement of physical stability and could be ascribed to the thicker architecture derived from interfacial adsorption of protein fragments and small peptides. Similar findings have been reported by other authors, who proposed that the formation of a gel-like network of adsorbed protein at the interface could provide a steric hindrance to oil droplets against coalescence (Lu *et al*., 2016; N. N. Wu *et al*., 2014; Q. T. Zhang *et al*., 2015).

3.9. Electrokinetic potential of emulsion droplets

The electrokinetic potential (i.e., ζ potential) of emulsion droplets stabilized with different FDHs is shown in Figure 2.7. The ζ potential of all samples was negative, indicating a predominance of negative charges over positive charges on the surface of the emulsion droplets. It has been generally accepted that the ζ potential of an emulsion is an indicative of its physical stability (Shanmugam & Ashokkumar, 2014). The higher the ζ potential absolute value, the more physically stable is the emulsion, because the repulsive forces between electrostatic charges with the same sign prevent the emulsion droplets from aggregating and collapsing.

For the emulsions obtained in this work, the ζ potential follows different patterns that can be related to its physical stability, as observed in the measurement of droplet size distribution. The emulsions formulated with WSP hydrolysates presented low initial values for the ζ potential (around -10 mV), which suggest less repulsive interactions and poor physical stability due to the tendency of the emulsion droplets to aggregate. For these emulsions, the zeta potential also increases and gets closer to zero when increasing storage time, indicating that destabilization is occurring due to the neutralization of positive and negative charges on the droplet surface caused by flocculation. This extreme has been confirmed by adding a deflocculant (SDS) to the emulsion prior to the measurement of droplet size

distribution and zeta potential, as described by Santos *et al*. (2018). According to the data presented in Table 2.4, D[4,3] of the emulsions after 14 days of storage at 4 °C was reduced with the addition of SDS in all cases, with percentual decreases ranging from 14 to 95 %. These results indicate that the increase in the average droplet size during storage was mainly due to flocculation, instead of coalescence. Comparable results were obtained by Benito-Román *et al*. (2020) for microemulsions of rice bran oil stabilized with pea protein and maltodextrin mixtures.

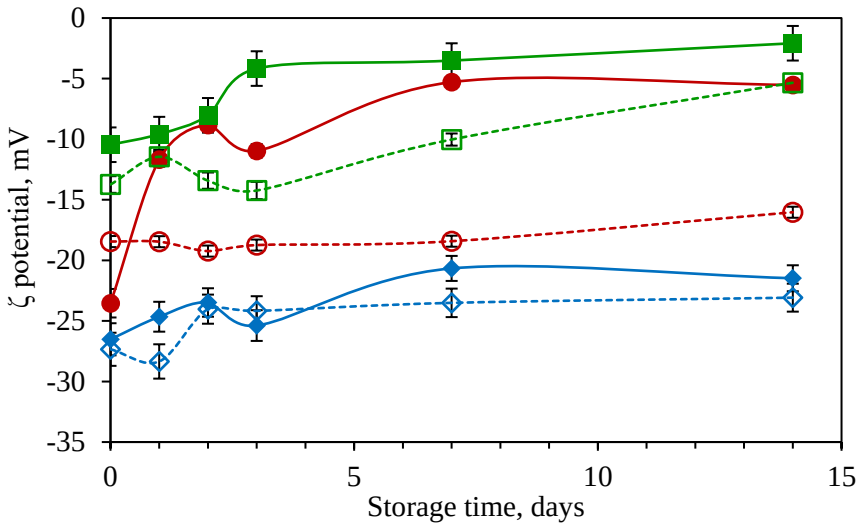

Figure 2.7. Evolution of the electrokinetic potential (ζ potential) of emulsions stabilized with freeze-dried hydrolysates (FDHs) during storage. FDHs obtained from fish meal (FM, ● ○), its water-soluble fraction (WSP ■ □), and its non-water-soluble fraction (NSP, ◆ ◇) by subcritical water hydrolysis (SWH, full symbols) and enzymatic hydrolysis with Alcalase® (Alc-H, hollow symbols). Lines are drawn to guide the eye.

The emulsions formulated with FM and NSP showed higher (in absolute value) zeta potential values, ranging from -18.5 to -27.3 mV. It has been suggested that the emulsions with zeta potential values of -11 to -20 mV were close to the threshold of destabilization, while the emulsions with higher absolute values of zeta potential (-41 to -50 mV) had good stability (Shanmugam & Ashokkumar, 2014). From the data presented in Figure 2.6 and the evolution of the droplet size distribution of the hydrolysates, the emulsions obtained with NSP hydrolysates are stable no matter the

hydrolysis method. On the contrary, the emulsions formulated with FM presented differences with the hydrolysis method. The SWH hydrolysate led to an emulsion with higher zeta potential (-23.5 mV) than the one obtained with the enzymatic FM hydrolysate (-18.5 mV).

However, the first emulsion rapidly crossed the destabilization threshold, showing a zeta potential of -11.5 mV after 1 day of storage, whereas the latter kept its physical stability and its zeta potential value along 14 days of storage. Again, the larger peptides produced by Alcalase®, compared to the smaller protein fragments and free amino acids obtained by SWH treatment offer an explanation to these results. The smaller the size of the peptides, the more likely to adsorb on the droplet surface, conferring its electrical charge (i.e.: higher zeta potential); however, an excessively small size of peptides and amino acids does not allow the formation of a thick protein layer around the oil droplet and the emulsion ultimately collapses. On the contrary, the larger peptides obtained with Alcalase® do not provide a high surface charge but they could act as Pickering-like stabilizers, giving strong emulsion architectures derived from interfacial adsorption of protein aggregates in thick layers, and effectively improving the creaming stability of emulsion (N. Li *et al*., 2022; Liu & Tang, 2013). Zeta potential results are also closely related to surface hydrophobicity since when the absolute value of zeta potential of protein solution becomes smaller and electrostatic repulsion is reduced, the protein molecules in the system tend to aggregate with each other. As a result, the hydrophobic groups of the protein become embedded in the protein aggregates; thus, reducing the surface hydrophobicity of the protein residues and decreasing emulsion stability (D. Li *et al*., 2020).

4. Conclusions

Subcritical water hydrolysis (SWH) raises as a green and efficient method to prepare fish protein hydrolysates from fish meal (FM), its water-soluble fraction (WSP) and insoluble fraction (NSP). Compared to enzymatic hydrolysis, SWH

provides higher hydrolysis yield, higher protein recovery, and higher degree of hydrolysis, no matter what the starting material was. The techno-functional properties of fish protein hydrolysates explored in this work are highly intercorrelated. i.e., small peptides and amino acids present good solubility in a broad pH range, which opens its utilization in pharmaceutical and cosmeceutical applications. The best emulsifying properties and highest emulsion stability were observed in fish protein hydrolysates with intermediate peptide sizes and high surface hydrophobicity, such as the NSP hydrolysates. This work demonstrates that fish protein hydrolysates can be prepared using water, the greenest solvent, as the extraction solvent and the hydrolytic agent. Furthermore, the prior fractionation by conventional water extraction allowed to obtain hydrolysates with different properties, which can be targeted to specific applications. In this work, the techno-functional properties of the NSP hydrolysates were improved, yielding emulsions with lower droplet sizes and better stability than other green alternatives such as enzymatic hydrolysis. On the other hand, the hydrolyzed WSP fraction did not present good emulsifying properties, although it represents a valuable source of N in the form of free and structural amino acids with numerous industrial applications.

CHAPTER 3

Membrane fractionation of hydrolysates of the water-soluble protein from tuna fish meal obtained by subcritical water and enzymatic treatments. Comparison of physical and chemical properties

Adapted from the article:

P. Barea, A.E. Illera, H. Candela, R. Melgosa, J.M. Benito, S. Beltrán, M.T. Sanz (2025).

"Membrane fractionation of hydrolysates of the water-soluble protein from tuna fish meal obtained by subcritical water and enzymatic treatments. Comparison of physical and chemical properties"

Bioresources and Bioprocessing, *12*, 16.

DOI: https://doi.org/10.1186/s40643-025-00850-3

Capítulo 3

Fraccionamiento por membrana de hidrolizados de proteína hidrosoluble de harina de atún obtenida por agua subcrítica y tratamientos enzimáticos. Comparación de sus propiedades físicas y químicas

Resumen

Se obtuvieron dos hidrolizados diferentes de la fracción de proteína soluble en agua (WSP) de harina de atún mediante tratamientos de agua subcrítica-CO_2 (subW-CO_2) y Alcalasa®. Los hidrolizados mostraron diferente composición química en cuanto a su perfil de aminoácidos libres (FAA) y distribución del peso molecular de sus péptidos. En consecuencia, se propusieron diferentes estrategias mediante el uso de un sistema de filtración frontal con membranas de lámina plana. Se propusieron dos pasos seguidos de nanofiltración (NF) para el fraccionamiento de hidrolizados de subW-CO_2 con membranas de poliamida (800–600 Da y 300–150 Da) que produjeron un primer retenido en el que se retuvo el 79 % de la fracción proteica, mientras que el 92 % de los FAA se retuvieron en el segundo paso con un índice de pureza del 29 %. Los hidrolizados de Alcalasa® se fraccionaron por ultrafiltración (UF, 10 kDa) seguidos de NF (1–1,1 kDa) con membranas de polietersulfona obteniendo un primer retenido con más del 65 % de retención de fracción proteica con un índice de pureza del 50 %. Aunque se observó una distribución de peso molecular relativamente amplia en todas las corrientes, las fracciones retenidas no disminuyeron significativamente las altas capacidades antioxidantes y quelantes del hierro de los hidrolizados originales del alimento.

Palabras clave: Hidrólisis proteica, filtración frontal (UF y NF), perfil de amino ácidos libres y de proteína, capacidad reductora y quelante, distribución de pesos moleculares.

Chapter 3

Membrane fractionation of hydrolysates of the water-soluble protein from tuna fish meal obtained by subcritical water and enzymatic treatments. Comparison of physical and chemical properties

Abstract

Two different hydrolysates of the water-soluble protein (WSP) fraction from tuna fish meal were obtained by subcritical water-CO_2 (subW-CO_2) and Alcalase® treatments. Hydrolysates showed different chemical composition regarding their free amino acid (FAA) profile and molecular weight distribution of the peptides generated. Consequently, different strategies were proposed by using a stirred dead-end filtration system equipped with flat sheet membranes. Two nanofiltration (NF) consecutive steps were proposed for fractionation of subW-CO_2 hydrolysates with polyamide membranes (800–600 Da and 300–150 Da) yielding a first retentate where 79 % of the protein fraction was retained, while 92 % of FAA were retained in the second step with a purity index of 29 %. Alcalase® hydrolysates were fractionated by ultrafiltration (UF, 10 kDa) followed by NF (1–1.1 kDa) with polyethersulfone membranes obtaining a first retentate with more than 65 % of protein fraction retention with a purity index of 50 %. Although a relatively wide molecular weight distribution was observed in all streams, the retentate fractions did not significantly diminish the high antioxidant and iron-chelating capacities of the original feed hydrolysates.

Key words: Protein hydrolysis, dead-end filtration (UF and NF), free amino acid and protein profile, reducing and chelating capacities, molecular weight distribution.

1. Introduction

Fisheries generate various solid by-products, such as filleting waste or heads which are typically converted into fish meal and oil. Fish meal is an essential ingredient in aquaculture due to its high protein content and nutritional value. However, there is a need to explore better methods for upgrading fish meal by discovering new valuable products within the fish meal production chain. In this regard, fish protein hydrolysates are considered highly promising in the food, pharmaceutical, and cosmetic industries due to their excellent nutritional, functional, and biological activities (Barea *et al*., 2024; Bourseau *et al*., 2009). Fish protein hydrolysates consist of amino acid sequences, often between 2–20 residues, embedded within the natural protein structure. The production of fish protein hydrolysates emerges as a promising approach to add value to fish by-products, offering improved properties compared to the native protein.

This study focuses on the production and fractionation of protein hydrolysates derived from tuna fish meal. Previous research has explored the potential of water as an environmentally friendly extraction and hydrolysis agent for this material (Barea *et al*., 2023). In the present work, the initial step involved extracting the water-soluble protein (WSP) fraction from tuna fish meal through water extraction at 80 °C. Subsequently, this WSP underwent hydrolysis using subcritical water (subW) treatment by employing CO_2 as a pressurization agent (subW-CO_2). subW refers to water in its liquid state within the temperature range of 100 to 374 °C and pressures up to 22 MPa. Under these specific conditions, water exhibits unique properties. Notably, the increased concentration of H^+ and OH^- ions in the aqueous medium enhances its catalytic activity, facilitating both acid- and base-like catalyst for hydrolysis reactions (Marcet *et al*., 2016). Additionally, the introduction of CO_2 into the subW medium increases acidity through carbonic acid formation, further catalyzing WSP hydrolysis. Hydrolysates obtained by subW-CO_2 treatment (from now on SWH) were compared with those from conventional enzymatic hydrolysis

with Alcalase (from now on Alc-H), showing different chemical composition in terms of the release of free amino acids (Barea *et al*., 2023).

In the literature, a relationship has been stablished between the physicochemical characteristics of peptides, such as their molar mass distribution and their biological activity. Specifically, fractions between 1 kDa and 4 kDa are considered the most promising for nutritional and/or pharmaceutical uses (Saidi *et al*., 2014b). Hence, it is worthwhile to further investigate fractionation and concentration steps of the peptides generated during hydrolysis (Abejón *et al*., 2018).

Membrane separation processes have been proposed for the fractionation of peptides and other valuables biomolecules. Membrane technology offers a clean separation process that can be conducted under mild conditions with relatively low energy consumption. It also provides high flexibility in system design. Several studies have investigated the fractionation of marine hydrolysates, employing methods such as ultrafiltration (UF) or combined UF-nanofiltration (NF) processes to isolate fractions enriched in specific molecular weight (MW) peptides or free amino acids. These approaches aim to develop novel products with enhanced functional properties. However, the majority of existing studies have exclusively focused on the fractionation of hydrolysates obtained through enzymatic treatments with proteases, neglecting the exploration of more sustainable hydrolysis processes such as those SWH (Abejón *et al*., 2018; Chorhirankul *et al*., 2024; Pezeshk *et al*., 2019; Picot *et al*., 2010; Roslan *et al*., 2018; Saidi *et al*., 2013).

The objective of this study was to investigate the integration of different hydrolysis treatments, applied to the WSP of tuna fish meal, along with membrane separation technology. Due to the significant release of free amino acids by subW-CO_2 treatment, various membranes were initially tested using a synthetic mixture of the major amino acids released by subW-CO_2 treatment. Based on these results, a two-step consecutive NF membrane process was studied for the fractionation of SWH and a two-step UF (1^{st} step) and NF (2^{nd} step) membrane process for Alc-H.

The different fractions generated during the membrane processes were characterized in terms of their chemical composition, focusing on protein content and free amino acids, hydrolysate size distribution and antioxidant activity.

2. Experimental

2.1. Raw Material

Tuna fish meal (*Thunnus* sp.) was used as the raw material in this study. It was kindly provided by *Sarval Bio-Industries Noroeste*, S.A.U. (A Coruña, Spain). The chemical composition of fish meal has been previously reported by Barea *et al*. (2023). The protein content was 51 ± 2 % (w/w) considering as N-factor a value of 5.0 previously established and the N-elemental content (Barea *et al*., 2023).

2.2. Water soluble protein extraction

The WSP was extracted by applying the optimal extraction conditions previously determined by the authors (Barea *et al*., 2023). Specifically, 16 g fish meal per 100 mL of distilled water were put in contact at 80 °C for 30 min. Subsequently, the water-soluble extract was separated from the solid, the non-soluble water fraction, by centrifugation at 5000 rpm for 15 min. The WSP was then subjected to hydrolysis by subW-CO_2 and enzymatic treatments.

2.3. Hydrolysis by subcritical water-CO_2 treatment

200 mL of WSP from fish meal were charged in a batch high pressure reactor of 0.5 L capacity. The reactor was covered by a ceramic heating jacket (230 V, 4000 W, ⌀ 95 mm, 160 mm height) to achieve the selected working temperature. A Pt100 sensor placed inside the reactor was connected to a PID system to control and register the temperature during the hydrolysis process. The temperature for the subW-CO_2 process was selected as 180 °C and the working pressure was set at 5 MPa by using CO_2 as pressurization agent. Temperature and pressure were selected based on

previous work by Barea *et al*., where subW hydrolysis was studied within a temperature range of 140–180 °C, showing a positive effect of temperature in the hydrolysis process (Barea *et al*., 2023). The use of CO_2 as pressurization agent enhanced the production of free amino acids compared to using an inert gas such as nitrogen, likely due to the associated pH reduction caused by CO_2 dissolution in water. Regarding working pressure, its effect on the hydrolysis performance was observed to be non-significant, compared with temperature and time, as long as water remains in the liquid state. Mild reaction pressures, in the range of 40 to 60 bar, were also identified as optimal for the hydrolysis of biomass proteins to produce free amino acids (Alonso-Riaño *et al*., 2021).

After 300 min of treatment, the vessel was cooled, and depressurization was performed once the temperature dropped below 90 °C. Samples were then frozen at -18 °C until analysis and further use.

2.4. Enzymatic hydrolysis

The commercial protease Alcalase® (Novozymes [Novonesis Group], Bagsvaerd, Denmark), kindly donated by Novo Industry, was selected in this work. For the enzymatic hydrolysis, 200 mL of the WSP extract were incubated at 60 °C and pH 8 obtained by adding NaOH. To initiate the hydrolysis, 225 U of Alcalase were added to the solution, as determined according to Pokhum *et al*. (2015) with some modifications (Barea *et al*., 2023). After 240 min of incubation, the final hydrolysate was heated in boiling water for 5–10 min to inactivate the protease. All hydrolysates were centrifuged at 5000 rpm for 15 min to remove any dust particle from the solutions. The centrifuged solution was frozen at -18 °C until analysis and further use.

2.5. Membrane filtration process

The membrane filtration studies were conducted using a dead-end stirred bench-scale stainless steel HP4750 batch cell supplied by Sterlitech Corporation

(Kent, WA, USA) with a 0.3 L capacity (Figure 3.1a). The module is provided with a magnetic stirrer, a manometer, an analytical balance, and a nitrogen cylinder. The shear field generated by the stirrer helps to control membrane fouling in the dead-end module by sweeping away any dissolved matter or solute that could accumulate on the membrane surface (Roslan *et al*., 2018). Additionally, it ensures uniform hydrodynamic conditions across the entire membrane surface. In any case, for each experiment, a new membrane was used to prevent any loss of permeability due to fouling. Disk samples of flat-sheet membranes were used with an effective permeate area of 14.6 cm^2. See the detailed configuration in Figure 3.1b.

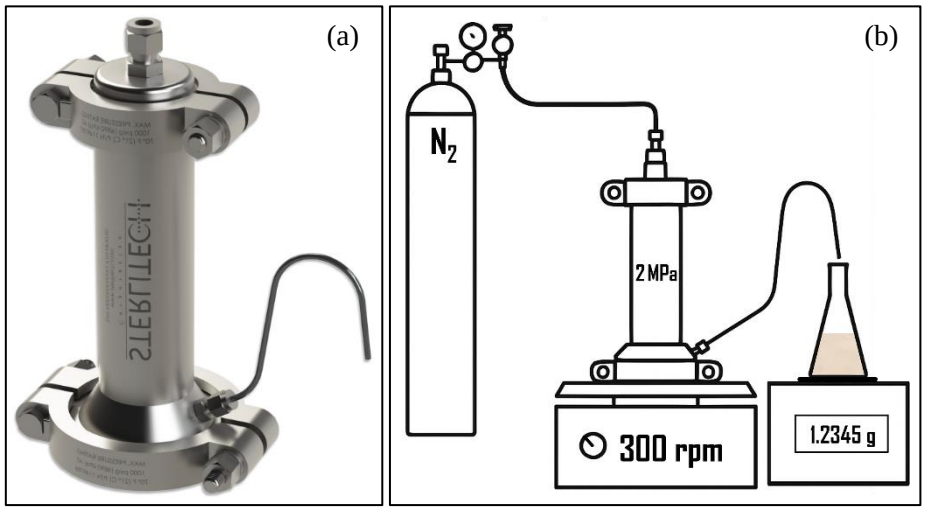

Figure 3.1. (a) Sterlitech membrane filtration reactor (Sterlitech). **(b)** Schematic diagram of the laboratory membrane filtration setup using the reactor.

Four flat sheet NF membranes were tested in this work. Three flat sheet polyamide thin-film composite (PA-TFC) NF membranes: NFG, NFW, and NFX (manufactured by Synder Filtration, CA, USA) were supplied by Sterlitech. They had different molecular weight cut off (MWCO) of ~600–800, ~300–500 and ~150–300 Da, respectively. Another NF membrane, NP010 (Microdyn-Nadir, GmbH, Wiesbaden, Germany), with a MWCO of 1–1.2 kDa, was also tested. NP010 was composed of polyethersulfone (PES) as active layer with a polyethylene / polypropylene (PE/PP) support layer. Additionally, a UF membrane, Synder-ST,

with a MWCO of 10 kDa, also made of PES as the active layer, was included in the study.

At the start of each filtration experiment, fresh membranes were tested by recirculating water until no further reduction in water flux was observed. This conditioning of the membranes ensured their wettability, stabilized the permeate flux, and removed any preservatives and wetting agents from their surface, thereby enhancing the overall membrane performance.

The filtration process was carried out at room temperature with a stirring speed of 300 rpm to simulate cross-flow filtration conditions. The transmembrane pressure was 2 MPa. The pressure on the permeate side was the atmospheric pressure for all the experiments conducted.

A feed solution volume of 200 mL was used for each filtration experiment. The permeate was collected continuously and weighed at regular intervals along the process. Once a certain mass concentration factor was reached, the experiment was interrupted. Samples of the feed, permeate and retentates fractions were collected for further analysis and stored at -18 °C.

Preliminary experiments were conducted using a synthetic amino acid aqueous mixture of alanine + glycine + proline, with a composition similar to that determined in the SWH. These experiments aimed to stablish the rejection characteristics of each membrane. Based on these results and the characterization of the molecular weight distribution of the hydrolysates, a two-step sequential NF process was proposed to fractionate the SWH, while a two-step UF/NF process was considered for the enzymatic hydrolysate (see Figure 3.2). In this operation mode, at the end of the first step, the permeate recovered was used as feed solution in the second filtration step.

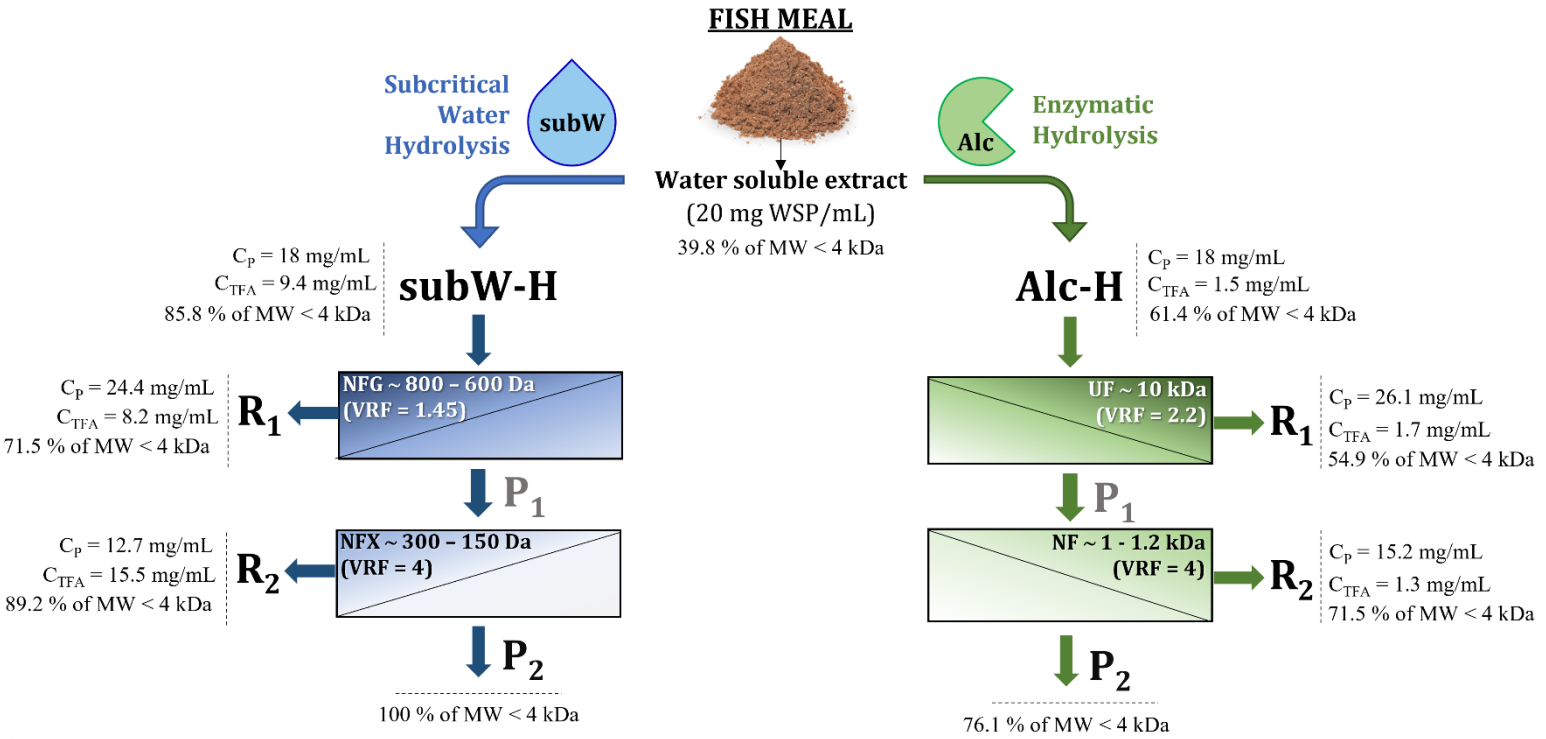

Figure 3.2. Membrane cascade approach to fractionate the protein and free amino acid fraction of SWH and Alc-H. $C_{dry\ matter}$ = dry matter concentration, C_p = protein concentration, C_{TFA} = total free amino acid concentration, mM Fe^{2+} = reducing capacity, percentage of iron chelating capacity.

2.5.1. Membrane performance parameters

The permeate flux was determined by weighing the permeate collected at a specific time:

$$J = \frac{1}{A_{membrane}} \cdot \frac{m_{permeate}}{t} \quad \textbf{[3.1]}$$

where J is the permeate flux, $kg \cdot m^{-2} \cdot h^{-1}$, $A_{membrane}$ is the effective membrane area, m^2, $m_{permeate}$ is the permeate mass, kg, and t is the filtration time, h.

The Volume Reduction Factor, VRF, is an important parameter in concentration operating mode and it is defined as:

$$VRF = \frac{V_F}{V_R} \quad \textbf{[3.2]}$$

where V_F and V_R are the initial feed and retentate volume ($V_R = V_F - V_P$), respectively, and V_P the permeate volume.

The retention percentage factor, R_i, reflects the performance of a membrane to retain certain solutes in a hydrolysate and it was evaluated according to Chorhirankul *et al*. (2024):

$$R_i(\%) = \left(1 - \frac{C_{P,i}}{C_{R,i}}\right) \cdot 100 \quad \textbf{[3.3]}$$

The concentration factor, CF, was evaluated as:

$$\text{Concentration factor} = CF = \frac{C_R}{C_F} \quad \textbf{[3.4]}$$

where $C_{P,i}$ $C_{R,i}$ and $C_{F,i}$ are the concentration of the solute, i, in the permeate, retentate and feed solutions, respectively.

The purity index of the peptide fraction or the free amino acids in the streams generated during fractionation, PI, was measured as the percentage of the corresponding fraction over the total dry matter content:

$$PI = \frac{C_{protein\ or\ amino\ acids,stream}}{C_{dry\ matter,stream}} \cdot 100 \quad \textbf{[3.5]}$$

The process yield, Y_i, was defined as the percentage of a certain component entering the system in the feed stream that was recovered in the product stream:

$$Y_i\ (\%) = \frac{mass\ of\ i\ in\ the\ product}{mass\ of\ i\ in\ the\ feed} \cdot 100 \quad \textbf{[3.6]}$$

The error of the mass balance, ε (i), was quantified by the relative error defined as the ratio of the mass residue of compound i when performing a mass balance around the unit operation to the initial amount of i expressed in percentage:

$$\varepsilon(i) = \frac{mass_{i,feed} - (mass_{i,R1} - mass_{i,R2} - mass_{i,P2})}{mass_{i,feed}} \cdot 100 \quad \textbf{[3.7]}$$

2.6. Analytical methods

2.6.1. Dry matter content

1 mL of each sample was placed in Petri dishes. The dry matter content was obtained by drying the samples in an oven at 105 ± 1 °C until constant weight was achieved. The results were expressed as mg of dry matter content/mL.

2.6.2. Total organic carbon and total nitrogen

A Total Organic Carbon Analyzer Shimadzu (TOC-V CSN) was used to quantify the concentration of total carbon (TC) and inorganic carbon (IC). Potassium hydrogen phthalate and sodium hydrogen carbonate were used as standards. The TOC concentration was then calculated by subtracting the IC concentration from the

obtained TC concentration. Total Nitrogen (TN) content was determined by using KNO_3 as standard. TOC and TN determination provides valuable information related to the total dissolved organic carbon representing the total dissolved organic molecules to help to understand the fractionation process and chemical composition of the streams generated by evaluating the molar ratio N:C.

2.6.3. Lowry method for protein determination

The Lowry method was carried out to determine the total protein content of the different streams generated in the fractionation process (Lowry *et al*., 1951). Briefly, the samples were conveniently diluted to 1 mL with deionized water. 5 mL of Lowry reagent were then added (Lowry reagent: 20 $g \cdot L^{-1}$ sodium potassium tartrate, 20 $g \cdot L^{-1}$ copper sulfate pentahydrate and 20 $g \cdot L^{-1}$ sodium carbonate in 0.1 M NaOH; in proportion 1:1:100). Samples were incubated for 15 min in the dark. Afterwards, 0.5 mL of Folin-Ciocalteu's phenol reagent, diluted 1:3 in distilled water, were added, and the mixture was let to stand for 30 min in the dark. Finally, absorbance was measured at 750 nm using a Jasco spectrophotometer and protein content was obtained based on a calibration curve using bovine serum albumin as standard.

2.6.4. Free amino acids

SubW-CO_2 and enzymatic hydrolysis would yield different products after treatment. These would include partially hydrolyzed proteins as peptides of different molecular weight, but also, free amino acids. The variety of these hydrolysis products will reflect the hydrolysis degree achieved by both methods. Free amino acids were determined in both SWH and Alc-H hydrolysates as well as in the different UF and NF streams. The amino acid profile was analyzed by gas chromatography after derivatization. The analysis was performed based on the original protocol by Hušek (1991) with some modifications. In a tube, 200 µL of the aqueous sample were mixed with 267 µL of a mixture of ethanol:pyridine (4:1), 33.3 µL of propylchloroformate (PCF) as the derivatization agent and 200 µL of Norvaline 0.2 mM (as internal standard). The tube containing the sample was gently

shaken twice for about 10 s each time, letting it rest for 1 min between shakes and carefully releasing the formed gas. Afterwards, 200 µL of chloroform containing 1 % of PCF were added to the mixture followed by 30 s of vortex stirring to ensure thorough mixing. The derivates were transferred to the organic phase, and an aliquot of this phase was injected in GC-FID instrument (Hewlett Packard, HP 5890 Series II). Aliquots of 4 µL of the derivatized amino acids were injected at 1:15 split ratio at 250 °C into a ZB-AAA column (Phenomenex Inc.), 10 m × 0.25mm I.D. The initial temperature of 110 °C was maintained for 1 min; then, the oven temperature was programmed from 110 to 320 °C at 32 °C/min. Helium was used as a carrier gas at 60 kPa and nitrogen was used as a make-up gas. The detector temperature was set at 320 °C. Amino acids were identified using pure standards for the different amino acids and with norvaline as internal standard.

The amino acid profile of the WSP was determined previous hydrolysis of the soluble protein before the derivatization. Acid hydrolysis was carried out using 6 N HCl at 100 °C for 24 h. Tryptophan, cysteine and methionine are partially or totally destroyed on this acid hydrolysis, so an alkaline hydrolysis was also carried out to determine these amino acids using a 4.2 M NaOH for 24 h at 110 °C (Barea *et al.*, 2023).

2.6.5. Determination of reducing and iron chelating capacity

Reducing capacity was assessed by the Ferric Reducing Antioxidant Power (FRAP) assay according to Benzie & Strain (1996). A solution of $FeSO_4 \cdot 7\,H_2O$ (0.1 M) was used as standard. Results were expressed in µmol Fe^{2+}/L.

The metal chelating activity was determined according to the method described by Ketnawa *et al.* (2016). 800 µL of the liquid samples were mixed with 10 µL of iron dichloride solution (2 mM) and 20 µL of Ferrozine (5 mM). After keeping the mixture for 10 min at room temperature, the absorbance was measured at 562 nm. The blank (sample with 30 µL of water instead of reagents) was subtracted from the

measured absorbance and the result was compared with the control measurement (water instead of sample). Results were expressed in % of iron chelating capacity.

2.6.6. Size Exclusion Chromatography

The molecular size distribution of the different samples was measured by Gel-Permeation Size Exclusion Chromatography coupled to a refraction index detector (GPC-SEC-RID, 1260 HPLC system, Agilent Technologies, CA, USA). The column system consisted of a Proteema precolumn (4.6 x 30 mm) and a micro column in series (4.6 x 250 mm) with a porosity of 100 Å and a particle size of 3 µm (PSS Polymer Standards Service GmbH), which allowed separation in the range from 100 to 150000 Da. Characterization of samples was performed in isocratic mode with 0.01 M NH_4Ac, at a flow rate of 0.3 mL/min at 35 °C. Standards used for the calibration consist of a pullulan standard set (from 342 Da to 343 kDa). Data were analyzed with Agilent OpenLab Data Analysis 2.5 software. After filtration through 0.45 µm syringe filters, a volume of 10 µL of samples and standards were injected. The total area of the chromatogram was integrated and separated into fractions of five molecular weight (MW) ranges (> 10000, 10000–6000, 6000–4000, 4000–2000, 2000–1000, 1000–300, and < 300 Da, respectively), expressed as the percentage of the total area.

3. Results and discussion

3.1. Production and characterization of subcritical water and enzymatic hydrolysates from WSP fraction

The production of the WSP fraction from tuna fish meal, as detailed in section 2.2, resulted in an aqueous solution with a concentration of 20.5 ± 0.8 mg of WSP/mL, as determined by the Lowry assay. subW-CO_2 hydrolysis and enzymatic hydrolysis were carried out to generate small peptides and free amino acids in the medium. This hydrolysis process was a crucial step that determined further design

strategies for the stages of separation, fractionation, and purification of small peptides and the free amino acids generated.

The amino acid profile of the SWH and the Alc-H is summarized in Table 3.1. Additionally, the amino acid profile of the WSP is also presented in Table 3.1, being glycine (199 ± 9 mg/g_{wsp}), proline (111 ± 5 mg/g_{wsp}), glutamic acid (including glutamic acid and glutamine, 103 ± 14 mg/g_{wsp}) and alanine (83 ± 7 mg/g_{wsp}) identified as the most abundant amino acids in the WSP fraction of fish meal.

subW-CO_2 and enzymatic treatments yielded hydrolysates with different properties and chemical composition (Barea *et al*., 2023). These authors showed the generation of peptides of smaller size by subW-CO_2 compared to enzymatic hydrolysis as supported by size exclusion chromatography. SWH yielded a higher amount of free amino acids (9.4 ± 0.9 mg/mL) compared to Alc-H (1.5 ± 0.2 mg/mL, see Table 3.1). Table 3.2 summarized the molecular weight (MW) distribution of both hydrolysates together with the MW distribution of the WSP. It can be observed that the Alc-H contains peptides with a higher degree of polymerization, accounting for 38.5 % (w/w) peptides with MW higher than 4000 Da, while this percentage was 14.1 % (w/w) for SWH. The high percentage of molecules with a MW lower than 300 Da and the higher amount of free amino acids must be highlighted in the SWH (Table 3.1). In any case, the percentage of peptides with MW higher than 4000 Da was lower in both hydrolysates than the distribution determined for the initial WSP extract with more than 60 % (w/w), 37.7 % (w/w) corresponding to the fraction of MW > 10000 Da. The different chemical composition determined the selection of the membrane separation cascade processes to concentrate the valuable fractions of the protein hydrolysates (see Figure 3.2).

Table 3.1. Amino acid profile of the WSP from fish meal. Characterization of the SWH at 180 °C and Alc-H at 60 °C: Free amino acid profile, total protein content, dry matter content and reducing and chelating capacity.

Amino acid	WSP	SWH	Alc-H
	aa profile, mg aa/g_{WSP}*	Free amino acids released, mg/mL	
Ala	83 ± 7	1.55 ± 0.05	0.135 ± 0.003
Gly	199 ± 9	3.05 ± 0.07	0.067 ± 0.006
Val	29 ± 5	0.22 ± 0.02	0.054 ± 0.005
Leu	36 ± 2	0.19 ± 0.3	0.07 ± 0.01
Ile	18 ± 2	0.09 ± 0.01	0.041 ± 0.004
Tre	31 ± 2	0.074 ± 0.005	0.024 ± 0.004
Ser	36 ± 5	0.14 ± 0.02	0.033 ± 0.006
Pro	111 ± 5	1.04 ± 0.07	0.047 ± 0.005
Asp	70 ± 7	0.94 ± 0.1	0.12 ± 0.02
Met	12 ± 2	0.15 ± 0.01	0.044 ± 0.009
Hyp	58 ± 9	0.39 ± 0.08	0.021 ± 0.009
Glu	103 ± 14	0.30 ± 0.03	0.06 ± 0.02
Phe	21 ± 2	0.32 ± 0.04	0.083 ± 0.07
Lys	37 ± 6	0.24 ± 0.02	0.13 ± 0.03
His	13 ± 2	0.46 ± 0.03	0.33 ± 0.01
Hyl	51 ± 18	0.062 ± 0.005	0.086 ± 0.003
Tyr	15 ± 3	0.082 ± 0.003	0.06 ± 0.01
Trp	54 ± 12	0.034 ± 0.005	0.042 ± 0.003
Cys	25 ± 9	0.057 ± 0.004	0.05 ± 0.01
Total	1002 ± 121	9.4 ± 0.9	1.5 ± 0.2
Dry matter, mg/mL	40 ± 2	48 ± 3	39 ± 1
Protein, mg/mL	20 ± 1	18 ± 1	18.6 ± 0.7
mM Fe^{2+}	0.57 ± 0.01	3.8 ± 0.2	0.48 ± 0.01
Chelating capacity, %	5.6 ± 1.3	68 ± 2	88 ± 1

Ala: alanine, Gly: glycine, Val: valine, Leu: leucine, Ile: isoleucine, Tre: threonine, Ser: serine, Pro: proline, Asp: aspartic acid, Met: methionine, Hyp: hydroxyproline, Glu: glutamic acid, Phe: phenylalanine, Lys: lysine, His: histidine, Hyl: hydroxylysine, Tyr: tyrosine, Trp: tryptophan, Cys: cysteine.
*20.5 ± 0.8 mg protein/mL.

Table 3.2. Molecular weight distribution (Da) of the WSP extract, SWH and Alc-H and their UF/NF fractions, expressed as % (w/w).

Molecular weight (Da)	> 10000	10000–6000	6000–4000	4000–2000	2000–1000	1000–300	< 300
WSP extract	37.7 ± 0.3	12.5 ± 0.2	10.0 ± 0.1	26.4 ± 0.3	8.4 ± 0.2	3.7 ± 0.1	1.30 ± 0.05
SWH	0.20 ± 0.05	10.5 ± 0.4	3.4 ± 0.1	18.7 ± 0.3	13.1 ± 0.3	15.9 ± 0.2	38.1 ± 0.4
NF, R1	2.1 ± 0.1	21.7 ± 0.3	4.6 ± 0.1	20.1 ± 0.2	9.5± 0.2	13.3 ± 0.3	28.6 ± 0.4
NF, R2	0.01 ± 0.00	7.7 ± 0.2	2.9 ± 0.1	17.4 ± 0.2	18.4 ± 0.3	15.7 ± 0.3	37.8 ± 0.5
NF, P2	0.00 ± 0.00	0.00 ± 0.00	0.00 ± 0.00	6.6 ± 0.1	23.7 ± 0.4	44.8 ± 0.5	24.8 ± 0.3
Alc-H	11.6 ± 0.2	16.8 ± 0.2	10.1 ± 0.2	30.2 ± 0.4	19.4 ± 0.4	5.1 ± 0.2	6.7 ± 0.1
UF, R1	14.2 ± 0.3	21.0 ± 0.4	10.0 ± 0.1	24.2 ± 0.4	19.8 ± 0.3	5.0 ± 0.1	5.8 ± 0.2
UF, R2	5.1 ± 0.2	14.0 ± 0.3	9.4 ± 0.2	34.4 ± 0.5	23.7 ± 0.4	5.7 ± 0.1	7.7 ± 0.2
UF, P2	2.3 ± 0.1	6.8 ± 0.1	14.8 ± 0.3	49.4 ± 0.4	10.8 ± 0.2	6.2 ± 0.2	9.6 ± 0.3

A higher reducing capacity was observed for the SWH compared to the Alc-H, 3.8 ± 0.2 and 0.48 ± 0.01 mM Fe^{2+}, respectively. However, the Alc-H exhibited higher iron chelating capacity with a value of 88 ± 1 % compared to 68 ± 2 % for SWH. It is important to note that the FRAP reducing capacity test is based on single electron transfer reactions, while transient metal ion chelation acts indirectly as an antioxidant mechanism by inhibiting radical chain reactions. The higher temperatures of subW-CO_2 treatment compared to enzymatic hydrolysis could lead to conformational changes of peptides hydrolysates leading to lower iron chelating capacity, although presenting peptides with low molecular weight distribution (Barea *et al*., 2024). Furthermore, the lower iron chelating capacity determined for SWH could also be related with the higher amount of free amino acid released into the medium. According to Guidea *et al*. (2020), metal chelating capacity of the free proteinogenic amino acids shows a moderate Fe^{2+} chelating activity with values of 4.90 ± 0.03, 65 ± 1 and 34 ± 3 % for the major free amino acids released by subW-CO_2 treatment: alanine, glycine and proline (see Table 3.1), respectively. It is important to note that Guidea *et al*. (2020) achieved these results by using standard amino acid solutions in known concentrations, in contrast to the complex matrices employed in this study.

3.2. Membrane concentration process in stirred dead-end filtration

3.2.1. Pure amino acid mixture filtration

First, the effectiveness of different NF membranes in retaining the major free amino acids released during subW-CO_2 treatment was studied. The feed amino acid concentrations were as follows: 1.5 ± 0.1 mg alanine/mL, 3.0 ± 0.1 mg glycine/mL ± 0.1 and 1.0 ± 0.1 mg proline/mL. After conditioning the membranes with water, permeation of the multicomponent pure amino acid mixture was performed with the four NF membranes used in this work (NFG, NFW, NFX of polyamide-TFC and NP010 of PES). Filtration experiments were ended at a VRF = 4. Additionally, the

amino acid retention for the UF-ST membrane was also tested for the pure amino acid mixture to cover all the membranes considered in this study. Figure 3.3a shows the permeate flux determined for the five membranes. The UF Synder ST membrane exhibited the highest permeate flux with an abrupt decay observed at the beginning of the process, 23 % of decrease, followed by a plateau around 2 VRF values. The total permeate flux for all the NF membranes was lower than for UF and there was observed a correlation between MWCO and membrane permeate flux for NF regardless of the membrane material (PES or PA-TFC). However, it must be highlighted that only slightly higher permeate flux were determined for NFX (300–500 Da) compared to NFW (150–300 Da). There was also observed an initial decay in J for the NF membranes with the highest MWCO (NFG and NP010), similar to the pattern observed for the UF-ST; with 17 % and 9 % of decrease for NP010 and NFG, respectively. On the contrary, the permeate flux exhibited a smooth maximum for NFW and NFX, followed by a slight decrease. Tamires *et al*. (2020) also observed a similar phenomenon for different NF membranes, where the permeate flux increased at the beginning of the filtration process, stabilizing after a certain time. This behavior was attributed to the swelling of the membrane, which provided greater flux initially and resulted in less rejection by the membrane.

At various VRF ratios, permeate samples were collected and analyzed for amino acid composition. A steady increase in the total amount of amino acids permeating through the membrane was observed as the value of the VRF ratio increased for the three amino acids and for each of the membranes studied (Figure 3.4a-c), being this increase less pronounced for the smallest pore size membrane, NFX.

A correlation was also observed between the MWCO for the series of NFG/NFW/NFX membranes and amino acid permeation, with higher permeation for all the three amino acids as the MWCO of the membrane increased. However, for the NP010 and UF membrane of PES polymer, there was no clear correlation between MWCO and permeation of the three amino acids. In fact, similar

percentages of the amino acids in the permeate stream were obtained for the NP010 membrane (1–1.2 kDa), the Synder-UF (10 kDa), and of the order of NFG membrane, especially for the smallest amino acids, alanine and glycine, probably due to the small molecular weight of these amino acids compared to the MWCO of these membranes. This was also reflected in the values of the retention percentage factor (R_{aa} %) of the amino acids (Eq. 3.3) and the yield of the amino acid in the retentate stream ($Y_{aa,\ retentate}$ %), see Figure 3.4d-f). For example, at VRF = 4.0, for the 600–800 Da NFG membrane, $R_{Glycine}$, the smallest amino acid, was 6 %, increasing to 45 % and 82 % for the 300–500 Da NFW and 150–300 Da NFX, membranes respectively, corresponding to values of $Y_{Glycine,retentate}$ of 26 %, 44 % and 76 %. The values for NP010 and UF membranes were of similar order as for the NFG membrane. These results support the idea that the amino acid separation occurs not only by size exclusion, but also by the interaction of the membrane polymer with the components of the feed, which might play an important role, as suggested by Chorhirankul (2024) in their study. For instance, values as high as 23 %, 24 % and 28 % for $Y_{Glycine,retentate}$, $Y_{Alanine,retentate}$ and $Y_{Proline,retentate}$ were obtained for 10 kDa UF-Synder membrane (MWCO >>>> $M_{W,amino\ acids}$).

The concentration factor, CF (Eq. 3.4), was also plotted for alanine, glycine and proline at the end of the process (VRF = 4) for all the membranes. According to the previously presented values, CF values significantly higher than the unity were only obtained for NFW and NFX membranes. Therefore, NFW or NFX membranes could be appropriate for amino acid concentration, and considering the higher retention values for all the amino acids, NFX membrane could be a good option as NF step to concentrate the high amount of free amino acid obtained in the SWH, previous removal of larger peptides.

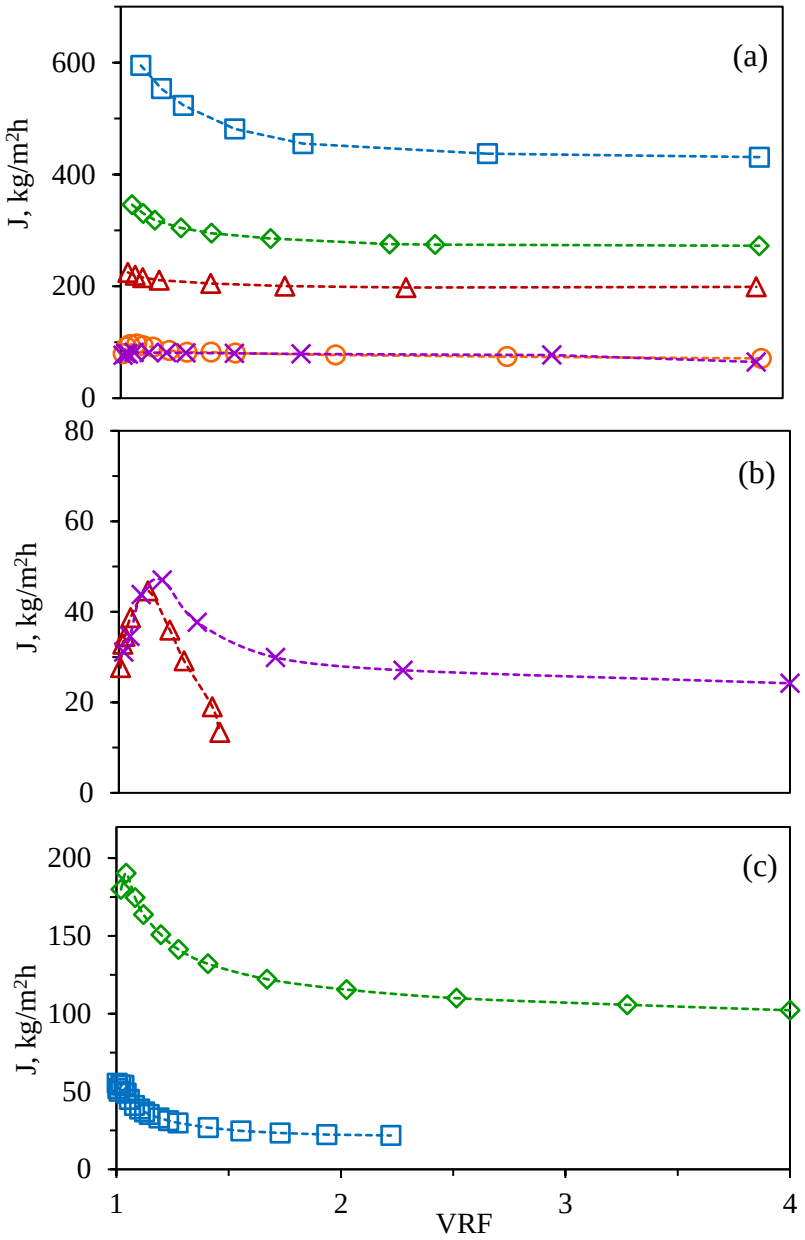

Figure 3.3. Total permeate flux (J) for **(a)** pure amino acid mixtures (□ UF-Synder, ◇ NP010, △ NFG, ○ NFW, × NFX). **(b)** SWH (△ 1st step NFG, × 2nd step NFX). **(c)** Alc-H (□ 1st step UF-Synder, ◇ 2nd step NP010). Lines are drawn to guide the eye.

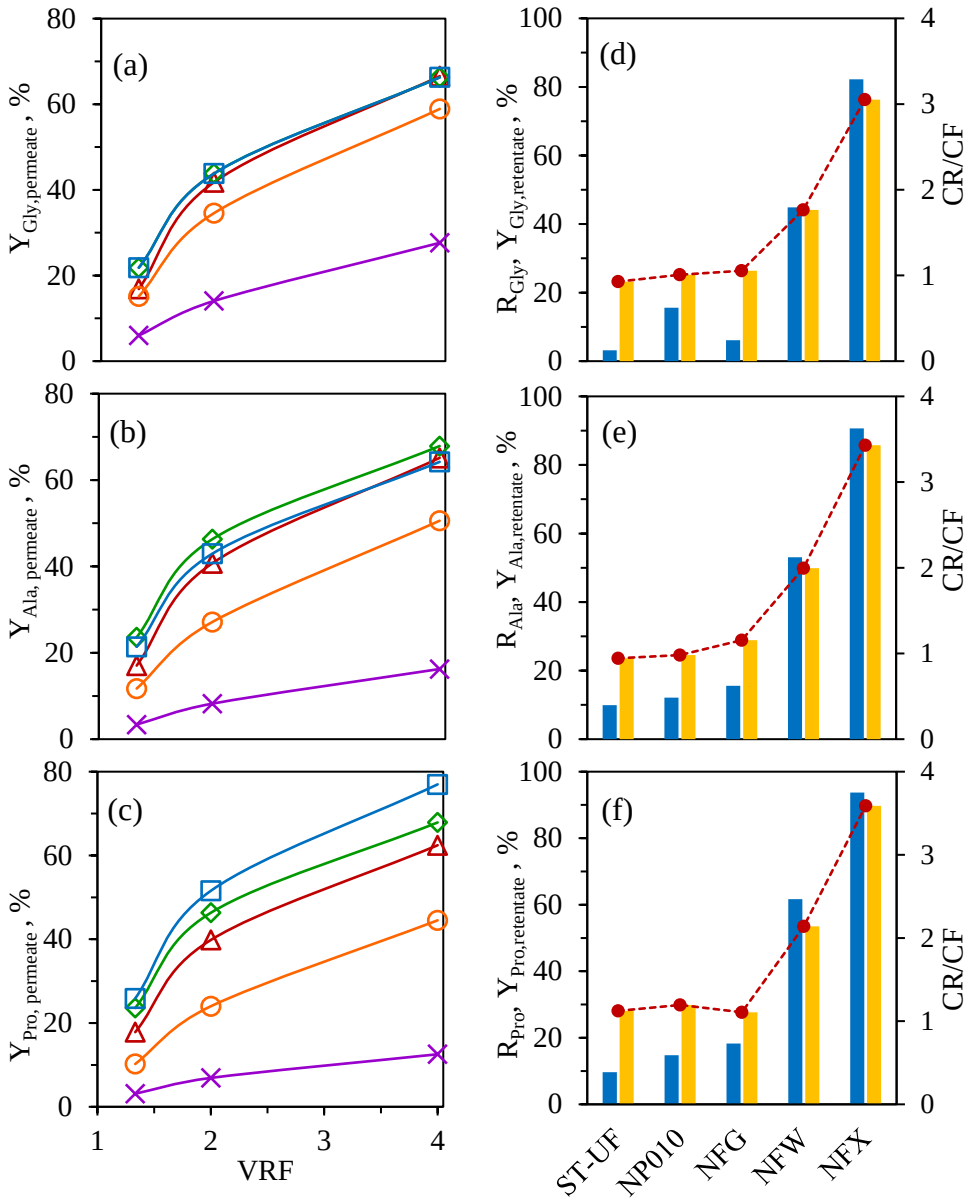

Figure 3.4. Percentage recovery of the amino acid in the permeate stream as a function of the concentration factor **(a)** glycine **(b)** alanine **(c)** proline for different membranes: □ UF-Synder, ◇ NP010, △ NFG, ○ NFW, × NFX. **(d, e, f)** Amino acid retention (■), percentage recovery in the retentate stream (■) and CR/CF (●) at VRF = 4 for the different membranes. Lines are drawn to guide the eye.

Additionally, a correlation was also observed between the molecular weight of the three amino acids and their corresponding retentions for each individual

membrane (see Figure 3.4). For instance, for the NFX membrane at VRF = 4, $R_{Glycine}$ = 82 %, $Y_{Glycine,retentate}$ = 76 % and CF = 3.1, were obtained for glycine (M_W = 75.07) while these parameters were evaluated as $R_{Alanine}$ = 91 %, $Y_{Alanine,retentate}$ = 86 % and CF = 3.4 for alanine (M_W = 89.09); and $R_{Proline}$ = 94 %, $Y_{Proline,retentate}$ = 90 % and CF = 3.6 for proline (M_W = 115.13). A similar pattern was observed for the other membranes with higher MWCOs (see Figure 3.4), but with lower values of the retention, amino acid recovery in the retentate and concentration factor, according to their increased permeation through the membrane.

Mass balances were performed for each amino acid, considering the initial mass in the feed and the collected mass in the retentate and permeate streams for all the tested membranes at the end of the filtration experiment (VRF = 4). The relative error in the mass balance was consistently lower than 10 %, except for experiment with UF membrane that reached deviations of 12 and 10 % for alanine and glycine, respectively.

3.2.2. Two-step nanofiltration process to fractionate subW-CO_2 hydrolysates

3.2.2.1. Permeate Flux

Based on the results obtained from the molecular weight distribution of the SWH and the separation of a pure amino acid mixture, a two-step NF process was proposed to fractionate the components of this hydrolysate (see Figure 3.2). Initially, the NFG membrane (~600–800 Da) was selected to retain the fraction of molecules in the SWH with MW higher than 800 Da, which approximately corresponds to 36 % of the total molecules in the hydrolysate (considering the molecules of MW higher than 1000 Da, as shown in Table 3.1). The permeate from this first step is expected to be enriched in the free amino acids present in the SWH. Therefore, the permeate obtained from this initial fractionation step was used as feed in a second filtration step using the NFX membrane. The NFX was chosen over the NFW membrane based on results obtained for filtration of a pure amino acid synthetic mixture, where

both membranes (NFX ~150–300 Da and NFW ~300–500 Da) showed similar permeate flux. However, the NFX membrane provided higher retention and concentration factors for individual free amino acids. The polyamide membrane series was considered in the SWH fractionation to maintain consistency in the polymer type throughout the NF sequence for this hydrolysate.

The permeate flux has been plotted in Figure 3.3b showing much lower values compared to the synthetic mixture of amino acids (Figure 3.3a), specially for NFG membranes. The initial permeate flux (J_o) for NFG membrane was 225 kg/m^{2}h in the amino acid mixture decreasing to 28 kg/m^{2}h for SWH. This result suggests that fouling on the membrane surface has a significant effect on permeation performance; peptides and free amino acids can be adsorbed on the polyamide membrane reducing the permeate flux (Tamires *et al*., 2020).

In the 1st stage, larger solutes with diameters larger than the membrane pores could be deposited on the membrane surface, causing the formation of a cake layer. Additionally, solutes of similar size to the pore size of the membrane could also partially seal the membrane pores. Due to low and continuously decreasing permeate flux, the experiment was stopped when the VRF reached 1.45, with a permeate flux of 13.4 kg/m^{2}h that corresponds to 0.33 g/min. This was before reaching the VRF of 4.0, which was studied for the pure amino acid mixture and would have resulted in an extended operation time. In the 2nd step of the sequential process, the decrease in the permeation flux for the NFX membrane was less pronounced, with J_o values of 77 kg/m^{2}h and 31 kg/m^{2}h for the amino acid mixture and the hydrolysate, respectively, at a VRF of 4.0 in this second step. The lower J decrease in permeation flux in the 2nd step was observed in other sequential processes, as reported by Saidi *et al*. (2013) in their study, due to the reduction of adsorption on the membrane surface, which is related to the lower amount of dry matter in the feed of the 2nd stage (P1). The initial content of dry matter in the SWH (feed of the 1st stage) was 48 mg dry matter/mL (Figure 3.2), while this concentration was reduced to 26 mg dry matter/mL in the P1 (feed of the 2nd stage). This low dry matter concentration in the

2nd stage allowed reaching a VRF of 4 in the second stage. Dry matter content was also determined in the R1, R2 and P2 streams, being 65, 53 and 18 mg/mL, respectively. The dry matter concentration allowed us to determine its retention percentages in the two consecutive stages, considering the corresponding feed entering the system as 61 and 67 % in the 1st and 2nd stages, respectively. For both membranes, the permeate flux initially increased from 28 to 45 kg/m^{2}h for NFG membrane and from 31 to 47.0 kg/m^{2}h for NFX membrane, and then decreased continuously until the end of the process. Swelling of the membrane could initially lead to higher flux, allowing more soluble solids to adhere to the membrane surface in a given time. This could result in a faster growth of the cake layer that led to faster decrease in permeate flux, especially for the NFG membrane.

Mass balance of the total dry matter has been plotted in Figure 3.5 considering the final streams R1, R2 and P2 of the consecutive process. At the end of the sequential step, most of the dry matter was retained in the first retentate (yield of 84.7 %), while only 10.3 % of the initial dry matter content of the feed was in R2 and P2. This is consistent with the low permeate flux in the first stage. The error of the mass balance, evaluated with Eq. 3.7, was determined as 5.3 % (Figure 3.5).

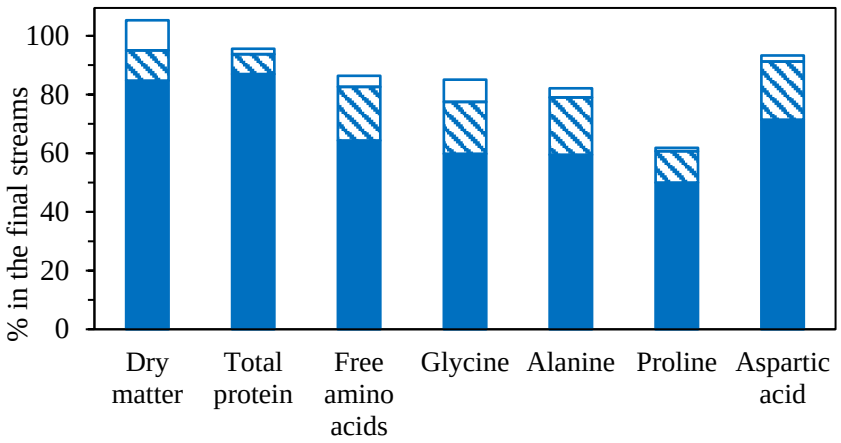

Figure 3.5. Mass balance of dry matter, protein content, free amino acids and the major free amino acids determined in SWH (retentate of the NFG step (■ R1), retentate of the NFX step (▨ R2) and permeate of the NFX step (□ P2).

3.2.2.2. Peptides and amino acid separation

Peptides

During the fractionation step, the protein concentration in the R1 (VRF = 1.45) increased up to 24.4 mg/mL (CF = 1.4, from 18 mg/mL). The highest protein concentration factor was reached in the second NF step increasing from 5.1 mg/mL (P1=F2) to 12.7 mg/mL (CF = 2.5). These results indicate that most of the protein fraction was rejected by the membranes and concentrated in the retentates in the two-step consecutive process. Figure 3.6a collects the retention percentages evaluated with the reported concentration data of the protein fraction, yielding 79 % and 91 % in the 1st and 2nd stages and purity indexes of 38 % and 24 %, in R1 and R2, respectively.

The mass balance of total protein content was determined and also plotted in Figure 3.5, showing that 87 % of the initial protein content was retained in the R1 and less than 2 % of the initial protein content was determined in the final permeate P2. The error of the mass balance, evaluated with Eq. 3.7, was less than 4.5 %, indicating that the material balance closely matches for the protein fraction and that it was not adsorbed on a great extent on the surface of the polyamide membranes.

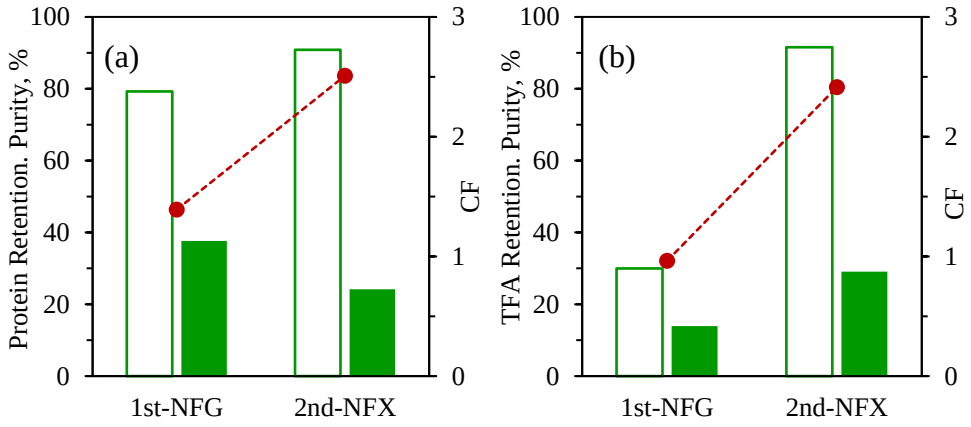

Figure 3.6. Retention percentages, purity and concentration factor of SWH (□ retention percentage, ■ purity index in the retentates, ● concentration factor). **(a)** Peptide fraction. **(b)** Total Free amino acids (TFA).

Total free amino acids

The retention percentage, purity and concentration factor of total free amino acids in the SWH have been plotted in Figure 3.6b. Total free amino acid content was evaluated as the sum of the individual free amino acids as determined by gas chromatography (section 3.1). The retention percentage in the 1st stage was 30 %. This value is slightly higher than the value previously reported for the individual amino acid in a synthetic pure amino acid mixture, which could be attributed to the a higher fouling degree observed during the SWH filtration in this first step. On the contrary, the rentention degree of total free amino acids in the 2nd stage (NFX membrane) was 92 %, within the range of values reported for individual amino acids in the synthetic mixture. The purity index for total free amino acids was 14 % and 29 % in the retentates of the consecutive steps, R1 and R2, respectively, achieving a concentration factor of 2.4 in the second step.

Table 3.1 reports the individual free amino acids determined in the SWH, with alanine, glycine and proline being the major free amino acids released. To evaluate the behavior of these individual amino acids, Figure 3.7a plots the concentration of these individual free amino acids in the different streams, along with the concentration of the total free amino acids. This Figure also includes aspartic acid since its percentage in the initial feed was 10.8 % of the total free amino acids (0.94 mg/mL, see Table 3.1), slightly lower than that of proline. The individual retention degree in each stage followed a similar pattern to the retention determined for the total free amino acids (see Figure 3.6a), with retention values higher than 85 % in the second stage of the consecutive process. For the smallest amino acids (glycine and alanine) the lowest value for the retention percentage was reached in the first stage, with values of 11.3 and 27.7 %, respectively.The highest concentration of total free amino acids was determined in the R2 (15.3 mg/mL), with glycine (5.8 mg/mL) and alanine (3.2 mg/mL) being the most abundant amino acids in R2, accounting both amino acids for 59 % of the total free amino acids in this stream.

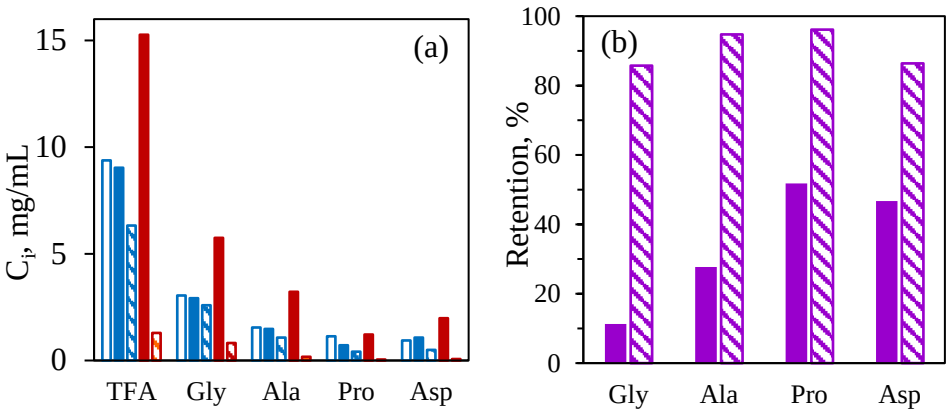

Figure 3.7. (a) Concentration of TFA and some individual free amino acids in the different streams □ SWH (initial hydrolysate), ■ R1, ▨ P1, ■ R2, ▨ P2. **(b)** Retention percentage of most abundant free amino acids in SWH (■ R1, ▨ R2). Gly = glycine, Ala = alanine, Pro = proline, Asp = aspartic acid.

The mass balance of total free amino acids and the selected individual free amino acids was evaluated and included in Figure 3.5. 64 % of the initial total free amino acid content was retained in the R1, 18 % in R2 and less than 4 % was determined in the final permeate P2. The error of the mass balance, evaluated with Eq. 3.7, yielded a higher error in the mass balance compared to the total protein fraction and the dry matter, with an error of 13.7 %. The errors in the mass balance for glycine, alanine and aspartic acid were of the same order (see Figure 3.5); however, the mass balance was not satisfactory for proline, which could be due to analytic problems (especially in the permeate fraction where its concentration was very low) or to adsorption on the membrane materials.

Total organic carbon and nitrogen content

It was determined by TOC-Analyzer, and evaluated in the different streams of this consecutive process. The values obtained allowed us to evaluate the molar ratio N:C in the different streams. The ratio N:C was in the range of 0.31–0.32 for the feed (SWH) and R1 and R2 fractions. These values agree with the N:C ratio reported by Rivas-Ubach *et al*. (2018) for peptides-type compounds (N:C = 0.3) indicating that most of the organic matter corresponds to protein-type compounds, which aligns

with the chemical composition of the initial extract of WSP. However, the N:C ratio in the final permeate P2 was higher, N:C = 0.49. This higher value could be consistent with the higher amount of glycine ($C_2H_5NO_2$, N:C = 0.5) in the final permeate compared to other peptides and free amino acids.

Molecular weight distribution

The MWD of the three diferent final streams (R1, R2 and P2) generated in the two consecutive steps are listed in Table 3.2. As described in section 3.1 the weight percentage of peptides of MW higher than 4000 Da accounted only for 14.1 % in the SWH, with only 0.2 % of MW higher than 10 kDa, due to higher hydrolytic power of the subW reaction medium due to the addition of CO_2. These higher MW peptides were concentrated in the R1 fraction, as this fraction accounted for 28.4 % (w/w) of the distribution (21.72 % in the range from 10 kDa to 6 kDa) . The significant flux reduction determined in the first step could therefore be related to the substantial membrane fouling due to the presence of these peptides of higher molecular ranges. However, R1 still contained a large peptide fraction with MW lower to the MWCO of NFG (600–800 Da, see Table 3.2). On the contrary, the percentage of peptides with MWCO higher than 4 kDa in R2 was 10.7 %, less than half of the percentage of R1. The lower concentration of these high MW molecules supports the fact that the permeate flux in the second step was relatively higher than in the first step. Peptides with MW below 4000 Da accounted for 89.3 % and 100 % in R2 and P2, respectively. However, the NFX retentate (R2) still contained peptides of MW below 300 Da, while peptides higher than 300 Da were also presented in the permeate (P2). Both membranes, NFG and NFX, initially swelled upon contact with the hydrolysate (see Figure 3.3b) that could lead to the permeation of peptides of higher MW than the MWCO of the membrane.

Although a certain trend was observed with the MWCO of the different streams, results indicate that the selected membranes did not achieve sharp separations, since a relative wide MW distribution of peptides was found in several fractions. Similar conclusions were drawn by Picot *et al*. (2010) in the treatment by UF and NF in a

consecutive process to fractionate Prolastin, a commercial hydrolysate obtained by controlled proteolysis of skins from North Atlantic lean fish. These authors observed that a first UF step with a modified polyethersulfone membrane (MWCO of 4 kDa) still produced a retentate with a large portion of peptides below 4000 Da (as high as 93 % by weight), even though high VFR was reached. Meanwhile, the NF retentate of the second step process proposed by Picot *et al*. (2010) still contained about 22 % of peptides below 300 Da (MWCO of the membrane).

3.2.2.3. Reducing and iron quelating capacity

The reducing capacity, expressed as mM Fe^{2+} and the iron quelating capacity of the different streams generated in the cascade process have been plotted in Figure 3.8. Both parameters followed a similar trend in the different streams. R1 and R2 presented higher reducing and iron quelating capacity than the corresponding permeates, with the highest value determined in the R1, 5.30 mM Fe^{2+} and 89 % of iron quelating capacity. The higher reducing capacity observed in the feed (F) and R1 could be due to a synergistic effect among the different peptides generated in the hydrolysis process, reducing this effect when the membrane fractionation was performed and peptides of higher MW were retained in the R1 fraction. There was a strong positive correlation between both, reducing and iron quelating capacities ($r = 0.9103$, p-value $= 0.0318 < 0.05$), according to the Pearson linear correlation. Furthermore, both parameters were visually correlated with the color of the different fractions; the darker the fraction, the higher the reducing and iron quelating capacity.

The lower reducing capacity for P1, R2 and P2 could be also attributed to its lower dry matter content. The following values of reducing capacity were obtained when expressing the results as mM Fe^{2+}/mg_{DM}: 0.079, 0.082, 0.054, 0.047, and 0.044 for F, R1, P1, R2 and P2, respectively. When evaluating the reducin capacity as mM $Fe^{2+}/mg_{protein}$ the following values for F, R1, P1, R2 and P2 were obtained: 0.21, 0.22, 0.28, 020, and 0.66, respectively, showing the highest value for P2, free of molecules of MW higher than 4000 Da.

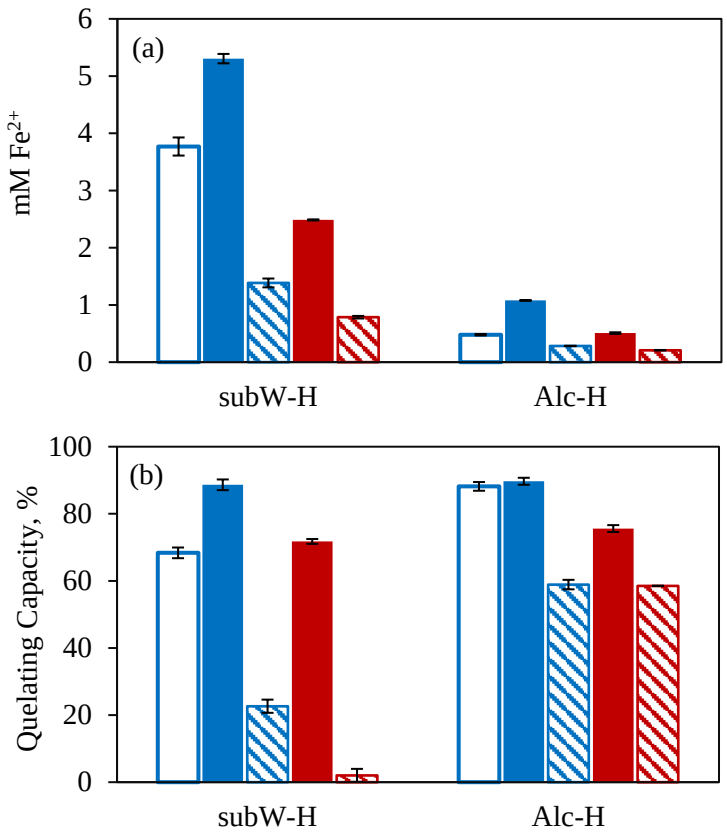

Figure 3.8. (a) Reducing capacity and **(b)** Iron quelating capacity of SWH and Alc-H in the different streams: ☐ initial hydrolysate, ■ R1, ▨ P1, ■ R2, ▨ P2.

3.2.3. Fractionation of Alcalase hydrolysates

3.2.3.1. Permeate Flux

Alc-H presented a low concentration of free amino acids (1.5 mg/L) with a peptide fraction of MW higher than 10 kDa of 11.6 % of the total peptide fraction (16.8 % close to the MWCO of the membrane, in the range of 6000–10000 Da, according to the distribution presented in Table 3.1). Based on this composition, the following cascade approach was proposed: (1) a 1st UF step by using the UF-Synder membrane with a MWCO of 10 kDa to remove the peptide fraction of higher MW, (2) the permeate from the UF step will be the feed of a 2nd NF step by using the NP010 membrane (Figure 3.3) to concentrate molecules with MW higher than 1000–

1200 Da but lower than 10000 Da. Due to the low concentration of free amino acids in the Alc-H, no concentration step was proposed for this fraction. The NP010 membrane was chosen over the NFG membrane to use the same polymer through the Alc-H fractionation sequence, specifically polyethersulfone polymer.

The permeate flux for both separation steps have been plotted in Figure 3.3b. A great reduction in the permeate flux was obtained when using the Alc-H compared to the amino acid mixture as feed, from 594 to 52 kg/m^{2}h for UF-Synder and from 346 to 180 kg/m^{2}h for NP010, respectively. Surprisingly, J was lower in the 1st step for UF-Synder (10 kDa) than in the 2nd separation step using NP010 NF membrane (1–1.2 kDa). This could be attributed to the larger pore size of UF-Synder membrane making it more susceptible to pore blocking and particle deposition, resulting in a greater permeate flux decline. However, fouling is a complex phenomenon depending on the characteristics of the membrane and the feed. Polyethersulfone membranes could be classified as hydrophobic when compared with polyamide membranes. In the literature, it has been described that the peptides usually adsorb more readily to hydrophobic materials compared to hydrophilic ones (such as NFG and NFX), which could lead to the observed high initial flux decrease for UF-Synder due to the formation of a dense cake layer by the peptides in the feed (Chorhirankul *et al*., 2024). Due to complex fouling processes observed during the first UF step, filtration was stopped when the VRF reached 2.2, corresponding to a permeate flux of 21.7 kg/m^{2}h, 0.53 g/min, to avoid prolonged operation times.

A less pronounced decrease in J was observed in the second separation step, compared to what was observed in the SWH fractionation. The higher permeate flux obtained with NP010 could be explained by considering the dry matter content in the different streams, similar to the performance of SWH. Dry matter in the feed, the Alc-H, was 39 mg/mL, while the dry matter concentration of the P1 stream (the feed of the 2nd stage) was 25 mg/mL. The dry matter retention coefficients were 52 and 71 % in the 1st and 2nd stages, respectively.

The values of dry matter concentration and VRF allowed us to evaluate the mass balances for the total dry matter considering the three final streams obtained in the process: R1, R2 and P2 (Figure 3.9). The yield for dry matter in the R1 stream was 61 %. This high retention of the dry matter in the first step also explains the low J values. This value was lower than the yield for SWH due to the higher MCWO of the UF membrane compared to that of the NFG membrane employed in SWH. Similar dry matter yields were obtained in the R2 and P2 fractions in the second fractionation steps, with values of 17 % and 15 %, respectively. The error of the mass balance, evaluated with Eq. 3.7, was determined to be 7 %.

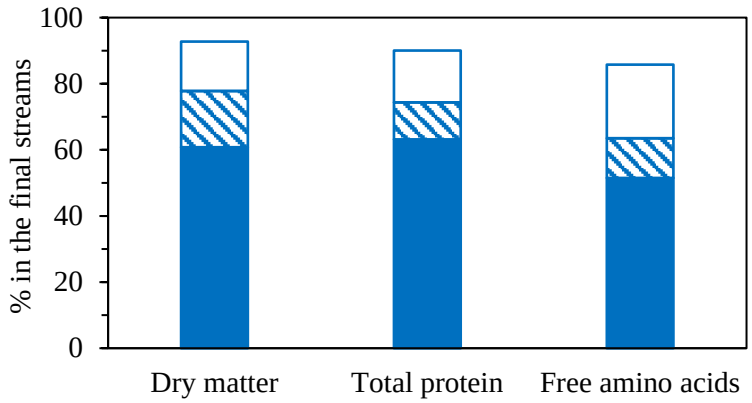

Figure 3.9. Mass balance of dry matter, protein content and free amino acids in Alc-H: retentate of the UF step (■ R1), retentate of the NP010 step (▧ R2) and permeate of the NP010 step (□ P2).

3.2.3.2. Peptides and amino acid separation

Peptides

The protein concentration was determined in the different streams generated in the consecutive fractionation steps for the Alc-H with values of 26.1, 9.0, 15.2 and 7.1 mg/mL in the R1, P1 (P1 = F2), R2 and P2 streams, respectively ($CF_{1st\ step}$ = 1.4 and $CF_{2nd\ step}$ = 1.7). The corresponding retention percentages for each stage have been plotted in Figure 3.10a. The protein retention percentages were lower than the values achieved for the SWH by two consecutive NF steps. The higher MWCO of

the UF-Synder membrane allowed a higher permeation of the protein fraction, although molecular weight distribution of Alc-H showed peptides with higher MW, yielding a moderate value of the retention percentage, 66 % (purity index 50 %). The second step yielded a retention percentage of the protein fraction of 54 % (purity index of 32 %) (Figure 3.10a). Therefore, there was still an important fraction of the protein content with MW lower than 1–1.2 kDa that would permeate through the NP010 NF membrane. This result can also be observed in the mass balance of the total protein fraction plotted in Figure 3.9. Most of the initial protein content was retained in R1, 63 %, but still 16 % was determined in the final permeate (P2), while 11 % of the initial protein fraction was retained in the R2 stream. The error of the mass balance, evaluated with Eq. 3.7, was determined to be 10 %. Although this value falls within the normal range for values in material balance errors, the higher deviation compared with the value determined in the SWH fractionation could be due to the adsorption of certain peptides on the PES membrane, as previously indicated.

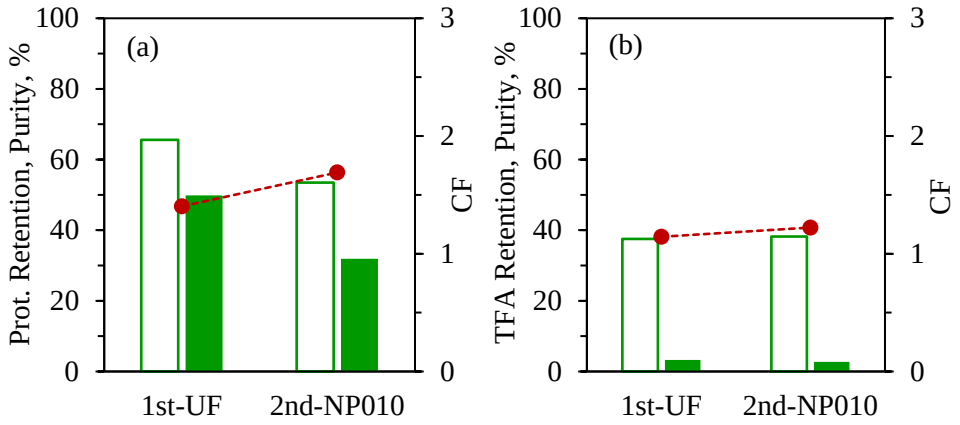

Figure 3.10. Retention percentages, purity in the retentates and concentration factor of Alc-H for: **(a)** the peptide fraction, and **(b)** total free amino acids (TFA). Retention percentage (□), Purity index (■), Concentration factor (●).

Total free amino acids

According to the MWCO of the membranes selected in the fractionation for the Alc-H, the retention percentage of free amino acids was low with values lower than

40 % for both separation steps and concentration factors close to 1 in both steps ($CF_{1st\ step}$ = 1.1 and $CF_{2nd\ step}$ = 1.2). The total free amino acid content in the Alc-H was relatively low compared to the SWH. Therefore, low purity indexes for total free amino acids were obtained in the R1 and R2 fractions, 3 % in both streams. The purity index for total free amino acids in the P2 stream was also not high due to the relatively high protein fraction content in this stream.

The mass balance of total free amino acids was evaluated and also included in Figure 3.9. 51.5 % of the initial total free amino acid content was retained in the R1, 12 % in R2 and 22 % was determined in the final permeate P2. The high percentage of the initial total free amino acids retained in R1 must be highlighted, especially considering that MW of amino acids ranges from 75.07 Da for glycine to 204.23 for tryptophan and the MWCO of UF-Synder membrane was 10 kDa. Adsorption and interactions with the adsorbed peptides on the PES membrane surface could lead to this retention of free amino acids in the R1 stream. The error of the mass balance (Eq. 3.7) was 14.2 %. The highest value for the mass balance error was also determined for total free amino acids in the SWH.

Total organic carbon and nitrogen content

The obtained values enabled the evaluation of the N:C molar ratio with similar values in the different streams: 0.30, 0.28, 0.33, 0.30 and 0.31 for F, R1, P1, R2 and P2, respectively. These values indicated that most of the organic matter correspond to protein-type compounds, according to the value reported by Rivas-Ubach *et al*. (2018) for these compounds (N:C = 0.3).

Molecular weight distribution

Table 3.2 listed the MWD of the three final streams generated (R1, R2 and P2) in the Alc-H fractionation. Slightly higher percentage of peptides with MW > 10 kDa (the MWCO of the membrane) was determined in R1 (14.2 %) compared to the initial feed (11.6 %), which did not show a sharp separation by the Synder-ST UF membrane. When using NP010 membrane in the second stage, NF retentate (R2)

still contained peptides with MW < 2 kDa (37.1 %). As it was also observed in the fractionation of the SWH, different MW classes of peptides were determined in all streams and only peptides with a size much smaller than the MWCO of the membrane were able to permeate freely in the first UF step and the second step with the NP010 membrane.

Saidi *et al*. also found that peptides with MW below 4 kDa were retained by a UF-4 kDa membrane in the study of fractionation of tuna dark muscle by-product hydrolysate by using Alcalase (Saidi *et al*., 2014a, 2014b). These authors also pointed out that only small peptides passed freely through the membrane. However, these authors when passing the Alcalase hydrolysate of this by-product through the NP010 NF membrane, the NF retentate was enriched in fractions with MW > 1 kDa and < 4 kDa while the NF permeate was completely free from peptide fractions with MW > 4 kDa and enriched in smaller peptide fraction, achieving a more effective separation in the NF than in the UF process.

3.2.3.3. Reducing and iron quelating capacity

The reducing and the iron quelating capacity of the streams generated in the separation of the Alc-H have been plotted in Figure 3.8. Reducing capacity of all the streams was considerably lower compared to those of the SWH, since the initial feed presented a low reducing capacity of 0.48 mM Fe^{2+}. In any case, the highest reducing capacity was observed in the R1 stream, where most of the peptide fraction was concentrated.

On the contrary, the Alc-H fractions exhibited stronger chelating capacity compared to the SWH. The iron chelating capacity was affected by membrane fractionation since the retentates fractions presented higher capacity than the permeates one, corresponding to the peptide fractions of higher MW in the retentates fractions. Girgih *et al*. (2013) also reported that the increased peptide chain length led to higher iron chelating capacity on salmon protein hydrolysates. These authors proposed that the strong metal chelating properties of long-chain peptides may be

due to synergistic effects of higher number of amino acid residues when compared to the shorter peptides while the lower chelating capacity of the permeates was attributed to the reduced additive and synergistic effect of the peptides in the permeate (narrow MW distribution).

4. Conclusions

This paper discusses the impact of a two-step membrane fractionation process on two different hydrolysates obtained from the water-soluble protein fraction from tuna fish meal generated by two different treatments, subW-CO_2 and Alcalase® treatment. These two treatments yielded two hydrolysates with different chemical composition regarding free amino acids and molecular weight of the peptides generated.

Due to the higher concentration of free amino acids and small peptides in the SWH, this hydrolysate and its fractions could have valuable applications in pharmaceutical and cosmeceutical industries, thanks to their good solubility in a broad pH range, as determined by Barea *et al*. (2024). In contrast, the larger peptides obtained from the Alc-H could act as emulsions stabilizers, providing strong emulsion structure due to interfacial adsorption of large peptides in thick layers, as suggested by Barea *et al*. in their evaluation of the techno-functional properties of fish meal hydrolysates (Barea *et al*., 2024). The different properties of both hydrolysates present a great opportunity for the development of novel foods, ingredients or cosmetics.

These MWD of the two hydrolysates led to different fractionation strategies. The two step NF process applied to the SWH resulted in a first retentate with higher protein fraction content, while maintaining its reducing capacity. In the retentate from the second NF step, 92 % of FAA were retained, with a purity index of 29 %, but a lower reducing capacity. This stream, rich in free amino acids, mainly alanine and glycine, could be of significant use in the food industry, as glycine is well known for its role as a sweeting agent and flavor enhancer.

On the other hand, for Alc-H a first UF and a second NF step led to a valuable first retentate with more than 65 % of protein retention with a purity index of 50 %, maintaining the high quelating capacity of the Alc-H and slightly higher reducing capacity.

The second step in the sequences proposed for both hydrolysates resulted in a lower membrane fouling degree, probably due to the reduced dry matter content in the stream fed to this second stage. In both processes, a relatively wide MW distribution of peptides was determined in all streams, and it was concluded that these membranes did not perform a sharp separation. In any case, it is important to highlight that GPC, as a technique for determining the MWD, is based on the assumption that the elution time is an accurate predictor of MWD of the peptide mixture, which may not always be true. Additionally, in this study, the calibration curve was obtained using pullulan standard set, rather than a broad range of small peptides of different MW, which might exhibit different interactions with the GPC column.

Another limitation faced by this study was the complex and pronounced membrane fouling observed during the first fractionation step proposed for each hydrolysate, which prevented achieving the VRF of 4. To improve the results, it would be valuable to investigate strategies to reduce membrane fouling and explore novel or different membranes. Additionally, as future work, scaling-up the process for industrial applications will present a significant challenge.

CHAPTER 4

Green extraction of isoflavones from okara using subcritical water: Kinetics, optimization, and comparison with other water-based sustainable methods

Adapted from the article:

P. Barea, A.E. Illera, R. Melgosa, Ó. Benito-Román, H. Candela, S. Beltrán, M.T. Sanz (2025).

"Green extraction of isoflavones from okara using subcritical water: Kinetics, optimization, and comparison with other water-based sustainable methods"

Food Chemistry, *482*, 144166.

DOI: https://doi.org/10.1016/j.foodchem.2025.144166

Capítulo 4

Extracción ecológica de isoflavonas de okara utilizando agua subcrítica: cinética, optimización y comparación con otros métodos sostenibles basados en agua

Resumen

El agua se ha explorado como agente de extracción verde para la extracción de isoflavonas de la okara. Primero, el agua subcrítica (subW) se exploró utilizando dos okaras diferentes: (1) lavada y seca (OKW) y (2) no pretratada (OKC). La familia de la genisteína fue la más abundante, con cantidades muy bajas en la familia de la gliciteína. Los datos cinéticos revelaron la interconversión de malonil-glucósidos en β-glucósidos al usar subW, con constantes de tasa de degradación crecientes para todas las isoflavonas con temperatura. Se obtuvo un máximo de 1229 μg de isoflavonas/g de okara seca a 120 °C después de 30 min para OKC. Las tecnologías de microondas (MAE) y ultrasonido (UAE) lograron el 72,8 % y el 75,4 % del rendimiento de subW. La productividad al máximo fue de 41,0, 82,5 y 92,8 μg de isoflavonas /(g de okara seca · min). Sin embargo, se obtuvo una fracción más alta de las formas más biodisponibles, β-glucósido + aglicona, usando subW.

Palabras clave: Okara, isoflavonas, agua subcrítica, cinéticas, extracción asistida por microondas, extracción asistida por ultrasonidos.

Chapter 4

Green extraction of isoflavones from okara using subcritical water: Kinetics, optimization, and comparison with other water-based sustainable methods

Abstract

Water has been explored as a green extraction agent for isoflavone extraction from okara. First, subcritical water (subW) was explored using two different okaras: (1) washed and dried (OKW) and (2) non-pre-treated (OKC). Genistein family was the most abundant, with very low quantities in the glycitein family. Kinetic data revealed interconversion of malonyl-glycosides to β-glycosides in subW, with increasing degradation rate constants for all isoflavones with temperature. A maximum of 1229 μg isoflavone/g of dried okara was obtained at 120 °C after 30 min for OKC. Microwave (MAE) and ultrasound (UAE) technologies achieved 72.8 % and 75.4 %, of the yield of subW. Productivity at the maximum was of 41.0, 82.5 and 92.8 μg isoflavone /(g dry okara · min) for subW, MAE, UAE. However, higher fraction of the more bioavailable forms β-glycoside + aglycone was obtained by subW.

Key words: Okara, isoflavones, subcritical water, kinetics, microwave-assisted extraction, ultrasound-assisted extraction.

1. Introduction

Okara is the main by-product of the soybean (*Glycine max*) industry. It is generated during the filtration stage of soybean-derived products, such as tofu, soy milk, and soy protein isolate. Soybean is the most widely cultivated and consumed legume globally, and more than 14 million tonnes of okara are produced every year, with approximately 1.1 kg produced per kilogram of soybeans processed (Mok *et al*., 2019). Despite its significant potential as a valuable by-product, okara is often discarded due to challenges related to its preservation and tendency to spoil rapidly. Okara presents high nutritional value, it is rich in fiber, proteins with good amino acid profile, lipids with beneficial fatty acids, B-group vitamins, antioxidants and essential minerals. It also contains a noteworthy concentration of isoflavones, as soybeans are the most important source of these flavonoids (Mok *et al*., 2019; Nkurunziza, Pendleton, Sivagnanam, *et al*., 2019). Therefore, it is worth exploring sustainable methods to valorize this by-product, with a focus on extracting the valuable fraction of bioactive compounds as an initial step in a cascade approach.

Isoflavones are flavonoids with an estrogen-like structure, commonly referred to as phytoestrogens, that confer functional properties and health benefits. Some of the most notable health benefits associated with isoflavones in blood plasma include anti-inflammatory effects, protection against colon cancer, anti-obesity properties, diabetes management, prevention of osteoporosis, enhancement of bone health, and support for the gut microbiota (Hsiao *et al*., 2020). These benefits are particularly relevant during periods of senescence and perimenopause, where supplementation with isoflavones, due to their structural similarity to estrogens, may be especially advantageous (Hsiao *et al*., 2020).

Twelve isoflavones have been isolated from soybeans, classified into four main groups: aglycones (genistein [GE], daidzein [DE], and glycitein [GYE]), β-glycosides (genistin [G], daidzin [D], and glycitin [GY]), malonyl-glycosides (malonyl-genistin [MG], malonyl-daidzin [MD], and malonyl-glycitin [MGY]), and

acetyl-glycosides (acetyl-genistin [AG], acetyl-daidzin [AD], and acetyl-glycitin [AGY]) (Jankowiak *et al*., 2014).

Malonyl-glycosides contain a malonyl group, which makes them the most thermolabile form, and they are the most common in nature. β-Glycosides contain only a glycoside group and are also common in nature. Aglycones, which are the native forms, have a non-polar structure and are less common in nature; however, they are the most bioavailable forms, followed by β-glycosides. The higher the bioavailability, the greater their capacity to provide health benefits (Hsiao *et al*., 2020; Nkurunziza, Pendleton, Sivagnanam, *et al*., 2019).

Isoflavone extraction typically involves at least two steps: extraction using a large amount of organic solvent, followed by purification through multiple chromatography columns. In this study, a green method for extracting isoflavones without using organic solvents was proposed using water under subcritical conditions. Subcritical water (subW) is an innovative green extraction technology that uses only water as a solvent at temperatures from 100 to 374 °C and pressures high enough to maintain water in its liquid state. Water exhibits unique properties under subcritical conditions. Its dielectric constant decreases due to hydrogen bond dissociation, while the ionic product of water (K_W) increases, resulting in a higher concentration of hydronium and hydroxide ions. This makes water a great solvent for both polar and non-polar substances, and it also exhibits acidic or basic catalytic properties, eliminating the need for additional chemical catalysts in the process (Barea *et al*., 2024; Nkurunziza, Pendleton, Sivagnanam, *et al*., 2019).

Many prior studies on isoflavone extraction have focused on using hydroalcoholic mixtures to achieve high extraction efficiency with 50–70 % aqueous ethanol solution (Jankowiak *et al*., 2014). When a significant amount of ethanol is needed in the solvent to work at low liquid-to-solid, either a large volume of ethanol or a drying pre-treatment step is required (Jankowiak *et al*., 2014). Consequently, subW extraction offers an eco-friendly and sustainable alternative to conventional

organic solvent-based methods for isoflavone extraction. The unique properties of water under subcritical conditions enhance its ability to dissolve bioactive compounds. By adjusting the temperature and pressure, both yield and selectivity can be optimized. Additionally, owing to its increased ionic product content, subW enables the simultaneous extraction and hydrolysis of isoflavone glycosides into aglycones, which are more bioavailable, without the need for extra acid hydrolysis steps.

The objective of this study was to investigate the potential of water under subcritical conditions as an extraction agent for the sustainable valorization of okara, proposing a first step under mild conditions for the recovery of isoflavones from okara, focusing mainly on the effect of extraction temperature. It is important to note that okara has a high moisture content exceeding 80 %, which contributes to its rapid spoilage. A key strength of this study is the examination of isoflavone extraction from crude okara without any pre-treatment, as water was chosen as the extraction agent. The results obtained by subW extraction were compared with conventional solvent extraction using different hydroalcoholic mixtures, as well as other water-based emerging extraction technologies, such as microwave and ultrasound-assisted extraction processes. A comparison will be established considering the extraction yield, isoflavone distribution, productivity, and energy consumption per gram of isoflavone in the extract. Additionally, a comprehensive kinetic study was conducted to explore the interconversion pathways between different groups of isoflavones under different extraction conditions by subW extraction.

2. Experimental

2.1. Raw Material

Okara was supplied by *Frías Nutrición* S.A.U. (Burgos, Spain), with a moisture content of 82.5 ± 0.1 % (w/w), making it highly susceptible to spoilage. Upon receipt, a portion of okara was conveniently washed and dried. When okara was tentatively dried without washing, either in a convection oven at 45 °C or vacuum

oven, it spoiled rapidly. Therefore, experiments were carried out with okara previously washed with distilled water at a ratio of 1:1 (w/v) (equivalent to 8.75 % of dry matter in water). The mixture was homogenized for 1 min and filtered. The washed okara (hereafter referred to as OKW) was subsequently dried in a convection oven at 45 °C for 24 h to a final moisture content of 5 % (w/w). OKW was stored at 5 °C without spoiling during storage. In contrast, another portion of the received okara was immediately frozen in individual small plastic bags without any prior treatment (no washing or drying) and is referred to as crude okara (OKC). To allow for a better comparison between both types of okara, all results in this study were expressed using the corresponding dry basis.

Isoflavone standards (purity ≥ 98 %) used for calibration in HPLC were purchased from various suppliers: daidzin (**D)** and genistin **(G)** from *TargetMol*; glycitin (**GY)** and malonyl-genistin (**MG)** from *ChemCruz*; daidzein (**DE)** from *Thermo Scientific*; glycitein **(GYE)** from *Chengdu Biopurify Phytochemicals*; genistein **(GE)** from *Fluorochem*; and malonyl-daidzin **(MD)** from *ChemFaces*.

2.2. Conventional extraction

Conventional solvent extraction of isoflavones was performed in an orbital shaker (Grant Instruments OLS 200, Shepreth Cambridgeshire, England). Extraction conditions were selected based on a previous study by Jankowiak *et al*. (2014). The authors identified 50 °C for 1h as the optimal extraction conditions. In this work, extractions were conducted at 50 °C for 30 min and 60 min using various ethanol-water mixtures, including 100 % ethanol, 70 % ethanol, 50 % ethanol, 30 % ethanol, and 100 % water. OKW was dissolved at a concentration of 5 % (w/v), equivalent to 4.75 % (w/v) on a dry basis. Times shorter than that reported by these authors were also considered to optimize yield and productivity.

2.3. Subcritical water (subW) extraction process

Subcritical water extraction was performed in a 0.5 L batch reactor covered with a ceramic heating jacket (230 V, 4000 W, ⌀ 95 mm, 160 mm height). A Pt100 sensor and PID system enabled the control and registration of the temperature, while a pressure gauge with a purge valve maintained the pressure inside the reactor during the process.

For each extraction, 200 mL of 4.75 % in a dry basis (w/v) OKW suspension was charged into the reactor. Higher okara loadings were not feasible owing to swelling of the raw material and stirring challenges. The treatment was conducted at various temperatures ranging from 110 °C to 160 °C at a pressure of 5 MPa using N_2 as the pressurization agent. The operating temperature and pressure were selected considering previous work when dealing with subW extraction of flavonoid compounds from food wastes such as onion skin wastes, concluding that extraction of phenolic compounds such as flavonoids was temperature sensitive with subW under mild conditions, 145 °C, resulting in the optimum extraction conditions, when covering the temperature range from 105 to 180 °C, observing degradation at temperatures higher than 160 °C (Benito-Román, 2020). Regarding the operating pressure, its effect on the performance of subW was observed to be non-significant, compared with temperature and time, as long as water remained in the liquid state. After determining the optimal extraction temperature, isoflavone extraction was performed from crude okara (OKC) using a 200 mL suspension at the same dry basis concentration of 4.75 % (w/v).

Isoflavone extraction kinetics were followed by withdrawing the samples at regular time intervals through the sampling port. After a certain treatment time, the reactor was cooled to 90 °C and depressurized to collect the final hydrolysate.

2.4. Microwave assisted extraction

The microwave assisted extraction (MAE) was conducted using a flexiWAVE microwave equipment (T_{max} = 300 °C, p_{max} = 10 MPa, Milestone SRL, Sorisole, Italy). Hydrolysis was performed in Teflon 100 mL batch vessels with constant stirring and temperature control. A heating ramp was set for 5 min with microwave power limited to 1000 W, with the actual average power used ranging from 150 to 200 W during the 5 min heating phase and 75–100 W to maintain the temperature during the rest of the process. Extractions were performed with OKC, using vessels containing 25 mL of OKC suspensions at 4.75 % (w/v) on a dry basis, at different temperatures (110–140 °C) and treatment times (5, 10, and 15 min). The temperature extraction conditions were chosen based on previous results of subW extractions and are of the order of extraction conditions reported for MAE tested by Tsubaki *et al.* (2009). in the range of 110 to 140 °C, with extraction times ranging from 5 to 45 min. The results were compared with those from subW extractions.

2.5. Ultrasound assisted extraction

A 750 W ultrasonic processor with a 13 mm probe (Vibra-Cell™ 75042, Sonics Material™ Inc., U.S.A.) was used to extract the isoflavones from okara. The samples were processed at a constant ultrasound frequency of 20 kHz and 100 % of amplitude, 79 μm according to the manufacturer's instructions. In each run 200 mL of an OKC aqueous suspension at 4.75 % (w/v) on a dry basis were placed in a thermostated vessel (⌀ = 4.8 cm, V = 199 cm^3) to regulate temperature by circulating water through the jacketed vessel from a thermostat bath, performing extractions at 50 °C. When dealing with UAE, the working temperature should be below the saturation vapor pressure of water at ambient pressure; therefore, 50 °C was selected for comparison with the hydroalcoholic conventional solvent extraction. The US probe was submerged at a constant depth of 2 cm from the bottom of the vessel (Illera, Sanz, Varona, *et al*., 2018). The treatment was administered in pulses, 5 s on and 5 s off, with a maximum treatment time of 30 min (1 h total process). Samples

were collected every 5 min to follow the kinetics, with additional aliquots collected at the start and at 2.5 min.

2.6. Analysis of the extracts

2.6.1. Extraction yield

An aliquot (1.5–2 mL of the final extract was filtered through a 0.22 µm syringe filter and dried at 105 °C to remove the solvent until a constant weight was achieved. The extraction yield was calculated as the ratio between the weight of the dry extract obtained after removing the solvent by considering the initial volume of the collected extract and the weight of the dried okara at the beginning of the extraction process.

2.6.2. Isoflavones (determination and quantification)

Isoflavones in the different extracts were analyzed using an HPLC/DAD system (Agilent 1260 Infinity II/HP Series 1100) equipped with a column system consisting of a precolumn (Phenomenex® AJ0-9000:2.1-4.6 mm) and an LC Column (Kinetex® 5µm Biphenyl: 4.6 mm x 250 mm) with a porosity of 100 Å. Prior to analysis, the extracts were filtered through 0.22 µm syringe filters. The column temperature was maintained at 25 °C. A gradient of two mobile phases was used for separation: (A) 1 % acetic acid in 0.005 M ammonium acetate (prepared in deionized water) and (B) 1 % acetic acid in 0.005 M ammonium acetate (prepared in ACN). The flow rate was set at 0.8 mL/min, with the gradient flow transitioning over 90 min from an initial concentration of 98 % (A) and 2 % (B) to final concentrations of 20 % (A) and 80 % (B).

A Diode Array Detector (HP Agilent 1100 HPLC G1315A DAD) was used to measure the signals and spectra of each sample from 190 nm to 950 nm. The wavelength used to measure and compare all chromatograms was 254 nm, complemented by measurements at 280 nm, 330 nm, and 370 nm. Additionally, analyzing the full spectrum helps match each peak with the corresponding isoflavone

standard. Standard solutions of eight isoflavones were used for calibration and identification. G, D, GE, DE, GYE, and MD were dissolved in methanol, whereas MG and GY were dissolved in ethanol and dimethyl sulfoxide (DMSO), respectively, owing to their low solubility in methanol. For data acquisition and treatment OpenLab CDS 2.5 was used.

The results are expressed as the amount of isoflavones per gram of dry okara. The purity of the isoflavones in the extract was expressed as the ratio of the mass of isoflavones to the mass of the total dry extract.

2.6.3. Total nitrogen

A Total Organic Carbon Analyzer Shimadzu (TOC-V CSN) was used to quantify the total nitrogen content. Through catalytic thermal decomposition, nitrogen-containing compounds are oxidized during combustion. The resulting nitrogen oxides (NO_X) were detected using a chemiluminescence detector and correlated with the original nitrogen concentration of the samples. Potassium nitrate (KNO_3) was used as a calibration standard.

2.6.4. Total phenolic content

Total phenolic content (TPC) was determined using the Folin-Ciocalteu reagent (VWR). Samples (100 µL) were diluted with 2.8 mL), and subsequently, Folin-Ciocalteu reagent (100 µL) was added, followed by the addition of 2.0 mL of sodium carbonate 7.5 % (w/v). After incubation for 1 h, absorbance was measured at 750 nm. Gallic acid was used as the standard for calibration, and the results were expressed as milligrams of gallic acid equivalents (GAE) per gram of dry sample.

2.6.5. Reducing capacity

The reducing capacity of okara extracts was assessed using the Ferric Reduction Antioxidant Power assay (FRAP), as proposed by Benzie & Strain (1996).

The standard used for the calibration was an $FeSO_4 \cdot 7H_2O$ solution (0.1 M), and the results were expressed as µmol of Fe^{2+} per gram of dry okara.

2.7. Statistical analysis

All samples were analyzed at least twice and expressed as the mean ± standard deviation of the replicates. Data were analyzed using software Statgraphics19 X64 and, the significance of the differences between sample results was determined based on an analysis of variance with Fisher's Least Significant Difference (LSD test) at *p*-value ≤ 0.05.

3. Results

3.1. Isoflavones extraction on pre-treated Okara (OKW)

3.1.1. Isoflavones extracted by conventional extraction

The discussion focuses on the eight isoflavones detailed in the Material section (section 2.1) among the 12 existing isoflavones. Acetyl forms and malonyl-glycitin were excluded because of the absence of the corresponding standards in this study. Notably, Jankowiak *et al*. (2014) studied the extraction of isoflavones from okara using different solvents, including a 70 % ethanol aqueous solution and concluded that malonyl-glycitin accounted for only 1.5 % of the total isoflavone content. Furthermore, among the three acetyl-glycosides, only acetyl-genistin was detected in the extracts, but it accounted for only 0.6 % of the total extracted isoflavones. When water was used as a solvent, Jankowiak *et al*. (2014) reported extraction percentages of 2.9 % for malonyl-glycitin and 1 % for acetyl-genistin. Tsubaki *et al*. (2009) also identified malonyl-glycitin as the least concentrated isoflavone when extraction was performed with water as solvent, noting its high susceptibility to degradation (ignoring also the presence of acetyl-glycosides). Therefore, it can be concluded that the sum of the eight predominant isoflavones (G, D, GY, GE, DE, GYE, MG, and MD) is a good approach for total isoflavone extraction.

Table 4.1 presents the total isoflavone extraction yield, as well as the yield of each individual isoflavone, for the aqueous, ethanol, and different ethanol-water mixtures used as solvents in this study. Extraction from OKW using only water at 50 °C for 30 min resulted in a total isoflavone yield of 281 ± 3 µg/g of dry okara (Table 4.1). As the ethanol concentration in the extraction solvent increased, the total isoflavone yield continuously increased, reaching a maximum of 439 ± 10 µg/g of dry okara in 50 % ethanol, representing a 56 % increase in yield. Further increase in ethanol concentration did not result in higher yields; for example, at 70 % ethanol, the yield decreased slightly to 411 ± 11 µg/g dry okara. The lowest yield was obtained using pure ethanol, with only 14 ± 1 µg of total isoflavones per gram of dry okara, indicating that isoflavones have a limited solubility in ethanol. Table 4.1 also lists the dielectric constant (ξ) values for the corresponding ethanol-water mixtures at 50 °C, as reported by Akerlof (1932). The dielectric constant is a physical property that influences, among other properties, the solvent capacity. According to Fakhree *et al*. (2010) , knowledge of the dielectric constant of mixed solvents can help predict the solubilities of bioactive compounds. Considering the dielectric constant values for the ethanol an aqueous mixture at 50 °C as reported by Akerlof (1932) it can be stablished that the highest extraction yield occurred at dielectric constant value between ethanol and water, with a value of $\xi = 42.92$ corresponding to 50 % ethanol-water mixture, whereas both higher dielectric constant values (e.g., pure water, $\xi = 69.85$) and lower values (e.g., pure ethanol, $\xi = 20.87$) were associated with lower extraction yields.

Table 4.1. Isoflavone extraction yield of OKW using different hydroalcoholic mixtures as solvents at 50 °C for 30 min. Values with letters (a–e) show significant differences in each row when applying the LSD method at *p*-value ≤ 0.05.

µg ISF /g dry okara	30 min					60 min				
	100% EtOH	70% EtOH	50% EtOH	30% EtOH	0% EtOH	100% EtOH	70% EtOH	50% EtOH	30% EtOH	0% EtOH
Malonyl-daidzin	2.1 ± 0.3^{a}	130 ± 3^{c}	145 ± 1^{d}	145 ± 0.3^{d}	112 ± 0.1^{b}	2.28 ± 0.01^{a}	135 ± 3^{c}	149 ± 4^{d}	149 ± 1^{d}	110 ± 1^{b}
Malonyl-genistin	2.03 ± 0.05^{a}	130 ± 4^{c}	147 ± 1^{d}	145 ± 2^{d}	87.9 ± 0.2^{b}	2.4 ± 0.2^{a}	136 ± 3^{c}	152 ± 1^{e}	148 ± 1^{d}	85.6 ± 0.5^{b}
Daidzin	1.1 ± 0.1^{a}	34.9 ± 0.9^{d}	34.9 ± 0.3^{d}	32.6 ± 0.7^{c}	30.8 ± 0.2^{b}	1.5 ± 0.2^{a}	37 ± 5^{c}	37 ± 2^{c}	35 ± 2^{bc}	30.3 ± 0.5^{b}
Glycitin	0.24 ± 0.02^{a}	11.5 ± 0.5^{b}	12 ± 2^{b}	11.5 ± 0.1^{b}	13 ± 2^{b}	0.33 ± 0.04^{a}	12 ± 1^{b}	12.6 ± 0.9^{b}	12.0 ± 0.4^{b}	11.9 ± 0.3^{b}
Genistin	1.76 ± 0.01^{a}	59 ± 2^{e}	54 ± 1^{d}	46 ± 3^{c}	32.5 ± 0.1^{b}	2.5 ± 0.3^{a}	63.7 ± 0.5^{e}	57.2 ± 0.3^{d}	48.7 ± 0.9^{c}	32.6 ± 0.4^{b}
Daidzein	4.0 ± 0.5^{a}	27.1 ± 0.4^{c}	27 ± 2^{c}	17.8 ± 0.02^{b}	3.46 ± 0.02^{a}	5.63 ± 0.07^{a}	28.5 ± 1^{c}	29.5 ± 0.9^{c}	19.0 ± 0.6^{b}	3.9 ± 0.4^{a}
Glycitein	0.39 ± 0.09^{a}	3.3 ± 0.3^{b}	3.6 ± 0.9^{b}	2.87 ± 0.01^{b}	1.0 ± 0.1^{a}	0.54 ± 0.03^{a}	3.6 ± 0.1^{c}	3.9 ± 0.4^{c}	2.86 ± 0.07^{b}	1.0 ± 0.2^{a}
Genistein	2.07 ± 0.01^{a}	15.0 ± 0.1^{c}	15 ± 2^{c}	7.2 ± 0.1^{b}	0.11 ± 0.01^{a}	2.86 ± 0.04^{b}	15.8 ± 0.1^{d}	16.1 ± 0.4^{d}	7.84 ± 0.06^{c}	0.16 ± 0.03^{a}
Total MG	4.1 ± 0.4^{a}	260 ± 7^{c}	292 ± 2^{d}	290 ± 2^{d}	199.9 ± 0.3^{b}	4.7 ± 0.2^{a}	272 ± 6^{c}	301 ± 5^{d}	297 ± 1^{d}	196 ± 1^{b}
Total βG	3.1 ± 0.1^{a}	105 ± 3^{c}	101 ± 3^{d}	90 ± 4^{d}	76 ± 2^{b}	4.3 ± 0.1^{a}	113 ± 4^{e}	107 ± 3^{d}	96 ± 2^{c}	75 ± 1^{b}
Total AG	6.5 ± 0.6^{a}	45.4 ± 0.8^{c}	46 ± 5^{c}	27.9 ± 0.1^{b}	4.6 ± 0.1^{a}	9.04 ± 0.05^{b}	48 ± 1^{d}	50 ± 2^{d}	29.7 ± 0.7^{c}	5.0 ± 0.6^{a}
Total ISF	14 ± 1^{a}	411 ± 11^{c}	439 ± 10^{d}	408 ± 6^{c}	281 ± 3^{b}	18.1 ± 0.3^{a}	432 ± 9^{c}	457 ± 9^{d}	422 ± 2^{c}	276 ± 1^{b}
Dielectric constant*	20.87	32.86	42.92	53.79	69.85	31.39	5.44	4.08	3.67	–1.98

*Akerlof (1932)

The most abundant forms in the extract were the malonyl-glycosides, followed by β-glycosides with only a small low proportion of aglycones, except in the case of pure ethanol. For the optimal solvent, 50 % ethanol-water mixture, malonyl-glycosides accounted for 66.5 % of the total isoflavones (slightly lower than the 71.3 % obtained with water alone), β-glycosides accounted for 22.9 % (lower than the 27.0 % extracted with water), while the aglycones made up 10.6 % (almost seven times higher than the 1.6 % extracted with water). This pattern is consistent with other studies that have shown that okara produced on an industrial scale predominantly contains malonyl-glycosides and β-glycosides, which are considered the more natural forms of isoflavones, similar to those found in soybeans. These forms are typically present when lower temperatures and shorter extraction times are used. Aglycones tend to accumulate only under more severe extraction conditions (Moras *et al*., 2017; Tsubaki *et al*., 2009). These findings align with those of Jankowiak *et al*. (2014), who reported higher concentrations of aglycones (386 μg/g dry okara, 37.9 % of the total isoflavones) compared to β-glycosides (35.1 %) and malonyl-glycosides (26.4 %) when using a 70 % ethanol-water solution, attributing this result to the production of okara at laboratory scale starting from crude soybean and submitting it to harsh conditions. In any case, focusing on valorization studies on industrial-scale raw materials, which could be more suitable for potential scaling-up processes, may be a more interesting approach.

Extractions for 1 h did not result in a significant increase in the concentrations of total or individual isoflavones. The total isoflavone yield after 1 h was approximately 4 % higher with the 50 % ethanol solvent and almost 2 % lower with pure water. Therefore, only the 30-min extraction data are presented here.

3.1.2. Isoflavones extraction by using water under subcritical conditions

The extraction efficiency of organic solvents and subW can be compared based on their dielectric constants, which is not the only factor affecting the isoflavone extraction process but is an important parameter to consider when determining the

optimal conditions for the extraction of some biocompounds. The results presented in Table 4.1 indicate that the 50 % ethanol-water mixture yielded the highest isoflavone extraction, corresponding to a dielectric constant value of 42.92. The physical properties of water under subcritical conditions undergo significant changes with temperature, showing a decrease in its dielectric constant and higher hydrolytic power owing to the increase in its ionic product. Therefore, subW has been explored as a potential greener alternative to hydroalcoholic mixtures for isoflavone extraction. An increase in the temperature in the subcritical region led to a decrease in the dielectric constant of water, becoming similar to that of organic solvents. The temperature range covered in this study was from 110 °C to 160 °C, which corresponds to dielectric constant values of approximately (graphical lecture at 100 bar) 53 and 41, respectively, of the order of ethanol-water mixtures with 30–50 % content of the alcohol (see Table 4.1) (Galamba *et al*., 2019). Therefore, in the temperature range covered in this work, subW exhibits dielectric constant values similar to those found in the most effective traditional isoflavone extractions using hydroalcoholic mixtures but avoids the use of any organic solvent. This reduction enhances the solvent effectiveness of water, allowing it to dissolve substances ranging from slightly polar to non-polar (Ali *et al*., 2025).

Figure 4.1a shows the total isoflavone extraction kinetics at selected temperatures. The kinetics of total isoflavone extraction include the time required to reach the operating temperature (initiated immediately after mixing), which was approximately 30 min. At the lowest temperatures tested (110 °C to 140 °C), a maximum was observed in the early stages of the extraction process, with the highest initial extraction rate and maximum occurring at 120 °C, which resulted in a maximum yield of 526.4 μg isoflavone /g dry okara after 30 min of treatment, 19.9 % higher than the yield obtained with a 50 % ethanol solution in a conventional extraction, (439 ± 10 μg /g dry okara). After this maximum, the isoflavone content decreased because of degradation. The rate of isoflavone degradation increased with an increase in temperature. At the highest temperature assayed (160 °C), a

continuous decrease in total isoflavone content was observed from the beginning due to a faster degradation rate than the extraction rate.

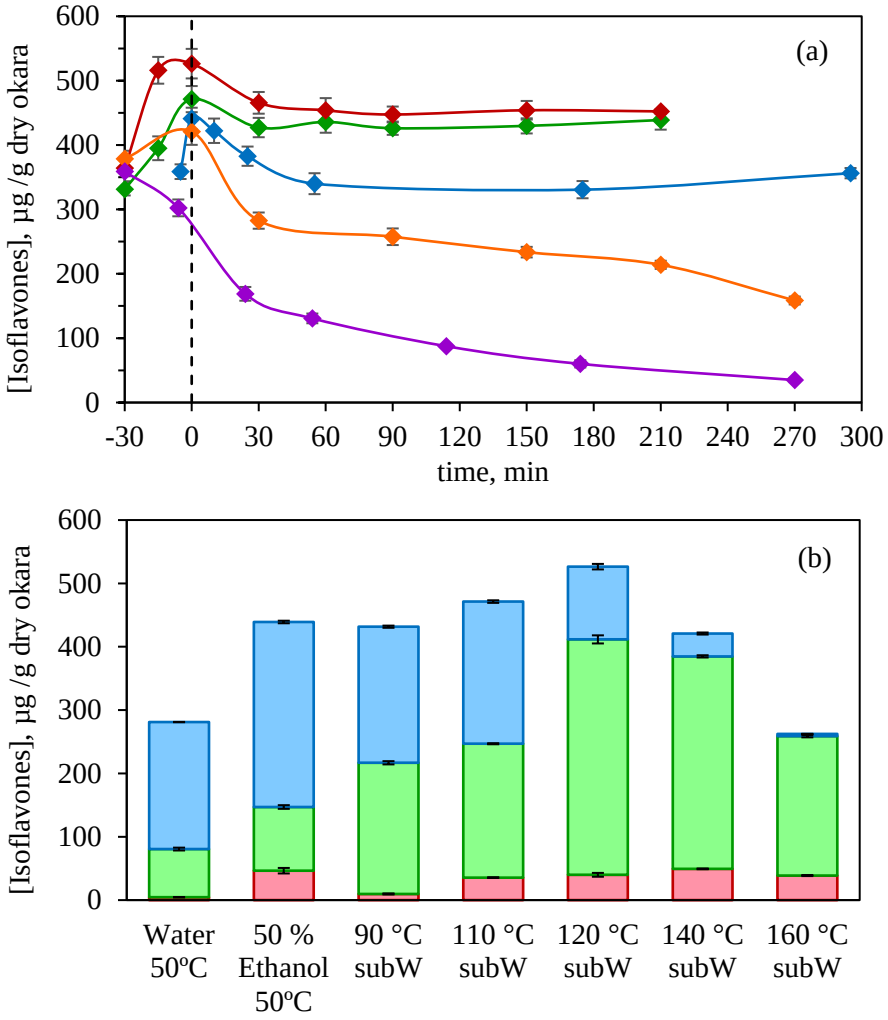

Figure 4.1. (a) Total isoflavone extraction (µg /g dry okara) by subW treatment for OKW, as a function of time (min), at different temperatures: 90 °C (◆); 110 °C (◆); 120 °C (◆); 140 °C (◆); 160 °C (◆). **(b)** Isoflavone profile (µg /g dry okara) after 30 min of water and 50 % ethanol extraction at 50 °C and for subW extractions at different temperatures: malonyl-glycosides (□), β-glycosides (□), aglycones (□).

Figure 4.1a shows the isoflavone extraction kinetics at 90 °C. Although water at 90 °C and atmospheric pressure is not under subcritical conditions, this

temperature was included in the study because of the rapid extraction rates observed under mild subcritical water conditions. Notably, for the treatment conducted at 90 °C, okara was added to the reactor only after the water temperature reached 90 °C because no pressurization was necessary at this temperature; the working temperature was attained within the first 5 min. At 90 °C, the isoflavone extraction also showed a maximum, followed by a decrease in the total isoflavone content over time.

The higher isoflavone extraction yield observed could be attributed to the tunable properties of water under subcritical water conditions, as previously discussed. The dielectric constant decreased with temperature, being similar to that of a 50 % ethanol aqueous mixture. However, at 120 °C, where maximum extraction was achieved (Figure 4.1), the extraction of isoflavones was higher when using subW than when using a 50 % ethanol aqueous mixture. This may indicate that this reaction medium promotes the extraction of isoflavones. A similar trend was observed in the extraction of bioactive compounds from onion skin waste when subW was used, in the temperature range from 105 to 180 °C, when compared with ethanolic aqueous mixtures, although they exhibited similar dielectric constant value (Benito-Román *et al.*, 2020). Therefore, other properties might play an important role, such as the ionic product of water, which increases with increasing temperature, resulting in higher concentrations of hydronium and hydroxide ions in the medium, favoring a hydrolytic medium that might lead to a higher extraction of isoflavones.

Furthermore, in the literature it has been reported that isoflavones and proteins interact strongly via non-covalent interactions, mainly hydrogen bonds and hydrophobic interactions (Jankowiak *et al.*, 2014; Le Bourvellec & Renard, 2012; Speroni *et al.*, 2010). The use of subcritical water (subW) could reduce protein-isoflavone interactions due to its higher ionic product (K_w), which, among other effects, leads to more acidic conditions that could potentially facilitate the hydrolysis of the protein fraction. To elucidate the relationship between the hydrolysis of the protein fraction and the increase in isoflavone extraction, the total nitrogen content

in the final extracts was determined (Table 4.2). It can be clearly observed that the protein content (N content) in the final extracts was higher for the subW extracts than for the conventional water and 50 % ethanol extracts. Although temperatures above 140 °C promoted higher protein hydrolysis in the extracts, degradation of the isoflavones occurred rapidly.

Table 4.2. Nitrogen content in final subcritical water and conventional extracts.

	OKW					
Ext. solvent	**Water**	**EtOH (50%)**	**subW**	**subW**	**subW**	**subW**
Temperature	**50 °C**	**50 °C**	**110 °C**	**120 °C**	**140 °C**	**160 °C**
[N], mg/L	159	112	521	575	723	969

For comparison, the isoflavone profile at the point of achieving the operating temperature (approximately 30 min for all subcritical water (subW) extractions) is presented in Figure 4.1b, which also includes the isoflavone profile for extractions at 50 °C using pure water and a 50 % ethanol aqueous solution as solvents. A clear increase in the total isoflavone content in the extraction medium was observed during the heating stage at temperatures lower than 120 °C, along with shifts in the proportion of each isoflavone group. For instance, the malonyl form percentage decreased from 47.6 % at 110 °C to 21.8 % at 120 °C, further reducing to just 1.3 % at 160 °C. In contrast, the β-glycoside form increased from 44.8 % at 110 °C to 70.6 % at 120 °C and reached 83.9 % at 160 °C of total isoflavone content. These findings are consistent with those of previous studies, which reported that malonyl-glycosides degrade at 100 °C, converting to β-glycosides due to thermal decomposition at these or higher temperatures (Rostagno *et al.*, 2004). Conventional extractions with water and 50 % ethanol showed higher malonyl form percentages (71.3 % and 66.5 %, respectively) and lower β-glycoside content than any subW hydrolysis method (27.0 % and 22.9 %, respectively). Among all extractions, subW at 120 °C yielded the highest total isoflavone concentration (526.4 µg/g), with the highest combined content of β-glycoside and aglycone (411.6 µg/g, 78.2 %), the two isoflavone groups of particular interest due to their bioactive properties.

Therefore, subcritical water treatment clearly modified the isoflavone profile due to chemical transformations, as observed during the non-isothermal heating period. An in-depth kinetic study of the interconversion between isoflavone forms at different temperatures was conducted during the isothermal period. Considering the isoflavones identified in this study, Figure 4.2 shows the kinetic profiles for the different forms of isoflavones within the genistein, daidzein, and glycitein families, in mole concentration (μmol/g dry okara). Among these, the genistein family was the most abundant group, followed by the daidzein family with the lowest quantities determined in the glycitein family (see Figure 4.2), which was approximately ten times lower than for the genistein family. Among all isoflavone groups, malonyl-glycosides were found to be the most thermosensitive forms, with concentrations decreasing consistently at all working temperatures, while temperatures exceeding 140 °C were necessary to observe β-glycoside degradation. Aglycones were found in low amounts, with daidzein showing the highest concentration.

Chien *et al*. (2005) also reported that malonyl-glycosides, the predominant form in nature, are easily degraded under moderate conditions leading to the formation of β-glycosides, which have been reported to be more bioavailable than malonyl-forms. The transition to aglycones, the least hydrophilic form of isoflavones, is less common in nature, but the most bioavailable form requires harsh conditions to remove the glycoside group. Similarly, Moras *et al*. (2017) reported an interchange between the highly thermolabile malonyl-glycosides and β-glycosides in the study of the extraction of isoflavones from soybean flour and soybean protein isolate using pressurized water extraction at temperatures exceeding 80 °C, with complete degradation at higher temperatures.

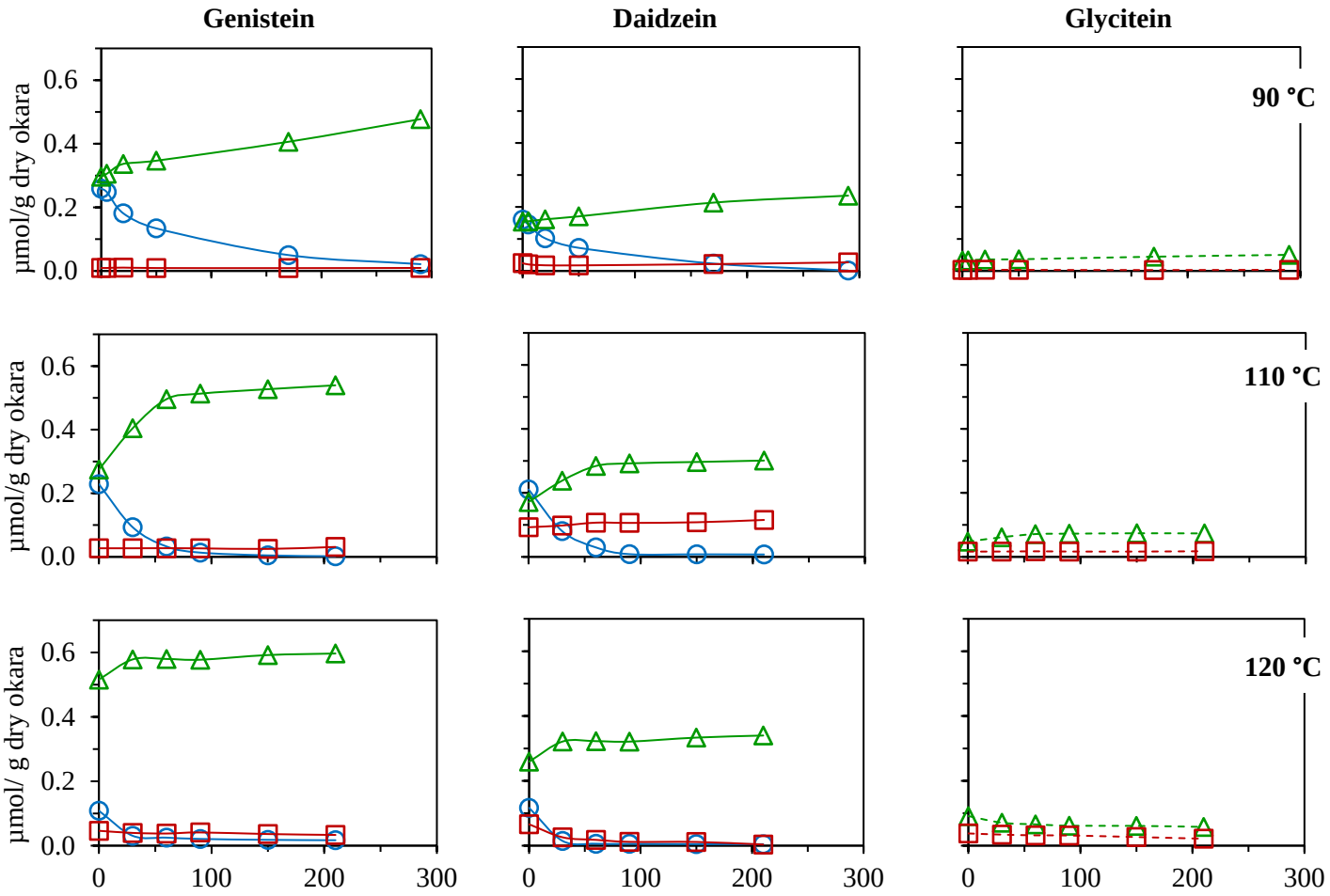
Genistein
Daidzein
Glycitein
90 °C
110 °C
120 °C
µmol/g dry okara
µmol/ g dry okara
0.0
0.2
0.4
0.6
0
100
200
300

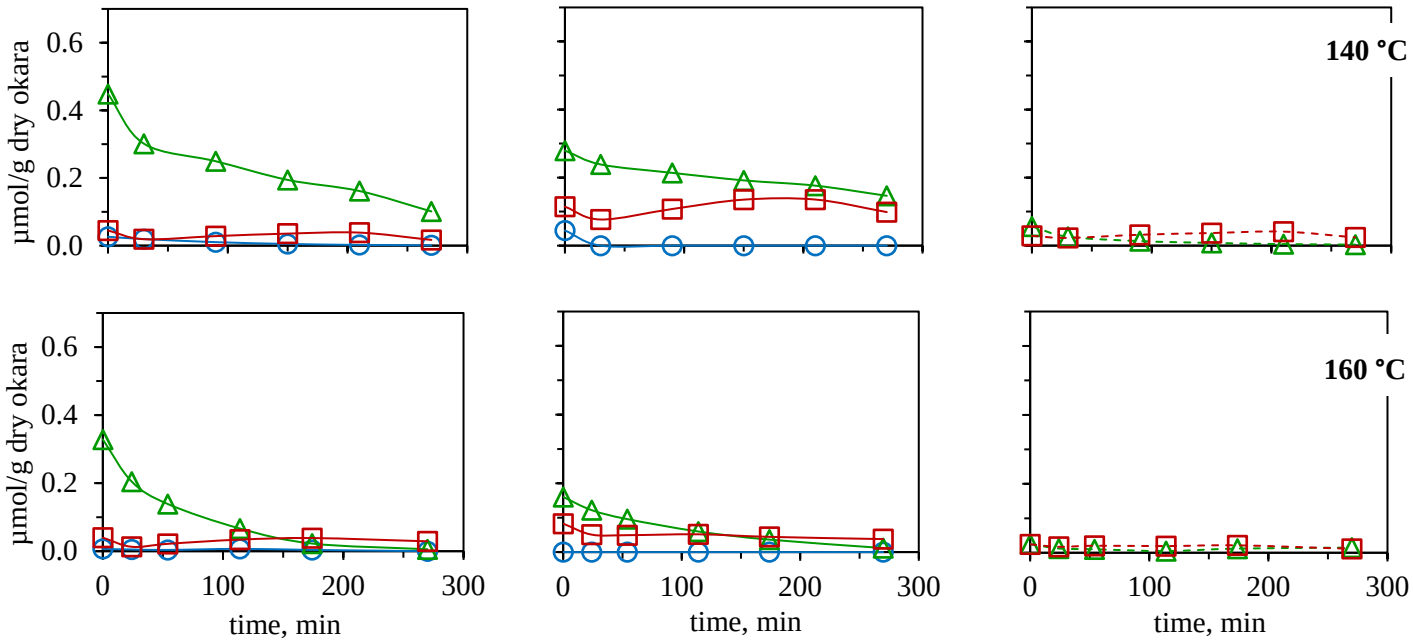

Figure 4.2. Kinetic curves of malonyl-glycosides (○), β-glycosides (△), and aglycones (□) of genistein (first column), daidzein (second column), and glycitein (third column) families at different temperatures (90 °C, 110 °C, 120 °C, 140 °C, and 160 °C from the first to the fifth row. Continuous lines represent the kinetic model of Eq. 4.1–4.3 (parameters listed in Table 4.3 and 4.4), and discontinuous lines for glycitein are used to guide the eye.

Moras *et al*. (2017) predicted optimal isoflavone extraction through subcritical water hydrolysis, obtaining a 61.0 % yield at 114 °C for 2 min with soybean protein isolate, and an 85.1 % yield at 122 °C for 14 min with soybean flour. These optimal temperatures align with the subW extractions in this study, although they require longer times, likely due to the use of soybean by-products rather than soybean flour or protein isolates, which contain higher and more easily extractable concentrations of these bioactive compounds. By contrast, Nkurunziza, Pendleton, & Chun (2019), reported optimal isoflavone extraction at 146.23 °C and 3.98 MPa for 213.5 min, differing from most studies and the present results; however, their work did not account for malonyl-glycosides, which represent the most significant fraction of total soybean isoflavones.

To further analyze the results presented in Figure 4.2, the interconversion pathways proposed among the three identified isoflavone forms are presented in the following scheme:

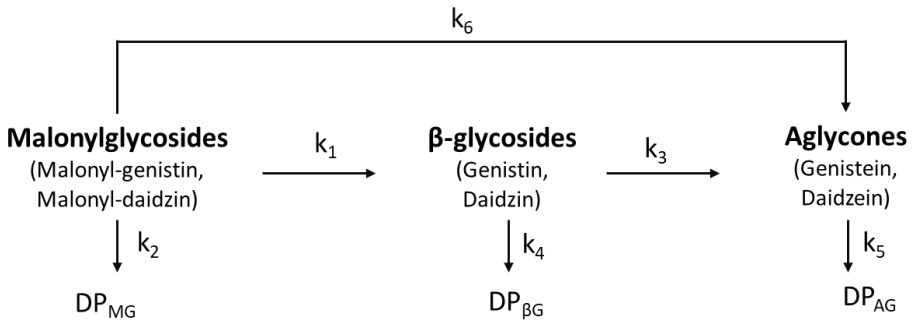

Scheme 4.1. Representation of the interconversion pathways between the three forms of each isoflavone analyzed in this study.

First-order reaction kinetics have frequently been used to analyze food components, and have been proven effective in describing the interconversion and degradation behaviors of isoflavones (Chien *et al*., 2005). Scheme 4.1 illustrates six different conversion pathways, each with an assigned reaction rate constant k. This model does not consider acetyl forms, as these were not determined in the present study:

$$\frac{dC_{MG}}{dt} = -(k_1 + k_2 + k_6)\, C_{MG} \quad \textbf{[4.1]}$$

$$\frac{dC_{\beta G}}{dt} = k_1 C_{MG} - (k_3 + k_4)\, C_{\beta G} \quad \textbf{[4.2]}$$

$$\frac{dC_{Ag}}{dt} = k_3 C_{\beta G} + k_6 C_{MG} - k_5\, C_{Ag} \quad \textbf{[4.3]}$$

where k_1 is the kinetic rate constant for the formation of β-glycoside from malonyl forms and k_3 and k_6 are the kinetic rate constants for the formation of aglycones (AG) from β-glycoside (βG) and malonyl-glycosides (MG) forms, respectively. k_2, k_4, and k_5 are the degradation kinetic constants of the malonyl, β-glycoside, and aglycone forms, respectively.

The rate constants for the proposed kinetic equations were obtained by simultaneously solving the set of differential equations for each model. These differential equations were solved numerically using a fourth-order Runge-Kutta method, and the parameters were obtained by minimizing the following objective function (O. F.) using the simplex Nelder-Mead method:

$$O.F. = \sqrt{\frac{\sum_{\text{all compounds}} \sum_{i=1}^{n} abs(C_{i,exp} - C_{i,calc})}{n}} \quad \textbf{[4.4]}$$

The kinetic parameters for the genistein and daidzein families are presented in Tables 4.3 and 4.4. Due to the absence of a malonyl-glycitin standard in this study, kinetic parameters were not obtained for the glycitein group. Nevertheless, as previously noted, glycitein isoflavones constituted less than 3–10 % of the total extracted mass of isoflavones, varying with extraction temperature. The temperature dependence of the reaction rate constants is described by the Arrhenius equation:

$$k = k_o \cdot \exp(E_a/RT) \quad \textbf{[4.5]}$$

Although the temperature-dependent trends for isoflavone form interconversions are not always fully consistent, several general conclusions can be

drawn. Generally, the degradation rate constants for all isoflavone forms increased with temperature, with malonyl-glycosides exhibiting the highest values. A deeper analysis of the isoflavone profiles of the genistein and daidzein families yielded similar conclusions, based on the kinetic rate constants presented in Tables 4.3 and 4.4. The ratio of the reaction rate constants for malonyl-glycoside interconversion (for both genistein and daidzein family) to the β-glycoside and aglycone forms versus degradation to other degradation products, $(k_1+k_6)/k_2$, suggests that interconversion to other isoflavone forms occurs more rapidly than degradation to other compounds, particularly at low temperatures. Furthermore, a $k_1/(k_3 + k_4)$ ratio greater than one indicates that the formation of β-glycosides from malonyl-glycosides is faster than their conversion to aglycones or degradation into other products. Similarly, a value greater than one for the ratio k_6/k_3 suggests that aglycone formation from malonyl-glycosides is faster than that from β-glycosides. Tables 4.3 and 4.4 also include the activation energy values for each interconversion step, showing generally high activation energies for all the steps, revealing high temperature sensitivity of all isoflavone forms in the subcritical water reaction medium. For both isoflavone families (genistein and daidzein), the most temperature-dependent interconversion was observed in the conversion of β-glycosides to aglycones (k_3) or other degradation products (k_4). The continuous lines shown in Figure 4.2 represent the kinetic model proposed, with the corresponding kinetic parameters listed in Tables 4.3 and 4.4.

Comparisons with literature are somewhat challenging due to variability in reported values, and most studies have reported changes in the isoflavone profile of soybean (no kinetics the by-product okara) subjected to different heating procedures, focusing on the genistein family. An *et al*. (2023) investigated the interconversion kinetics for the genistein family in isoflavone extraction from soybean in subW, at temperatures ranging from 100 °C to 180 °C from 3 to 30 min. Similar to the findings of this study, they observed a general trend of increasing degradation rate constants with increasing temperature, with malonyl-genistein being the most thermosensitive.

Table 4.3. Reaction rate constants of genistein family compounds and activation energy (kJ/mol) for isoflavone interconversion.

T, °C		90	110	120	140	160	Ea
MG→G	**k_1**	$6.84 \cdot 10^{-3}$	$3.36 \cdot 10^{-2}$	$1.88 \cdot 10^{0}$	$7.63 \cdot 10^{-2}$	$8.05 \cdot 10^{-1}$	76
MG→DP	**k_2**	$4.10 \cdot 10^{-3}$	$9.11 \cdot 10^{-6}$	$9.15 \cdot 10^{-1}$	$2.25 \cdot 10^{0}$	$1.11 \cdot 10^{0}$	164
G→GE	**k_3**	$7.42 \cdot 10^{-9}$	$1.04 \cdot 10^{-6}$	$2.89 \cdot 10^{-8}$	$2.98 \cdot 10^{-3}$	$5.92 \cdot 10^{-2}$	312
G→DP	**k_4**	$7.41 \cdot 10^{-9}$	$9.11 \cdot 10^{-7}$	$2.85 \cdot 10^{-8}$	$2.83 \cdot 10^{-3}$	$5.60 \cdot 10^{-3}$	277
GE→DP	**k_5**	$1.90 \cdot 10^{-4}$	$1.70 \cdot 10^{-4}$	$1.73 \cdot 10^{-3}$	$2.95 \cdot 10^{-2}$	$2.83 \cdot 10^{0}$	185
MG→GE	**k_6**	$1.53 \cdot 10^{-5}$	$9.80 \cdot 10^{-6}$	$2.32 \cdot 10^{-4}$	$4.16 \cdot 10^{-1}$	$7.85 \cdot 10^{-1}$	186

Table 4.4. Reaction rate constant of daidzein family compounds and activation energy (kJ/mol) for isoflavone interconversion.

T, °C		90	110	120	140	160	Ea
MD→D	**k1**	$6.14 \cdot 10^{-3}$	$1.92 \cdot 10^{-2}$	$1.68 \cdot 10^{0}$	–	–	197
MD→DP	**k2**	$5.63 \cdot 10^{-3}$	$9.90 \cdot 10^{-3}$	$1.11 \cdot 10^{0}$	$2.74 \cdot 10^{0}$	–	171
D→DE	**k3**	$2.34 \cdot 10^{-9}$	$4.29 \cdot 10^{-5}$	$2.12 \cdot 10^{-7}$	$1.69 \cdot 10^{-3}$	$9.09 \cdot 10^{-3}$	280
D→DP	**k4**	$2.25 \cdot 10^{-9}$	$4.87 \cdot 10^{-7}$	$1.63 \cdot 10^{-7}$	$1.69 \cdot 10^{-3}$	$9.09 \cdot 10^{-3}$	316
DE→DP	**k5**	$1.45 \cdot 10^{-4}$	$1.35 \cdot 10^{-4}$	$2.31 \cdot 10^{-2}$	$1.30 \cdot 10^{-3}$	$4.13 \cdot 10^{-3}$	79
MD→DE	**k6**	$2.68 \cdot 10^{-8}$	$2.28 \cdot 10^{-3}$	$1.01 \cdot 10^{-3}$	–	–	453

A detailed analysis of their kinetic rate constants also suggests that genistin formation occurs faster than its consumption due to genistein formation or its degradation into other products. Additionally, they observed that genistein forms more rapidly from the acetyl form (as an intermediate of the malonyl group) than from the β-glycoside form. Regarding activation energies for the different steps, these authors (An *et al.*, 2023) identified the degradation of genistein to unknown compounds as the most sensitive process with an activation energy of 1086 kcal/mol (4539.5 kJ/mol). This is an exceptionally high value compared to the data in this study or any other reported activation energies for kinetic processes.

Other kinetic studies in the literature also focus on the interconversion and degradation of isoflavone forms in soybean, but in media other than subW. Chien *et al*. (2005) analyzed the interconversion and degradation of pure isoflavones during dry or moist heating at 100, 150 and 200 °C. Isoflavone standards (malonyl-genistin, acetyl-genistin, genistin, and genistein) were dissolved in methanol, and then the solution was placed in sealed ampoules that were immersed in an oil bath preheated to the selected temperature. On the other hand, Niamnuy *et al*. (2012), studied the drying kinetics of soybean, along with the inter-conversion and degradation of soy isoflavones, using gas-fired infrared combined with hot air vibrating drying at various temperatures (50, 70, 130 and 150 °C). Zhang & Chang (2016) treated soymilk, obtained by soaking and blanched soybean at 80 °C for 2 min, by UHT (ultra-high temperature) at 135 to 150 °C for 10 to 50 s with a pilot plant-scale Microthermics processor. In any case, in these studies, first-order kinetic models effectively described the changes among the isoflavone forms during heating, with the malonyl-glycosides showing the highest degradation rate constants. Therefore, it can be concluded that the isoflavone profile, particularly malonyl-glycosides, is greatly affected by the heating process.

3.1.2.1. TPC and antioxidant activity of OKW subW extractions

Figures 4.3a and 4.3b show the total polyphenol content (TPC) and reducing capacity, according to the FRAP assay, in the OKW subW extracts. Both parameters followed a similar trend, with the highest TPC and reducing capacity observed at 160 °C, while much lower values were recorded at lower temperatures of 110 °C and 120 °C. This pattern contrasts with the isoflavone content, which was higher at lower temperatures, whereas significant degradation was noted at higher temperatures.

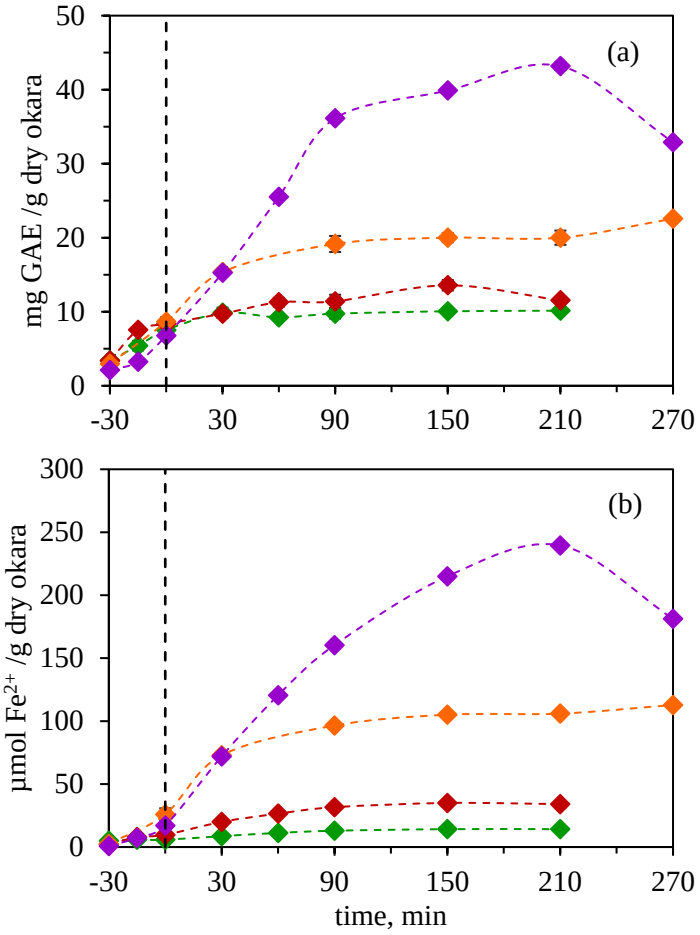

Figure 4.3. (a) Profile of total polyphenol content from OKW extracts by subW extraction (mg GAE /g dry okara). **(b)** Antioxidant activity of OKW subW extracts measured by FRAP (µmol Fe^{2+} /g dry okara), as a function of time (min). 110 °C (◆); 120 °C (◆); 140 °C (◆); 160 °C (◆).

These high TPC and reducing capacity values are likely due to browning reactions that occur at elevated temperatures, producing antioxidant compounds independent of isoflavone concentration (Rimbach *et al*., 2003). Maillard Reaction Products (MRP), formed between sugars and amino groups during the treatment of okara at high temperatures, significantly influence the antioxidant capacity of these extracts. MRP are known for their ability to scavenge oxygen radicals and chelate metals (B. Li *et al*., 2012; Yilmaz & Toledo, 2005). Given these insights, it is evident that the high antioxidant activity observed at higher temperatures results from the

degradation of compounds with strong antioxidant properties. These samples displayed more intense browning at elevated temperatures owing to MRP formation.

Regarding the correlation between these two assays, it can be concluded that TPC and antioxidant capacity are directly correlated. However, isoflavone content does not show such a strong correlation due to the much higher antioxidant properties of other compounds generated during processing, primarily MRP.

3.2. Isoflavones extraction on crude okara (OKC)

3.2.1. Extraction by subcritical water

OKC has a high moisture content, exceeding 80 % (w/w). During the beverage and solid residue separation process in soymilk production, a substantial amount of isoflavones remained in the retained solution. In the washing procedure of OKC to produce the OKW, the washing water contained approximately 40–55 μg of isoflavones/mL. This significant loss of isoflavones during the washing and drying processes makes OKC a promising candidate for further exploration to recover valuable isoflavones. Furthermore, the drying process is energy-intensive, and in the case of okara, it is particularly challenging to dry because of its tendency to spoil quickly during the drying processes unless it was not previously washed.

To explore OKC as a direct source of isoflavones, an extraction process was conducted using subcritical water (subW) at the optimal extraction temperature of 120 °C, previously determined using OKW as a reference, and at the same ratio of dry okara/solvent, 4.75 % (w/v) in a dry basis. For comparative purposes, the total isoflavone content during subW extraction at 120 °C for both OKW and OKC is plotted in Figure 4.4. The most notable difference observed was in the initial isoflavone content at the beginning of the extraction, with values of 364 and 716 μg isoflavone/g of dry okara for OKW and OKC, respectively. As previously noted, the higher initial isoflavone content in OKC was attributed to the isoflavones retained in the solution from okara and the beverage separation process. For both OKW and

OKC, isoflavone content initially increased, reaching a maximum at 30–35 min, and then decreased due to isoflavone degradation at long treatment times. After 60 min, the levels stabilized. As described in Figure 4.2, in the early stages of the treatment, malonyl forms were partially degraded but converted into more thermally stable β-glucoside forms; this plateau was observed after 60 min.

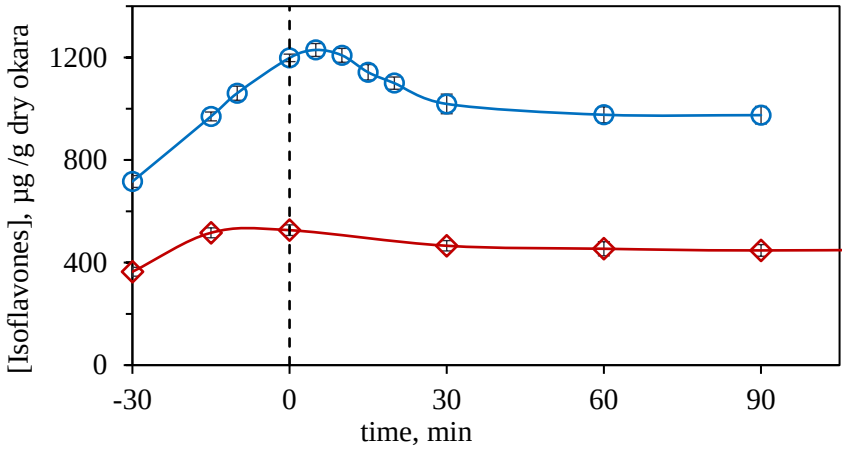

Figure 4.4. Isoflavone extraction (µg/g dry okara) by subW treatment under the same conditions (120 °C, 5 MPa) as a function of time (min). ◇ OKW, ○ OKC.

At the maximum, isoflavone content reached 1229 and 526.4 µg/g dry okara, for OKC and OKW, respectively, with OKC yielding over twice as much isoflavone content as OKW. The initial isoflavones extraction rate, evaluated up to the maximum, was also higher for OKC, 13.7 µg/g·min; nearly twice that of OKW (7.4 µg/g·min). The slower extraction rate in the OKW may have resulted from thermal drying. In Figure 4.5, an HPLC chromatograms of the isoflavones identified in this work for OKC was plotted after 30 min and 60 min of treatment to observe the interchange between isoflavone forms as well as its degradation at longer operation times.

The isoflavone extraction yield from OKC exceeds previous findings in the literature. Jankowiak *et al*. (2014) reported yields below 600 µg isoflavones/g okara, when using water as solvent, with a biomass concentration of 5 % dry okara at

temperatures ranging from 20 °C to 95 °C, which resulted in higher aglycone concentration due to lab-scale production of okara, as previously indicated. Even with changes in solvent, as reported by Jankowiak *et al*. (2014), such as adjusting the pH (yielding 911 μg/g at pH 10) or adding ethanol (1018 μg/g, 70 % ethanol), the extraction yields were lower than those obtained in this study, which used only pressurized water under mild conditions as a green solvent.

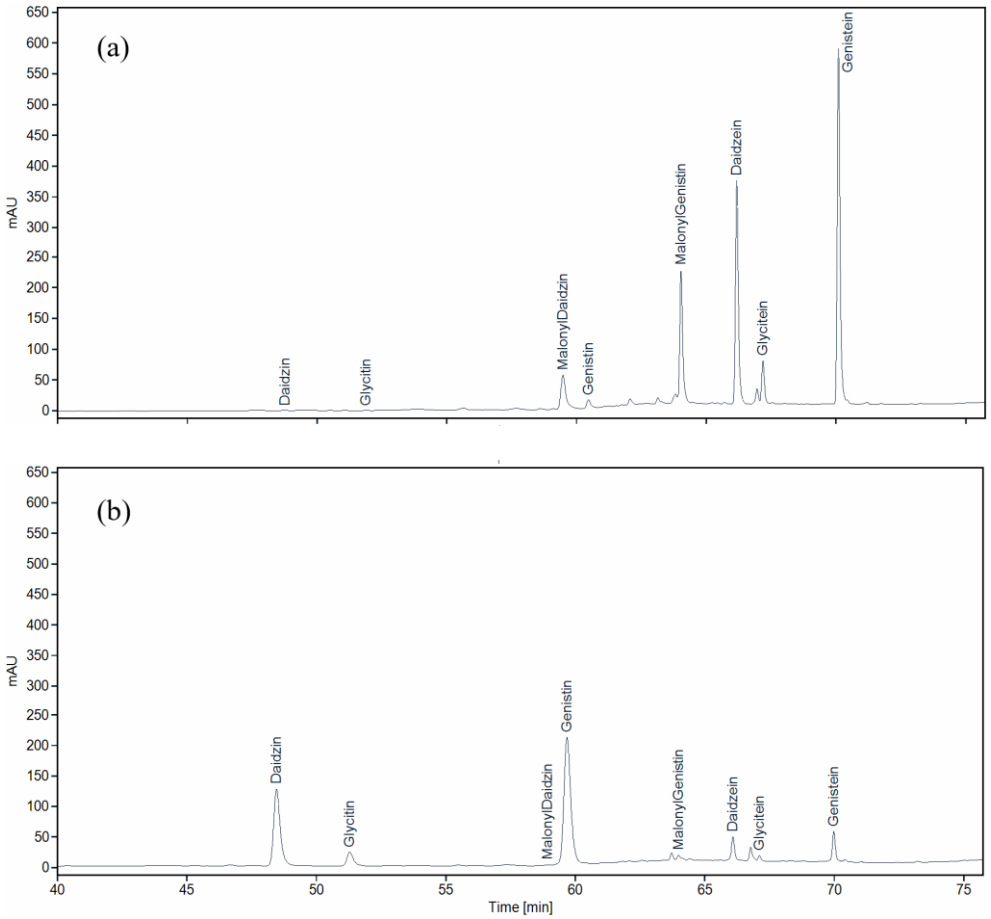

Figure 4.5. HPLC chromatograms corresponding to isoflavone extraction from crude okara with subW at 120 °C. **(a)** after 30 min of treatment and **(b)** after 60 min of treatment.

Isoflavone extraction from OKC was also conducted using the optimal hydroalcoholic mixture composition determined for OKW in conventional extractions (50 % ethanol-water) in a pressurized vessel at 5 MPa and 120 °C. The

highest extraction yield was achieved 30 min after initiating the heating process, with a value of 1216.6 µg/g OKC, which was similar to the value obtained using water alone. These results demonstrate that the use of pressurized fluids facilitates high isoflavone extraction yields when employing only water as the solvent, thereby eliminating the need for additional organic solvents when compared to conventional solvent extraction.

3.2.2. Comparison of isoflavones extraction by other methods

The results of isoflavone extraction from OKC were compared with those of other innovative and emerging extraction methods, including microwave assisted extraction (MAE) and ultrasound assisted extraction (UAE). The experiments were performed using OKC with 4.75 % dry okara in water.

3.2.2.1. Microwave assisted extraction

Figure 4.6a shows the extraction kinetics of total isoflavones from OKC using MAE at temperatures ranging from 110 to 140 °C. Experiments were not conducted at 160 °C because of the fast degradation of isoflavones observed at this temperature in previous subW treatments. At all the tested temperatures, an initial increase in isoflavone content was observed in the medium, except at 140 °C, where the degradation rate of isoflavones was faster than their extraction rate. The highest yields were achieved at lower temperatures of 110, 115, and 120 °C after 5 min of treatment, reaching similar values of 895, 885, and 888 µg/g dry okara, respectively. After reaching these peaks, the degradation rates increased at higher temperatures.

The profiles of the individual isoflavones at different temperatures are plotted in Figure 4.7. It can be observed that at any higher temperature or time tested, the destruction of the malonyl forms is more notable than the formation or extraction of β-glycosides or aglycones, as the global recount of isoflavones is much lower. Treatments at 115 °C and 120 °C showed values similar to those at 110 °C, as the more thermolabile forms were not so affected in short times. In contrast, from 130

to 140 °C, the malonyl form degradation was more notable, while the β-glycoside concentration increased, but at a lower rate, notably decreasing the global quantity of isoflavones in the final extracts.

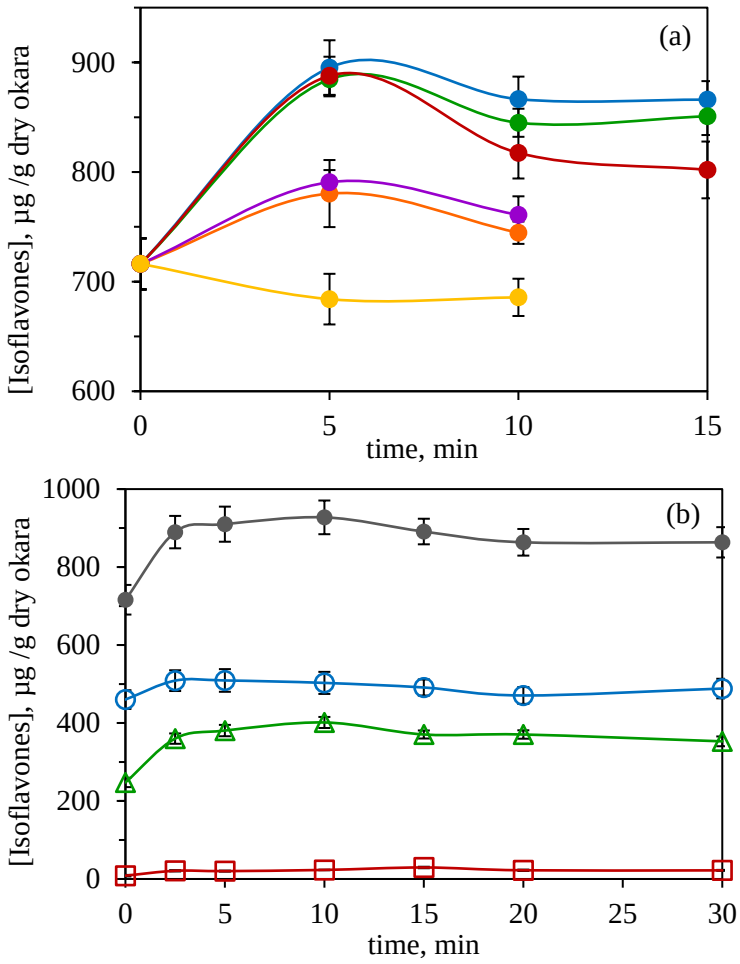

Figure 4.6. Total isoflavone extraction from OKC (µg /g dry okara). **(a)** MAE treatment, as a function of time (min), at different temperatures. 110 °C (●); 115 °C (●); 120 °C (●); 130 °C (●); 135 °C (●); 140 °C (●). **(b)** UAE treatment at 50 °C, as a function of time (min). Total isoflavones (●), subdivided in: malonyl-glycosides (○), β-glycosides (△), and aglycones (□).

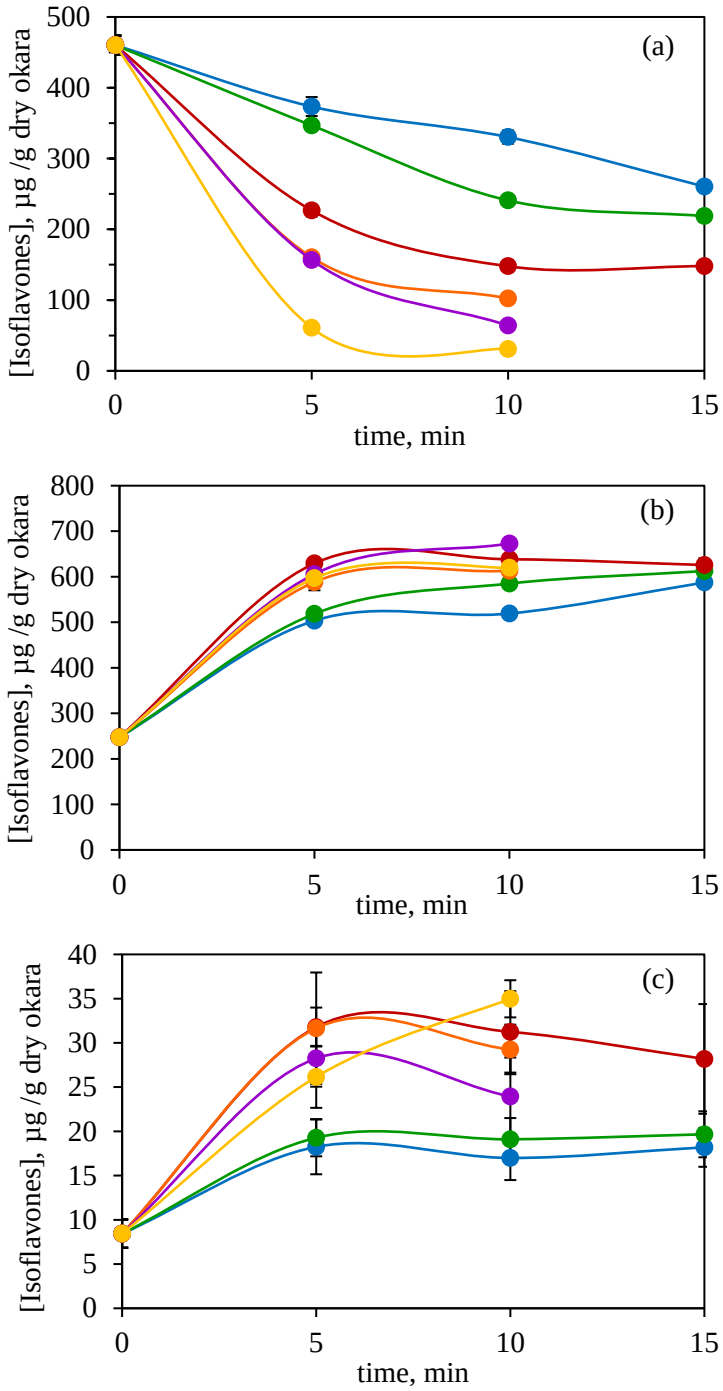

Figure 4.7. MAE isoflavone extraction for the different isoflavones form. **(a)** Malonyl-glycoside **(b)** β-glycosides **(c)** Aglycones. 110 °C (●); 115 °C (●); 120 °C (●); 130 °C (●); 135 °C (●); 140 °C (●).

Few studies have addressed isoflavone extraction from okara using MAE. Tsubaki *et al*. (2009), reported the highest isoflavone yield from okara using water as solvent at 120 °C, with a 2-min heating period followed by 5 min of treatment, achieving 2191 μg/g dry okara. This value decreases as the temperature increases above 120 °C. At a low temperature of 60 °C, Tsubaki *et al*. (2009) achieved a yield of 2159 μg/g of dry okara, but consisting of 59 % malonyl forms and 34 % β-glycosides. In contrast, at 120 °C, the proportion shifted to 22 % for malonyl-glycosides and 69 % for β-glycosides. In any case, these values are much higher than the values usually reported for isoflavone extraction from okara (Jankowiak *et al*., 2014; Nkurunziza, Pendleton, & Chun, 2019).

3.2.2.2. Ultrasound assisted extraction

Isoflavone extraction from OKC was performed using UAE with a similar dry solid content of 4.75 % in water as the extraction solvent at 50 °C. The remaining experimental conditions are detailed in Section 2.6. The UAE results are shown in Figure 4.6b. After 10 min of treatment, the isoflavone concentration reached a maximum of 928 μg/g dry okara. From that point until the end of the process (30 min), a slight decrease was observed owing to isoflavone degradation.

Regarding the isoflavone forms, under the selected UAE conditions, slight degradation of malonyl-glycosides was observed, with the highest value of 509 μg/g of dry okara decreasing to 471–485 μg/g after 20–30 min of extraction. Similarly, β-glycosides reached a peak of 401 μg/g in dry okara and then decreased to 353 μg/g after 30 min of UAE. The total aglycone content increased from 8 μg/g to 29 μg/g during the extraction period.

3.2.2.3. Comparison of extraction technologies

Figure 4.8 and Table 4.5 compare the optimal extraction experiment for each technology applied to isoflavone extraction from OKC, as well as the best subW result for OKW. SubW achieved the highest isoflavone yield (1229 μg isoflavone/g

dry okara) at 120 °C, 5 MPa, and 30 min of treatment. MAE and UAE technologies achieved 72.8 % and 75.4 % of the extraction efficiency of subW, respectively, with values of 895 and 928 μg isoflavone/g dry okara, respectively. The differences in the distribution of each isoflavone form among the four extraction technologies must be highlighted. The highest ratio of [β-glycoside + aglycone] to [malonyl-glycoside] was determined in the subW extracts. According to Scheme 1, subW treatment modifies the isoflavone profile owing to chemical transformations, and malonyl-glycosides are easily degraded under moderate conditions in subW, leading to the formation of β-glycosides.

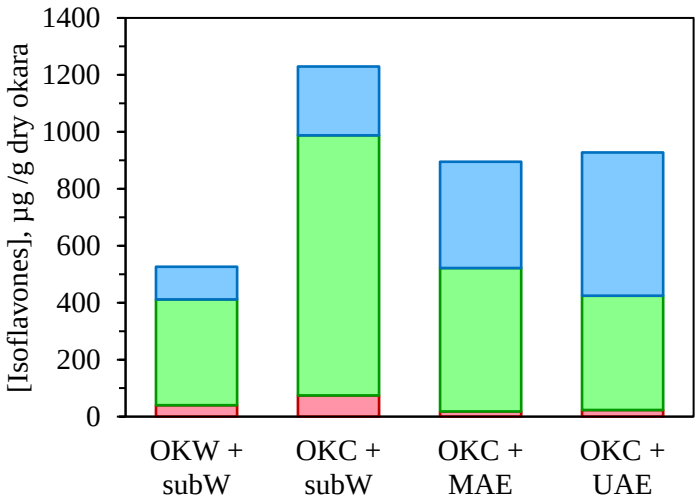

Figure 4.8. Total isoflavone extraction (μg/g dry okara) and distribution of each isoflavone form (malonyl-glycosides, β-glycosides, aglycone) for the best extraction results obtained from each of the three methods studied (subW at 120 °C for 30 min, MAE at 110 °C for 5 min, and UAE at 50 °C for 10 min).

Because the maximum extraction yield was achieved at different treatment times, at the maximum isoflavone extraction yield, the productivity was evaluated considering time for comparison purposes, with values of 41.0, 82.5 and 92.8 μg isoflavone /g dry okara min for subW, MAE, and UAE, respectively. Although the lower productivity values were achieved by subW extraction, when considering the distribution of different isoflavone forms, subW exhibited a significantly higher ratio

of [β-glycoside + aglycone] to [malonyl-glycoside] at 4.09, compared to 1.40 and 0.84 for MAE and UAE, respectively, being these two isoflavones forms more noteworthy in terms of their functional properties (Hsiao *et al.*, 2020). Thus, it can be concluded that subW treatment promoted the transformation of malonyl-glycoside into β-glycoside and aglycone forms, as shown in Figure 4.2 and Table 4.5. Table 4.5 also presents the total extraction yield along with the corresponding percentage of isoflavone content in the dry extracts, showing higher isoflavone concentrations in the dry extracts obtained from the subW and MAE extractions.

Table 4.5. Parameters for comparison of isoflavone extraction from crude okara (OKC) by subW, MAE, and UAE.

	Total ISF, µg/g OKC	Ratio ISF, [β+A]/[M]	Productivity, µg ISF/g·min	Dry ext., %	ISF in dry extract, %	Energy, J/µg ISF
subW	1229	4.09	41	2.05	0.30	88
MAE	895	1.40	83	1.46	0.29	213
UAE	928	0.84	93	2.24	0.20	52

Further comparisons of the three technologies were performed in terms of energy consumption (see Table 4.5). UAE exhibited the lowest energy consumption per µg of extracted isoflavone, 52 J/µg isoflavone, followed by subW at 88 J/µg isoflavone, with MAE having the highest energy consumption at 213 J/µg isoflavone. Ultrasound-assisted extraction achieved the highest productivity, while maintaining the lowest energy consumption. This efficiency could be attributed to the cavitation effect generated in the solvent by ultrasonic waves, which allows the solvent to rapidly and effectively penetrate most matrices (Bustamante-Rangel *et al.*, 2018). However, it is important to highlight the significantly more favorable [β-glycoside + aglycone] to [malonyl-glycoside] ratio achieved with subW compared with UAE, which recorded the lowest ratio among the three extraction techniques studied in this work (Table 4.5).

4. Conclusions

This work represents the first stage of a broader project aimed at the complete valorization of okara focusing on the obtention of isoflavones by water-based sustainable methods. Two types of okara were tested: (1) washed and dried okara and (2) untreated okara. Untreated okara resulted in higher isoflavone yields (1229.2 µg isoflavones /g dry okara, at 120 °C for 30 min) and energy savings by avoiding the drying stage.

A kinetic study revealed that subW promoted the interconversion between isoflavone forms and increased beta-glucosides. MAE and UAE technologies reached 72.8 and 75.4 % of subW extraction efficiency. UAE exhibited the highest productivity and lowest energy consumption. However, subcritical water extraction produced a significantly more favorable [β-glycoside + aglycone] to [malonyl-glycoside] ratio, as these two forms more bioavailable fractions.

These technologies offer potential for industrial-scale applications, providing improved efficiency, reduced processing times, and environmentally friendly alternatives to conventional extraction methods.

CHAPTER 5

Cascade valorization of okara by subcritical water hydrolysis: assessment of protein and amino acid profile in batch and semi-continuous systems

Adapted from:

P. Barea, R. Melgosa, A.E. Illera, H. Candela, S. Beltrán, M.T. Sanz

"Cascade valorization of okara by subcritical water hydrolysis: assessment of protein and amino acid profile in batch and semi-continuous systems"

Manuscript submitted to: *Journal of Environmental Chemical Engineering.*

Capítulo 5

Valorización en cascada de okara mediante hidrólisis con agua subcrítica: evaluación del perfil proteico y de aminoácidos en sistemas discontinuos y semicontinuos

Resumen

Este estudio evaluó la hidrólisis con agua subcrítica (SWH) como estrategia verde dentro de un proceso en cascada para la recuperación de proteínas a partir de okara previamente sometida a un proceso de valorización de sus isoflavonas (OK-2). Los resultados se compararon con la okara sin tratar (OK-1).

La extracción en discontinuo se realizó a 180 °C durante 3 h y 5 MPa en un reactor de 0.5 L. En estas condiciones, la recuperación total de aminoácidos a partir de OK-2 fue del 81 ± 3 % (12.6 g/L), con un 20 ± 1 % de aminoácidos libres, predominando el ácido glutámico y un perfil favorable de aminoácidos esenciales. Estos resultados fueron semejantes o incluso superiores a los de OK-1, con mayores rendimientos en aminoácidos ligados (61 ± 2 % frente a 50 ± 1 %) y porcentaje de extracción de los esenciales (78 ± 3 % frente a 71 ± 4 %), indicando que la extracción previa de isoflavonas no afectó negativamente la hidrólisis proteica.

La hidrólisis de OK-2 también se realizó en modo semicontinuo en un reactor de 2 L, en dos etapas (180 °C y 270 °C). La segunda etapa permitió una extracción significativamente mayor, alcanzando una recuperación del 70.4 % de proteínas (1.22 g/L) y un 10 % de aminoácidos libres, con predominio del ácido glutámico.

En conjunto, la okara se confirma como un subproducto prometedor para procesos en cascada, combinando una primera etapa suave de extracción de isoflavonas con una segunda extracción/hidrólisis proteica de mayor severidad. Ambas configuraciones de agua subcrítica resultaron eficientes para este propósito.

Palabras clave: Agua subcrítica, okara, isoflavonas, proteína, perfil de aminoácidos.

Chapter 5

Cascade valorization of okara by subcritical water hydrolysis: assessment of protein and amino acid profile in batch and semi-continuous systems

Abstract

This study evaluated subcritical water hydrolysis (SWH) as a green strategy within a cascade process for protein recovery from okara previously subjected to an isoflavone valorization process (OK-2). The results were compared with untreated okara (OK-1).

Batch extraction was carried out at 180 °C for 3 h and 5 MPa in a 0.5 L reactor. Under these conditions, the total amino acid recovery from OK-2 reached 81 ± 3 % (12.6 g/L), with 20 ± 1 % of free amino acids, mainly glutamic acid, and a favorable profile of essential amino acids. These results were comparable or even superior to those of OK-1, showing higher yields of bound amino acids (61 ± 2 % over 50 ± 1 %) and a greater extraction percentage of essential amino acids (78 ± 3 % over 71 ± 4 %), indicating that the previous extraction of isoflavones did not negatively affect protein hydrolysis.

Hydrolysis of OK-2 was also performed in a semicontinuous mode in a 2 L reactor, in two stages (180 °C and 270 °C). The second stage enabled a significantly higher extraction, achieving a 70.4 % protein recovery (1.22 g/L) and 10 % of free amino acids, with glutamic acid as the predominant compound.

Overall, okara is confirmed as a promising by-product for cascade processes, combining a mild first stage for isoflavone extraction with a second, more severe stage for protein extraction/hydrolysis. Both subcritical water configurations proved efficient for this purpose.

Key words: Subcritical water, okara, isoflavones, protein, amino acid profile.

1. Introduction

Okara is the primary by-product of soybean (*Glycine max*) processing, generated during the production of soymilk and tofu in the filtration phase. As the most widely cultivated and consumed legume worldwide, soybean plays a central role in global food systems. The demand for soybean-based products grows yearly, guided by an increasing awareness of their nutritional benefits, the increasingly extended use of soybean oil and the rising adoption of plant-based diets as alternatives. Soymilk and tofu, in whose production okara results as a by-product, are ones of the greatest substitutes for cow's milk and animal meat, respectively (Barea, Illera, Melgosa, *et al*., 2025; Colletti *et al*., 2020).

World production of soybean in 2023 reached 378 million tonnes (Mt), a 5.1 % increment from 2022. The leading producer is Brazil (152 Mt) followed by EEUU and Argentina. In Spain, production reached 7670 t (FAO, 2025a). Global production is estimated to increase up to 398 Mt in 2023/24, with forecasts predicting a continued annual growth of 6.1 %, reaching approximately 423 Mt in 2024/25 and predicted to keep increasing for 2025/26 and upcoming years (FAO, 2025b). For every 1 t of soybean processed, approximately 1.1 t of wet okara are generated as a by-product (Barea, Illera, Melgosa, *et al*., 2025). Therefore, the global production of wet okara can be estimated around 465 Mt only in 2025.

Okara has been extensively studied for its isoflavone content, with numerous works focusing on the hydrolysis, concentration, and purification of these compounds. Isoflavones are the most distinctive phytochemicals in soybean, present in high concentrations and known for their functional properties and health benefits due to their estrogen-like structure (Barea, Illera, Melgosa, *et al*., 2025; Hsiao *et al*., 2020). Beyond isoflavones, one of the most valuable compounds in okara is protein, being present in high concentrations and offering a complete amino acid profile with all essential amino acids (Colletti *et al*., 2020). However, their extraction from okara have received far less attention in published literature and even fewer when

considering detailed amino acid distribution of the hydrolysates, which is essential for evaluating the potential use of okara extracts.

In previous studies, isoflavone extraction has been optimized using various techniques, standing out subcritical water hydrolysis (SWH) in mild conditions as the most effective method (Barea, Illera, Melgosa, *et al*., 2025). Therefore, subW is also proposed here as a promising green alternative for protein extraction from the remaining solid after isoflavone extraction, still rich in protein, as a novel green method that has demonstrated efficiency on extracting valuable compounds as protein from different food by-products. subW uses pressurized liquid water at temperatures between 100 and 374 °C. These conditions make water act as both an acid and a base catalyst, due to a decrease in its dielectric constant and an increase in the ionic product (Kw), enhancing the hydrolysis of proteins into smaller peptides and free amino acids without requiring any added chemicals or enzymes (Barea *et al*., 2024; Haq *et al*., 2025).

Compared to enzymatic hydrolysis, which is the most commonly reported method for protein extraction/hydrolysis from okara (de Figueiredo *et al*., 2018; Ningrum *et al*., 2025), SWH offers significant advantages, such as shorter reaction times, higher degrees of hydrolysis, and greater release of amino groups (Barea *et al*., 2023). SWH not only maximizes protein hydrolytic efficiency, but also enhances bioactive properties of hydrolysates. It is effective, avoids producing unwanted residues like salts, and reduces the risk of damaging sensitive amino acids. All these factors make it a highly promising method for sustainably valorizing protein-rich by-products (Haq *et al*., 2025).

Peptides exhibit enhanced bioactive properties that are inactive in their native protein structure until released through hydrolysis. Several of these bioactive peptides, including soybean-derived peptides, have been associated with antidiabetic, antihypertensive (ACE-inhibition), antithrombotic or mineral-binding effects, besides antioxidant capacity (Haq *et al*., 2025; Marcet *et al*., 2016; Moure *et*

al., 2006). Moure *et al*. (2006) reported that non-refined hydrolysates displayed higher antioxidant activity than purified ones. Low-molecular-weight peptides and free amino acids are associated with enhanced bioactivities. In addition to bioactive properties, hydrolyzed peptides also possess valuable techno-functional properties such as emulsifying and foaming capacity. Techno-functional and bioactive properties are closely related to the physicochemical characteristics of the hydrolysates, particularly peptide size and amino acid profile. Consequently, protein hydrolysates rich in these functional and bioactive molecules are considered promising ingredients for applications in nutraceuticals, functional foods, pet feed, and in clinical nutrition (Barea *et al*., 2024; Marcet *et al*., 2016).

The aim of this study is to evaluate the efficiency of SWH as a green and highly effective technology for protein hydrolysis, in two different configurations (batch and semi-continuous), in a cascade extraction approach from pre-treated okara with subW at mild conditions to extract and valorize the isoflavones present in okara (Barea, Illera, Melgosa, *et al*., 2025). Protein release and amino acid profile were analyzed in this work. Results were compared with those obtained using untreated okara to assess the advantageous of performing a cascade valorization strategy.

2. Experimental

2.1. Raw material

Okara was supplied by *Frías Nutrición* S.A.U. (Burgos, Spain). This by-product presents 82.5 % moisture, and it will be referred from now on as OK-1 (equivalent to OKC in previous Chapter 4). Characterization of the raw material was performed according to the methodology detailed in section 2.3.

2.2. Subcritical water process for okara valorization

In this study, a cascade approach was proposed to selectively fractionate compounds of high added value present in the OK-1 using subW, as illustrated in

Figure 5.1. Initially, mild conditions (120 °C) were selected based on previous studies to extract the isoflavone fraction present in the crude okara (OK-1) using a batch reactor (Figure 5.2) (Barea, Illera, Melgosa, *et al*., 2025). Following this initial step, a liquid extract rich in bioactive compounds was generated. The solid residue remaining after filtration (OK-2) was subjected to more severe conditions, ranging from 180 °C and 270 °C, to extract/hydrolyze the protein fraction and other structural components. This second step was conducted in both, batch (Figure 5.2) and semi-continuous (Figure 5.3) configurations for comparison.

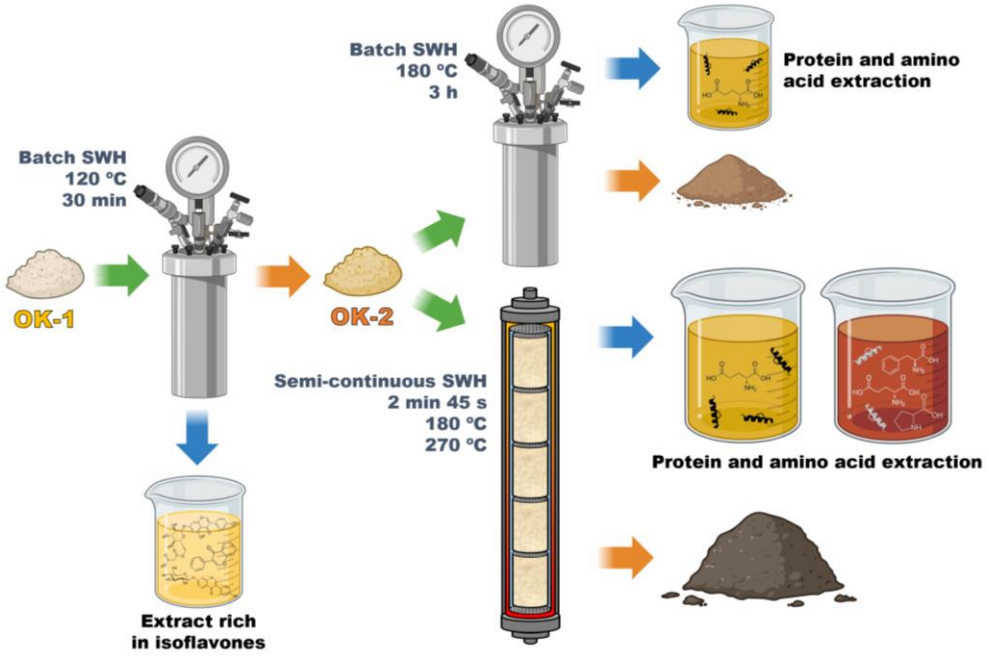

Figure 5.1. Schematic representation of the experimental flow diagram for the cascade valorization of okara by subcritical water hydrolysis (SWH). First step: Isoflavone extraction from OK-1 at 120 °C. Second step: protein extraction from OK-2.

2.2.1. Batch reactor

The batch subW experiments were carried out in a lab-built batch reactor system with a total internal volume of 0.5 L (see Figure 5.2). The reactor was externally heated using a ceramic heating jacket (230 V, 4000 W, ⌀ 95 mm, 160 mm

height). A Pt100 temperature sensor placed inside the reactor was connected to a PID controller to regulate and monitor the temperature during the reaction. A needle valve connected to a cooling system enabled sample collection during hydrolysis.

In a typical run, 9.5 g of dry biomass (considering the moisture content) and 200 mL of distilled water were loaded into the reactor. Operating pressure was fixed at 5 MPa by using nitrogen as pressurization agent, being this pressure enough to keep water in its liquid state at the testing operating temperatures of this work in the batch configuration. Two sequential batches were performed. First, crude okara (OK-1) was charged into the reactor to obtain an extract rich in isoflavones working at 120 °C (Barea, Illera, Melgosa, *et al*., 2025); this process was carried out several times in order to obtain a considerable quantity of solid residue (OK-2). This solid residue was further subjected to more severe conditions, setting the operating temperature at 180 °C, see Figure 5.1. This temperature was set based on previous works as it was sufficient to promote protein hydrolysis from different sources (Barea *et al*., 2023).

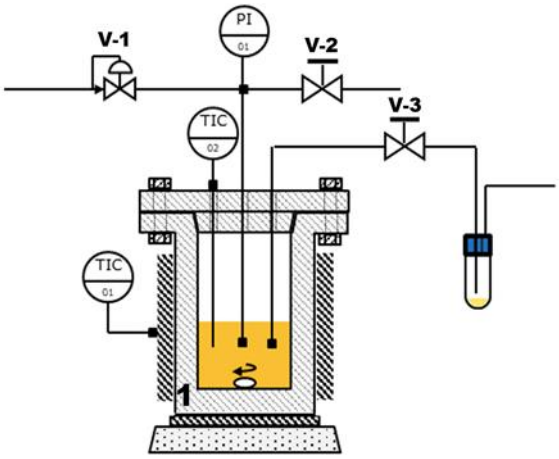

Figure 5.2. Batch subW configuration: **(1)** Steel reactor; **V-1**: gas inlet (N_2); **V-2**: pressure purge valve; **V-3**: sampling valve; **TIC-01**: external temperature control; **TIC-02**: extraction temperature control; **PI-01**: internal pressure gauge.

After each treatment step, the reactor was cooled and depressurized when the internal temperature dropped below 90 °C. The hydrolysates were filtered through Whatman No. 5 paper to separate solids and then stored at −18 °C until analysis.

2.2.2. Semi-continuous reactor

Semi-continuous subW experiments were carried out in a pilot-scale installation (*Eurotechnica GmbH*, Germany) equipped with a reactor of 2.3 L (*Sitec-Sieber Engineering AG*) and a plunger-pump (NP25/12-500, *Speck*), allowing a maximum operating temperature and pressure of 300 °C and 20 MPa, respectively (Figure 5.3). A tube with five baskets was fitted into the reactor which made it easier to introduce and distribute the sample evenly along the reactor, avoiding agglomeration in the bottom. The tube is closed at the top and bottom with metallic filters preventing the passage of any solid into the different connections of the equipment. The heating of the jacketed reactor is achieved by circulating the heating fluid through the jacket. Until the desired temperature was achieved water was circulated through a bypass circuit avoiding extraction during heating. Temperature of the heating fluid is regulated by smart controller integrated into the heater unit (Oil Advanced D1-300-9-50, 380-415 V, 50 Hz, *Single, Group GmbH*), able to reach temperatures up to 300 °C.

In a typical run, 100 g on a dry basis (considering the humidity content) were loaded into the reactor by conveniently placing 20 g on a dry basis in each one of the vessels previously described. Two different temperatures were sequentially applied starting from 180 °C and going further to 270 °C. This two-step approach is designed to achieve high protein recovery in a shorter time frame, avoiding the need for extended treatment.

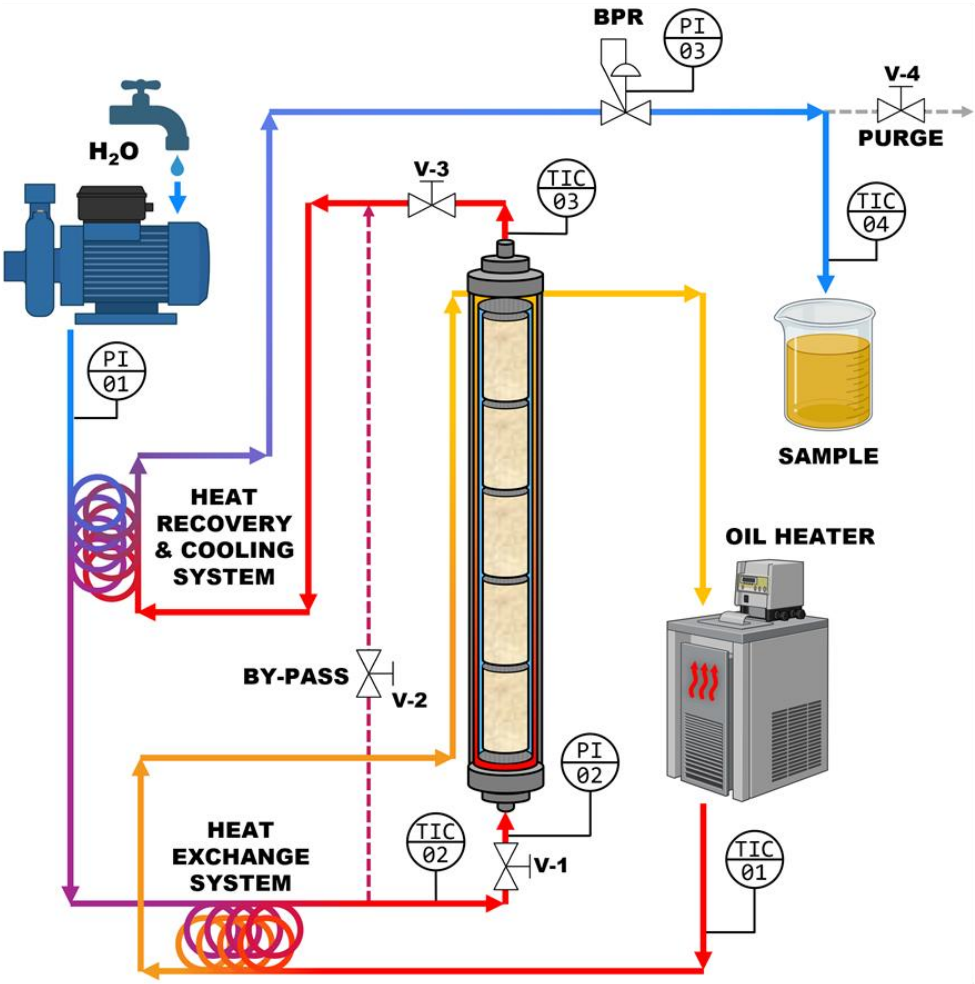

Figure 5.3. Semi-continuous subW configuration: **BPR**: system back-pressure-regulator; **V-1**: reactor inlet valve; **V-2**: by-pass valve; **V-3**: reactor outlet valve; **V-4**: purge valve; **TIC-01**: heating fluid temperature; **TIC-02**: reactor inlet temperature; **TIC-03**: reactor outlet temperature; **TIC-04**: system outlet temperature (sampling); **PI-01**: system inlet pressure; **PI-02**: reactor inlet pressure; **PI-03**: system (regulated by BPR) pressure.

The pump frequency was fixed at 5 Hz providing a water flux of 0.84 L/min and the system was pressurized to 9 MPa to keep water in its liquid state when working at the highest temperature. Initially, water was recirculated through the bypass line. Once the desired water temperature was reached for the first extraction step, 180 °C, the bypass valve was closed and water began to flow through the

biomass in the reactor. The effluent was collected continuously, and samples were taken every 1–2 L for analysis. After this first extraction step at 180 °C, the bypass valve was opened again and pre-heating water up to 270 °C was achieved in the bypass circuit, repeating the process. After completion of the whole process and cooling of the equipment to below 60 °C (as recommended by the manufacturer), the reactor was opened, and the remaining solid was recovered. Aliquots from each collected liquid fraction were filtered through Whatman No. 5 paper to remove suspended solids and stored at -18 °C until further analysis.

Comparison of the results obtained in subW in both configurations will be compared by evaluating the severity factor. This factor is a dimensionless parameter that integrates time and temperature to assess the intensity of hydrothermal treatments. It was evaluated through Eq. 5.1:

$$\text{Severity factor} = \log(R_0); \quad R_0 = t \cdot \exp\left(\frac{T-100}{14.75}\right) \qquad \textbf{[5.1]}$$

where t is the residence time (min) and T the temperature (°C). The constant 14.75 reflects the activation energy for glycosidic bond cleavage (first-order kinetics), while 100 °C is the reference temperature for hemicellulose depolymerization (Illera *et al*., 2025).

2.3. Analysis

2.3.1. Saccharide profile and quantification

The polysaccharide fraction and derived products were analyzed by high-performance liquid chromatography (HPLC) following the National Renewable Energy Laboratory (NREL) protocols (A. Sluiter *et al*., 2008). The HPLC system was equipped with a Bio-Rad Aminex HPX-87H column and its corresponding pre-column, using 0.005 M H_2SO_4 as the mobile phase at a flow rate of 0.6 mL/min. Detection was performed with both a refractive index detector and a variable wavelength detector (VWD) set at 210 nm; both detectors and the column were

maintained at 40 °C. A sample volume of 10 μL was injected after filtration through 0.22 μm syringe filters (Scharlab).

Briefly, extractives-free solid samples were subjected to two steps of acid hydrolysis, according to the NREL protocol. The acid insoluble residue (AIR) was rinsed with deionized water, dried 4 h at 105 °C and weighed. Ash content was determined by weight difference after placing AIR in a muffle furnace at 575 °C for 24 h. Insoluble lignin was calculated as the difference between AIR and ash. For polysaccharide determination, hydrolysates were neutralized with $CaCO_3$ to pH 5–6 and filtered through a 0.22 μm syringe filters before HPLC determination. Monomers and sugar-derived compounds were directly measured in liquid extracts after filtering through a 0.22 μm pore size syringe filter and quantifying its yield considering biomass total sugars (Eq. 5.2). Oligomeric structural sugars in liquid hydrolysates were quantified by comparing monomer concentrations before and after acid autoclave hydrolysis (Eq. 5.3).

$$\text{Monomer yield (\%)} = \frac{(\text{Monomeric sugar})_{\text{hydrolysate}}}{(\text{Total sugar})_{\text{initial biomass}}} \times 100 \qquad \textbf{[5.2]}$$

$$\text{Oligomer yield (\%)} = \frac{(\text{Total} - \text{Monomeric sugar})_{\text{hydrolysate}}}{(\text{Total sugar})_{\text{initial biomass}}} \times 100 \qquad \textbf{[5.3]}$$

The total yield of each sugar was calculated as the sum of its monomeric and oligomeric fractions.

Compounds were identified by comparing their retention times with pure analytical-grade standards. Xylose and galactose were determined by enzymatic spectrophotometric kits, due to the fact that both sugars elute at the same time in the current HPLC setup. L-Arabinose/D-Galactose Assay Kit (700004264, Megazyme) and D-Xylose Assay Kit (700004355, Megazyme) were used to determine the concentration of both monomers.

2.3.2. Lipid content

The oil content of the okara was determined by Soxhlet extraction (Buchi B-811) using hexane as solvent.

2.3.3. Protein content

Protein in the samples was estimated from the nitrogen content present in the samples as measured by the elemental analysis. The *N*-factor was calculated from the total amino acid profile (free + bound amino acids) and elemental nitrogen data, according to the NREL standard protocols (NREL Laboratory Analytical Procedures).

The purity of the protein hydrolysate was calculated by considering the total soluble solids as shown in Eq. 5.4:

$$\text{Purity}\ (\%) = \frac{(\text{Protein})_{\text{hydrolysate}}}{(\text{Total extracted solids})_{\text{hydrolysate}}} \times 100 \qquad \textbf{[5.4]}$$

2.3.4. Elemental analysis

Elemental composition (C, H, N, S) of raw material and the remaining solids was determined by an elemental micro-analyzer EA Flash 2000 apparatus (Thermo Scientific, USA) with a thermal conductivity detector (TCD) integrated. Temperature in the oven and gas flow were set, respectively, at 900 °C and 250 mL/min for oxygen and 140 mL/min for helium, serving the latter as the carrier gas. An additional helium flow of 100 mL/min is used as reference for the detector. Calibration was performed with 4-aminobenzenesulfonamide as standard.

2.3.5. Total soluble solids

Aliquots of 1 mL of the final hydrolysate were filtered through a 0.22 μm syringe filter and dried in an oven at 105 ± 1 °C until constant weight allowing to calculate the percentage of solids in each liquid extract.

2.3.6. Amino acid profile and quantification

The amino acids were analyzed by gas chromatography (Hewlett-Packard, 6890 series) with flame ionization detection (GC-FID). Derivatization of amino acids is required prior to analysis to increase their volatility, allowing them to be analyzed by GC without requiring excessively high temperatures that would otherwise lead to their thermal degradation. The derivatization was carried out following the method detailed by Barea, Illera, Candela, *et al*. (2025) based on the method reported by Hušek (1991), which involves a mixture of ethanol:pyridine, Norvaline as internal standard, propyl-chloroformate (PCF) as derivatization agent and chloroform with 1 % PCF as organic phase. 4 μL of the organic phase were injected at 1:15 split ratio at 250 °C into a ZB-AAA column (10 m × 0.25 mm I.D., Phenomenex Inc.). The initial temperature of 110 °C was maintained for 1 min; then, the oven temperature was programmed from 110 to 320 °C at 32 °C/min. Helium was used as a carrier gas at 60 kPa and nitrogen was used as a make-up gas. The detector temperature was set at 320 °C. Amino acids were identified using pure standards for the different amino acids and with norvaline as internal standard.

Amino acid profile of structural amino acids was determined after acid hydrolysis using 6 N HCl at 100 °C during 24 h and further derivatization. Tryptophan, cysteine and methionine are lost by acid hydrolysis, so an alkaline hydrolysis (4.2 M NaOH at 100 °C during 24 h) was also carried out to determine these amino acids (Barea, Illera, Candela, *et al*., 2025). Glutamine and asparagine can be underestimated being considered as glutamic acid and aspartic acid respectively, due to deamination; however, they have been reported accordingly in the results.

In the liquid hydrolysates, the difference between total amino acids (after acid or alkaline hydrolysis) and free amino acids (Eq. 5.5) in each sample was considered as bound amino acids (Eq. 5.6), representing peptides or proteins present in a non-free form in solution:

$$\text{Free aa (\%)} = \frac{(\text{Free aa})_{\text{hydrolysate}}}{(\text{Total aa})_{\text{initial biomass}}} \times 100 \quad \textbf{[5.5]}$$

$$\text{Bound aa (\%)} = \frac{(\text{Total aa} - \text{Free aa})_{\text{hydrolysate}}}{(\text{Total aa})_{\text{initial biomass}}} \times 100 \quad \textbf{[5.6]}$$

The hydrolysis yield of each amino acid in the semi-continuous SWH configuration was calculated as the ratio between the cumulative amount of free amino acid released during each interval and the initial total content of that amino acid in the raw biomass.

2.3.7. Total Nitrogen

Total nitrogen (TN) in the hydrolysates was quantified using a Total Organic Carbon Analyzer (Shimadzu TOC-V CSN). Nitrogen-containing compounds were oxidized by catalytic thermal decomposition during combustion, producing nitrogen oxides (NO_X) which can be detected by a chemiluminescence detector integrated in the instrument. Potassium nitrate (KNO_3) was used as the calibration standard.

The nitrogen content of each hydrolysate, together with its corresponding amino acid profile, was used to calculate the specific nitrogen-to-protein conversion factor (N factor), which in turn was applied to estimate accurately the protein content of each hydrolysate.

2.4. Statistical analysis

All the samples were produced and analyzed at least two times, and expressed as mean ± standard deviation of the replicates. Data was analyzed using the software Statgraphics19 X64, the significance of the differences between samples results was

determined based on an analysis of the variance with the Fisher's Least Significant Difference (LSD test) at *p*-value ≤ 0.05.

3. Results

3.1. Characterization of okara

The chemical composition on a dry basis of the original okara (OK-1) is showed in Table 5.1. The protein content was 26.9 ± 0.5 % (w/w). The applied N-factor was 5.04 as determined with the amino acid profile of the raw material reported in Table 5.2.

The amino acid distribution of okara is presented in Table 5.2. Glutamic acid was the most abundant amino acid (57 ± 4 $mg/g_{dryOK-1}$), followed by aspartic acid (23 ± 1 $mg/g_{dryOK-1}$), representing 28 % and 11 % of the amino acids, respectively. These values are consistent with previous reports in the literature, although some differences may exist depending on the crop origin and cultivar (Colletti *et al*., 2020; Kumar *et al*., 2016). OK-1 exhibits a great amino acid profile with a potentially high nutritional value in its hydrolysates, owning a 38 % of essential amino acids (EAA) in its profile (78 ± 2 $mg/g_{dryOK-1}$). Lysine (15 ± 1 $mg/g_{dry\ OK-1}$), phenylalanine (14.6 ± 0.8 $mg/g_{dry\ OK-1}$), isoleucine (12.4 ± 0.3 $mg/g_{dry\ OK-1}$), leucine (11.4 ± 0.7 $mg/g_{dry\ OK-1}$), and valine (9.3 ± 0.4 $mg/g_{dry\ OK-1}$) were the most prevalent EAAs. The EAA profile was consistent with other values reported in the literature. For example, Colletti *et al*. (2020) reported the same dominant EAAs, although leucine was the most abundant (phenylalanine was reported together with tyrosine). Kumar *et al*. (2016) also found leucine as most abundant, followed by phenylalanine, while maintaining the same top five EAAs.

Extractives in water were 12.2 ± 0.5 % (w/w), which included 3.3 $g/100\ g_{dry\ OK-1}$ of water-soluble protein. Ash and lipid content was 3.3 ± 0.1 % (w/w) and 9.5 ± 0.4 % (w/w), respectively. The major sugars present in the OK-1 were galactans and glucans, with values of 12 ± 1 % (w/w) and 10 ± 1 % (w/w),

respectively. Acid insoluble lignin accounted for 8.3 ± 0.4 % (w/w). Data more detailed can be found in Table 5.1. The elemental analysis composition of OK-1 yielded values of 49.9 ± 0.4 % (w/w) of C, 5.9 ± 0.2 % (w/w) of N and 8.0 ± 0.1 % (w/w) of H.

Table 5.1. Detailed composition (on a dry basis) of raw material (OK-1), solid residue after subW batch treatment at 120 °C (OK-2), solid residue after subW batch treatment and solid residue after subW 2-step semi-continuous treatment.

Compound	OK-1, %	OK-2, %	Residue (OK-2) Batch, %	Residue (OK-2) Semi-cont., %
Extractives H_2O	12.2 ± 0.5	n.d.	n.d.	n.d.
Ext. in EtOH	5.3 ± 0.5	n.d.	n.d.	n.d.
Saccharides	32 ± 4	29 ± 2	44 ± 2	3.1 ± 0.2
Glucans	*10 ± 1*	*15.9 ± 0.7*	*38 ± 2*	*0.91 ± 0.01*
Galactans	*12 ± 1*	*6.2 ± 0.3*	*4.1 ± 0.2*	*0.00 ± 0.00*
Xylans	*2.0 ± 0.3*	*1.4 ± 0.1*	*0.07 ± 0.01*	*0.00 ± 0.00*
Arabinans	*3.9 ± 0.9*	*2.3 ± 0.2*	*0.032 ± 0.003*	*0.00 ± 0.00*
Uronic acids	*3.9 ± 0.5*	*2.9 ± 0.4*	*0.22 ± 0.02*	*2.2 ± 0.2*
Protein	26.9 ± 0.5	32.8 ± 0.6	8.3 ± 0.4	10.5 ± 0.4
Lipid	9.5 ± 0.4	n.d.	n.d.	n.d.
polar	*1.8 ± 0.3*	*n.d.*	*n.d.*	*n.d.*
non-polar	*7.8 ± 0.2*	*n.d.*	*n.d.*	*n.d.*
Lignin	16 ± 1	31.7 ± 0.3	48 ± 3	83 ± 2
soluble	*8 ± 1*	*6.1 ± 0.1*	*3.0 ± 0.2*	*2.5 ± 0.1*
non-soluble	*8.3 ± 0.4*	*25.6 ± 0.3*	*45 ± 3*	*81 ± 2*
Ash	3.3 ± 0.1	4.0 ± 0.1	5.5 ± 0.2	6.1 ± 0.4
Elemental				
C, % (w/w)	49.9 ± 0.4	53.9 ± 0.3	60.1 ± 0.7	68.1 ± 0.2
N, % (w/w)	5.9 ± 0.2	7.0 ± 0.3	1.70 ± 0.08	2.7 ± 0.6
O, % (w/w)	32.9 ± 0.5	26.6 ± 0.4	24 ± 1	14 ± 1
H, % (w/w)	8.0 ± 0.1	8.5 ± 0.1	9.0 ± 0.1	9.3 ± 0.3
Molar ratio				
N:C	0.10 ± 0.01	0.11 ± 0.01	0.024 ± 0.001	0.034 ± 0.008
O:C	0.49 ± 0.01	0.37 ± 0.01	0.36 ± 0.01	0.22 ± 0.01
H:C	1.92 ± 0.03	1.89 ± 0.02	1.80 ± 0.03	1.64 ± 0.05

n.d.: not determined

Table 5.2. Amino acid profile of OK-1, of OK-2. Percentages of amino acids released in the liquid phase as free (free aa %, Eq 5.5) and bound amino acids (bound aa %, Eq. 5.6) from OK-2 hydrolysate (5 % (w/w)) by using batch subW at 180 °C for 3 h. Percentages of individual amino acids remaining in the final solid residue after treatment (remaining aa %) and amino acid profile in the solid residue ($mg/g_{dry\ solid}$).

Amino Acid	Initial aa, $mg/g_{dry\ OK\text{-}1}$	Initial aa, $mg/g_{dry\ OK\text{-}2}$	Liquid hydrolysate from OK-2			Solid residue from OK-2	
			Free aa, %	Bound aa, %	Total aa, %	Remaining aa, %	Remaining aa, $mg/g_{dry\ solid}$
Ala	7.9 ± 0.4[a]	8.9 ± 0.8[a]	18 ± 2	68 ± 11	86 ± 13	23 ± 2	2.02 ± 0.08
Gly	10 ± 1[a]	9.7 ± 0.9[a]	17 ± 2	54 ± 6	71 ± 8	24 ± 3	2.3 ± 0.1
Val	9.3 ± 0.4[a]	9 ± 1[a]	4.8 ± 0.5	75 ± 8	80 ± 9	22 ± 3	1.94 ± 0.09
Leu	11.4 ± 0.7[a]	12 ± 1[a]	4.0 ± 0.4	79 ± 7	83 ± 7	23 ± 3	2.7 ± 0.2
Ile	12.4 ± 0.3[b]	10.5 ± 0.4[a]	3.9 ± 0.2	68 ± 6	72 ± 6	20 ± 1	2.09 ± 0.09
Thr	1.2 ± 0.1[a]	1.4 ± 0.1[a]	7 ± 2	81 ± 11	88 ± 13	15 ± 3	0.21 ± 0.03
Ser	8.0 ± 0.1[b]	6.4 ± 0.1[a]	6 ± 2	65 ± 2	71 ± 4	20 ± 3	1.3 ± 0.2
Pro	11.0 ± 0.5[a]	11 ± 1[a]	7.4 ± 0.7	73 ± 15	80 ± 16	18 ± 2	1.9 ± 0.1
Asn	1.3 ± 0.2[a]	0.81 ± 0.04[a]	12.3 ± 0.9	64 ± 12	76 ± 13	26 ± 1	0.21 ± 0.01
Asp	23 ± 1[a]	27 ± 2[a]	26 ± 2	66 ± 5	92 ± 7	2.6 ± 0.5	0.7 ± 0.1
Met	4.8 ± 0.2[a]	4.1 ± 0.2[a]	29 ± 1	16 ± 4	45 ± 5	53 ± 5	2.2 ± 0.2
Hyp	0.81 ± 0.04[b]	3.1 ± 0.2[a]	13.2 ± 0.9	72 ± 5	85 ± 6	23 ± 2	0.70 ± 0.02
Glu	57 ± 4[b]	43.1 ± 0.8[a]	46 ± 2	37 ± 4	83 ± 6	12.2 ± 0.5	5.3 ± 0.2
Phe	14.6 ± 0.8[a]	13 ± 1[a]	8.0 ± 0.6	72 ± 14	80 ± 15	21 ± 2	2.8 ± 0.2
Cys	1.0 ± 0.1[a]	0.9 ± 0.1[a]	4.9 ± 0.8	85 ± 13	90 ± 14	7 ± 2	0.06 ± 0.01
Gln	0.44 ± 0.04[a]	0.4 ± 0.1[a]	65 ± 12	14 ± 3	79 ± 15	15 ± 3	0.064 ± 0.001
Lys	15 ± 1[a]	12.1 ± 0.8[a]	4.5 ± 0.7	74 ± 5	79 ± 6	14 ± 3	1.7 ± 0.4
His	6.1 ± 0.5[a]	5.1 ± 0.6[a]	19 ± 3	65 ± 8	84 ± 11	14 ± 3	0.7 ± 0.1
Tyr	5.0 ± 0.1[a]	5.4 ± 0.7[a]	9 ± 2	80 ± 13	89 ± 15	18 ± 3	0.96 ± 0.08
Hyl	1.34 ± 0.03[b]	0.94 ± 0.03[a]	11 ± 2	79 ± 3	90 ± 5	12 ± 4	0.11 ± 0.04
Trp	2.6 ± 0.1[a]	3.0 ± 0.1[b]	4.0 ± 0.5	85 ± 1	89 ± 2	19 ± 1	0.57 ± 0.02
TAA	204 ± 5[a]	187 ± 3[a]	20 ± 1	61 ± 2	81 ± 3	16.3 ± 0.4	30.5 ± 0.6
EAA	78 ± 2[a]	70 ± 2[a]	7.6 ± 0.3	70 ± 3	78 ± 3	21 ± 1	14.9 ± 0.5

Ala: alanine, Gly: glycine, Val: valine, Leu: leucine, Ile: isoleucine, Thr: threonine, Ser: serine, Pro: proline, Asn: asparagine, Asp: aspartic acid, Met: methionine, Hyp: hydroxyproline, Glu: glutamic acid, Phe: phenylalanine, Cys: cysteine, Gln: glutamine, Lys: lysine, His: histidine, Tyr: tyrosine, Hyl: hydroxylysine, Trp: tryptophan. TAA: total amino acids, EAA: total essential amino acids. Values with different letters (a, b) in "initial aa" columns are significantly different (LSD method at p-value ≤ 0.05).

Composition values were consistent with those reported by O'Toole (1999) for three different soybean cultivars, which showed protein contents ranging from 25.4 to 28.4 %, lipid contents from 9.3 to 10.9 %, insoluble fiber between 40.2 and 43.6 % containing 11.7 ± 1.4 % of lignin. O'Toole (1999) used a nitrogen conversion value for the proteins of 5.71 while the one calculated in this paper is 5.04. Insoluble fiber values subtracting its lignin content corresponds to approximately 30 %, value that agree with actual insoluble saccharide content in OK-1.

Other studies report several values and wider ranges for okara biomolecule contents, with protein between 15.2 and 33.4 %, fat between 8.3 and 10.9 %, total fiber between 42.4 and 58.1 %, and ash between 3.0 and 4.5 % (B. Li *et al*., 2012; Vong & Liu, 2016). The values obtained in the present work are within the mid-range of these reported values. The total fiber values reported in these studies, which do not separate lignin, are in agreement with the sum of saccharides and lignin determined in the present one, 48 ± 5 %.

3.2. First valorization step. Isoflavones extraction

OK-1 was subjected to a first valorization step (Figure 5.1) according to the optimal experimental conditions found in previous works (Barea, Illera, Melgosa, *et al*., 2025) and reported in Chapter 4, 120 °C and 30 min of subW treatment. After treatment, a liquid hydrolysate was obtained with a high content of isoflavones, more than 1200 µg of isoflavones per g of dry OK-1. Details of isoflavones profile and quantification can be found in previous work by Barea, Illera, Melgosa, *et al*. (2025).

The solid residue generated after treatment will be referred as OK-2. Chemical characterization of this solid was performed and detailed in Table 5.1, together with the data of OK-1 for a better comparison. Due to the solubilization and extraction of the easily extractable compounds in this first step, concentration for some of the insoluble compounds increased in the OK-2, especially insoluble acid lignin increasing its value up to 25.6 ± 0.3 % (w/w). Glucans content also increased

compared to OK-1, 15.9 ± 0.7 % (w/w), while galactans decreased to 6.2 ± 0.3 % (w/w). The protein content was assessed by the total nitrogen content determined in the elemental analysis and the amino acid profile of the OK-2 reported in Table 5.2. The total protein content was also higher in the OK-2 compared to OK-1, 32.8 ± 0.6 % (w/w) according to the higher N content of the residue OK-2 determined by elemental analysis (53.9 ± 0.3 % (w/w) of C, 7.0 ± 0.3 % (w/w) of N and 8.5 ± 0.1 % (w/w) of H). There were no significant differences in the total amino acid (TAA) content between OK-1 and OK-2 with similar amino acid profile for OK-1 and OK-2, being the major amino acids glutamic and aspartic acids, although slightly lower values were determined for glutamic acid in the OK-2 probably due to its high solubility in polar solvents. Similar content of EAA was found in the OK-2 (37.4 %) compared to OK-1. The same five EAA as in OK-1 were predominant in OK-2 (12.1 ± 0.8, 13 ± 1, 10.5 ± 0.4, 12 ± 1, 9 ± 1 mg/$g_{dry\ OK\text{-}2}$, maintaining their relative order). The high protein content of the solid residue offers a great potential for further valorization to extract/hydrolyze its protein content.

3.3. Second valorization step. Protein extraction

3.3.1. Batch configuration

The solid reside generated after the subW treatment contains a considerable protein content (32.8 ± 0.6 %) with a valuable amino acid profile (Table 5.2). This solid residue was subjected to a second subW fractionation at 180 °C for 3 h (5 % (w/w) of dry biomass loading into the extractor) to analyze the extraction/hydrolysis of this fraction.

Table 5.2 reports the quantification of individual free (Eq. 5.5) and bound (Eq. 5.6) amino acids in the liquid hydrolysate, as well as the amino acid profile of the remaining protein fraction in the solid residue after treatment. subW treatment yielded more than 80 % (81 ± 3 %) of total amino acid extraction indicating a highly effective hydrolysis under subcritical water conditions. In the liquid hydrolysate 20 ± 1 % were determined as free amino acids and 61 ± 2 % as bound amino acids in

small peptides released to the extraction medium, referring these percentages to the total initial individual amino acids determined in the OK-2.

Glutamic acid reached 1.70 ± 0.07 mg/mL in the hydrolysate, 83 ± 7 % of initial total in OK-2. Glutamic acid accounted for 24 % of the total amino acids extracted in OK-2 hydrolysate. Focusing in the free amino acid fraction, glutamic acid represents more than half of it, 53 % (noticeable in Figure 5.3). This composition offers a great potential in different food application. Despite not being an EAA, glutamic acid has an important role as a neurotransmitter, besides, it is commonly used to produce glutamate and also contributes to the synthesis of antioxidant compounds such as glutathione (Sano, 2009). Glutamate is known as the main compound behind the umami taste and acts as a natural flavor enhancer, it can improve the taste of foods reducing salt levels, helping promote healthier eating without raising fat or calorie intake. It is also a versatile amino acid that plays roles in flavor perception, metabolic pathways, and neural signaling (Jinap & Hajeb, 2010).

Other prevalent amino acids in the OK-2 hydrolysate, such as aspartic acid, have applications in pharmaceutical, chemical, and cosmetic industries as precursors for active compounds. Meanwhile, essential amino acids like isoleucine are primarily used as supplements in food and feed industries, and others (including the rest of more prevalent EAA: lysine, leucine, phenylalanine, and valine) are commonly used in both sectors (Madhariya *et al.*, 2023).

After this second subW step, a solid residue was generated whose elemental composition has been also presented in Table 5.1. The percentage of this solid residue accounted for 54 % of the OK-2 charged into the extractor. According to the high protein extraction/hydrolysis as determined in the liquid stream with free and bound amino acids profile, the nitrogen content on the solid (Table 5.1) was only 1.70 ± 0.08 % (w/w) while the C content increased up to 60.1 ± 0.7 % (w/w). The N:C molar ratio (Table 5.1) decreases markedly from 0.11 in OK-2 to 0.02 in the

corresponding residue after treatment, confirming the substantial hydrolysis of nitrogen-containing compounds. This is consistent with a relative concentration of saccharides and lignin, which are rich in carbon. In contrast, the slight decrease in O:C and H:C molar ratios (from 0.37 to 0.36 and from 1.89 to 1.80, respectively), suggests that the levels of oxygen and hydrogen bound to the remaining carbon-rich structures were mainly preserved during the process.

The amino acid profile of this residual solid is presented in Table 5.2. Analyzing the individual amino acid composition, it is observed that 16.3 ± 0.4 % of the total initial amino acid content in the OK-2 introduced into the reactor remains in the final solid fraction. Glutamic acid remains the predominant amino acid in this solid, with a concentration of 5.3 ± 0.2 mg/g dry solid (Table 5.2), although only 12.2 ± 0.5 % of the initial amount persists, followed by phenylalanine and leucine, with concentrations of 2.8 ± 0.2 and 2.7 ± 0.2 mg/g dry solid, respectively, representing 21 ± 2 % and 23 ± 3 % of their initial quantities.

Comparison of these data with previously published studies remains challenging due to the limited availability of detailed amino acid distribution data in okara hydrolysates, as noted by Kumar *et al*. (2016). This highlights the importance of this study, which proposes a two-step valorization process to extract both bioactive compounds, isoflavones and proteins (focusing on detailed amino acid profiles).

As concluded by Wiboonsirikul *et al*. (2013), protein extraction from okara using subcritical water hydrolysis (SWH) requires high temperatures to achieve effective results, yielding 7 g/L of extracted protein when operated at 240 °C for 5 min (corresponding to a severity factor of 4.82, Eq. 5.1). These authors showed slower protein extraction at 170 °C with increasing protein extraction from 5 to 40 min with value of 2.5 g/L to 4.0 g/L of protein, respectively. No results are shown after that time, but the trend presented by these authors suggests that the extraction would likely continue increasing. In this work, considering the OK-2 charged into

the reactor and the percentage of amino acids (either free or bound) in the liquid hydrolysate a concentration of 7.2 g of total amino acids/L would be yield in this work (log R_0 = 4.61, Table 5.3). However, a direct comparison of extraction yield is not possible, as the proportion of initial protein recovered is not reported.

In comparison with other studies that employed more severe extraction conditions, it is noteworthy that, in terms of the severity factor for amino acid extraction, some authors reported achieving their highest amino acid yields at considerably higher severity values (Quitain *et al*., 2001; Rogalinski *et al*., 2005). Specifically, Quitain *et al*. (2001) identified optimal yields at severity factors of 5.6, 5.9, and 6.2 (250 °C for 15–60 min), whereas Rogalinski *et al*. (2005) observed maximum extraction at severity factors of 5.6 and 5.7 (290 °C for 1.1–1.3 min). These values are evidently higher than the severity factor employed in the present study (4.61, Table 5.3), indicating that more extreme conditions are generally necessary to maximize amino acid release.

Table 5.3. Severity factor evaluated according to Eq. 5.1 calculated for each one of the treatments carried out in the present work in addition to isoflavone optimum extraction from previous studies.

	Isoflavones from OK-1	**Protein from OK-2**		
	Batch	**Batch**	**Semi-continuous**	
Temperature, °C	120	180	180	270
Time, min	30	180	2.75*	2.75*
Severity factor	2.07	4.61	2.79	5.44
Free aa recovery, %	n.d.	20 ± 1	1.7	11.1
Protein recovery, %	n.d.	81 ± 3	18.3	52.2

*Residence time of the liquid in the semi-continuous reactor (τ = V/F)
n.d.: not determined

Several studies in the literature have focused on protein recovery from okara using conventional alkaline extraction. For example, C. Y. Ma *et al*. (1996) achieved a 53 % protein recovery by adjusting the pH to 9.0 with NaOH at 80 °C, followed by isoelectric precipitation, obtaining a final extract with over 80 % protein purity.

Similarly, Tao *et al*. (2019) used "extreme alkaline" conditions (up to pH 12.0) in combination with pre-treatments such as steam-cooking, ultrasonication, or pressurization at 50 MPa. Among these, steam-cooking resulted in the highest protein recovery level (63 ± 2 %) but lower than to those reported in the present study (81 ± 3 %). Despite the high purities obtained by alkaline methods, they involve the use of strong chemicals and achieved lower recovery rates than the subcritical water hydrolysates presented in OK-2.

Enzymatic methods have also been widely explored as greener alternatives. de Figueiredo *et al*. (2018) used Viscozyme as a pre-treatment and obtained an extract with 56 % protein purity. Although this purity surpasses the protein purity obtained for OK-2 hydrolysate (28.2 %, Eq. 5.4), the recovery yield was substantially lower, reaching only 29.8 % of the initial protein, much less than the 81 ± 3 % of total amino acid hydrolysis obtained for the present OK-2 extraction.

3.3.1.1. Effect of isoflavones pre-extraction on protein extraction

To check if the initial treatment at 120 °C to extract the isoflavones could have an effect of protein extraction from the solid residue generated (OK-2), a similar treatment was conducted for OK-1 at 180 °C to analyze the extraction/hydrolysis from the crude okara.

The amino acid profile of the liquid hydrolysates of OK-1 and OK-2 at 180 °C for 3 h, as free and bound amino acids expressed in mass, have been plotted together in Figure 5.4 allowing a direct comparison. For each amino acid, the bars represent the distribution into free amino acids in the hydrolysate, bound amino acids in the hydrolysate, and remaining amino acids in the solid residue after treatment. This representation helps to confirm that the sum of the different amino acid fraction closely approximates the total content initially present for each amino acid.

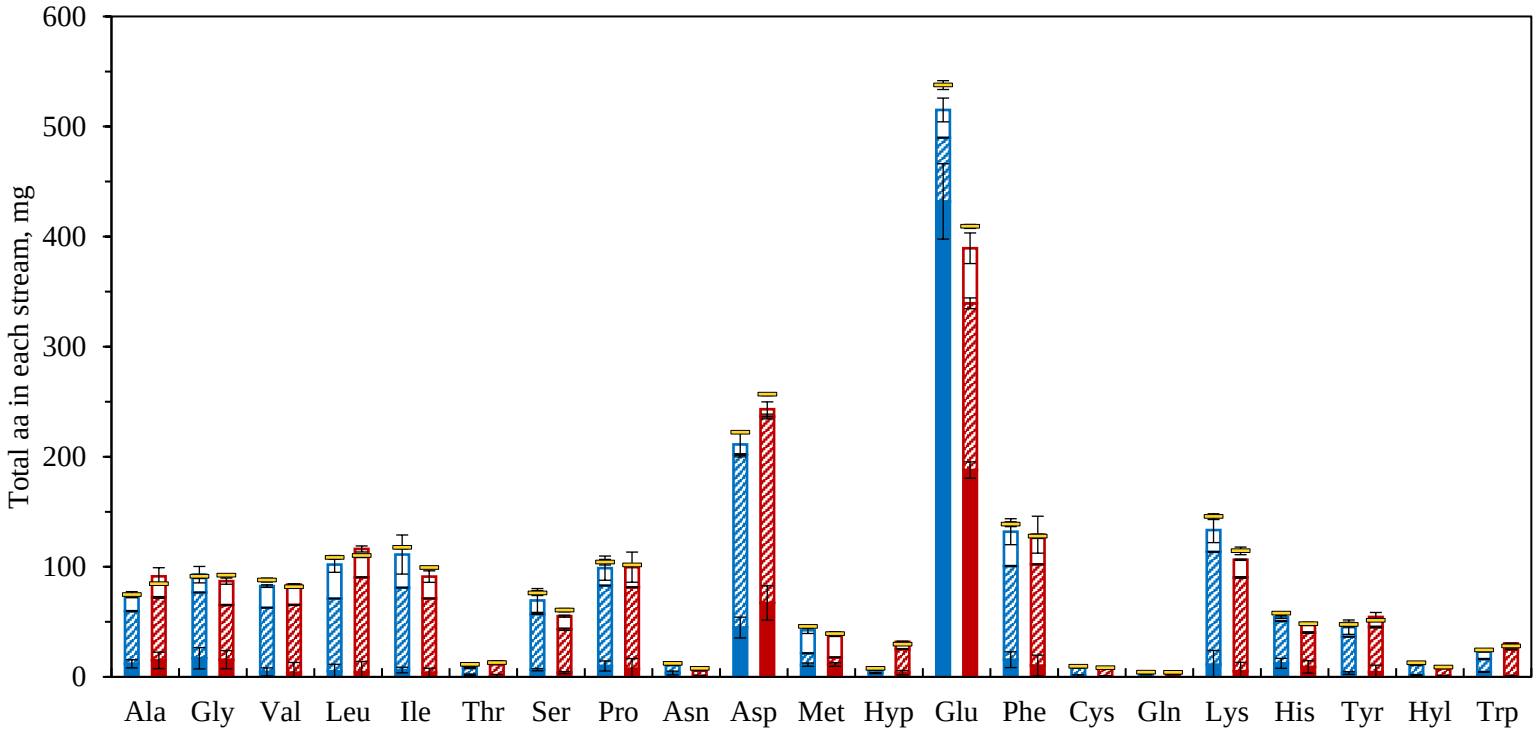

Figure 5.4. Amino acid profile distribution after subW treatment at 180 °C for 3 h from OK-1 and OK-2 hydrolysates. Free aa: OK-1 ■, OK-2 ■; bound aa: OK-1 ▨, OK-2 ▨; remaining aa on solid: OK-1 □, OK-2 □; initial total value: — (total mg).

The subcritical water hydrolysis of both biomass samples, OK-1 and OK-2, resulted in comparable free amino acid extraction efficiencies, with total yields of 81 ± 2 % and 81 ± 3 % for OK-1 and OK-2, respectively (Table 5.2, Figure 5.4). However, the proportion of free amino acids was higher in the fraction extracted from OK-1 (31 ± 1 %) compared to OK-2 (20 ± 1 %). This discrepancy is likely attributable to the loss of easily extractable amino acids during the isoflavone extraction process that produces OK-2. The hydrolysate of OK-2 exhibited a higher percentage of bound amino acids (61 ± 2 % compared to 50 ± 1 %), which are derived from more complex or less accessible proteins.

In any case, it can be concluded that OK-2 hydrolysates do not present disadvantages as a functional ingredient compared to the original by-product OK-1. Regarding protein extraction/hydrolysis, a higher extraction of the existing EAA (78 ± 3 % over 71 ± 4 % for OK-2 and OK-1, respectively) and a higher bound-to-free amino acid ratio can be observed. Furthermore, bioactive properties are attributed to peptides obtained in SWH hydrolysates (bound aa in these hydrolysates), as attributed antioxidant, antihypertensive and antidiabetic activities, additionally to foaming and emulsifying properties (Marcet *et al*., 2016). Besides, since OK-2 had been previously subjected to isoflavone extraction, its valorization gains additional relevance.

To assess the scalability and potential improvements of this approach, a semi-continuous SWH scaled-up system was subsequently investigated.

3.4. Subcritical water semi-continuous extraction

Subcritical water hydrolysis was also performed using a semi-continuous, scaled-up pilot plant to compare protein extraction/hydrolysis from this biomass with previous results presented in a batch configuration.

Semi-continuous subW treatment was performed at two different temperature steps: the first at 180 °C, and the second at higher temperature, 270 °C, intended to

maximize remaining protein and amino acid extraction. Pump flow rate was 0.84 L/min, leading to a residence time of 2.75 min for the liquid.

3.4.1. Protein extraction assessment

Protein extraction from the semi-continuous subW treatment was calculated based on the elemental nitrogen content of each sample and the N-factor previously calculated for OK-2 according to its amino acid profile. Eight samples were taken from each one of the temperature intervals.

Figure 5.5a represents in a bar chart the concentration of protein extracted on each one of the 16 samples collected through both temperature intervals. At 270 °C, the concentration of the protein fraction in the collected extracts is generally much higher than at 180 °C. In both cases, a peak concentration was observed, followed by a subsequent decline in the protein concentration within the extracts. The highest protein concentration was observed in the 12th sampling, with 2331 mg/L (corresponding 4^{th} sample of the second interval at 270 °C). In the first interval, at 180 °C, the peak was reached in the fifth sample, with 407 mg/L, 5.7 times lower than the previous value. This highlights 270 °C as a much more effective temperature for achieving protein hydrolysis in short residence times under the current configuration.

Figure 5.5b represents the accumulation of extracted protein as a function of time. Protein showed moderate accumulate protein productivity (g/h) in the samples recovered during the first interval at 180 °C, the overall increase across this first interval was limited, with an initial slope of 22.6 g/h ($22.6 \cdot t(h) + 7.4$; $R^2 = 0.99$). According to values presented in Figure 5.5a, the extraction levelled off in the final three sampling points.

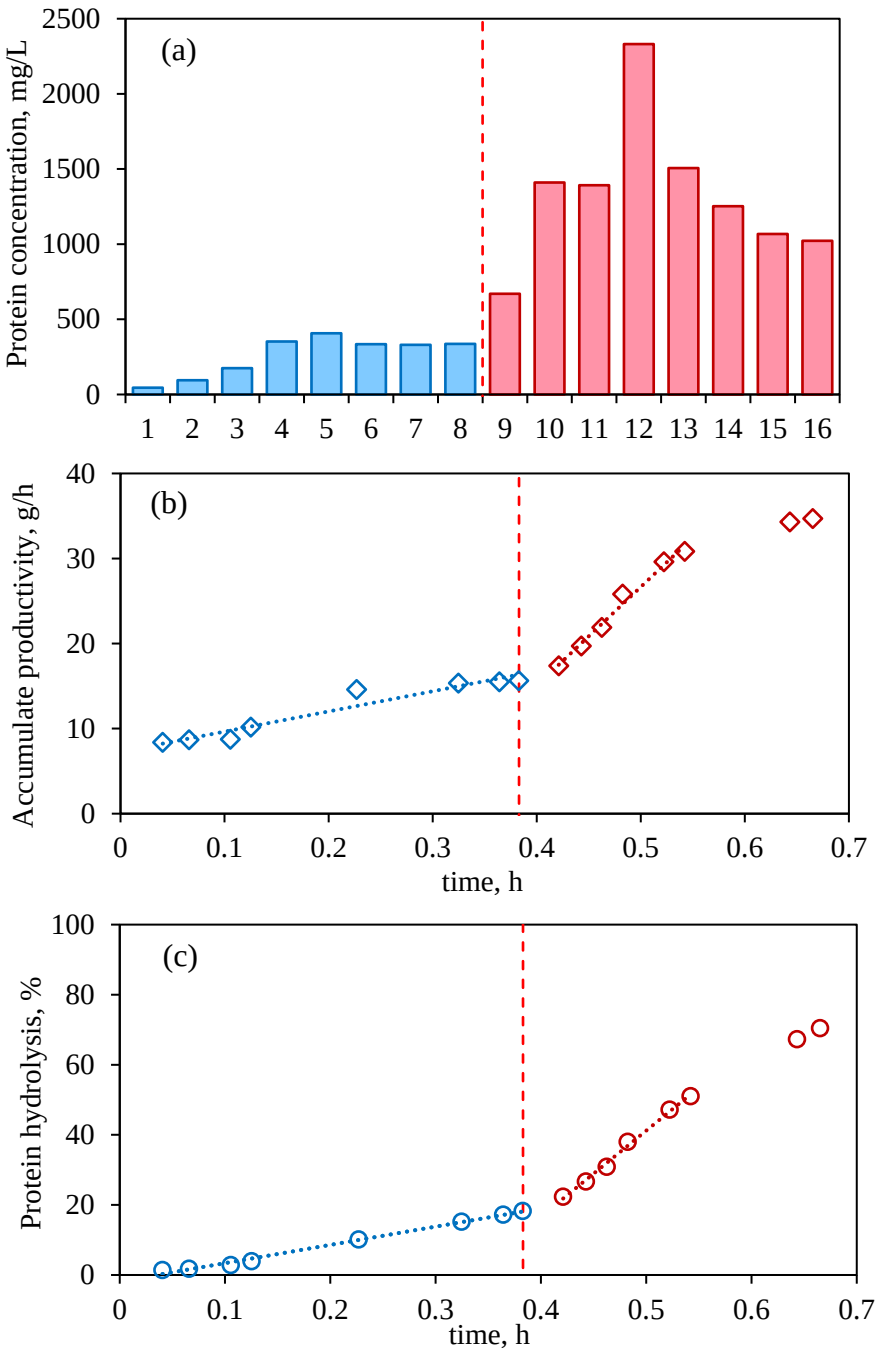

Figure 5.5. (a) Protein concentration (mg/L) in each extract 1–16. **(b)** Accumulated protein extraction productivity (g/h) as a function of time. **(c)** Accumulated protein degree of hydrolysis (%) in 2 L semi-continuous reactor from OK-2: 180 °C interval, **blue**; 270 °C interval, **red**; Intervals division, **- -**.

Second interval at 270 °C showed higher extraction and therefore higher accumulated productivity, presenting the first six points an initial slope of 116.0 g/h ($116.0 \cdot t(h) + 17.4$; $R^2 = 0.98$), more than 5 times higher than in the first case. In these first six points of the interval, accumulated productivity increased from starting 15.6 to 30.8 g/h (Figure 5.5b). The concentration of the last two collected samples at this temperature determined the level off observed in the accumulate productivity at the end of the process, finishing the experiment with a value of 34.7 g/h.

Figure 5.5c shows the percentage of protein hydrolyzed in the liquid effluent as a function of time, which is calculated on base to the grams of protein extracted on each sample relative to the initial protein content. During the first interval at 180 °C, a total of 6.0 g of protein was extracted, corresponding to 18.3 % of the initial protein content (Figure 5.5c).

In the second interval at 270 °C, an additional 17.1 g of protein were recovered (23.1 g in the full process considering the 6.0 g of the first interval), accumulating 52.1 % in total protein in this second step and 70.4 % of the total initial protein content in the whole process (Figure 5.5c). These results demonstrate that the second step, at 270 °C and short residence time of 2.75 min, led to a significantly higher extent of hydrolysis.

No specific studies have been found on semi-continuous subW extraction of proteins from okara. Available literature about protein recovery from okara focuses on batch systems (Wiboonsirikul *et al*., 2013).

The residual solid resulting from this comprehensive treatment exhibited a significant reduction in mass, constituting only 12.8 % of the initial OK-2. This process led to a marked solubilization of the majority of organic components, being acid-insoluble lignin the wide majority of the remaining solid (Table 5.1). Saccharides in the residual solid decreased from 29 ± 2 % in OK-2 to 3.1 ± 0.2 %, and proteins from 32.8 ± 0.6 % to 10.5 ± 0.4 %. Conversely, acid-insoluble lignin emerged as the predominant fraction in the residue, increasing from 25.6 ± 0.3 % to

81 ± 2 %, indicating the effective removal of most non-lignin compounds and the concentration of recalcitrant lignin.

These compositional changes are also evident in the molar elemental ratios of the solids. The N:C ratio decreased from 0.11 to 0.03, confirming the substantial removal of nitrogenous compounds, due to hydrolysis of proteins and peptides. A decrease was also observed in the O:C ratio, from 0.37 to 0.22, and in the H:C ratio, from 1.89 to 1.64, due to an increase in the C content of this residue. These reductions suggest that, in addition to nitrogen loss, the process induced partial dehydration and deoxygenation reactions (associated with a decrease in the amount of OH, carboxyl (COOH), and carbonyl (C=O) groups as reported by Alonso-Riaño *et al.* (2021), which are consistent with the thermal degradation and condensation of saccharide structures and the enrichment of lignin. This confirms that the solid residue remaining after high-temperature treatment is predominantly a carbon-rich, low-polarity matrix, mainly consisting of condensed lignin structures, containing negligible amounts of hydrophilic compounds like saccharides and proteins.

3.4.2. Amino acid profile assessment

Free amino acids were quantified in each collected sample from the semi-continuous process to evaluate the degree of protein breakdown into individual amino acids across the two intervals, 180 and 270 °C.

First interval of the treatment at 180 °C accumulated a total of 358.6 mg of free amino acids which corresponds to a 1.7 % of the initial amino acid content which represents 60 mg of free amino acid per g of protein extracted. The distribution of individual free amino acids accumulated during this interval is shown in Figure 5.6a. There is a remarkably high proportion of glutamic acid (42.3 %) in the extract, followed by aspartic acid (16.2 %), consistent with previous batch results at the same temperature. Among the essential amino acids (EAAs), valine and methionine showed the proportion in the extraction, 11.3 % and 10.1 %, respectively.

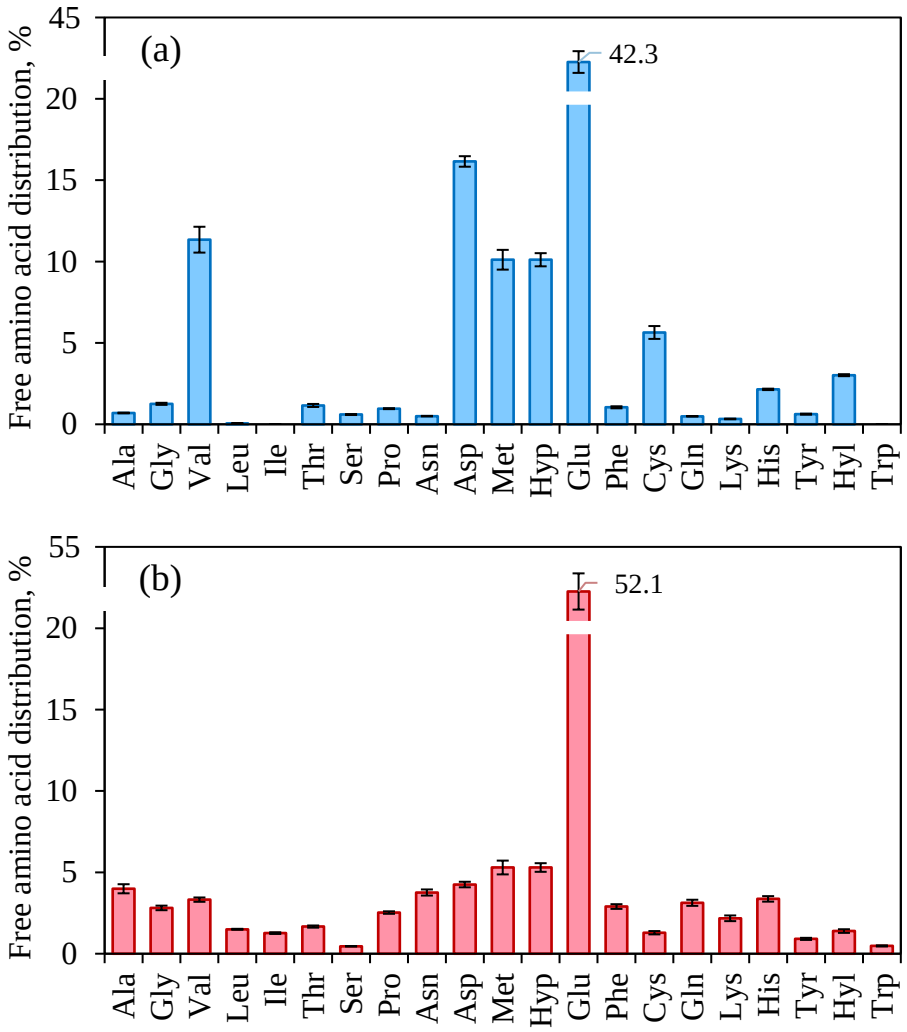

Figure 5.6. Free amino acid distribution (%) respect the total amino acids extracted by semi-continuous SWH. **(a)** First interval at 180 °C (■). **(b)** Second interval at 270 °C (■).

In the second interval the solid in the reactor was further summited to 270 °C. Considering only this interval, 2080.2 mg of free amino acids were accumulated, 5.8 times higher than during the first interval. These results correspond with 11.1 % of the total initial amino acid content in the biomass charged into the extractor, 121.7 mg of free amino acid per g of protein (17.1 g of protein were extracted in this interval). The individual free amino acid distribution in the extract after the second

interval is represented in the Figure 5.6b. The dominance of glutamic acid was also very pronounced (52.1 %), but it showed a wider distribution in the presence of free amino acids compared to the first interval at 180 °C. The following most abundant amino acids were methionine and hydroxyproline, both with 5.3 %, almost 10 times lower than glutamic acid.

The full process yielded 2438.8 mg of free amino acids, corresponding to 13.0 % of the total amino acids introduced, 105.7 mg per gram of extracted protein (23.1 g considering the full process). Remarkably greater results were observed during the second interval.

Figure 5.7 shows the hydrolysis yield (calculated as defined in section 2.3.6) for each individual free amino acid after both intervals.

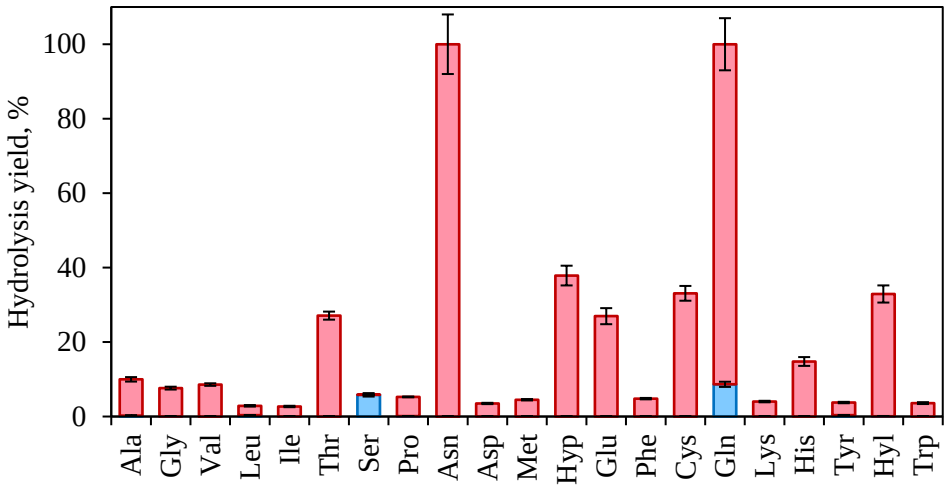

Figure 5.7. Hydrolysis yield (%) of each amino acid after two intervals of semi-continuous SWH extraction from OK-2, represented in blue (■) 180 °C first interval and in red (■) 270 °C second interval.

Asparagine and glutamine reached 100 %, likely due to their conversion into aspartic acid and glutamic acid via deamidation during hydrolysis. Although this may lead to misinterpretation in the quantification of certain hydrolysates, it is not considered a significant issue in this case, as both asparagine and glutamine are

among the least abundant amino acids in the original biomass; their likely measurement as their corresponding acids, far more prevalent, would not meaningfully affect any other results.

Aside from these, hydroxyproline (37.9 %), cysteine (33.1 %), and hydroxylysine (32.9 %) showed the highest yields, followed by threonine (27.1 %) and glutamic acid (27.0 %).

3.4.3. Comparison of batch and semi-continuous results

Total accumulated protein productivity of semi-continuous process resulted 34.7 g protein/h. This value was higher than the one obtained in the experiment in the batch reactor, 0.84 g/h more than 40 times higher. However, when considering the total water volume of both processes under the experimental conditions tested in this work, the semi-continuous system resulted in much more diluted extracts. The final concentration in the batch configuration was 12.6 g/L. This value was much higher than the highest value determined at 270 °C in the 12th collected samples, 2.3 g/L, (Figure 5.5a).

The yield of free amino acids was lower in the semicontinuous configuration compared with the free amino acid yield obtained in the batch reactor. For a better comparison in terms of time and temperature applied to each process, the severity factors of the different processes were listed in Table 5.3. The severity factor for the batch process was 4.61, while two different severity factors were evaluated for the semi-continuous process considering the two different temperature intervals: log R_0 = 2.79 at 180 °C and log R_0 = 5.44 at 270 °C.

The lower severity factor at 180 °C applied in the semicontinuous configuration can explain the difference between the free amino acid released in both configurations at the same temperature. The severity factor for this 270 °C second interval was 5.44, higher than the one evaluated in the batch reactor. This could lead to partial free amino acid degradation in the medium, specially of the most thermal

sensitive amino acids. Moreover, the medium free amino acid concentration extracted in the semi-continuous reactor just in the second interval at 270 °C was 0.149 g/L, considering the accumulated free amino acid and the volume extracted. Prior results from OK-2 in the batch reactor showed a free amino acid concentration of 1.8 g/L, 12 times higher.

The overall distribution differs from that of the batch reactor, where glutamic acid was also dominant, but higher levels of aspartic acid and EAA such as lysine, phenylalanine, valine, leucine, and isoleucine were recovered when using batch configuration.

The high concentration of glutamic acid as free amino acid must be highlighted for all the experiments, despite its reported thermolability. Glutamic acid, along with cysteine, is among the most thermolabile amino acids, in contrast to glycine and valine, which are the most thermally resistant. Glutamic acid lactamization into pyroglutamic acid (PGA) occurs at 230, 260 and 290 °C from 1 min under subW conditions and being stable for, at least, 20 min (Abdelmoez *et al*., 2010). PGA could be being detected as the real amino acid, although this has not been confirmed nor measured in the present study. That potential transformation may open up alternative valorization pathways, as it has shown cosmetic and pharmacological applications and as an intermediate in peptide and pharmaceutical synthesis (de Mello *et al*., 1995), although its presence was not directly identified.

3.5. Structural saccharides hydrolysis

Saccharide fraction corresponds to 29 ± 2 % in OK-2 on a dry basis. Most abundant structural sugars on OK-2 are glucans, with 15.9 ± 0.7 % (w/w) of total biomass followed by galactans, 6.2 ± 0.3 % (w/w) (Table 5.1).

Saccharide fraction hydrolysis was assessed by the degree of hydrolysis determined by quantifying the total free and structural sugars dissolved in each hydrolysate considering original values of each biomass.

Figure 5.8 shows the degree of hydrolysis achieved for each of the four determined sugars for both subW configurations, in their respective final extracts, referring to the free sugars on solution as "monomer" (Eq. 5.2) and for the ones being part of a more complex saccharide in solution as "oligomer" (Eq. 5.3).

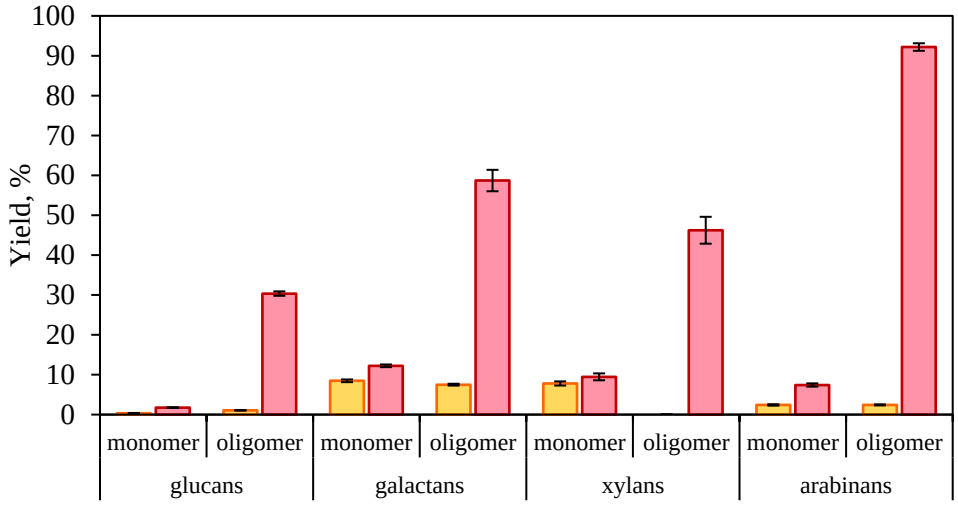

Figure 5.8. Degree of hydrolysis (%) of each structural sugar (glucans, galactans, xylans and arabinans) after subW treatments. Batch SWH (180 min at 180 °C), ; semi-continuous SWH (including 23 min at 180 °C and 17 min at 270 °C), .

Batch subW resulted in 0.14 g of total sugar release, from the total 2.46 g in the initial material charged into the reactor, yielding a 5.7 % degree of hydrolysis. In the case of semi-continuous subW, the degree of hydrolysis reached 48.6 % (extracting 12.6 g from the initial 25.9 g material charged into the baskets), corresponding to an 8.5 times higher degree of hydrolysis compared to batch configuration. This can be attributed to the higher severity factor (Table 5.3), of the second interval in the semicontinuous configuration at 270 °C, 5.44, while this value was 4.61 in case of batch system after 180 minutes.

The present data challenge some finding in the existing literature on okara treatment by subW (Sun *et al*., 2018; Wiboonsirikul *et al*., 2013). Sun *et al*. (2018) asserted that subW treatment at temperatures ranging from 160–230 °C for 10 min

results in decreased carbohydrate extraction as the temperature increases. Similarly, Wiboonsirikul *et al*. (2013), reported a reduction in carbohydrate content in the okara subW hydrolysates with increasing temperature and treatment time, having studied temperatures in the range of 170–260 °C for periods of 2–120 min.

Regarding the degree of hydrolysis of individual sugars (Figure 5.8), it is noteworthy that the extraction performed under the semi-continuous subW configuration yielded substantially higher amounts of sugars compared to the batch mode, likely due to the higher temperatures applied. The extraction was enhanced for both monomeric and oligomeric sugars; however, the difference was particularly pronounced in the case of oligomers, which were predominant over monomers in the semi-continuous configuration. This suggests that polysaccharides underwent partial hydrolysis without complete depolymerization into monomeric sugars, despite the severity of the treatment conditions.

In the batch configuration, the relation of monomers and oligomers was barely similar, representing the monomers a 51.9 % of the sugars extracted (and 48.1 % the oligomers). Among the polysaccharides, galactans exhibited the highest degree of hydrolysis (16.0 %), accounting for 69.2 % of the total sugars in solution (50.2 mg monomeric galactose and 44.5 mg oligomeric galactans the total 137 mg of sugars recovered). Xylans and arabinans followed, with hydrolysis of 7.8 % and 4.8 %, respectively, while glucans showed a limited 1.4 %.

In the semi-continuous SWH system, after both thermal intervals, the proportion of monomeric sugars only reached 10.7 %. Galactans again displayed the highest conversion rate, followed by xylans and arabinans, with values of 12.2 %, 9.5 %, and 7.4 %, respectively, while glucans remained the least hydrolyzed (1.7 %). Oligomers constituted the dominant fraction (89.3 %) of the dissolved sugars. Among these, galactans and glucans were the most abundant, accounting for 58.7 % and 30.3 %, respectively, with glucans being the most prevalent in solution (38.3 %) despite not presenting the highest yield.

Overall, these results indicate that treatment at 270 °C for a short residence time (severity factor = 5.44; Table 5.3) not only does not hinder carbohydrate extraction (as reported in some previous studies) but instead enhances it, particularly when compared with the milder batch configuration.

4. Conclusions

Subcritical water hydrolysis as a green and novel process provides a great protein extraction from okara, yielding high protein recovery and free and bound amino acid profiles. subW treatment in batch configuration (180 °C for 3h) extracted 81 % of the total amino acids in OK-2, with a purity of 28.2 %. Comparing results with non-treated okara (OK-1), pre-extracted okara (OK-2) showed higher amount of extracted protein.

Semi-continuous SWH showed much higher extraction at 270 °C in the second interval than at 180 °C in the first one. However, batch configuration resulted in better protein concentration results (12.6 over 1.22 g/L), free amino acid hydrolysis (20 over 10 %) and overall productivity (1.8 over 0.149 g/L) and hydrolysis yield (81 over 70.4 %). Remarkably, short-time treatment at 270 °C enhanced the release of structural sugars, especially in oligomeric form, which contradicts some previous literature works.

Overall, this work supports a two-step green valorization of okara, maximizing its potential as a source of free amino acids and bioactive peptides under SWH conditions, especially in the batch configuration.

CHAPTER 6

Protein recovery from okara by reduced-pressure alkaline pre-treatment: Optimization and techno-economic assessment

Adapted from:

P. Barea, S.S. Queiroz, C. Cabrera, B. Ruengsrichaiya, M.T. Sanz, S.I. Mussatto

"Protein recovery from okara by reduced-pressure alkaline pre-treatment: Optimization and techno-economic assessment"

Manuscript in preparation

Capítulo 6

Recuperación de proteínas de okara mediante pretratamiento alcalino a presión reducida: optimización y evaluación tecno-económica

Resumen

Este estudio evalúa la optimización y la escalabilidad industrial del pretratamiento alcalino a presión reducida (RPAP) para la extracción de proteínas de okara, un subproducto de alto valor generado durante la producción de leche de soja y tofu. Se analizó la influencia de la concentración de NaOH (20–180 mM), la presión de vacío (30,0–101,3 kPa) y el tiempo de extracción (5–120 min) sobre el rendimiento proteico y la selectividad hacia los carbohidratos. Los mayores valores de recuperación de proteínas (~90 %) y selectividad (~90 %) se obtuvieron bajo dos condiciones óptimas: (A) 45,5 kPa y 180 mM de NaOH por 60 min, y (B) 30,0 kPa y 100 mM de NaOH durante 120 min. Ambos procesos superaron en eficiencia a la extracción alcalina convencional y a otros métodos de referencia.

Se realizó una evaluación tecno-económica (TEA) a escala industrial mediante simulación en Aspen Plus®, considerando una capacidad anual de procesamiento de 7700 t de okara húmeda. Aunque el proceso A alcanzó una extracción óptima en menor tiempo, su elevado consumo de álcali incrementó significativamente los costos operativos. En cambio, el proceso B, más largo, pero con menor uso de reactivos, resultó un 20 % más rentable anualmente sin afectar la productividad, gracias a la operación continua en tres reactores. En conjunto, el proceso B se perfila como la opción más adecuada para la extracción de proteínas de okara a gran escala mediante RPAP, combinando menor gasto químico y económico.

Palabras clave: Pretratamiento alcalino a presión reducida, evaluación tecno-económica, okara, proteína, valorización de subproductos.

Chapter 6

Protein recovery from okara by reduced-pressure alkaline pre-treatment: Optimization and techno-economic assessment

Abstract

This study evaluates the optimization and industrial scalability of reduced-pressure alkaline pre-treatment (RPAP) for protein extraction from okara, a high-value by-product generated during the production of soy milk and tofu. The effects of NaOH concentration (20–180 mM), vacuum pressure (30.0–101.3 kPa), and extraction time (5–120 min) were analyzed in relation to protein yield and selectivity toward carbohydrates. The highest protein recovery (~90 %) and selectivity (~90 %) were achieved under two optimal conditions: (A) 45.5 kPa and 180 mM NaOH for 60 min, and (B) 30.0 kPa and 100 mM NaOH for 120 min. Both processes outperformed conventional alkaline extraction and other benchmark methods in terms of efficiency.

Based on both optimized conditions, a techno-economic assessment (TEA) was carried out at an industrial scale using Aspen Plus® simulation, considering an annual processing capacity of 7700 t of wet okara. Although process A achieved optimal extraction in a shorter time, its high alkali consumption significantly increased operating costs. In contrast, process B (longer but with lower reagent usage) proved to be 20 % more cost-effective annually without compromising productivity, owing to continuous batch operation using three reactors. Overall, process B emerges as the most suitable configuration for large-scale okara protein extraction via RPAP, combining reduced chemical input with improved economic performance.

Key words: Reduced-pressure alkaline pre-treatment, Tecno-economic assessment, okara, protein, by-product valorization.

1. Introduction

Okara, an insoluble by-product generated during the processing of soybeans for soymilk and tofu production, represents a significantly underutilized biomass rich in proteins, fiber, isoflavones, and other bioactive compounds (Chang & Liu, 2012; Mok *et al*., 2019). Each kilogram of dry soybeans utilized in the elaboration of soymilk or tofu yields approximately 1.1 kg of wet okara. Global soybean production in 2025 is projected to reach 423 million tonnes (Mt), with approximately 4.7 % allocated to tofu and soymilk production. This is anticipated to result in the generation of approximately 22 Mt of okara worldwide by 2025 (Barea, Illera, Melgosa, *et al*., 2025; FAO, 2025b; Ritchie *et al*., 2025). Despite its high protein content (approximately 25–28 % dry mass) and excellent amino acid profile, the high moisture content of okara (commonly around 80 %) and its rapid spoilage present challenges for valorization, and in most cases forces it to be discarded (O'Toole, 1999; Vong & Liu, 2016).

Traditional protein extraction from okara typically employs alkaline methods at elevated temperatures, often exceeding 100 °C. These conventional alkaline extractions necessitate high alkali concentrations and extended processing times, raising concerns regarding chemical consumption, environmental impact, protein quality degradation, and loss of functional properties. The process is further complex due to the substantial chemical usage, which do not meet sustainability requirements, and the high energy requirements for heating to temperatures above boiling point in industrial settings for large-scale biomass treatment. Additionally, the co-extraction of carbohydrates reduces hydrolysate purity, thereby compromising downstream applications (da Fonseca *et al*., 2023; Eze, 2019; Freitas *et al*., 2019; Tang *et al*., 2024).

Reduced-pressure alkaline pre-treatment (RPAP) offers a sustainable alternative by combining vacuum pressure with alkaline extraction under milder conditions (lower temperatures and notably reduced chemical use), thereby

decreasing energy consumption, minimizing oxygen exposure, and enhancing selectivity by limiting sugar co-extraction (da Fonseca *et al*., 2023). Conducted using a rotary evaporator under vacuum, RPAP improves protein purity and preserves larger peptides, which are critical for food formulations requiring texture and stability (Cunha & Pintado, 2022; da Fonseca *et al*., 2023; Wouters *et al*., 2016). While the RPAP process remains to utilize NaOH, optimizing the process to reduce alkali usage, as well as adjusting time and pressure, can enhance sustainability and scalability, thereby decreasing the carbon footprint and operational costs (da Fonseca *et al*., 2023).

In light of these challenges and opportunities, this study examines RPAP extraction conditions, including vacuum pressure, NaOH concentration, and time, to optimize protein yield and selectivity from okara while minimizing chemical inputs. Furthermore, a techno-economic assessment (TEA) at an industrial scale complements the experimental work, identifying viable operational parameters that balance technical performance with economic viability.

Techno-economic assessment (TEA) is a crucial methodology employed to evaluate the economic viability and technical performance of industrial processes by integrating process simulation data with detailed cost analyses (Cabrera Camacho *et al*., 2020; Koutinas *et al*., 2016). TEA typically involves estimating capital costs, operating expenses, and potential revenues, and enabling the identification of cost parameters that could influence process profitability and scalability (Mailaram *et al*., 2022). This approach facilitates the analysis of variables, design optimization, and investment decisions. By employing TEA, researchers and industry can compare process alternatives, predict return on investment, and evaluate sustainability at early development stages, connecting the gap between laboratory findings and industrial applications (Cabrera Camacho *et al*., 2020; Mailaram *et al*., 2022).

In the context of by-product valorization, such as protein extraction from okara, TEA ensures that proposed technologies achieve efficiency, economic viability, and

sustainability, particularly in the present work, by comparing processes to determine which should be scaled-up for industrial application.

2. Experimental

2.1. Raw material

The okara provided by *Frías Nutrición* S.A.U. (Burgos, Spain) exhibits a moisture content of 82.5 ± 0.1 % (w/w), consistent with reports of its high-water content and susceptibility to spoilage due to rapid microbial growth. On a dry matter basis, this by-product contains 32 ± 4 % saccharides, 26.9 ± 0.5 % protein, 9.5 ± 0.4 % lipids, and 16 ± 1 % lignin, with a nearly equal distribution of soluble (8 ± 1 %) and insoluble (8.3 ± 0.4 %) fractions (see Table 5.1, Chapter 5). These values confirm okara potential as a nutrient-rich substrate for valorization and protein extraction applications.

2.2. Reduced-pressure alkaline pre-treatment (RPAP)

Reduced-pressure alkaline pre-treatment (RPAP) or alkaline extraction under reduced pressure, is a process based on treating biomass with NaOH under vacuum conditions in a rotary evaporator. The combination of alkaline medium, reduced pressure and mild temperatures promotes the solubilization of proteins by breaking protein-matrix interactions, while limiting carbohydrate release. This makes RPAP particularly suitable for selectively extracting proteins from okara yielding hydrolysates with minimal carbohydrate contamination.

Okara was subjected to RPAP using a rotary evaporator (IKA RV 10 control, Germany). In each experiment, 24 g of dry biomass (around 132 g of wet okara) were mixed with an aqueous NaOH solution to reach 480 mL considering the humidity already present in okara, obtaining a 5 % dry okara solution. The treatment was carried out at 70 °C in a 1000 mL round-bottom flask, stirring at 100 rpm and under specific alkali concentration, time, and vacuum pressure conditions, ranging

from 20–180 mM, 5–120 min, and 30.0–45.5 kPa, respectively. After pre-treatment, it was centrifuged at 10000 rpm for 20 min using 50 mL tubes in a Thermo Scientific Multifuge X3R. The liquid fraction was neutralized with 2 M HCl to a pH range of 6–7 and subsequently collected for the analysis of protein and total carbohydrates. The solid fraction was washed with deionized water, neutralized with 2 M HCl to neutral pH, and dried at 50 °C for 24 h.

2.3. Analysis

2.3.1. Total protein

Total protein concentration was determined using the Bradford assay following the 96-well plate protocol. Protein standards of bovine serum albumin (BSA) were prepared in buffer at concentrations ranging from 0.1 to 1.4 mg/mL. For the assay, 5 μL of each standard, blank (buffer only), or unknown sample was pipetted into individual wells of a 96-well microplate. Subsequently, 250 μL of Bradford Reagent was added to each well, and the plate was mixed on a shaker for approximately 30 s. The samples were incubated at room temperature for 5 minutes, and their absorbance was measured at 595 nm using a microplate reader (Sigma-Aldrich, 2021). The protein concentration of unknown samples was calculated by interpolating their net absorbance values from the standard curve, reporting the results as mg per mL of extract.

Furthermore, yield and selectivity of protein were also calculated. Yield of protein (Eq. 6.1) extraction was calculated in relation to the initial total protein present in okara. Protein selectivity (Eq. 6.2) was determined to evaluate the quality of the obtained protein hydrolysate in relation to the total solubilized compounds. Since RPAP theoretically does not promote carbohydrate solubilization, this parameter helps to assess the quality of the hydrolysate by considering the minimal release of non-protein compounds, particularly sugars, providing an indicator of how efficient is the protein extraction method.

$$\text{Yield (\%)} = \left(\frac{\text{Protein } \left({}^{g}/_{L}\right) \times \text{Extracted volume (L)}}{\text{Initial protein (g)}}\right) \times 100 \qquad \textbf{[6.1]}$$

$$\text{Selectivity (\%)} = \left(\frac{\text{Protein } \left({}^{g}/_{L}\right)}{\text{Protein } \left({}^{g}/_{L}\right) + \text{Carbohydrates } \left({}^{g}/_{L}\right)}\right) \times 100 \qquad \textbf{[6.2]}$$

2.3.2. Total carbohydrates

Total carbohydrates were quantified by the Anthrone assay developed by the BCBT group (DTU, Denmark) based on previously described methodologies (Ballesteros *et al.*, 2017; Tiwari, 2015). A stock solution of glucose (300 µg/mL) was prepared in deionized water and used to generate calibration standards ranging from 10 to 300 µg/mL. The Anthrone-Sulfuric acid reagent was freshly prepared by dissolving 0.01 g of Anthrone in 10 mL of concentrated sulfuric acid (95–98 %) and protected from light. For the assay, 50 µL of standards, samples, or blanks were pipetted into a 96-well plate and mixed with 150 µL of Anthrone-Sulfuric acid reagent. The plate was cooled at 4 °C for 10 min, incubated at 100 °C and 500 rpm for 20 min, and then cooled to room temperature for 20 min. Absorbance was measured at 620 nm using a microplate reader. Carbohydrate concentrations were determined by interpolation from the glucose standard curve and expressed as glucose equivalents, reporting the results as mg per mL of extract.

2.4. Statistical analysis

All the samples were produced in duplicate and analyzed at least three times each, and expressed as mean ± standard deviation of the replicates. Data was analyzed using the software Statgraphics19 X64, the significance of the differences between samples results was determined based on an analysis of the variance with the Fisher's Least Significant Difference (LSD test) at p-value ≤ 0.05.

2.5. Techno-Economical Assessment

Techno-economical-assessment (TEA) is a methodology that integrates process modelling and economic analysis to evaluate the technical viability, costs, and profitability of industrial processes. It estimates capital and operating costs, identifies key parameters influencing performance, and supports decision-making by quantifying economic viability, risks, and potential improvements. In this work TEA was used with the aim of helping to opt to the most profitable process to extract proteins from okara by using RPAP, after having determined different experiments with comparable great results of extraction and selectivity. The application used to carry out this assessment was Aspen Plus®.

The industrial prices of drinking water (0.113 €/t) and electricity (0.191 €/kWh) used were recovered from Spain as the process is supposed to be carried out there (*CNMC*, 2025). HCl (217 €/t) and NaOH (233 €/t) industrial prices used were recovered from European data, from April 2025 (van Breugel, 2025a, 2025b).

Almost all the equipment were obtained from Aspen Plus® database while generating the flowchart, with the exception of the reactor for the extraction and the filter to separate liquid and solid after the process, which were needed to be more specifical to fit the correct scale-up of the system without over-increasing the overall cost. The prices were corrected by using the CEPCI cost index to adapt previous prices to the inflation using 2024 data (University of Manchester, 2024).

Reactor for extraction chosen from Humbird *et al*. (2011) was F-303 (3rd Seed Fermentor, 2000-gallon skid complete, SS304), with a total cost of 104913€ per unit, adapted to 2024 prices. The filter chosen was S-505 Pressure Filter Larox, 384 m^2 filtration area, SS316 (Humbird *et al*., 2011); after a size correction, based on (Mailaram *et al*., 2022), the cost of the filter reached 310801 €, adapted to 2024 prices.

Once a reactor with a correct volume and outcome flux has been chosen, loading times (τ_{ul}) can be calculated as the outcome flux divided by the total volume of the reactor. As reported by Koutinas *et al*. (2016), this τ_{ul} corresponds to the reactor uploading time. In most cases, the downloading time (τ_{dl}) is approximately the same and can be considered equal. Knowing the upload, download, and treatment time (τ_t), the required number of reactor units (N_F) of known dimensions can be calculated using Eq. 6.3. When the resulting number of reactor units is not an integer, it must always be rounded up to the next whole number to ensure that the system can handle the total flow.

$$\text{Reactor units} = N_F = \left(\frac{\tau_{ul} + \tau_{dl} + \tau_t}{\tau_{ul}}\right) \quad \textbf{[6.3]}$$

Total annual cost (TAC) is a very useful value when assessing cost of a new process. It includes the cost of the assembling of the system per year plus the operating cost of the whole process in that year. Commonly, 3 years are considered to payback the equipment/system, in which the year cost of the process is the one calculated as shown in Eq. 6.4. After that payback period of three years, the cost of the process only considers the operating cost, assuming the recovery of the cost of assembling the machinery for the entire process in previous years.

$$\text{TAC} = \left(\frac{\text{Capital cost}}{\text{Payback period}}\right) + \text{Operating cost} \quad \textbf{[6.4]}$$

Additionally, *Frías Nutrición* reports that the disposal cost of their okara side stream typically ranges from 20–40 €/t of okara, which would correspond to approximately 150000–300000 €/year considering 7700 t of okara production in 2025. This amount will not be considered on the TEA tables in the results, setting the okara feedstock at 0 €.

3. Results

3.1. Protein extraction and selectivity

For the optimization of RPAP methodology in terms of protein extraction from okara the first trials were carried out in the conditions shown in Table 6.1. Time and temperature were fixed to 60 min and 70 °C, respectively, based on optimal results from da Fonseca *et al*. (2023), who obtained the best results of protein extraction from BSG (brewer's spent grain) when using 180 mM NaOH, 45.5 kPa (at 70 °C for 60 min).

Table 6.1. Effect of pressure, and NaOH concentration on protein extraction from 5 % okara at 70 °C for 60 min: protein concentration, yield, carbohydrate concentration, and selectivity.

P, kPa	NaOH, mM	Protein, mg/mL	Yield, %	Carbohydrates, mg/mL	Selectivity, %
45.5	20	0.57 ± 0.04^{a}	3.3 ± 0.4^{a}	0.57 ± 0.01^{a}	50 ± 2^{a}
	60	4.5 ± 0.2^{b}	27 ± 2^{c}	1.5 ± 0.1^{bc}	75 ± 2^{c}
	100	11.4 ± 0.9^{e}	67 ± 5^{g}	1.42 ± 0.09^{bc}	89 ± 1^{ef}
	140	13.8 ± 0.5^{f}	81 ± 3^{hi}	1.4 ± 0.1^{bc}	90.7 ± 0.7^{f}
	180	15.5 ± 0.7^{g}	91 ± 3^{j}	1.58 ± 0.08^{c}	90.8 ± 0.6^{f}
30.0	20	1.6 ± 0.1^{a}	9 ± 1^{b}	0.62 ± 0.05^{a}	72 ± 2^{b}
	60	6.9 ± 0.3^{c}	41 ± 2^{e}	1.3 ± 0.1^{b}	84 ± 1^{d}
	100	14.1 ± 0.2^{f}	83 ± 1^{i}	1.3 ± 0.1^{b}	91.3 ± 0.6^{f}
	140	14.2 ± 0.2^{f}	83 ± 1^{i}	1.4 ± 0.1^{bc}	91.0 ± 0.6^{f}
	180	13.8 ± 0.5^{f}	81 ± 2^{hi}	1.50 ± 0.09^{bc}	90.2 ± 0.6^{f}
101.3	100	6.1 ± 0.3^{c}	36 ± 2^{d}	1.4 ± 0.2^{bc}	82 ± 2^{d}
	140	9.3 ± 0.6^{d}	55 ± 4^{f}	1.4 ± 0.2^{bc}	87 ± 2^{e}
	180	13.3 ± 0.5^{f}	78 ± 3^{hi}	1.5 ± 0.2^{bc}	90 ± 1^{f}

Values with different letters (a, j) in each column are significantly different when applying the LSD method at p-value ≤ 0.05.

In this study, the optimal conditions determined by da Fonseca *et al*. (2023) were initially tested (180 mM and 45.5 kPa), but experiments were extended to other

conditions: NaOH concentrations of 20, 60, 100 and 140 mM were tested at the same pressure, in order to assess if less alkaline medium presented similar efficiency as 180 mM NaOH. In the same way, trying to enhance protein extraction or to reduce the NaOH needed, the same five concentrations were also tested at 30.0 kPa (minimum pressure near saturation conditions at the working temperature). The most effective concentrations were also tested at atmospheric pressure (101.3 kPa), as in the conventional alkaline extraction method, in order to assure that the vacuum was enhancing the extraction process. Protein yield was calculated based on Eq. 6.1, (being protein concentration in raw okara 26.9 ± 0.5 %), and protein selectivity as shown in Eq. 6.2.

The data presented in Table 6.1 indicate that the highest protein concentration (15.5 ± 0.7 mg/mL) was achieved under conditions identical to those reported by da Fonseca *et al.* (2023): 45.5 kPa and 180 mM (on BSG in their study), with a temperature of 70 °C for 60 minutes. The present protein concentration results correspond to a notably high protein yield and selectivity of 91 ± 3 % and 90.8 ± 0.6 %, respectively, noticeably higher than the 80 % recovery and 76.8 % selectivity reported for BSG by these authors.

Comparable selectivity was observed in other extractions conducted at 45.5 kPa with 140 mM NaOH, 30.0 kPa with 180, 140, and 100 mM NaOH, and atmospheric pressure with 180 mM NaOH (Table 6.1). These extractions also demonstrated good protein concentration, still below the optimal result. Notably, only one of those extractions utilized 100 mM NaOH (at 30.0 kPa), a low NaOH concentration, yet achieved high protein extraction and selectivity (14.1 ± 0.2 mg/mL and 91.3 ± 0.6 %, respectively). This method also extracted significantly fewer carbohydrates compared to the extraction at 45.5 kPa and 180 mM NaOH, unlike the other high extractions mentioned, which were significantly similar to both. The rest of the results obtained with 100 mM or lower concentrations of NaOH were markedly inferior in both protein recovery yield and selectivity.

Given the importance of maximizing protein extraction while minimizing NaOH usage, further testing was conducted around the conditions of 45.5 kPa – 180 mM NaOH and 30.0 kPa – 100 mM NaOH to determine if higher protein yield or purity could be achieved. Table 6.2 separately presents four different conditions related to these values, each sampled from 5 to 120 minutes, to establish the optimal extraction time over a wider range. The combinations of vacuum pressures and NaOH concentrations were: 45.5 kPa and 100 mM NaOH (Table 6.2.A); 30.0 kPa and 100 mM NaOH (Table 6.2.B); 45.5 kPa and 180 mM NaOH (Table 6.2.C); 30.0 kPa and 180 mM NaOH (Table 6.2.D).

As shown in Table 6.2, protein recovery and selectivity varied depending on the operating conditions. Under 45.5 kPa and 100 mM NaOH (experiment A), the highest protein concentration (14.4 ± 0.1 mg/mL, 85 ± 1 % recovery) was reached after 120 min, together with one of the best selectivity values (88.7 ± 0.6 %). In experiment B (30.0 kPa and same NaOH concentration, 100 mM), the maximum protein concentration (15.2 ± 0.1 mg/mL, 89 ± 1 % recovery) was also obtained at 120 min, showing higher protein recovery and selectivity (89.6 ± 0.4 %).

When NaOH concentration was increased to 180 mM (experiments C and D, Table 6.2), the extraction became more efficient at shorter times. In experiment C (45.5 kPa), excellent performance was achieved at both 60 and 120 min; however, the 60 min extract was selected as the most suitable, combining high protein concentration (15.1 ± 0.9 mg/mL, 89 ± 5 % recovery) with a great selectivity value (90.1 ± 0.8 %). Under 30.0 kPa (experiment D), the highest values of protein recovery and selectivity were lower than those obtained previously (at 60 min: 14 ± 1 mg/mL, 82 ± 8 % recovery, and 90 ± 1 % selectivity).

Figure 6.1 shows protein and carbohydrate concentrations during the four kinetic assays presented in Table 6.2. Protein extraction increased markedly under all conditions, rising from 4–6 mg/mL at 5 min to 12–15 mg/mL at 60 min, and reaching 14–15 mg/mL at 120 min (almost a three-fold increase in some cases). In

contrast, carbohydrate concentrations only presented a slightly increase, from ~1 mg/mL at 5 min to 1.5–1.7 mg/mL at 60 min, and 1.7–1.8 mg/mL at 120 min, not even coming close to doubling its value. These results highlight the strong capacity of RPAP to selectively extract proteins while limiting carbohydrate release, thereby achieving very high selectivity values under all tested conditions.

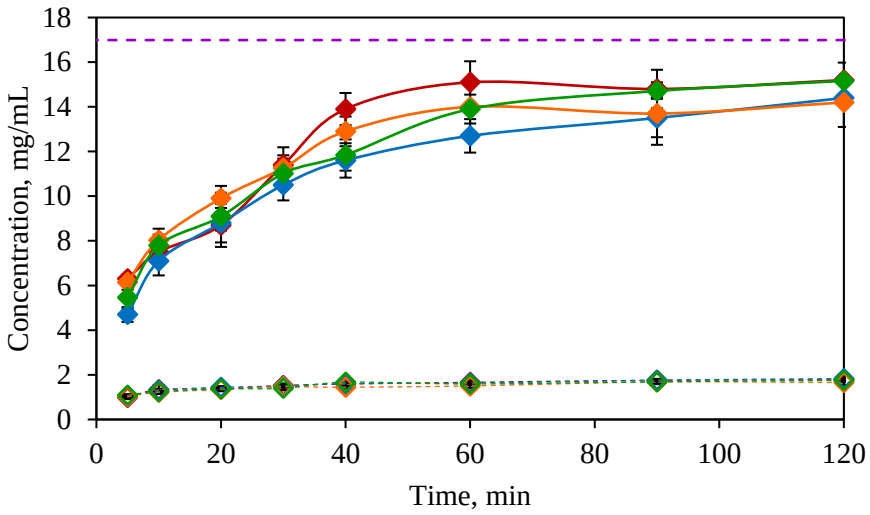

Figure 6.1. Protein (◆) and carbohydrate (◇) concentration (mg/mL) as a function of time. Vacuum pressure and NaOH concentration, respectively: 45.5 kPa and 100 mM, ◆ ◇; 30.0 kPa and 100 mM, ◆ ◇; 45.5 kPa and 180 mM, ◆ ◇; 30.0 kPa and 180 mM, ◆ ◇; maximum protein value, - -. Lines are drawn to guide the eye.

Figure 6.2 shows the protein extraction yields from Table 6.2 as a function of time, facilitating the identification of the conditions that resulted in the highest extraction efficiencies. The best-performing conditions in Table 6.2 were 45.5 kPa with 180 mM NaOH at 60 minutes, matching the optimal conditions previously reported in Table 6.1 (89 ± 4 % in Table 6.2 versus 91 ± 3 % in Table 6.1; the average of both values was used in the subsequent analysis), and 30.0 kPa with 100 mM NaOH at 120 minutes, which improved upon the corresponding result in Table 6.1 by extending the extraction time (yield increased from 83 ± 1 % to 89 ± 1 %).

Table 6.2. Effect of time, pressure, and NaOH concentration on protein extraction from 5 % okara at 70 °C: protein concentration, yield, carbohydrate concentration, and selectivity. **A:** 45.5 kPa, 100 mM NaOH. **B:** 30.0 kPa, 100 mM NaOH. **C:** 45.5 kPa, 180 mM NaOH. **D:** 30.0 kPa, 180 mM NaOH.

	Time, min	Pressure, kPa	[NaOH], mM	Protein, mg/mL	Yield, %	Carbohydrates, mg/mL	Selectivity, %
A	**5**	**45.5**	**100**	4.7 ± 0.3^{a}	28 ± 2^{a}	1.03 ± 0.08^{a}	82 ± 2^{a}
	10			7.1 ± 0.7^{b}	42 ± 3^{b}	1.31 ± 0.07^{b}	84 ± 1^{b}
	20			8.8 ± 0.3^{c}	52 ± 2^{c}	1.44 ± 0.04^{c}	85.9 ± 0.6^{c}
	30			10.5 ± 0.7^{d}	62 ± 3^{d}	1.5 ± 0.1^{cd}	88 ± 1^{d}
	40			11.6 ± 0.8^{e}	68 ± 4^{e}	1.60 ± 0.08^{de}	88 ± 1^{d}
	60			12.7 ± 0.8^{f}	75 ± 4^{f}	1.63 ± 0.06^{e}	88.6 ± 0.7^{d}
	90			13.5 ± 0.9^{f}	79 ± 4^{f}	1.76 ± 0.06^{f}	88 ± 1^{d}
	120			14.4 ± 0.1^{g}	85 ± 1^{g}	1.8 ± 0.1^{f}	88.7 ± 0.6^{d}
B	**5**	**30.0**	**100**	5.5 ± 0.5^{a}	32 ± 3^{a}	1.09 ± 0.04^{a}	83.4 ± 1.4^{a}
	10			7.8 ± 0.5^{b}	46 ± 2^{b}	1.25 ± 0.03^{b}	86.2 ± 0.8^{b}
	20			9 ± 1^{c}	54 ± 7^{c}	1.4 ± 0.1^{c}	87 ± 2^{b}
	30			11.0 ± 0.7^{d}	65 ± 1^{d}	1.4 ± 0.1^{c}	88.8 ± 0.9^{cd}
	40			11.8 ± 0.7^{d}	70 ± 3^{e}	1.67 ± 0.05^{de}	87.6 ± 0.7^{bc}
	60			13.9 ± 0.6^{e}	82 ± 1^{f}	1.59 ± 0.06^{d}	89.7 ± 0.6^{d}
	90			14.7 ± 0.3^{ef}	87 ± 1^{g}	1.69 ± 0.07^{de}	89.7 ± 0.4^{d}
	120			15.2 ± 0.1^{f}	89 ± 1^{g}	1.76 ± 0.07^{e}	89.6 ± 0.4^{d}

C	**5**	**45.5**	**180**	6.3 ± 0.2^{a}	37 ± 1^{a}	0.98 ± 0.07^{a}	86.5 ± 0.9^{ab}
	10			7.5 ± 0.5^{b}	44 ± 3^{b}	1.3 ± 0.2^{b}	85 ± 2^{a}
	20			8.7 ± 0.8^{c}	51 ± 4^{c}	1.4 ± 0.1^{bc}	86 ± 1^{a}
	30			11.4 ± 0.8^{d}	67 ± 4^{d}	1.52 ± 0.09^{cd}	88 ± 1^{bc}
	40			13.9 ± 0.7^{e}	82 ± 4^{e}	1.6 ± 0.1^{de}	89.7 ± 0.8^{d}
	60			15.1 ± 0.9^{f}	89 ± 5^{f}	1.7 ± 0.1^{ef}	90.1 ± 0.8^{d}
	90			14.8 ± 0.9^{ef}	87 ± 4^{ef}	1.76 ± 0.02^{f}	89.4 ± 0.6^{cd}
	120			15.2 ± 0.8^{f}	89 ± 4^{f}	1.78 ± 0.07^{f}	89.5 ± 0.6^{cd}
D	**5**	**30.0**	**180**	6.1 ± 0.3^{a}	36 ± 2^{a}	1.04 ± 0.03^{a}	85.6 ± 0.8^{a}
	10			8.0 ± 0.5^{b}	47 ± 3^{b}	1.21 ± 0.05^{b}	86.9 ± 0.8^{b}
	20			9.9 ± 0.2^{c}	58 ± 1^{c}	1.34 ± 0.05^{c}	88.1 ± 0.5^{c}
	30			11.3 ± 0.6^{d}	66 ± 3^{d}	1.5 ± 0.1^{d}	88.5 ± 0.9^{cd}
	40			12.9 ± 0.7^{e}	76 ± 3^{e}	1.44 ± 0.03^{cd}	89.9 ± 0.5^{e}
	60			14 ± 1^{f}	82 ± 8^{ef}	1.50 ± 0.09^{d}	90 ± 1^{e}
	90			14 ± 1^{f}	82 ± 7^{ef}	1.7 ± 0.1^{e}	89 ± 1^{cde}
	120			14 ± 1^{f}	82 ± 6^{f}	1.7 ± 0.1^{e}	89.4 ± 0.9^{de}

Values with different letters (a, g) in each column from each one of the 4 sub-tables are significantly different when applying the LSD method at p-value ≤ 0.05.

None of the highest yields obtained under the other two kinetics, 45.5 kPa with 100 mM NaOH at 120 minutes, and 30.0 kPa with 180 mM NaOH at 60–120 minutes exceeded the values achieved under the two conditions mentioned above.

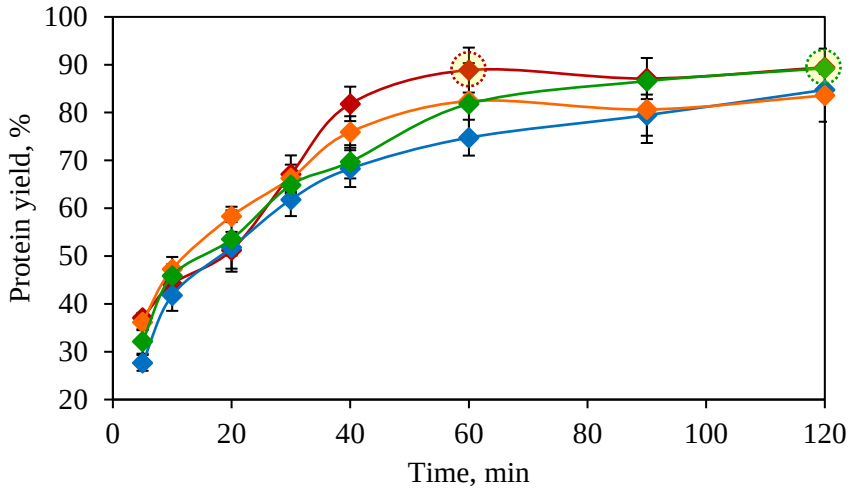

Figure 6.2. Protein yield (%) as a function of time. Vacuum pressure and NaOH concentration, respectively: 45.5 kPa and 100 mM, ◆; 30.0 kPa and 100 mM, ◆; 45.5 kPa and 180 mM, ◆; 30.0 kPa and 180 mM, ◆. Conditions: A (◌); B (◌).

Conditions (A) 60–45.5–180 and (B) 120–30.0–100 (min – kPa – mM NaOH) yielded the highest protein extractions (15.3 ± 0.3 and 15.2 ± 0.1 mg/mL), corresponding to the outstanding extraction yields of 90 ± 6 % and 89 ± 1 %, respectively (Figure 6.2). From now on, these two highest yield extraction conditions will be referred to as “A” and “B”, respectively (Figure 6.2).

Figure 6.3 illustrates protein selectivity as a function of the protein-to-carbohydrate ratio. A clear non-linear trend, resembling a logarithmic or quadratic behavior, is observed across the four extraction conditions, with higher ratios generally associated with greater selectivity, trending to stabilize in selectivities around 90 %. Interpreting together Figures 6.1 and 6.3 it is concluded that carbohydrate release is too modest to compromise selectivity, even at the highest protein recoveries (~90 %).

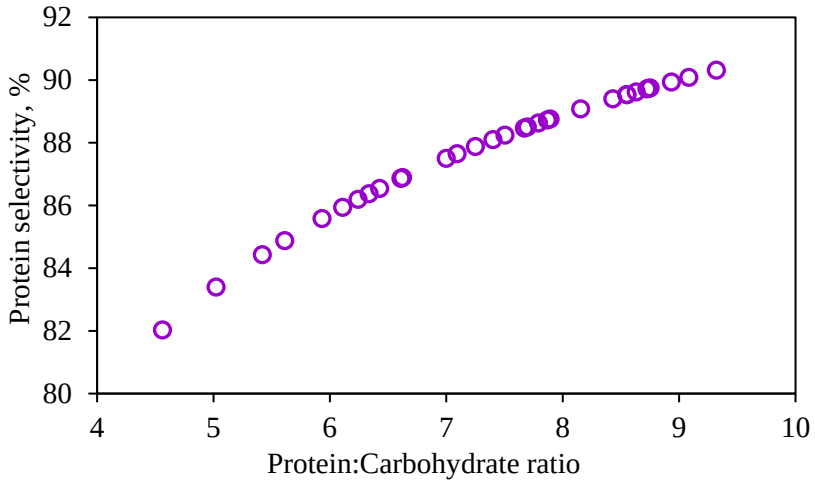

Figure 6.3. Protein selectivity (%) as a function of the ratio Protein:Carbohydrate. All conditions from Table 6.2 represented (○).

In summary, optimizing extraction conditions maximizes protein yield while minimizing carbohydrate co-extraction, leading to purer protein fractions. This confirms that, within the RPAP method, targeting the highest protein solubilization is advantageous without incurring significant carbohydrate contamination.

Selectivity in cases A and B (90.4 ± 0.3 % and 89.6 ± 0.4 %, respectively) was considered statistically similar, and although not the highest value observed among all the obtained results (91.3 ± 0.6 %), it was nearly so. As noted earlier, protein recovery was regarded as the more relevant parameter, particularly when selectivity values fall within the narrow range of 89–91 %.

No studies have been identified in the literature regarding protein extraction from okara using vacuum pressure technologies nor alkaline treatment assessed with reduced pressure. Most published research has focused on conventional alkaline extraction, which generally involves protein solubilization under alkaline conditions followed by precipitation (Eze *et al.*, 2022). While this approach achieves moderate recovery yields, it is constrained by prolonged processing times and the requirement for elevated temperatures.

Recent advances have explored modifications of alkaline extraction. Ultrasonic-assisted alkaline extraction, for instance, has been shown to remarkably enhance protein yield and quality through cavitation effects that disrupt the okara matrix. Eze *et al*. (2022) reported recovery rates of up to 84 % at pH 12 and 60 °C using ultrasonic treatment (20 kHz, 50 min). Tang *et al*. (2024) further demonstrated that alternating ultrasonic/alkaline treatments (on/off ultrasonic pulses applied before and after alkaline extraction) improved protein purity (around 80 %) and functional stability, achieving 17 % recovery compared with 13 % for conventional alkaline extraction and 15 % for continuous ultrasonic-assisted extraction; however, these last recovery levels remain relatively low.

Other approaches include enzymatic assisted alkaline extraction, in which proteolytic enzymes facilitate protein release prior to alkaline treatment (de Figueiredo *et al*., 2018; Orts *et al*., 2019). de Figueiredo *et al*. (2018) reported 29.8 % recovery using Viscozyme (a multi-enzyme complex which consists of cellulase, hemicellulase, arabinase, beta-glucanase and xylanase), under optimized conditions (53 °C, pH 6.2, 4 % enzyme, for 2 h) intending to disrupt the cell wall and facilitate protein release followed by extraction with 1 M NaOH. Similarly, but in this case employing proteases, Orts *et al*. (2019) demonstrated that subtilisin treatment at pH 10 and 55 °C for 2 h solubilized up to 49 % of okara protein, while also generating bioactive peptides and increasing isoflavone extraction, thereby improving the functional properties of the extract.

Emerging physical technologies have also shown promise reporting protein extraction yields of up to 94 % at 100 MPa (Preece *et al*., 2017). Plazzotta *et al*. (2021) applied high-pressure homogenization in sequential steps from 50 to 150 MPa prior to alkaline extraction with 1 M NaOH; every condition in that process being considerably harsher compared with the present work, which employs milder NaOH concentrations (0.10–0.18 M), sub-atmospheric pressure, and works at moderate temperatures (Plazzotta *et al*., 2021; Preece *et al*., 2017).

Overall, these alternative technologies demonstrate the potential to improve the efficiency of conventional alkaline extraction of okara proteins. Nevertheless, the use of vacuum pressure as a primary extraction mechanism has not yet been reported for okara valorization, underscoring both the novelty and significance of the present study.

Since it is currently not possible to compare the present results with other vacuum pressure extraction technologies applied to okara due to the limited number of studies, it is also relevant to compare them with different novel and sustainable techniques, such as the previously obtained results for protein extraction from the same okara using subcritical water treatment. As reported in Chapter 5, batch subcritical water treatment at 180 °C and 5 MPa for 3 h yielded a total amino acid extraction of 81 ± 2 %. This yield is slightly lower than that obtained in the present work using RPAP. However, it is important to note that the method described in Chapter 5 did not involve any chemical reagents, relying solely on water, pressure, and temperature. Therefore, it can be considered a significantly more sustainable process.

Since extractions A and B achieved the best protein recovery while also presenting high selectivity, they were selected for further comparison to determine the optimal RPAP condition for okara protein valorization. To this end, a techno-economic assessment was proposed at industrial scale to evaluate the cost of each scaled-up process. Since both conditions performed similarly in extraction and selectivity, the economic evaluation was expected to be decisive: one process requires twice the time and higher vacuum, while the other consumes more NaOH but operates in half the time with lower vacuum.

3.2. Techno economical assessment (TEA)

Cost of the process was estimated as an industrial scaled-up system based on yearly production of okara by our provider, *Frías Nutrición*. This planning was carried out by using Aspen Plus®.

The process was elaborated in Aspen Plus® following the Figure 6.4 flowchart. The extraction reactor (Reactor-01) chosen was 3rd Seed Fermentor SS304 (Humbird *et al.*, 2011), with a volume of 7570 L and an outcome flux of 3375 L/h. This results on an upload time (τ_{ul}) of 2.24 h, same as the download time. For both cases A and B, total time of treatment, considering treatment time (1 h for case A and 2 h for case B), load time (2.24 h) and download time (2.24 h), last 5.48 and 6.48 h, respectively. By using Eq. 6.3, considering these times, the total number needed of this type of reactor can be calculated, resulting on 3 units of the reactor in both of the processes:

$$\textbf{Case A} \rightarrow \text{Reactor units} = \left(\frac{2.24+2.24+1}{2.24}\right) = 2.45 \rightarrow 3 \text{ units}$$

$$\textbf{Case B} \rightarrow \text{Reactor units} = \left(\frac{2.24+2.24+2}{2.24}\right) = 2.89 \rightarrow 3 \text{ units}$$

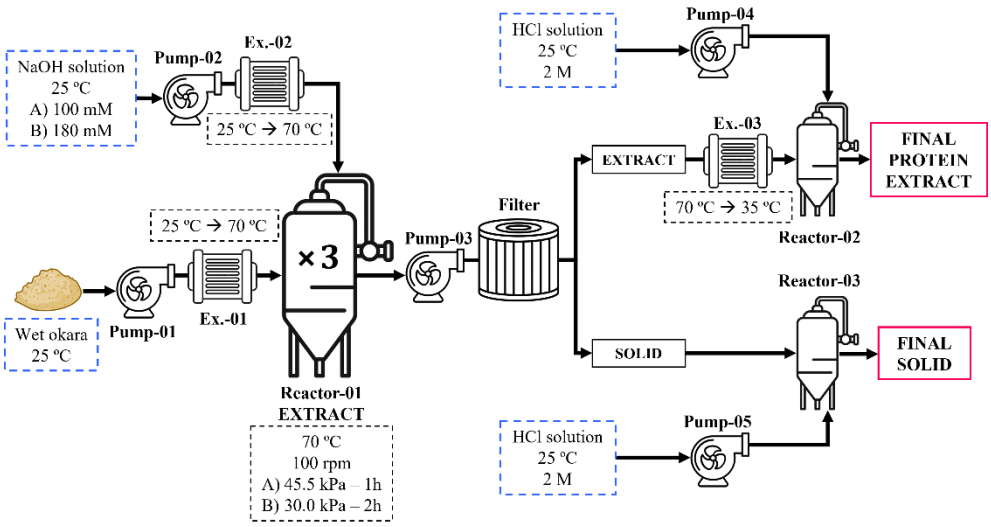

Figure 6.4. Flowchart of the scaled-up version of the RPAP process shaped during the techno-economical assessment. All the equipment taken into account for the capital cost: 5 pumps (Pump-00), 3 heat exchangers (Ex.-00), 3 reactors (Reactor-00), and one separation filter after the extraction.

The process represented in Figure 6.4 is either valid for case A and case B, with the only differences on the concentration of the initial NaOH and the time and pressure applied to the extraction. In terms of the equipment the only difference

between both processes would be the separation pressure filter (see Table 6.3), which is not exactly the same due to a slight difference in the actual cake flow, calculated by Aspen Plus®.

Figure 6.5 represents in a Gantt chart the operation process carried out with the three existing extraction reactors simultaneously in a cascade configuration. Each time a reactor is filled by pump 1 and 2 (e.g., Reactor-I), the filling of the next reactor (Reactor-II) begins, at the same time the extraction process begins in the filled reactor. The filling process continues in this same manner with following reactors (Reactor-III and again R-I, R-II, etc.), that always are going to be empty when the uploading pumps are ready, as can be observed in Figure 6.5. Each time an extraction process ends (either 1 or 2 hours depending on process A or B, respectively), the emptying stage of that reactor begins. As with uploading, once one reactor has been downloaded, it starts the downloading of the following one.

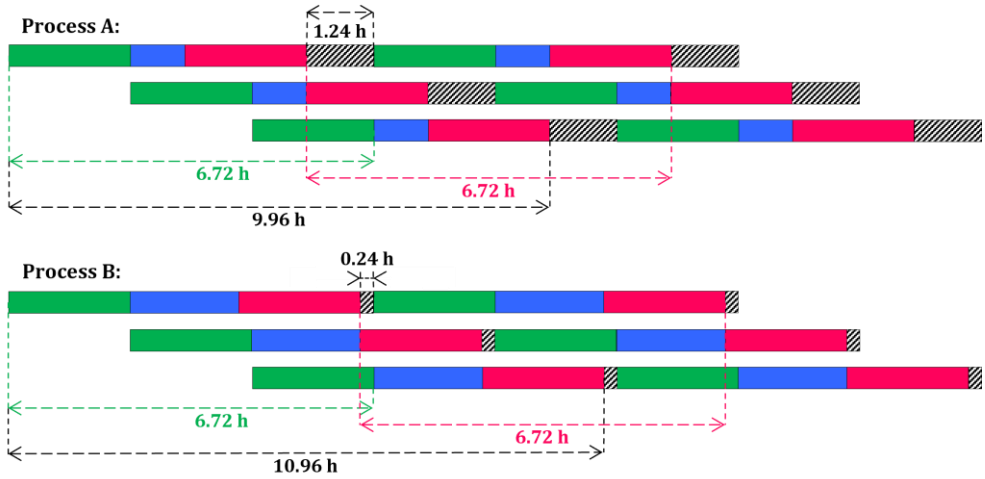

Figure 6.5. Gantt chart representation of cascade scheduling for raw material upload, RPAP extraction and download, in three simultaneous batch reactors. Upload (■, 2.24 h), extraction (■, A: 1 h, B: 2 h), download (■, 2.24 h), and free time (▨, A: 1.24 h, B: 0.24 h).

The upload, extraction, and download processes can be carried out without any process interruptions or overlaps due to the previously calculated number of reactors (N_F) required. In both processes, the N_F value obtained was less than 3, being 3

reactors the optimal number and also allowing for some free time from when each reactor is downloaded until it is refilled again, 1.24 h in case A and 0.24 h in case B, which would allow for some flexibility in the process. In both processes A (5.48 h) and B (6.48 h), the time since the raw materials are loaded into a reactor until the same one is reloaded again is 6.72 h.

By using this conformation system, this extra time does not affect the process once it is already ongoing, since from the moment the first download is obtained (only when starting-up the system, process B lasts 1 hour more than A, 10.96 instead of 9.96 h), the time required to complete one extract extraction cycle (every 3 subsequent downloads) will continue to be 6.72 h for both processes, not affecting the extra 1 h of the case B from then on. Both processes can be considered equal in terms of production quantity.

Once the process is ongoing, every 2.24 h a reactor is downloaded after treating 7570 L, including almost 380 kg dry okara (approximately 2.2 t wet) and 55–30 kg of pure NaOH in cases A–B. In this way in a full year the 7700 t of okara produced by *Frías Nutrición* can be treated more than enough. In every download (2.24 h), approximately 92 kg of protein would be extracted. Considering the 7700 t of wet okara generated yearly, the total protein extracted from this by-product would round 326 t.

The cost of the whole equipment for each process is shown in Table 6.3, where is represented the cost of each equipment of the system, including both the machinery itself and its corresponding assembling, resulting in the total cost of the whole okara protein extraction system.

The most expensive part of the system are the three extractors, costing almost 1.02 M€. It is followed by the filtering system rounding 0.456 M€. The other two reactors destinated to neutralize both final streams are also al remarkable cost, around 0.32 M€. The rest of the systems needed for the processes present a much moderate cost costing around than 0.46 M€ if considering all (3 heat exchangers

costing around 0.218 M€ together and 5 pumps costing around 0.241 M€ together). The two cases are represented on the Table 6.3, however, the only difference between the two processes is the cost of the separation system, which is affected by the actual filter cake flow generated by Aspen Plus® after elaborating the whole process in the program. Actual cake flow of the filter in case A was 1062.9 kg/h while in case B was 1058.4 kg/h. This make that difference of 1402 € between the two processes (456866 € in A and 455464 € in B), which will be considered imperceptible as it represents less than 0.06 % of the capital cost. Overall system capital cost in both cases approximately 2.58 M€.

Table 6.3. Calculated cost of all the equipment and installation costs necessary at industrial scale to carry out the RPAP process to all the okara produced yearly by *Frías Nutrición*.

Equipment		A, €	B, €
(Pump-01)	**Pump for okara**	45500 €	
(Pump-02)	**Pump for NaOH**	54900 €	
(Pump-03)	**Pump for product**	55300 €	
(Pump-04)	**Pump HCl into extract**	42900 €	
(Pump-05)	**Pump HCl into solid**	42900 €	
(Ex.-01)	**Heating system for okara**	62300 €	
(Ex.-02)	**Heating system for NaOH**	73300 €	
(Ex.-03)	**Cooling system for extract**	83100 €	
(Reactor-01)	**Reactor for extraction [×3]**	1019896 €	
(Reactor-02)	**Reactor to neutralize extract**	328100 €	
(Reactor-03)	**Reactor to neutralize solid**	313200 €	
(Filter)	**Filter for separation**	456866 €	455464 €
	Total	2578262 €	2576860 €

Once the industrial scale-up was set, the operational cost of a year of processing the 7700 t of okara generated by *Frías Nutrición* were calculated for both cases (Table 6.4). Total operating cost of the process A in a year ascend to 198075 €, while process B reached 158590 €, an 80 % of the case A. As reflected in Table 6.4, the

cost of NaOH and HCl in the case A is higher due to use a much higher concentration than in case B, every ton of 100 mM and 180 mM NaOH cost 1.26 € and 2.16 € respectively. Total NaOH cost every year ascend from 25734 € to 44481 € when comparing case B and A. In the same way much more 2M HCl is needed to neutralize both streams after the extraction, needing 2628 t in case A instead of 1402 t of case B, which makes a cost ascend from 23871 € to 44758 € when comparing case B and A respectively.

Table 6.4. Operational cost calculations for process A and B. Divided into raw materials and energy/water consuming processes.

	Cost, €/t	Quantity, t/year		Operating cost, €/year	
		A	B	A	B
Raw materials					
Wet okara	0.00	7700	7700	0.00 €	0.00
NaOH [100mM]	1.26	–	20497	–	25734
NaOH [180mM]	2.16	20583	–	44481	–
HCl [2 M]	17.03	2628	1402	44758	23871
Energy / water					
Cooling Water	0.10	32980	33013	2862	2865
Steam	47.40	2518	2520	103571	103661
Pump system	–	–	–	2402	2459
Total	–	–	–	198075 €	158590 €

In the other hand, treatment time in case B doubles case A, from 1 h to 2 h, which was expected to increase heat exchangers systems costs; moreover, vacuum during the process is also higher, from 45.5 kPa in case A to 30.0 kPa in case B. As shown in Table 6.4, cooling water, steam, and pump systems did not almost increase its price from case A to case B (from 108836 € in case A to 108985 € in case B). Creating a higher vacuum atmosphere and maintaining it and the temperature for 2 h instead of 1 h did not affect the cost of the process, the most energy consuming process is to increase the temperatures from 25 °C to 70 °C in both inlets, being very low energy consuming maintaining it (being its cost practically imperceptible), whether for 1 or 2 h. Consequently, the great difference on costs due to the chemicals

(from 49605 € in case B to 89239 € in case A in terms of raw materials, approximately 40000 € difference) is the part that made the overall difference between the two processes, leading to the conclusion that process B is much more cost-effective than A due to the notably less use of chemicals, in addition to be considered a greener process.

TAC can be calculated by using capital cost values and operating cost of both cases (Eq. 6.4). It will be considered 3 years as payback period, based in common payback period stated in these types of industrial scale-up approaches.

$$\textbf{Case A} \rightarrow \text{TAC} = \left(\frac{2\,578\,262\ €}{3\ \text{years}}\right) + 198\,075\ € = 1\,057\,496\ € / \text{year}$$

$$\textbf{Case B} \rightarrow \text{TAC} = \left(\frac{2\,576\,860\ €}{3\ \text{years}}\right) + 158\,590\ € = 1\,017\,543\ € / \text{year}$$

Total annual cost of the first 3 years of each configuration of the process would present a difference of almost 40000 € (39953 €) each year (1.057 M€ in case A and 1.017 M€ in case B), being the cost of process B a 96.2 % of the process A, not presenting a high difference in these 3 years. The following years the cost of the process would be only considered by the operating cost of treating 7700 t of wet okara per year, resulting in 198075 € in case A and 158590 € in case B (saving 39485 €/year, a 20 % of case A operating cost), in these following years, as the cost is much slighter in both cases and the difference almost the same, the difference in the ratio of prices is much remarkably, being the case B an 80 % cheaper after the 3rd year.

Figure 6.6 represents the total cost of each one of the processes in 4 different periods of time: after 3 years, just having accomplished the capital cost of the equipment calculated by TAC; 5 years, comprising those three years and two more which only sum the operating cost, being more notably the difference; 10 years, comprising five years more of only operating cost; and 25 years, comprising 15 years more of only operating cost.

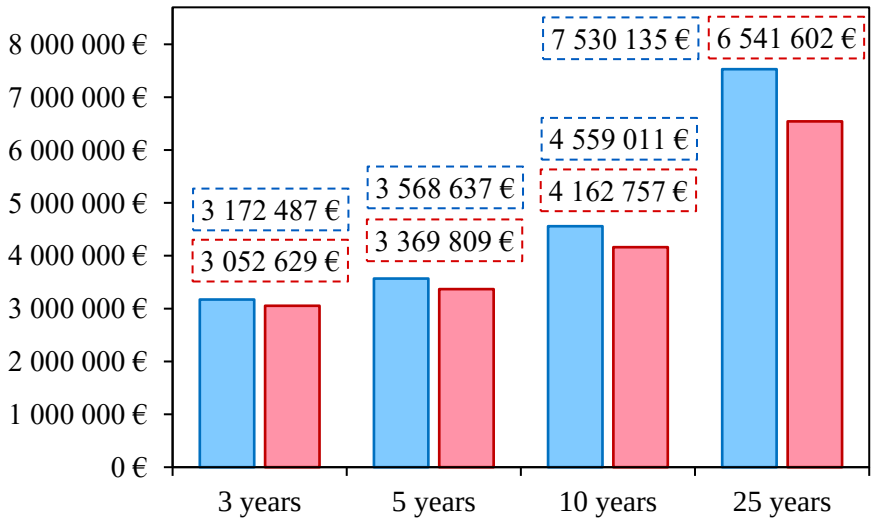

Figure 6.6. Representation of total cost of processes A (🟦) and B (🟥) accumulated after 3, 5, 10 and 25 years.

Results of this timeline cost study show that case B is more profitable whatever is the year-duration of the industrial process, being higher the difference with case A as more years pass after the three years of paying the whole system equipment. Cost of the processes per amount of years is shown detailed in Figure 6.6. Case B cost a 96.2 % less after 3 years (difference of almost 0.12 M€ –119858 €–), a 94.4 % less after 5 years (difference of almost 0.20 M€ –198828 €–), a 91.3 % less after 10 years (difference of almost 0.40 M€ –396254 €–), and an 86.9 % less after 25 years reaching a difference of almost 1 M€ cost (988534 €).

4. Conclusions

Optimization of RPAP for protein extraction from okara revealed two optimal processes at 70 °C: 45.5 kPa with 180 mM NaOH for 60 min (process A) and 30.0 kPa with 100 mM NaOH for 120 min (process B). Both achieved the highest, and not significantly different, recovery rates, with protein yields of 90 ± 6 and 89 ± 1 % and selectivity values of 90.4 ± 0.3 and 89.6 ± 0.4 %, respectively.

Despite their comparable extraction efficiency, the techno-economic assessment (TEA) revealed marked differences between both processes at industrial scale. While process A achieved optimal results in shorter relative extraction time, its higher alkali consumption substantially increased both chemical costs, including neutralization. In contrast, process B required longer relative reaction time but consumed significantly less chemicals, leading to 20 % lower operating costs and overall improved sustainability, especially in the long-term cost analysis. Moreover, the higher relative treatment time and vacuum pressure in B not only did not affect to the overall cost but also allowed treating the same amount of sample than in A by using the combination of the same 3 reactors simultaneously.

Therefore, although both configurations are technically feasible and highly efficient, process B represents the most economically and environmentally advantageous option for large-scale RPAP implementation. These results indicate that minimizing chemical input, rather than reducing treatment time (which proved irrelevant with three reactors configuration) or vacuum pressure, is the critical factor for improving the cost-effectiveness and scalability of okara protein valorization.

CONCLUSIONS

CONCLUSIONS

Although each chapter contains its own conclusions from the different experimental studies carried out in this PhD Thesis, the following general conclusions can be established:

Subcritical water extraction represents a highly effective green alternative to non-sustainable methodologies for protein extraction from food by-products, applicable to protein from both animal sources, such as tuna fish meal, and plant/vegetal sources, like soybean okara. The process is optimized for tuna fish meal by using CO_2 as a pressurization agent, due to its ability to lower the pH of the matrix, while protein extraction from okara is enhanced by using N_2 as an inert gas. This methodology provides great protein extraction from both biomasses yielding high protein recoveries and great bound and free amino acids profile.

Other methodologies such as enzymatic treatments with proteases (Alcalase® and Novozym®), were tested presenting good results, though with significantly lower efficiency compared to subcritical water extraction, which demonstrated much higher release of amino groups and free amino acids within similar timeframes and did not require additional catalysts.

Regarding the functional properties of fish meal hydrolysates, subW resulted as an efficient method to obtain fish protein hydrolysates from fish meal (FM), its water-soluble fraction (WSP) and insoluble fraction (NSP). In comparison to enzymatic hydrolysis, subW provided higher hydrolysis yields, higher protein recovery, and a greater degree of hydrolysis. These hydrolysates, particularly from the insoluble fraction, showed great emulsifying and foaming abilities, influenced by peptide size and the balance between hydrophobic and hydrophilic regions, which makes them valuable for food, pharmaceutical, and cosmetic applications.

The two-step fractionation of the protein hydrolysates facilitated the effective separation of proteins, peptides, and free amino acids according to molecular size, which enhances the functional potential of each fraction. Hydrolysate fractions with higher concentrations of free amino acids and small peptides, mainly obtained from subW hydrolysis, demonstrate great value for pharmaceutical and cosmeceutical applications due to their excellent solubility across a broad pH range. Conversely, hydrolysate fractions with larger peptides, mostly obtained through enzymatic hydrolysis, are promising as emulsion stabilizers by providing a strong structure through the interfacial adsorption of large peptides.

Subcritical water under mild conditions is also effective for hydrolyzing isoflavones from okara, and serves as a preparatory step for further valorization of the protein-rich by-product by applying subcritical water at harsher conditions. Microwave- and ultrasound-assisted extractions (MAE and UAE) also showed favorable results for isoflavone extraction, with UAE being particularly effective by achieving the highest productivity and lowest energy consumption. However, both methods produced fewer valuable hydrolysates than subcritical water, which achieved the optimal isoflavone yield and the most favorable ratio of bioavailable forms.

Scaling up the batch subW system to a semi-continuous subW extraction configuration, using okara (pre-treated for isoflavone extraction), yielded positive outcomes in terms of free amino acid and total protein hydrolysis. Nevertheless, the semi-continuous approach, mainly due to the dilution characteristic of this type of configuration, demonstrated lower hydrolysis yields and protein concentrations, reduced free amino acid hydrolysis, and significantly lower overall productivity compared to the original batch system.

Reduced-pressure alkaline pre-treatment (RPAP) proved to be an excellent methodology for replacing traditional, highly-chemical using, protein extraction methods from okara, especially when optimizing both the recovery yield and purity

of the extract. This approach achieved exceptional protein selectivity due to minimum co-extraction of carbohydrates.

Techno-economic assessment (TEA) resulted to be a helpful tool for evaluating the viability of industrial-scale implementation of RPAP. This analysis facilitated the selection of optimal conditions balancing economy and sustainability, given that two alternatives provided excellent and comparable results. It also enabled estimation of the capital cost for constructing the processing system and the annual operating costs associated with treating all the okara generated each year by the supplier.

Future research should focus on the comprehensive valorization of okara residues generated during the extraction processes described in this work, particularly targeting the high carbohydrate content remaining after protein recovery using RPAP. Prior enzymatic saccharification of these carbohydrates could enable their subsequent use as substrates for fermentation, facilitating the production of high-value bioproducts such as lactic acid, which is currently of significant interest within the department.

Simultaneously, techno-economic assessment (TEA) will play a main role in scaling up promising extraction methodologies, such as batch subcritical water extraction, enabling an integral comparison of these novel technologies and providing a robust evaluation of their feasibility and sustainability for industrial application of the different novel and green technologies used along this work.

REFERENCES

REFERENCES

Abdelmoez, W., Nakahasi, T., & Yoshida, H. (2007). Amino Acid Transformation and Decomposition in Saturated Subcritical Water Conditions. *Industrial & Engineering Chemistry Research*, *46*(16), 5286–5294. https://doi.org/10.1021/ie070151b

Abdelmoez, W., Yoshida, H., & Nakahasi, T. (2010). Pathways of amino acid transformation and decomposition in saturated subcritical water conditions. *International Journal of Chemical Reactor Engineering*, *8*(1). https://doi.org/10.2202/1542-6580.1903

Abdelmoez, W., & Yoshida, H. (2013). Production of amino and organic acids from protein using sub-critical water technology. *International Journal of Chemical Reactor Engineering*, *11*(1), 369–384. https://doi.org/10.1515/ijcre-2013-0017

Abejón, R., Belleville, M. P., Sanchez-Marcano, J., Garea, A., & Irabien, A. (2018). Optimal design of industrial scale continuous process for fractionation by membrane technologies of protein hydrolysate derived from fish wastes. *Separation and Purification Technology*, *197*, 137–146. https://doi.org/10.1016/j.seppur.2017.12.057

Adler-Nissen, J. (1979). Determination of the degree of hydrolysis of food protein hydrolysates by trinitrobenzenesulfonic acid. *Journal of Agricultural and Food Chemistry*, *27*, 1256–1262. https://doi.org/10.1021/jf60226a042

Ahmed, R., & Chun, B. S. (2018). Subcritical water hydrolysis for the production of bioactive peptides from tuna skin collagen. *Journal of Supercritical Fluids*, *141*, 88–96. https://doi.org/10.1016/j.supflu.2018.03.006

Akerlof, G. (1932). Dielectric constants of some organic solvent-water mixtures at various temperatures. *Journal of the American Chemical Society*, *54*(11), 4125–4139. https://doi.org/10.1021/ja01350a001

Alavi, F., & Ciftci, O. N. (2023). Purification and fractionation of bioactive peptides through membrane filtration: A critical and application review. *Trends in Food Science and Technology*, *131*, 118–128. https://doi.org/10.1016/j.tifs.2022.11.024

Ali, M. S., Ho, T. C., Razack, S. A., Haq, M., Roy, V. C., Park, J. S., Kang, H. W., & Chun, B. S. (2023). Oligochitosan recovered from shrimp shells through subcritical water hydrolysis: Molecular size reduction and biological activities. *Journal of Supercritical Fluids*, *196*. https://doi.org/10.1016/j.supflu.2023.105868

Ali, M. S., Haq, M., Park, S. W., Han, J. M., Kim, J. W., Choi, M. S., Lee, S. M., Park, J. S., Chun, M. S., Lee, H. J., & Chun, B. S. (2025). Recent advances in recovering bioactive compounds from macroalgae and microalgae using subcritical water extraction: Prospective compounds and biological activities. Food Chemistry, 142602. https://doi.org/10.1016/j.foodchem.2024.142602

Alonso, E. (2018). The role of supercritical fluids in the fractionation pre-treatments of a wheat bran-based biorefinery. *Journal of Supercritical Fluids*, *133*, 603–614. https://doi.org/10.1016/j.supflu.2017.09.010

Alonso-Riaño, P., Sanz, M. T., Benito-Román, O., Beltrán, S., & Trigueros, E. (2021). Subcritical water as hydrolytic medium to recover and fractionate the protein fraction and phenolic compounds from craft brewer's spent grain. *Food Chemistry*, *351*. https://doi.org/10.1016/j.foodchem.2021.129264

Alonso-Riaño, P. (2022). *Integral valorization of brewer´s spent grain by emerging technologies* [PhD Thesis, University of Burgos]. Universidad de Burgos. https://doi.org/10.36443/10259/7801

Alonso-Riaño, P., Ramos, C., Trigueros, E., Beltrán, S., & Sanz, M. T. (2023). Study of subcritical water scale-up from laboratory to pilot system for brewer's spent grain valorization. *Industrial Crops and Products*, *191*, 1–13. https://doi.org/10.1016/j.indcrop.2022.115927

An, J. H., Ko, M. J., & Chung, M. S. (2023). Thermal conversion kinetics and solubility of soy isoflavones in subcritical water extraction. *Food Chemistry*, *424*, 136430. https://doi.org/10.1016/j.foodchem.2023.136430

Antonov, Y. A., Zhuravleva, I. L., Cardinaels, R., & Moldenaers, P. (2015). Structural studies on the interaction of lysozyme with dextran sulfate. *Food Hydrocolloids*, *44*, 71–80. https://doi.org/10.1016/j.foodhyd.2014.09.006

Arogundade, L. A., Mu, T. H., & Akinhanmi, T. F. (2016). Structural, physicochemical and interfacial stabilization properties of ultrafiltered African yam bean (*Sphenostylis stenocarpa*) protein isolate compared with those of isoelectric protein isolate. *LWT - Food Science and Technology*, *69*, 400–408. https://doi.org/10.1016/j.lwt.2016.01.049

Asghar, A., Afzaal, M., Saeed, F., Ahmed, A., Ateeq, H., Shah, Y. A., Islam, F., Hussain, M., Akram, N., & Shah, M. A. (2023). Valorization and food applications of okara (soybean residue): A concurrent review. *Food Science and Nutrition*, *11*(7), 3631–3640. https://doi.org/10.1002/fsn3.3363

Aspevik, T., Egede-Nissen, H., & Oterhals, Å. (2016). A systematic approach to the comparison of cost efficiency of endopeptidases for the hydrolysis of Atlantic salmon (*Salmo salar*) by-products. *Food Technology and Biotechnology*, *54*(4), 421–431. https://doi.org/10.17113/ft b.54.04.16.4553

Aspevik, T., Oterhals, Å., Rønning, S. B., Altintzoglou, T., Wubshet, S. G., Gildberg, A., Afseth, N. K., Whitaker, R. D., & Lindberg, D. (2017). Valorization of Proteins from Co- and By-Products from the Fish and Meat Industry. *Topics in Current Chemistry*, *375*(3), 123–150. https://doi.org/10.1007/s41061-017-0143-6

Atef, M., & Mahdi Ojagh, S. (2017). Health benefits and food applications of bioactive compounds from fish byproducts: A review. *Journal of Functional Foods*, *35*, 673–681. https://doi.org/10.1016/j.jff.2017.06.034

Avelar, Z., Rodrigues, R. M., Pereira, R. N., & Vicente, A. A. (2022). Future food proteins—Trends and perspectives. *Future Foods: Global Trends, Opportunities, and Sustainability Challenges*, 267–285. https://doi.org/10.1016/B978-0-323-91001-9.00007-4

Ballesteros, L. F., Teixeira, J. A., & Mussatto, S. I. (2017). Extraction of polysaccharides by autohydrolysis of spent coffee grounds and evaluation of their antioxidant activity. *Carbohydrate Polymers*, *157*, 258–266. https://doi.org/10.1016/j.carbpol.2016.09.054

Barea, P., Melgosa, R., Illera, A. E., Alonso-Riaño, P., Díaz de Cerio, E., Benito-Román, Ó., Beltrán, S., & Sanz, M. T. (2023). Production of small peptides and low molecular weight amino acids by subcritical water from fish meal: Effect of pressurization agent. *Food Chemistry*, *418*. https://doi.org/10.1016/j.foodchem.2023.135925

Barea, P., Melgosa, R., Benito-Román, Ó., Illera, A. E., Beltrán, S., & Sanz, M. T. (2024). Green fractionation and hydrolysis of fish meal to improve their techno-functional properties. *Food Chemistry*, *452*, 139550. https://doi.org/10.1016/j.foodchem.2024.139550

Barea, P., Illera, A. E., Melgosa, R., Benito-Román, Ó., Candela, H., Beltrán, S., & Sanz, M. T. (2025). Green extraction of isoflavones from okara using subcritical water: Kinetics, optimization, and comparison with other water-based sustainable methods. *Food Chemistry*, *482*. https://doi.org/10.1016/j.foodchem.2025.144166

Barea, P., Illera, A. E., Candela, H., Melgosa, R., Benito, J. M., Beltrán, S., & Sanz, M. T. (2025). Membrane fractionation of hydrolysates of the water-soluble protein from tuna fish meal obtained by subcritical water and enzymatic treatments. Comparison of physical and chemical properties. *Bioresources and Bioprocessing*, *12*(1). https://doi.org/10.1186/s40643-025-00850-3

Benito-Román, Ó., Sanz, M. T., Illera, A. E., Melgosa, R., Benito, J. M., & Beltrán, S. (2019). Pectin methylesterase inactivation by High Pressure Carbon Dioxide (HPCD). *Journal of Supercritical Fluids*, *145*. https://doi.org/10.1016/j.supflu.2018.11.009

Benito-Román, Ó., Sanz, M.T., & Beltrán, S. (2020). Microencapsulation of rice bran oil using pea protein and maltodextrin mixtures as wall material. *Heliyon*, *6*, 3615. https://doi.org/10.1016/j.heliyon.2020.e03615

Benzie, I. F. F., & Strain, J. J. (1996). The Ferric Reducing Ability of Plasma (FRAP) as a Measure of "Antioxidant Power": The FRAP Assay. *Analytical Biochemistry*, *239*, 70–76. https://doi.org/10.1006/abio.1996.0292

Bobone, S., Van De Weert, M., & Stella, L. (2014). A reassessment of synchronous fluorescence in the separation of Trp and Tyr contributions in protein emission and in the determination of conformational changes. *Journal of Molecular Structure*, *1077*, 68–76. https://doi.org/10.1016/j.molstruc.2014.01.004

Boisen, S., Bech-Andersen, S., & Eggum, B. O. (1987). A critical view on the conversion factor 6.25 from total nitrogen to protein. *Acta Agriculturae Scandinavica*, *37*, 299–304. https://doi.org/10.1080/00015128709436560

Bourseau, P., Vandanjon, L., Jaouen, P., Chaplain-Derouiniot, M., Massé, A., Guérard, F., Chabeaud, A., Fouchereau-Péron, M., Le Gal, Y., Ravallec-Plé, R., Bergé, J.-P., Picot, L., Piot, J.-M., Batista, I., Thorkelsson, G., Delannoy, C., Jakobsen, G., & Johansson, I. (2009). Fractionation of fish protein hydrolysates by ultrafiltration and nanofiltration: impact on peptidic populations. *Desalination*, *244*, 303–320. https://doi.org/10.1016/j.desal.200

Brishti, F. H., Chay, S. Y., Muhammad, K., Ismail-Fitry, M. R., Zarei, M., Karthikeyan, S., & Saari, N. (2020). Effects of drying techniques on the physicochemical, functional, thermal, structural and rheological properties of mung bean (*Vigna radiata*) protein isolate powder. *Food Research International*, *138 Part B*, 109783. https://doi.org/10.1016/j.foodres.2020.109783

Bryant, M. (2025). *Overfishing Statistics & Facts You Should Know In 2025 (source: FAO)*. Worldanimalfoundation.Org. https://worldanimalfoundation.org/advocate/overfishing-statistics/

Bustamante-Rangel, M., Delgado-Zamarreño, M. M., Pérez-Martín, L., Rodríguez-Gonzalo, E., & Domínguez-Álvarez, J. (2018). Analysis of Isoflavones in Foods. *Comprehensive Reviews in Food Science and Food Safety*, *17*, 391–411. https://doi.org/10.1111/1541-4337.12325

Cabrera Camacho, C. E., Alonso-Fariñas, B., Villanueva Perales, A. L., Vidal-Barrero, F., & Ollero, P. (2020). Techno-economic and Life-Cycle Assessment of One-Step Production of 1,3-Butadiene from Bioethanol Using Reaction Data under Industrial Operating Conditions. *ACS Sustainable Chemistry and Engineering*, *8*(27), 10201–10211. https://doi.org/10.1021/acssuschemeng.0c02678

Carr, A. G., Mammucari, R., & Foster, N. R. (2011). A review of subcritical water as a solvent and its utilization for the processing of hydrophobic organic compounds. *Chemical Engineering Journal*, *172*(1), 1–17. https://doi.org/10.1016/j.cej.2011.06.007

Chang, S. K. C., & Liu, Z. (2012). Soymilk and Tofu Manufacturing. *Handbook of Plant-Based Fermented Food and Beverage Technology*, *1–2*, 139–162. https://doi.org/10.1201/b12055-11

Chen, Y., Chen, J., Chang, C., Chen, J., Cao, F., Zhao, J., Zheng, Y., & Zhu, J. (2019). Physicochemical and functional properties of proteins extracted from three microalgal species. *Food Hydrocolloids*, *96*, 510–517. https://doi.org/10.1016/j.foodhyd.2019.05.025

Cheng, H., Zhu, X., Zhu, C., Qian, J., Zhu, N., Zhao, L., & Chen, J. (2008). Hydrolysis technology of biomass waste to produce amino acids in sub-critical water. *Bioresource Technology*, *99*(9), 3337–3341. https://doi.org/10.1016/j.biortech.2007.08.024

Chien, J. T., Hsieh, H. C., Kao, T. H., & Chen, B. H. (2005). Kinetic model for studying the conversion and degradation of isoflavones during heating. *Food Chemistry*, *91*(3), 425–434. https://doi.org/10.1016/j.foodchem.2004.06.023

Chorhirankul, N., Janssen, A. E. M., & Boom, R. M. (2024). UF fractionation of fish protein hydrolysate. *Separation and Purification Technology*, *330*, 125232. https://doi.org/10.1016/j.seppur.2023.125232

Chun, B. S., Lee, S. C., Ho, T. C., Micomyiza, J. B., Park, J. S., & Lee, H. J. (2022). Subcritical Water Hydrolysis of Comb Pen Shell (*Atrina pectinata*) Edible Parts to Produce High-Value Amino Acid Products. *Marine Drugs*, *20*(6). https://doi.org/10.3390/md20060357

CNMC. (2025). Comparador de Ofertas de Energía. https://comparador.cnmc.gob.es/

Cocero, M. J., Cabeza, Á., Abad, N., Adamovic, T., Vaquerizo, L., Martínez, C. M., & Pazo-Cepeda, M. V. (2018). Understanding biomass fractionation in subcritical & supercritical water. *Journal of Supercritical Fluids*, *133*, 550–565. https://doi.org/10.1016/j.supflu.2017.08.012

Colletti, A., Attrovio, A., Boffa, L., Mantegna, S., & Cravotto, G. (2020). Valorization of by-products from soybean (*Glycine max* (L.) Merr.) processing. *Molecules*, *25*(9), 2129. https://doi.org/10.3390/molecules25092129

Corredig, M., Young, N., & Dalsgaard, T. K. (2020). Food proteins: processing solutions and challenges. *Current Opinion in Food Science*, *35*, 49–53. https://doi.org/10.1016/j.cofs.2019.12.010

Cunha, S. A., & Pintado, M. E. (2022). Bioactive peptides derived from marine sources: Biological and functional properties. *Trends in Food Science and Technology*, *119*, 348–370. https://doi.org/10.1016/j.tifs.2021.08.017

da Fonseca, Y. A., Gurgel, L. V. A., Baêta, B. E. L., Dragone, G., & Mussatto, S. I. (2023). Reduced-pressure alkaline pretreatment as an innovative and sustainable technology to extract protein from brewer's spent grain. *Journal of Cleaner Production*, *416*. https://doi.org/10.1016/j.jclepro.2023.137966

Das, D., Mir, N. A., Chandla, N. K., & Singh, S. (2021). Combined effect of pH treatment and the extraction pH on the physicochemical, functional and rheological characteristics of amaranth (*Amaranthus hypochondriacus*) seed protein isolates. *Food Chemistry*, *353*, 129466. https://doi.org/10.1016/j.foodchem.2021.129466

de Figueiredo, V. R. G., Yamashita, F., Vanzela, A. L. L., Ida, E. I., & Kurozawa, L. E. (2018). Action of multi-enzyme complex on protein extraction to obtain a protein concentrate from okara. *Journal of Food Science and Technology*, *55*(4), 1508–1517. https://doi.org/10.1007/s13197-018-3067-4

de Mello, C. F., De La Vega, D. D., Pizutti, L. T., Lopes, F. P., Rubin, M. A., Homerich, J. G., Melo, C. R., Somer, J. E., Souza, D. O., & Wajner, M. (1995). Neurochemical effects of l-pyroglutamic acid. *Neurochemical Research*, *20*(12), 1437–1441. https://doi.org/10.1007/BF00970591

Diniz, G. S., Barbarino, E., Oiano-Neto, J., Pacheco, S., & Lourenço, S. O. (2013). Gross chemical profile and calculation of nitrogen-to-protein conversion factors for nine species of fishes from coastal waters of Brazil. *Latin American Journal of Aquatic Research*, *41*, 254–264. https://doi.org/10.3856/vol41-issue2-fulltext-5

Domenico Ziero, H., Buller, L. S., Mudhoo, A., Ampese, L. C., Mussatto, S. I., & Carneiro, T. F. (2020). An overview of subcritical and supercritical water treatment of different biomasses for protein and amino acids production and recovery. *Journal of Environmental Chemical Engineering*, *8*. https://doi.org/10.1016/j.jece.2020.104406

Esteban, M. B., García, A. J., Ramos, P., & Márquez, M. C. (2010). Sub-critical water hydrolysis of hog hair for amino acid production. *Bioresource Technology*, *101*, 2472–2476. https://doi.org/10.1016/j.biortech.2009.11.054

Etemadian, Y., Ghaemi, V., Shaviklo, A. R., Pourashouri, P., Sadeghi Mahoonak, A. R., & Rafipour, F. (2021). Development of animal/ plant-based protein hydrolysate and its application in food, feed and nutraceutical industries: State of the art. *Journal of Cleaner Production*, *278*. https://doi.org/10.1016/j.jclepro.2020.123219

Eze, O. F. (2019). *Extraction of proteins from soybean residue (okara) and investigation of their physicochemical properties and their application as emulsifiers* [PhD Thesis, University of Reading]. https://api.semanticscholar.org/CorpusID:208691022

Eze, O. F., Chatzifragkou, A., & Charalampopoulos, D. (2022). Properties of protein isolates extracted by ultrasonication from soybean residue (okara). *Food Chemistry*, *368*, 130837. https://doi.org/10.1016/j.foodchem.2021.130837

Fakhree, M. A., Delgado, D. R., Martínez, F., & Jouyban, A. (2010). The Importance of Dielectric Constant for Drug Solubility Prediction in Binary Solvent Mixtures: Electrolytes and Zwitterions in Water + Ethanol. *American Association of Pharmaceutical Scientists*, *11*(4), 1726–1729. https://doi.org/10.1208/S12249-010-9552-3

FAO. (1986). *The production of fish meal and oil*. Chapter 3: The process. FAO Fisheries Technical Paper, 142(1). FAO. https://www.fao.org/4/x6899e/X6899E04.htm

FAO. (2020). *The State of World Fisheries and Aquaculture 2020. Sustainability in action*. FAO. https://doi.org/10.4060/ca9229en

FAO. (2022). *The State of World Fisheries and Aquaculture 2022. Towards Blue Transformation*. FAO. https://doi.org/10.4060/cc0461en

FAO. (2023). *The State of Food Security and Nutrition in the World 2023*. *Urbanization, agrifood systems transformation and healthy diets across the rural–urban continuum*. FAO. https://doi.org/10.4060/cc3017en

FAO. (2024). *The State of World Fisheries and Aquaculture 2024*. *Blue Transformation in action*. FAO. https://doi.org/10.4060/cd0683en

FAO. (2025a). FAOSTAT: Crops and Livestock Products (QLC) [database]. Retrieved July 16, 2025, from https://www.fao.org/faostat/es/#data/QCL

FAO. (2025b). *Food Outlook. Biannual report on global food markets*. FAO. https://doi.org/10.4060/cd5655en

Folador, J. F., Karr-Lilienthal, L. K., Parsons, C. M., Bauer, L. L., Utterback, P. L., Schasteen, C. S., Bechtel, P. J., & Fahey, G. C. (2006). Fish meals, fish components, and fish protein hydrolysates as potential ingredients in pet foods. *Journal of Animal Science*, *84*(10), 2752–2765. https://doi.org/10.2527/jas.2005-560

Freitas, C. S., Vericimo, M. A., da Silva, M. L., da Costa, G. C. V., Pereira, P. R., Paschoalin, V. M. F., & Del Aguila, E. M. (2019). Encrypted antimicrobial and antitumoral peptides recovered from a protein-rich soybean (*Glycine max*) by-product. *Journal of Functional Foods*, *54*, 187–198. https://doi.org/10.1016/j.jff.2019.01.024

Friedman, M. (2004). Applications of the Ninhydrin Reaction for Analysis of Amino Acids, Peptides, and Proteins to Agricultural and Biomedical Sciences. *Journal of Agricultural and Food Chemistry*, *52*, 385–406. https://doi.org/10.1021/jf030490p

Fritzsche, H., & Phillips, M. (2025). *Electromagnetic radiation - Microwaves, Wavelengths, Frequency*. Britannica. Retrieved August 10, 2025, from https://www.britannica.com/science/electromagnetic-radiation/Microwaves

Galamba, N., Paiva, A., Barreiros, S., & Simões, P. (2019). Solubility of Polar and Nonpolar Aromatic Molecules in Subcritical Water: The Role of the Dielectric Constant. *Journal of Chemical Theory and Computation*, *15*(11), 6277–6293. https://doi.org/10.1021/acs.jctc.9b00505

Gehring, C., Davenport, M., & Jaczynski, J. (2009). Functional and nutritional quality of protein and lipid recovered from fish processing by-products and underutilized aquatic species using isoelectric solubilization/precipitation. *Current Nutrition & Food Science*, *5*, 17–39. https://doi.org/10.2174/157340109787314703

Ghalamara, S., Brazinha, C., Silva, S., & Pintado, M. (2024). Valorization of Fish Processing By-Products: Biological and Functional Properties of Bioactive Peptides. *Current Food Science and Technology Reports*, *2*(4), 393–409. https://doi.org/10.1007/s43555-024-00045-5

Girgih, A. T., Udenigwe, C. C., Hasan, F. M., Gill, T. A., & Aluko, R. E. (2013). Antioxidant properties of Salmon (*Salmo salar*) protein hydrolysate and peptide fractions isolated by reverse-phase HPLC. *Food Research International*, *52*(1), 315–322. https://doi.org/10.1016/j.foodres.2013.03.034

Guérard, F., Dufossé, L., Broise, D., & Binet, A. (2001). Enzymatic hydrolysis of proteins from yellowfin tuna (*Thunnus albacares*) wastes using Alcalase. *Journal of Molecular Catalysis B: Enzymatic*, *11*, 1051–1059. https://doi.org/10.1016/S1381-1177(00)00031-X

Guidea, A., Zăgrean-Tuza, C., Moț, A. C., & Sârbu, C. (2020). Comprehensive evaluation of radical scavenging, reducing power and chelating capacity of free proteinogenic amino acids using spectroscopic assays and multivariate exploratory techniques. *Spectrochimica Acta - Part A: Molecular and Biomolecular Spectroscopy*, *233*, 118158. https://doi.org/10.1016/j.saa.2020.118158

Halim, N. R. A., Yusof, H. M., & Sarbon, N. M. (2016). Functional and bioactive properties of fish protein hydrolysates and peptides: A comprehensive review. *Trends in Food Science and Technology*, *51*, 24–33. https://doi.org/10.1016/j.tifs.2016.02.007

Hames, B., Scarlata, C., & Sluiter, A. (2008). *Determination of Protein Content in Biomass* (Laboratory Analytical Procedure, NREL/TP-510-42625). National Renewable Energy Laboratory. https://www.nrel.gov/docs/gen/fy08/42625.pdf

Hao, G., Cao, W., Li, T., Chen, J., Zhang, J., Weng, W., Osako, K., & Ren, H. (2019). Effect of temperature on chemical properties and antioxidant activities of abalone viscera subcritical water extract. *The Journal of Supercritical Fluids*, *147*, 17–23. https://doi.org/10.1016/J.SUPFLU.2019.02.007

Haq, M., Chun, M. S., Ali, M. S., Han, J. M., Kim, J. W., Park, S. W., Choi, M. S., Lee, S. M., Park, J. S., Lee, H. J., & Chun, B. S. (2025). Molecular size reduction and functional properties of Atlantic salmon waste protein treated by subcritical water. *International Journal of Biological Macromolecules*, *309*, 142888. https://doi.org/10.1016/j.ijbiomac.2025.142888

He, X. H., Liu, H. Z., Liu, L., Zhao, G. L., Wang, Q., & Chen, Q. L. (2014). Effects of high pressure on the physicochemical and functional properties of peanut protein isolates. *Food Hydrocolloids*, *36*, 123–129. https://doi.org/10.1016/j.foodhyd.2013.08.031

Herdina, A. P., Handayani, E., Rohmawati, S., Isfanaya, N. K., & Sopandi, T. (2024). Evaluation of the Nutritional Composition of Fish Meal Production. *International Journal of Agriculture & Environmental Science*, *11*(4), 42–46. https://doi.org/10.14445/23942568/ijaes-v11i4p106

Hsiao, Y.H., Ho, C.T., & Pan, M.H. (2020). Bioavailability and health benefits of major isoflavone aglycones and their metabolites. *Journal of Functional Foods*, *74*, 104164. https://doi.org/10.1016/j.jff.2020.104164

Humbird, D., Davis, R., Tao, L., Kinchin, C., Hsu, D., Aden, A., Schoen, P., Lukas, J., Olthof, B., Worley, M., Sexton, D., & Dudgeon, D. (2011). *Process design and economics for biochemical conversion of lignocellulosic biomass to ethanol: Dilute-acid pretreatment and enzymatic hydrolysis of corn stover* (NREL/TP-5100-47764). National Renewable Energy Laboratory. https://www.nrel.gov/docs/fy11osti/47764.pdf

Hušek, P. (1991). Amino acid derivatization and analysis in five minutes. *FEBS Letters*, *280*(2), 354–356. https://doi.org/10.1016/0014-5793(91)80330-6

Illera, A. E., Sanz, M. T., Varona, S., Beltrán, S., Melgosa, R., & Solaesa, A. G. (2018). Effect of thermosonication batch treatment on enzyme inactivation kinetics and other quality parameters of cloudy apple juice. *Innovative Food Science and Emerging Technologies*, *47*, 71–80. https://doi.org/10.1016/j.ifset.2018.02.001

Illera, A. E., Sanz, M. T., Beltran, S., Melgosa, R., Solaesa, A. G., & Ruiz, M. O. (2018). Evaluation of HPCD batch treatments on enzyme inactivation kinetics and selected quality characteristics of cloudy juice from Golden delicious apples. *Journal of Food Engineering*, *221*, 141–150. https://doi.org/10.1016/j.jfoodeng.2017.10.017

Illera, A. E., Candela, H., Barea, P., Bermejo-López, A., Beltrán, S., & Sanz, M. T. (2025). Microwave technology as a green and fast alternative for furfural production and biomass pre-treatment using corn stover: Energetic and economic evaluation. *Industrial Crops and Products*, *223*. https://doi.org/10.1016/j.indcrop.2024.120095

Iwata, K., Ishizaki, S., Handa, A., & Tanaka, M. (2000). Preparation and characterization of edible films from fish water-soluble proteins. *Fisheries Science*, *66*, 372–378. https://doi.org/10.1046/j.1444-2906.2000.00057.x

Jain, B. (2015). Development and Acceptability Evaluation of Soy Milk Obtained from Soy. *Journal of Dairy Science and Technology*, *4*(1), 10–14.

Jankowiak, L., Kantzas, N., Boom, R., & Van Der Goot, A. J. (2014). Isoflavone extraction from okara using water as extractant. *Food Chemistry*, *160*, 371–378. https://doi.org/10.1016/j.foodchem.2014.03.082

Jinap, S., & Hajeb, P. (2010). Glutamate. Its applications in food and contribution to health. *Appetite*, *55*(1), 1–10. https://doi.org/10.1016/j.appet.2010.05.002

Kang, K., Quitain, A. T., Daimon, H., Noda, R., Goto, N., Hu, H. Y., & Fujie, K. (2001). Optimization of amino acids production from waste fish entrails by hydrolysis in sub- and supercritical water. *Canadian Journal of Chemical Engineering*, *79*, 65–70. https://doi.org/10.1002/cjce.5450790110

Ketnawa, S., Martínez-Alvarez, O., Benjakul, S., & Rawdkuen, S. (2016). Gelatin hydrolysates from farmed Giant catfish skin using alkaline proteases and its antioxidative function of simulated gastro-intestinal digestion. *Food Chemistry*, *192*, 34–42. https://doi.org/10.1016/j.foodchem.2015.06.087

Koh, B. B., Lee, E. J., Ramachandraiah, K., & Hong, G. P. (2019). Characterization of bovine serum albumin hydrolysates prepared by subcritical water processing. *Food Chemistry*, *278*, 203–207. https://doi.org/10.1016/j.foodchem.2018.11.069

Koutinas, A. A., Yepez, B., Kopsahelis, N., Freire, D. M. G., de Castro, A. M., Papanikolaou, S., & Kookos, I. K. (2016). Techno-economic evaluation of a complete bioprocess for 2,3-butanediol production from renewable resources. *Bioresource Technology*, *204*, 55–64. https://doi.org/10.1016/j.biortech.2015.12.005

Kumar, V., Rani, A., & Husain, L. (2016). Investigations of amino acids profile, fatty acids composition, isoflavones content and antioxidative properties in soy okara. *Asian Journal of Chemistry*, *28*(4), 903–906. https://doi.org/10.14233/ajchem.2016.19548

Labster. (n.d.). *Protein Structure*. Labster. Retrieved September 8, 2025, from https://theory.labster.com/protein-structure/

Lamp, A., Kaltschmitt, M., & Lüdtke, O. (2020). Protein recovery from bioethanol stillage by liquid hot water treatment. *Journal of Supercritical Fluids*, *155*. https://doi.org/10.1016/j.supflu.2019.104624

Le Bourvellec, C., & Renard, C. M. (2012). Interactions between polyphenols and macromolecules: Quantification methods and mechanisms. *Critical Reviews in Food Science and Nutrition*, *52*(3), 213–248. https://doi.org/10.1080/10408398.2010.499808

Lehninger, A. L. (1984). *Principios de bioquímica* (P. Van Eikeren, Ed.). Editorial Omega.

Li, B., Qiao, M., & Lu, F. (2012). Composition, Nutrition, and Utilization of Okara (Soybean Residue). *Food Reviews International*, *28*(3), 231–252. https://doi.org/10.1080/87559129.2011.595023

Li, C., Xue, H., Chen, Z., Ding, Q., & Wang, X. (2014). Comparative studies on the physicochemical properties of peanut protein isolate-polysaccharide conjugates prepared by ultrasonic treatment or classical heating. *Food Research International*, *57*, 1–7. https://doi.org/10.1016/j.foodres.2013.12.038

Li, D., Zhao, Y., Wang, X., Tang, H., Wu, N., Wu, F., Yu, D., & Elfalleh, W. (2020). Effects of (+)-catechin on a rice bran protein oil-in-water emulsion: Droplet size, zeta-potential, emulsifying properties, and rheological behavior. *Food Hydrocolloids*, *98*, 105306. https://doi.org/10.1016/j.foodhyd.2019.105306

Li, N., Wang, Y., Gan, Y., Wang, S., Wang, Z., Zhang, C., & Wang, Z. (2022). Physicochemical and functional properties of protein isolate recovered from Rana chensinensis ovum based on different drying techniques. *Food Chemistry*, *396*, 133632. https://doi.org/10.1016/j.foodchem.2022.133632

Liu, F., & Tang, C. H. (2013). Soy protein nanoparticle aggregates as pickering stabilizers for oil-in-water emulsions. *Journal of Agricultural and Food Chemistry*, *61*, 8888–8898. https://doi.org/10.1021/jf401859y

López, D. N., Boeris, V., Spelzini, D., Bonifacino, C., Panizzolo, L. A., & Abirached, C. (2019). Adsorption of chia proteins at interfaces: Kinetics of foam and emulsion formation and destabilization. *Colloids and Surfaces B: Biointerfaces*, *180*, 503–507. https://doi.org/10.1016/j.colsurfb.2019.04.067

Lowry, O. H., Rosebrough, N. J., Farr, A. L., & Randall, R. J. (1951). Protein measurement with the Folin phenol reagent. *The Journal of Biological Chemistry*, *193*, 265–275. https://doi.org/10.1016/s0021-9258(19)52451-6

Lu, W., Chen, X. W., Wang, J. M., Yang, X. Q., & Qi, J. R. (2016). Enzyme-assisted subcritical water extraction and characterization of soy protein from heat-denatured meal. *Journal of Food Engineering*, *169*, 250–258. https://doi.org/10.1016/j.jfoodeng.2015.09.006

Lv, Y., Chen, L., Liu, F., Xu, F., & Zhong, F. (2023). Improvement of the encapsulation capacity and emulsifying properties of soy protein isolate through controlled enzymatic hydrolysis. *Food Hydrocolloids*, *138*, 108444. https://doi.org/10.1016/j.foodhyd.2022.108444

Ma, C. Y., Liu, W. S., Kwok, K. C., & Kwok, F. (1996). Isolation and characterization of proteins from soymilk residue (okara). *Food Research International*, *29*(8), 799–805. https://doi.org/10.1016/0963-9969(95)00061-5

Ma, M., Ren, Y., Xie, W., Zhou, D., Tang, S., Kuang, M., Wang, Y., & Du, S. K. (2018). Physicochemical and functional properties of protein isolate obtained from cottonseed meal. *Food Chemistry*, *240*, 856–862. https://doi.org/10.1016/j.foodchem.2017.08.030

Madhariya, G., Diwan, S., Chauhan, R., Chandrawanshi, N. K., & Mahish, P. K. (2023). *Current applications of biomolecules in biotechnology*. In *Handbook of Biomolecules: Fundamentals, Properties and Applications*, 397–418. Elsevier. https://doi.org/10.1016/B978-0-323-91684-4.00027-X

Mailaram, S., Narisetty, V., Ranade, V. V., Kumar, V., & Maity, S. K. (2022). Techno-Economic Analysis for the Production of 2,3-Butanediol from Brewers' Spent Grain Using Pinch Technology. *Industrial and Engineering Chemistry Research*, *61*(5), 2195–2205. https://doi.org/10.1021/acs.iecr.1c04410

Marcet, I., Álvarez, C., Paredes, B., & Díaz, M. (2016). The use of sub-critical water hydrolysis for the recovery of peptides and free amino acids from food processing wastes. Review of sources and main parameters. *Review of Sources and Main Parameters. Waste Management*, *49*, 364–371. https://doi.org/10.1016/j.wasman.2016.01.009

Martin-Orue, C., Bouhallab, S., & Garem, A. (1998). Nanofiltration of amino acid and peptide solutions: Mechanisms of separation. *Journal of Membrane Science*, *142*(2), 225–233. https://doi.org/10.1016/S0376-7388(97)00325-6

Melgosa, R., Trigueros, E., Sanz, M. T., Cardeira, M., Rodrigues, L., Fernández, N., & Simoes, P. (2020). Supercritical CO2 and subcritical water technologies for the production of bioactive extracts from sardine (*Sardina pilchardus*) waste. *Journal of Supercritical Fluids*, *164*. https://doi.org/10.1016/j.supflu.2020.104943

Melgosa, R., Marques, M., Paiva, A., Bernardo, A., Fernández, N., Sá-Nogueira, I., & Simões, P. (2021). Subcritical water extraction and hydrolysis of cod (*Gadus morhua*) frames to produce bioactive protein extracts. *Foods*, *10*(6). https://doi.org/10.3390/foods10061222

Mok, W. K., Tan, Y. X., Lee, J., Kim, J., & Chen, W. N. (2019). A metabolomic approach to understand the solid-state fermentation of okara using *Bacillus subtilis* WX-17 for enhanced nutritional profile. *AMB Express*, *9*(1). https://doi.org/10.1186/s13568-019-0786-5

Montazeri Shatouri, M., Khabir, Z., Pirozzi, I., Demir Soker, P., & Haynes, P. A. (2025). Composition and Detailed Characterization of Amino Acids, Peptides, Proteins, Fatty Acids, and Minerals of Tuna Trimming Fish Meal. *ACS Food Science and Technology*, *5*(3), 1145–1155. https://doi.org/10.1021/acsfoodscitech.4c00992

Moras, B., Rey, S., Vilarem, G., & Pontalier, P.-Y. (2017). Pressurized water extraction of isoflavones by experimental design from soybean flour and Soybean Protein Isolate. *Food Chemistry*, *214*, 9–15. https://doi.org/10.1016/j.foodchem.2016.07.053

Moure, A., Domínguez, H., & Parajó, J. C. (2006). Antioxidant properties of ultrafiltration-recovered soy protein fractions from industrial effluents and their hydrolysates. *Process Biochemistry*, *41*(2), 447–456. https://doi.org/10.1016/j.procbio.2005.07.014

Nguyen, T. A. H., Ngo, H. H., Guo, W. S., Zhang, J., Liang, S., & Tung, K. L. (2013). Feasibility of iron loaded "okara" for biosorption of phosphorous in aqueous solutions. *Bioresource Technology*, *150*, 42–49. https://doi.org/10.1016/j.biortech.2013.09.133

Niamnuy, C., Nachaisin, M., Poomsa-Ad, N., & Devahastin, S. (2012). Kinetic modelling of drying and conversion/degradation of isoflavones during infrared drying of soybean. *Food Chemistry*, *133*(3), 946–952. https://doi.org/10.1016/j.foodchem.2012.02.010

Ningrum, A., Vanidia, N., Wardani, D. W., Priyanto, A., Manikharda, Kumalasari, R., Ekafitri, R., Kristanti, D., Setiaboma, W., Sarifudin, A., Siti Halimatul Munawaroh, H., & Lawrence Fuhrmann, P. (2025). Valorization of soybean residues (Okara): technofunctional properties of okara hydrolysates using papain. *International Journal of Food Properties*, *28*(1). https://doi.org/10.1080/10942912.2025.2519838

Nkurunziza, D., Pendleton, P., & Chun, B. S. (2019). Optimization and kinetics modeling of okara isoflavones extraction using subcritical water. *Food Chemistry*, *295*, 613–621. https://doi.org/10.1016/j.foodchem.2019.05.129

Nkurunziza, D., Pendleton, P., Sivagnanam, S. P., Park, J. S., & Chun, B. S. (2019). Subcritical water enhances hydrolytic conversions of isoflavones and recovery of phenolic antioxidants from soybean byproducts (okara). *Journal of Industrial and Engineering Chemistry*, *80*, 696–703. https://doi.org/10.1016/j.jiec.2019.08.044

Novozymes. (2025a). *Alcalase® Pure*. https://www.novozymes.com.cn/en/en/dairy/products/dairy-protein-hydrolysis/alcalase-pure

Novozymes. (2025b). *Novozym® 11028*. https://novozymes.com.cn/en/en/animal-protein/products/novozym-11028

Orts, A., Revilla, E., Rodriguez-Morgado, B., Castaño, A., Tejada, M., Parrado, J., & García-Quintanilla, A. (2019). Protease technology for obtaining a soy pulp extract enriched in bioactive compounds: isoflavones and peptides. *Heliyon*, *5*(6), 0–6. https://doi.org/10.1016/j.heliyon.2019.e01958

O'Sullivan, J., Beevers, J., Park, M., Greenwood, R., & Norton, I. (2015). Comparative assessment of the effect of ultrasound treatment on protein functionality pre- and post-emulsification. *Colloids and Surfaces A: Physicochemical and Engineering Aspects*, *484*, 89–98. https://doi.org/10.1016/j.colsurfa.2015.07.065

O'Toole, D. K. (1999). Characteristics and use of okara, the soybean residue from soy milk production - A review. *Journal of Agricultural and Food Chemistry*, *47*(2), 363–371. https://doi.org/10.1021/jf980754l

Ovissipour, M., Abedian, A., Motamedzadegan, A., Rasco, B., Safari, R., & Shahiri, H. (2009). The effect of enzymatic hydrolysis time and temperature on the properties of protein hydrolysates from Persian sturgeon (*Acipenser persicus*) viscera. *Food Chemistry*, *115*, 238–242. https://doi.org/10.1016/j.foodchem.2008.12.013

Paiva dos Santos, K., Mellinger-Silva, C., Santa Brígida, A. I., & Barros Gonçalves, L. R. (2020). Modifying Alcalase activity and stability by immobilization onto chitosan aiming at the production of bioactive peptides by hydrolysis of tilapia skin gelatin. *Process Biochemistry*, *97*, 27–36. https://doi.org/10.1016/j.procbio.2020.06.019

Park, J. S., Jeong, Y. R., & Chun, B. S. (2019). Physiological activities and bioactive compound from laver (*Pyropia yezoensis*) hydrolysates by using subcritical water hydrolysis. *Journal of Supercritical Fluids*, *148*, 130–136. https://doi.org/10.1016/j.supflu.2019.03.004

Park, J. S., Roy, V. C., Kim, S. Y., Lee, S. C., & Chun, B. S. (2022). Extraction of edible oils and amino acids from eel by-products using clean compressed solvents: An approach of complete valorization. *Food Chemistry*, *388*, 132949. https://doi.org/10.1016/j.foodchem.2022.132949

Petrova, I., Tolstorebrov, I., & Eikevik, T. M. (2018). Production of fish protein hydrolysates step by step: Technological aspects, equipment used, major energy costs and methods of their minimizing. *International Aquatic Research*, *10*, 223–241.

Pezeshk, S., Ojagh, S. M., Rezaei, M., & Shabanpour, B. (2019). Fractionation of Protein Hydrolysates of Fish Waste Using Membrane Ultrafiltration: Investigation of Antibacterial and Antioxidant Activities. *Probiotics and Antimicrobial Proteins*, *11*(3), 1015–1022. https://doi.org/10.1007/s12602-018-9483-y

Picot, L., Ravallec, R., Martine, F. P., Vandanjon, L., Jaouen, P., Chaplain-Derouiniot, M., Guérard, F., Chabeaud, A., Legal, Y., Alvarez, O. M., Bergé, J. P., Piot, J. M., Batista, I., Pires, C., Thorkelsson, G., Delannoy, C., Jakobsen, G., Johansson, I., & Bourseau, P. (2010). Impact of ultrafiltration and nanofiltration of an industrial fish protein hydrolysate on its bioactive properties. *Journal of the Science of Food and Agriculture*, *90*(11), 1819–1826. https://doi.org/10.1002/jsfa.4020

Plaza, M., & Turner, C. (2015). Pressurized hot water extraction of bioactives. *Trends in Analytical Chemistry*, *71*, 39–54. https://doi.org/10.1016/j.trac.2015.02.022

Plazzotta, S., Moretton, M., Calligaris, S., & Manzocco, L. (2021). Physical, chemical, and techno-functional properties of soy okara powders obtained by high pressure homogenization and alkaline-acid recovery. *Food and Bioproducts Processing*, *128*, 95–101. https://doi.org/10.1016/j.fbp.2021.04.017

Pokhum, C., Chawengkijwanich, C., & Kobayashi, F. (2015). Enhancement of Non-thermal Treatment on Inactivation of Glucoamylase and Acid Protease Using CO2 Microbubbles. *Journal of Food Processing & Technology*, *6*, 2–6. https://doi.org/10.4172/2157-7110.1000498

Polgár, L. (1989). *Mechanisms of protease action*. CRC Press.

Pommié, C., Levadoux, S., Sabatier, R., Lefranc, G., & Lefranc, M. P. (2004). IMGT standardized criteria for statistical analysis of immunoglobulin V-Region amino acid properties. *Journal of Molecular Recognition*, *17*(1), 17–32. https://doi.org/10.1002/jmr.647

Preece, K. E., Hooshyar, N., & Zuidam, N. J. (2017). Whole soybean protein extraction processes: A review. *Innovative Food Science and Emerging Technologies*, *43*, 163–172. https://doi.org/10.1016/j.ifset.2017.07.024

Quitain, A. T., Sato, N., Daimon, H., & Fujie, K. (2001). Production of valuable materials by hydrothermal treatment of shrimp shells. *Industrial and Engineering Chemistry Research*, *40*(25), 5885–5888. https://doi.org/10.1021/ie010439f

Ratnaningsih, E., Reynard, R., Khoiruddin, K., Wenten, I. G., & Boopathy, R. (2021). Recent advancements of UF-based separation for selective enrichment of proteins and bioactive peptides - A review. *Applied Sciences*, *11*(3), 1–36. https://doi.org/10.3390/app11031078

Rekha, C. R., & Vijayalakshmi, G. (2013). Influence of processing parameters on the quality of soycurd (tofu). *Journal of Food Science and Technology*, *50*(1), 176–180. https://doi.org/10.1007/s13197-011-0245-z

Rimbach, G., Matsugo, S., Minihane, A. M., Rimbachy, G., De Pascual-Teresay, S., Ewinsy, B. A., Matsugo, S., Uchida, Y., Minihaney, A. M., Turnery, R., Vafeiadouy, K., & Weinbergz, P. D. (2003). Antioxidant and free radical scavenging activity of isoflavone metabolites. *Xenobiotica*, *33*(9), 913–925. https://doi.org/10.1080/0049825031000150444

Ritchie, H. (2024). *Drivers of Deforestation*. Our World In Data. Retrieved August 8, 2025, from https://ourworldindata.org/drivers-of-deforestation#is-our-appetite-for-soy-driving-deforestation-in-the-amazon

Ritchie, H., & Roser, M. (2024). *Fish and Overfishing*. Our World In Data. Retrieved August 6, 2025, from https://ourworldindata.org/fish-and-overfishing

Ritchie, H., Rosado, P., & Roser, M. (2025). *Soybean production – FAO*. [Dataset; processed by Our World in Data]. FAO. Retrieved August 8, 2025, from https://archive.ourworldindata.org/20251014-161652/grapher/soybean-production.html

Rivas-Ubach, A., Liu, Y., Bianchi, T. S., Tolić, N., Jansson, C., & Paša-Tolić, L. (2018). Moving beyond the van Krevelen Diagram: A new stoichiometric approach for compound classification in organisms. *Analytical Chemistry*, *90*(10), 6152–6160. https://doi.org/10.1021/acs.analchem.8b00529

Rivas-Vela, C. I., Amaya-Llano, S. L., Castaño-Tostado, E., & Castillo-Herrera, G. A. (2021). Protein hydrolysis by subcritical water: A new perspective on obtaining bioactive peptides. *Molecules*, *26*, 1–15. https://doi.org/10.3390/molecules26216655

Rodrigues, L. A., Matias, A. A., & Paiva, A. (2021). Recovery of antioxidant protein hydrolysates from shellfish waste streams using subcritical water extraction. *Food and Bioproducts Processing*, *130*, 154–163. https://doi.org/10.1016/j.fbp.2021.09.011

Rogalinski, T., Herrmann, S., & Brunner, G. (2005). Production of amino acids from bovine serum albumin by continuous sub-critical water hydrolysis. *Journal of Supercritical Fluids*, *36*(1), 49–58. https://doi.org/10.1016/j.supflu.2005.03.001

Rogalinski, T., Liu, K., Albrecht, T., & Brunner, G. (2008). Hydrolysis kinetics of biopolymers in subcritical water. *The Journal of Supercritical Fluids*, *46*(3), 335–341. https://doi.org/10.1016/j.supflu.2007.09.037

Roslan, J., Mustapa Kamal, S. M., Khairul, K. F., & Abdullah, N. (2018). Evaluation on performance of dead-end ultrafiltration membrane in fractionating tilapia by-product protein hydrolysate. *Separation and Purification Technology*, *195*, 21–29. https://doi.org/10.1016/j.seppur.2017.11.020

Rostagno, M. A., Palma, M., & Barroso, C. G. (2004). Pressurized liquid extraction of isoflavones from soybeans. *Analytica Chimica Acta*, *522*(2), 169–177. https://doi.org/10.1016/j.aca.2004.05.078

Saidi, S., Deratani, A., Amar, R. B., & Belleville, M. P. (2013). Fractionation of a tuna dark muscle hydrolysate by a two-step membrane process. *Separation and Purification Technology*, *108*, 28–36. https://doi.org/10.1016/j.seppur.2013.01.048

Saidi, S., Deratani, A., Belleville, M. P., & Amar, R. B. (2014a). Antioxidant properties of peptide fractions from tuna dark muscle protein by-product hydrolysate produced by membrane fractionation process. *Food Research International*, *65*, 329–336. https://doi.org/10.1016/j.foodres.2014.09.023

Saidi, S., Deratani, A., Belleville, M. P., & Amar, R. B. (2014b). Production and fractionation of tuna by-product protein hydrolysate by ultrafiltration and nanofiltration: Impact on interesting peptides fractions and nutritional properties. *Food Research International*, *65*, 453–461. https://doi.org/10.1016/j.foodres.2014.04.026

Salo-Väänänen, P. P., & Koivistoinen, P. E. (1996). Determination of protein in foods: Comparison of net protein and crude protein (N x 6.25) values. *Food Chemistry*, *57*, 27–31. https://doi.org/10.1016/0308-8146(96)00157-4

Sano, C. (2009). History of glutamate production. *American Journal of Clinical Nutrition*, *90*(3), 728S-732S. https://doi.org/10.3945/ajcn.2009.27462F

Santos, J., Calero, N., Muñoz, J., & Cidade, M. T. (2018). Development of food emulsions containing an advanced performance xanthan gum by microfluidization technique. *Food Science and Technology International*, *24*, 373–381. https://doi.org/10.1177/1082013218756140

Sari, Y. W. (2015). *Biomass and its potential for protein and amino acids: valorizing agricultural by-products*. [PhD Thesis, Wageningen University]. Wageningen University. https://doi.org/10.18174/341569

Schaich, K. M. (2016). Analysis of Lipid and Protein Oxidation in Fats, Oils, and Foods. In *Oxidative Stability and Shelf Life of Foods Containing Oils and Fats*, 1–131. Elsevier. https://doi.org/10.1016/B978-1-63067-056-6.00001-X

Sganzerla, W. G., Viganó, J., Castro, L. E. N., Maciel-Silva, F. W., Rostagno, M. A., Mussatto, S. I., & Forster-Carneiro, T. (2022). Recovery of sugars and amino acids from brewers' spent grains using subcritical water hydrolysis in a single and two sequential semi-continuous flow-through reactors. *Food Research International*, *157*. https://doi.org/10.1016/j.foodres.2022.111470

Shahidi, F., Varatharajan, V., Peng, H., & Senadheera, R. (2019). Utilization of marine by-products for the recovery of value-added products. *Journal of Food Bioactives*, *6*, 10–61. https://doi.org/10.31665/jfb.2019.6184

Shanmugam, A., & Ashokkumar, M. (2014). Ultrasonic preparation of stable flax seed oil emulsions in dairy systems - Physicochemical characterization. *Food Hydrocolloids*, *39*, 151–162. https://doi.org/10.1016/j.foodhyd.2014.01.006

Shon, H. K., Phuntsho, S., Chaudhary, D. S., Vigneswaran, S., & Cho, J. (2013). Nanofiltration for water and wastewater treatment - A mini review. *Drinking Water Engineering and Science*, *6*(1), 47–53. https://doi.org/10.5194/dwes-6-47-2013

Sigma-Aldrich. (2021). *Bradford Reagent Procedure*, 1–6. Sigma-Aldrich.

Slizyte, R., Rommi, K., Mozuraityte, R., Eck, P., Five, K., & Rustad, T. (2016). Bioactivities of fish protein hydrolysates from defatted salmon backbones. *Biotechnology Reports*, *11*, 99–109. https://doi.org/10.1016/j.btre.2016.08.003

Sluiter, A., Hames, B., Ruiz, R., Scarlata, C., Sluiter, J., Templeton, D., & Crocker, D. (2008). *Determination of structural carbohydrates and lignin in Biomass* (Laboratory Analytical Procedure, NREL/TP-510-42618). National Renewable Energy Laboratory. https://www.nrel.gov/docs/gen/fy13/42618.pdf

Sluiter, J., Ruiz, R., Scarlata, C., Sluiter, A., & Templeton, D. (2010). Compositional analysis of lignocellulosic feedstocks. 1. Review and description of methods. *Journal of Agricultural and Food Chemistry*, *58*(16), 9043–9053. https://doi.org/10.1021/jf1008023

Soy Nutrition Institute Global. (2025). *U.S. Grown Soy*. Soy Nutrition Institute. Retrieved August 9, 2025, from https://sniglobal.org/us-grown-soy/

Speroni, F., Milesi, V., & Añón, M. C. (2010). Interactions between isoflavones and soybean proteins: Applications in soybean-protein-isolate production. *LWT - Food Science and Technology*, *43*(8), 1265–1270. https://doi.org/10.1016/j.lwt.2010.03.011

Sterlitech. (n.d.). *HP4750 assembly & operation manual*. Sterlitech.

Sun, H., Yuan, X., Zhang, Z., Su, X., & Shi, M. (2018). Thermal Processing Effects on the Chemical Constituent and Antioxidant Activity of Okara Extracts Using Subcritical Water Extraction. *Journal of Chemistry*, *2018*. https://doi.org/10.1155/2018/6823789

Tamayo-Tenorio, A., Kyriakopoulou, K. E., Suarez-Garcia, E., van den Berg, C., & van der Goot, A. J. (2018). Understanding differences in protein fractionation from conventional crops, and herbaceous and aquatic biomass - Consequences for industrial use. *Trends in Food Science and Technology*, *71*, 235–245. https://doi.org/10.1016/j.tifs.2017.11.010

Tamires, D., Vollet, G., Fernández, G., Gadioli, A., Baú, C., Dupas, M., & Martínez, J. (2020). Concentration of bioactive compounds from grape marc using pressurized liquid extraction followed by integrated membrane processes. *Separation and Purification Technology*, *250*, 117206. https://doi.org/10.1016/j.seppur.2020.117206

Tang, L., Liu, X., Bai, S., Zhao, D., Guo, X., Zhu, D., Su, G., Fan, B., Wang, B., Zhang, L., & Wang, F. (2024). Okara protein extracted by alternating ultrasonic/alkali treatment and its improved physicochemical and functional properties. *Ultrasonics Sonochemistry*, *111*, 107129. https://doi.org/10.1016/j.ultsonch.2024.107129

Tao, X., Cai, Y., Liu, T., Long, Z., Huang, L., Deng, X., Zhao, Q., & Zhao, M. (2019). Effects of pretreatments on the structure and functional properties of okara protein. *Food Hydrocolloids*, *90*, 394–402. https://doi.org/10.1016/j.foodhyd.2018.12.028

Tiwari, A. (2015). *Practical Biochemistry: A Student Companion*.

Trigueros, E., Alonso-Riaño, P., Ramos, C., Diop, C. I. K., Beltrán, S., & Sanz, M. T. (2021). Kinetic study of the semi-continuous extraction/hydrolysis of the protein and polysaccharide fraction of the industrial solid residue from red macroalgae by subcritical water. *Journal of Environmental Chemical Engineering*, *9*. https://doi.org/10.1016/j.jece.2021.106768

Trigueros, E., Sanz, M. T., Alonso-Riaño, P., Beltrán, S., Ramos, C., & Melgosa, R. (2021). Recovery of the protein fraction with high antioxidant activity from red seaweed industrial solid residue after agar extraction by subcritical water treatment. *Journal of Applied Phycology*, *33*, 1181–1194. https://doi.org/10.1007/s10811-020-02349-0

Tsubaki, S., Nakauchi, M., Ozaki, Y., & Azuma, J. I. (2009). Microwave heating for solubilization of polysaccharide and polyphenol from soybean residue (Okara). *Food Science and Technology Research*, *15*(3), 307–314. https://doi.org/10.3136/fstr.15.307

United Nations. (2023). *United Nations Sustainable Development Goals – Zero Hunger*. Retrieved August 4, 2025, from https://www.un.org/sustainabledevelopment/hunger/

University of Manchester. (2024). *Chemical Engineering Plant Cost Index*. University of Manchester. https://www.training.itservices.manchester.ac.uk/public/gced/CEPCI.html?reactors/CEPCI/index.html

van Breugel, M. (2025a). *Hydrochloric Acid price index*. Businessanalytiq. Retrieved April 21, 2025, from https://businessanalytiq.com/procurementanalytics/index/hydrochloric-acid-price-index/

van Breugel, M. (2025b). *Sodium hydroxide price index*. Businessanalytiq. Retrieved April 21, 2025, from https://businessanalytiq.com/procurementanalytics/index/sodium-hydroxide-price-index/

Van Walsum, G. P. (2001). Severity function describing the hydrolysis of xylan using carbonic acid. *Applied Biochemistry and Biotechnology - Part A Enzyme Engineering and Biotechnology*, *91–93*, 317–329. https://doi.org/10.1385/ABAB:91-93:1-9:317

Villamil, O., Váquiro, H., & Solanilla, J. F. (2017). Fish viscera protein hydrolysates: Production, potential applications and functional and bioactive properties. *Food Chemistry*, *224*, 160–171. https://doi.org/10.1016/j.foodchem.2016.12.057

Vinatoru, M., Mason, T. J., & Calinescu, I. (2017). Ultrasonically assisted extraction (UAE) and microwave assisted extraction (MAE) of functional compounds from plant materials. *Trends in Analytical Chemistry*, *97*, 159–178. https://doi.org/10.1016/j.trac.2017.09.002

Vogelsang-O'Dwyer, M., Sahin, A. W., Bot, F., O'Mahony, J. A., Bez, J., Arendt, E. K., & Zannini, E. (2023). Enzymatic hydrolysis of lentil protein concentrate for modification of physicochemical and techno-functional properties. *European Food Research and Technology*, *249*(3), 573–586. https://doi.org/10.1007/s00217-022-04152-2

Vong, W. C., & Liu, S. Q. (2016). Biovalorization of okara (soybean residue) for food and nutrition. *Trends in Food Science and Technology*, *52*, 139–147. https://doi.org/10.1016/j.tifs.2016.04.011

Ween, O., Stangeland, J. K., Fylling, T. S., & Aas, G. H. (2017). Nutritional and functional properties of fishmeal produced from fresh by-products of cod (*Gadus morhua L.*) and saithe (*Pollachius virens*). *Heliyon*, *3*, 343. https://doi.org/10.1016/j.heliyon.2017.e00343

Wiboonsirikul, J., Mori, M., Khuwijitjaru, P., & Adachi, S. (2013). Properties of extract from okara by its subcritical water treatment. *International Journal of Food Properties*, *16*(5), 974–982. https://doi.org/10.1080/10942912.2011.573119

Windsor, M. L. (1971). *Fish Meal*. FAO. https://www.fao.org/4/x5926e/x5926e01.htm

Wisuthiphaet, N., & Kongruang, S. (2015). Production of fish protein hydrolysates by acid and enzymatic hydrolysis. *Journal of Medical and Bioengineering*, *4*, 466–470. https://doi.org/10.12720/jomb.4.6.466-470

Wouters, A. G. B., Rombouts, I., Fierens, E., Brijs, K., & Delcour, J. A. (2016). Relevance of the Functional Properties of Enzymatic Plant Protein Hydrolysates in Food Systems. *Comprehensive Reviews in Food Science and Food Safety*, *15*(4), 786–800. https://doi.org/10.1111/1541-4337.12209

Wu, H., Forghani, B., Abdollahi, M., & Undeland, I. (2022). Lipid oxidation in sorted herring (*Clupea harengus*) filleting co-products from two seasons and its relationship to composition. *Food Chemistry*, *373*, 131523. https://doi.org/10.1016/j.foodchem.2021.131523

Wu, N. N., Zhang, J. B., Tan, B., He, X. T., Yang, J., Guo, J., & Yang, X. Q. (2014). Characterization and interfacial behavior of nanoparticles prepared from amphiphilic hydrolysates of β-conglycinin-dextran conjugates. *Journal of Agricultural and Food Chemistry*, *62*, 12678–12685. https://doi.org/10.1021/jf504173z

Yilmaz, Y., & Toledo, R. (2005). Antioxidant activity of water-soluble Maillard reaction products. *Food Chemistry*, *93*(2), 273–278. https://doi.org/10.1016/j.foodchem.2004.09.043

Yourchisin, D. M., & Van Walsum, G. P. (2004). Comparison of microbial inhibition and enzymatic hydrolysis rates of liquid and solid fractions produced from pretreatment of biomass with carbonic acid and liquid hot water. *Applied Biochemistry and Biotechnology - Part A Enzyme Engineering and Biotechnology*, *115*(1–3), 1073–1086. https://doi.org/10.1385/ABAB:115:1-3:1073

Yuan, H., Luo, Z., Ban, Z., Reiter, R. J., Ma, Q., Liang, Z., Yang, M., Li, X., & Li, L. (2022). Bioactive peptides of plant origin: distribution, functionality, and evidence of benefits in food and health. *Food and Function*, *13*(6), 3133–3158. https://doi.org/10.1039/d1fo04077d

Zaviezo, D., & Dale, N. (1994). Nutrient content of tuna meal. *Poultry Science*, *73*(6), 916–918. https://doi.org/10.3382/ps.0730916

Zhang, Q. T., Tu, Z. C., Wang, H., Huang, X. Q., Fan, L. L., Bao, Z. Y., & Xiao, H. (2015). Functional properties and structure changes of soybean protein isolate after subcritical water treatment. *Journal of Food Science and Technology*, *52*, 3412–3421. https://doi.org/10.1007/s13197-014-1392-9

Zhang, Y., & Chang, S. K. C. (2016). Isoflavone Profiles and Kinetic Changes during Ultra-High Temperature Processing of Soymilk. *Journal of Food Science*, *81*(3), C593–C599. https://doi.org/10.1111/1750-3841.13236

Zhu, G., Zhu, X., Fan, Q., Liu, X., Shen, Y., & Jiang, J. (2010). Study on production of amino acids from bean dregs by hydrolysis in sub-critical water. *Chinese Journal of Chemistry*, *28*(10), 2033–2038. https://doi.org/10.1002/cjoc.201090339

Zhu, X., Zhu, C., Zhao, L., & Cheng, H. (2008). Amino Acids Production from Fish Proteins Hydrolysis in Subcritical Water. *Chinese Journal of Chemical Engineering*, *16*(3), 456–460. https://doi.org/10.1016/s1004-9541(08)60105-6